# ANALYTICA CHIMICA ACTA

*International monthly devoted to all branches of analytical chemistry*
*Revue mensuelle internationale consacrée à tous les domaines de la chimie analytique*
*Internationale Monatsschrift für alle Gebiete der analytischen Chemie*




ELSEVIER PUBLISHING COMPANY

AMSTERDAM

*Anal. Chim. Acta*, Vol. 56, No. 2, 157–332, September 1971
Published monthly

## Publication Schedule for 1971

In the interests of rapid publication it has been found necessary to schedule 5 volumes for appearance in 1971. Since monthly publication will be maintained, this implies that 2 of the volumes will each consist of three issues, while 3 of the volumes will each consist of only 2 issues. The following provisional schedule applies:

| | | |
|---|---|---|
| Vol. **53**, No. **1** | January 1971 | |
| Vol. **53**, No. **2** | February 1971 | **(completing Vol. 53)** |
| Vol. **54**, No. **1** | March 1971 | |
| Vol. **54**, No. **2** | April 1971 | |
| Vol. **54**, No. **3** | May 1971 | **(completing Vol. 54)** |
| Vol. **55**, No. **1** | June 1971 | |
| Vol. **55**, No. **2** | July 1971 | **(completing Vol. 55)** |
| Vol. **56**, No. **1** | August 1971 | |
| Vol. **56**, No. **2** | September 1971 | |
| Vol. **56**, No. **3** | October 1971 | **(completing Vol. 56)** |
| Vol. **57**, No. **1** | November 1971 | |
| Vol. **57**, No. **2** | December 1971 | **(completing Vol. 57)** |

Subscription price: $17.50 or Dfl. 63.— per volume plus postage. Total subscription price for 1971: $87.50 or Dfl. 315.— plus postage. Additional cost for copies by airmail available on request. For subscribers in the U.S.A. and Canada, 2nd class postage paid at New York, N.Y. For advertising rates apply to the publishers.

Subscriptions should be sent to:

ELSEVIER PUBLISHING COMPANY P.O. Box 211, Amsterdam, The Netherlands

## GENERAL INFORMATION

*Languages*

Papers will be published in English, French or German.

*Submission of papers*

Papers should be sent to:

PROF. PHILIP W. WEST,
Coates Chemical Laboratories,
College of Chemistry and Physics,
Louisiana State University,
Baton Rouge 3,
La. 70803 (U.S.A.)

or to:

DR. A. M. G. MACDONALD,
Department of Chemistry,
The University,
P.O. Box 363
Birmingham B15 2TT (Great Britain)

*Reprints*

Fifty reprints will be supplied free of charge. Additional reprints (minimum 100) can be ordered at quoted prices. They must be ordered on order forms which are sent together with the proofs.

# P.P.B. Sensitivity for $1925 with PAR Model 174 Polarographic Analyzer


**ANALYZE**

- **Organics**
- **Pharmaceuticals**
- **Pollutants**
- **Metals**

**BY**

- **Differential Pulse**
- **Pulse**
- **Tast**
- **DC Polarography**

The PAR™ Model 174 Polarographic Analyzer complete with drop timer costs just $1925. Its part-per-billion sensitivity could heretofore only be found in units costing five times as much. The Model 174 brings all the analytical applications of ultra-sensitive polarographic techniques within the reach of any lab. For complete information, call or write Princeton Applied Research Corporation, Box 565, Princeton, New Jersey 08540; telephone (609) 452-2111.

**PRINCETON APPLIED RESEARCH CORPORATION**

115

Export price approximately 5% higher

428

# Comprehensive Biochemistry

*edited by*

MARCEL FLORKIN, *Professor of Biochemistry, University of Liège (Belgium) and*

ELMER H. STOTZ, *Professor of Biochemistry, University of Rochester, School of Medicine and Dentistry, Rochester, N.Y. (U.S.A.)*

**Section I**

PHYSICO-CHEMICAL AND ORGANIC ASPECTS OF BIOCHEMISTRY

This section is intended neither as a textbook of organic nor of physical chemistry, but rather as a collection of chapters which seem generally pertinent in the interpretation of biochemical techniques and in the understanding of the chemistry of biological compounds and reaction mechanisms.

Vol. 1. Atomic and Molecular Structure
Vol. 2. Organic and Physical Chemistry
Vol. 3. Methods for the Study of Molecules
Vol. 4. Separation Methods

**Section II**

CHEMISTRY OF BIOLOGICAL COMPOUNDS

Deals with the organic and physical chemistry of the major organic constituents of living material. This section includes a sound treatment of the important biological high polymers—their shape and physical properties. A number of substances peculiar to plants, certain isoprenoids, flavonoids, tannins, lignins, and plant hormones, often omitted from textbooks of biochemistry, are also covered.

Vol. 5. Carbohydrates
Vol. 6. Lipids—Amino Acids and Related Compounds
Vol. 7. Proteins (Part 1)
Vol. 8. Proteins (Part 2) und Nucleic Acids
Vol. 9. Pyrrole Pigments; Isoprenoid Compounds; Phenolic Plant Constituents
Vol. 10. Sterols, Bile Acids and Steroids
Vol. 11. Water-Soluble Vitamins, Hormones, Antibiotics

**Section III**

BIOCHEMICAL REACTION MECHANISMS

Section III is devoted primarily to Enzymes, focusing attention on the chemistry and function of the coenzymes. Other chapters treat thermodynamic and kinetic aspects of enzyme catalysis, hydrolytic enzymes displaying "active center" characteristics, and chelation and stereochemical considerations in enzyme catalysis. Much attention is given to biological oxidation mechanisms.

Vol. 12. Enzymes—General Considerations
Vol. 13. Enzyme Nomenclature (2nd revised edition)
Vol. 14. Biological Oxidations
Vol. 15. Group-Transfer Reactions
Vol. 16. Hydrolytic Reactions; Cobamide and Biotin Coenzymes

*Subscribers who place a standing order for the whole series will be entitled to an overall 20% discount. Detailed brochure available on request.*

**Elsevier**

Book Division, P.O. BOX 3489,
Amsterdam – The Netherlands

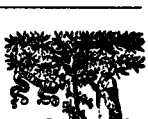

**Section IV**

METABOLISM

This section concerns itself with the degradative and biosynthetic pathways of carbohydrates, lipids, amino acids, porphyrins, purines, pyrimidines, etc., with special emphasis on experimental data as evidence for the metabolic schemes now admitted. Not only mammalian metabolism, but also the related metabolism in other organisms is treated. Special sections are devoted to the metabolism of special organs in the mammal, and highly characteristic variations of metabolism occurring in non-mammals. Abnormal cellular metabolism and the resulting disease states are discussed in detail.

Vol. 17. Carbohydrate Metabolism
Vol. 18. Lipid Metabolism
Vol. 18S. Pyruvate and Fatty Acid Metabolism
Vol. 19. Metabolism of Amino Acids, Proteins, Purines, and Pyrimidines
Vol. 20. Metabolism of Cyclic Compounds
Vol. 21. Metabolism of Vitamins and Trace Elements

**Section V**

CHEMICAL BIOLOGY

Section V is devoted to a number of topics which, in an earlier state of development, were primarily descriptive and included in the field of biology, but which have been rapidly brought to study at the molecular level. Besides the chapters often grouped under 'molecular biology', Section V also deals with modern aspects of bioenergetics, immunochemistry, photobiology, and a consideration of the molecular phenomena that underlie the evolution of organisms.

Vol. 22. Bioenergetics
Vol. 23. Cytochemistry
Vol. 24. Biological Information Transfer. Immunochemistry
Vol. 25. Regulatory Functions, Membrane Phenomena
Vol. 26A. Extracellular and Supporting Structures
Vol. 26B. Extracellular and Supporting Structures (continued)
Vol. 26C. Extracellular and Supporting Structures (continued)
Vol. 27. Photobiology, Ionizing Radiations
Vol. 28. Morphogenesis, Differentiation and Development
Vol. 29. Comparative Biochemistry. Molecular Evolution

---

Further volumes in the series not related to Section V

Vol. 30. History of Biochemistry
Vol. 30A. (part I). Protobiochemistry
Vol. 30A. (part II). From Protobiochemistry to Biochemistry
Vol. 30B. The Unravelling of Metabolic Pathways
Vol. 30C. The Molecular Basis of Biological and Physiological Concepts
Vol. 31. General Index

# Bibliography of Paper and Thin-Layer Chromatography 1966-1969

## and survey of applications

(supplementary volume No. 2, 1971)

Published in conjunction with the JOURNAL OF CHROMATOGRAPHY

Edited by K. MACEK, I. M. HAIS, J. KOPECKÝ, J. GASPARIČ, V. RÁBEK and J. CHURÁČEK

6½ x 9½", ca. 990 pages, Fall 1971, approx. Dfl. 125.00, ISBN 0-444-40953-x

This volume covers developments in both paper and thin-layer chromatography from 1966 to 1969 and is a continuation of earlier bibliographies.

The present volume contains 8695 entries, which give the names of the authors, title of the paper or book (translated title for papers in languages other than English, French or German) and the complete literature reference. For papers published in the less accessible periodicals the respective reference in *Chemical Abstracts* or *Zeitschrift für Analytische Chemie* has also been included. Since the title of a paper does not always give information concerning the particular chromatographic problem involved, an indication of the subject matter has in many cases been added at the end of the reference.

The book contains a General Part dealing with general reviews and books as well as with the theory and techniques, and a Special Part, which is subdivided into chapters according to the chemical structure of the compounds, or exceptionally, according to their biological activity (vitamins, antibiotics, insecticides, pharmaceuticals), physical properties (dyes) or technical importance (plastics, antioxidants). Cross-references are used in cases where papers contain data which could be included in several chapters.

The subject matter is based on a systematic search of about 70 journals which regularly publish papers of chromatographic interest, and a less regular search in other available journals, reprints, etc.

The bibliography contains an Author Index and a very extensive List of Substances Chromatographed in which an effort has been made to include as many substances as possible.

**Contents:**

GENERAL PART. General reviews and books. Principles, theory and information of general interest in PC and TLC. Techniques used in both PC and TLC. Techniques of PC. Techniques of TLC.

SPECIAL PART. Hydrocarbons. Alcohols. Phenols. Oxo compounds. Carbohydrates. Carboxylic acids. Lipids. Organic peroxides. Compounds containing heterocyclic oxygen. Steroids. Cardiac glycosides and saponins. Terpene derivatives. Amines, amides and related nitrogen compounds. Nitro and nitroso compounds. Amino acids. Peptides. Elucidation of the primary structure of peptides and proteins. Proteins. Purines, pyrimidines, nitrogenous constituents of nucleic acids. Alkaloids. Other compounds with heterocyclic nitrogen. Organic sulfur compounds. Organic phosphorus compounds. Organometallic and related compounds. Vitamins. Antibiotics. Pesticides. Dyes and pigments. Plastics. Application in pharmacy and toxicology. Some technical products and complex mixtures. Inorganic compounds. Radioactive substances. Author index.

List of substances chromatographed.

*Still available:*

**Bibliography of Paper and Thin-Layer Chromatography 1961-1965**

6½ x 9½", 1041 pages, 1968, Dfl. 95.00 (ca. $ 26.25), ISBN 0-444-40676-x

Elsevier
Journal Division, P.O. Box 211
Amsterdam - The Netherlands

*Analytica Chimica Acta*
Elsevier Publishing Company, Amsterdam
Printed in The Netherlands



# WOLFGANG SCHÖNIGER

## 1920–1971

Unfassbar ist es für die Analytiker und Mikrochemiker in aller Welt, dass Dr. Wolfgang Schöniger ein unerbittlich hartes Schicksal im 51. Lebensjahr mitten aus seinem blühenden Leben und Schaffen gerissen hat. Am 24. Februar 1971 starb dieser Mikrochemiker von Weltruf völlig unerwartet an den Folgen eines Unfalles in Basel.

Geboren am 4. August 1920 in Karlsbad-Weheditz (Land Böhmen, Tschechoslowakei), absolvierte Wolfgang Schöniger das Staatsrealgymnasium in Karlsbad. Im Herbst 1939 begann er an der deutschen Technischen Hochschule in Prag das Studium der Chemie, das er im Frühjahr 1945 beendete. Zu Beginn des Jahres 1946 trat er zunächst als wissenschaftliche Hilfskraft in das Medizinisch-Chemische Institut und PREGL-Laboratorium der Universität Graz ein. Von September 1949 bis Oktober 1953 wirkte Schöniger als Universitätsassistent an diesem, damals von Prof. Dr. Hans Lieb geleiteten Institut und entfaltete in diesem Zeitraum eine reiche und fruchtbare analytische Tätigkeit, die ihren Niederschlag in 23 Veröffentlichungen über zahlreiche Probleme, insbesondere der organischen Mikroanalyse, fand. In diese Jahre akademischer Tätigkeit fielen auch Studienreisen nach den U.S.A. und Schweden. Nach diesen frühzeitig an der Universität errungenen Erfolgen entschied sich Dr. Schöniger eine industrielle Laufbahn einzuschlagen.

Am 1. Oktober 1953 trat er in die Sandoz AG, Basel, mit dem Auftrag ein, eine leistungsfähige mikrochemische Abteilung aufzubauen. Aus bescheidenen Anfängen heraus hat Dr. Schöniger dieses für eine aktive pharmazeutische Forschung unentbehrliche Laboratorium geschaffen, es mit modernsten Geräten ausgestattet und einen hervorragenden Mitarbeiterstab herangebildet. Die prompte und zuverlässige Arbeit dieser Abteilung hatte zur Folge, dass bald alle in den Laboratorien der Sandoz hergestellten neuen Verbindungen zur Mikroanalyse der Arbeitsgruppe Schöniger anvertraut wurden. Mit Begeisterung, Ausdauer, aufbauendem Willen und getragen von profunden Sachkenntnissen widmete sich Dr. Schöniger dieser Aufgabe und pflegte dabei wertvolle Kontakte mit allen in diesem Fachgebiet massgeblichen Hochschul-Instituten und analytischen Laboratorien der grossen Chemiewerke der Welt. Seine Aufgeschlossenheit zu den sich rasch ändernden Problemen befähigten ihn, mit wachen Augen stets an der vordersten Front seines Forschungsgebietes beteiligt zu sein und die Ergebnisse für die industriellen Aufgaben nutzbringend anzuwenden.

Ein einziges Zeugnis für diese Aktivität mag hier angeführt sein. Schöniger schuf eine durch ihre Einfachheit, Eleganz und rasche Durchführbarkeit bestechende Methode zur Bestimmung von Halogenen, die heute als *Schöniger-Methode* weltweit bekannt ist. Es wird heute kaum ein analytisches Laboratorium geben, in welchem diese Methodik nicht erfolgreiche Anwendung findet. Besonders wichtig ist diese *Schöniger-Methode* in ihrer Erweiterung auf die Messung der Radioaktivität von künstlich markierten organischen Verbindungen, eine Variante, die zu einer wesent-

lichen Bereicherung der modernen Arzneimittelforschung führte.

Zahlreiche Fachgremien waren um die Mitarbeit Dr. Schöniger's bemüht. So war er Mitglied und Chairman of the Commission on Microchemical Techniques and Trace Analysis of the Analytical Chemistry Division of IUPAC, Vorstandsmitglied der Gesellschaft Schweizerischer Mikroanalytiker und der Österreichischen Gesellschaft für Mikrochemie und Analytische Chemie u.v.a.m. Auch verschiedenen internationalen Fachzeitschriften schenkte Dr. Schöniger seinen Rat als Mitherausgeber, so *Talanta* und *Analytica Chimica Acta.* Er war Träger des Fritz-Feigl-Preises und Ehrenmitglied der American Microchemical Society. In über 50 Vorträgen und weiteren 41 Publikationen war Dr. Schöniger bemüht, die immer komplexer werdenden Entwicklungen chemischer und physikalisch-chemischer analytischer Verfahren in klarer Form zu präsentieren und weiten Kreisen zugänglich zu machen.

In Anerkennung seiner grossen Verdienste erhielt Dr. Schöniger bereits im Jahre 1959 die Prokura der Sandoz AG. Weitere grosse Aufgaben wurden ihm in dieser Firma übertragen, so die Planung eines neuen grossen Analytik-Gebäudes. Seine organisatorische Begabung und die grosse Sachkenntnis liessen ihn auch hier Ausserordentliches vollbringen. Es ist eine Tragik, dass es ihm das Schicksal nicht vergönnt hat, das Resultat dieser seiner Bemühungen und seines grossen Einsatzes zu erleben.

Mit Dr. Schöniger ist nicht nur ein hervorragender Wissenschaftler dahingegangen, sondern auch ein wertvoller und liebenswerter Mensch. Seine wohlüberlegte Kompromissbereitschaft äusserte sich in der Achtung vor einer anderen Meinung und ebensosehr auch in der überzeugenden Vertretung eines ihm berechtigt und wissenschaftlich fundiert erscheinenden Standpunktes. Seine treffenden Bemerkungen, seine klar vorgebrachten, stets konstruktiven Vorschläge, aber auch sein alles überstrahlender Humor und sein befreiendes Lachen sind allen noch im Ohr, die Wolf Schöniger gekannt haben. Das tiefe Mitgefühl aller Kollegen gilt seiner Gattin und seinen drei Kindern.

Der tragische Heimgang von Dr. Wolfgang Schöniger hat in die Reihe der Mikroanalytiker eine Lücke gerissen, die kaum zu schliessen sein wird.

Hans Spitzy, Graz, 14. April 1971

*Analytica Chimica Acta*
Elsevier Publishing Company, Amsterdam
Printed in The Netherlands



# A CATALOG OF LASER-STIMULATED INFRARED EMISSION SPECTRA

D. M. HAILEY*, H. M. BARNES**, C. WOODWARD AND J. W. ROBINSON
*Department of Chemistry, Louisiana State University, Baton Rouge, La. 70803 (U.S.A.)*
(Received 7th May 1971)

Previous communications from this laboratory[1-3] have reported the stimulation of infrared emission from organic molecules with a carbon dioxide laser beam. The main requirement in a compound for laser-stimulated emission appears to be a suitably low vapor pressure, so that an adequate number of molecules are presented to the laser radiation. It has been found that the infrared emission process takes place with a wide variety of compounds.

This paper presents laser-stimulated infrared emission spectra for thirty-six compounds. Significant features of the spectra are discussed, and the emission peaks correlated with bond vibrations and the appropriate infrared absorption spectra.

## EXPERIMENTAL

As in previous studies[1-3] the radiation was provided by a Perkin-Elmer Model 6200 molecular gas laser. The spectrometer was a Beckman Model IR-10, modified and operated with fully open slits as described previously[2]. A glass sample cell fitted with Irtran-2 windows was used. The windows were held in position either by epoxy adhesive, or by mounting in camera lens holders, which were fixed to the cell with adhesive tape.

The experimental procedure adopted was similar to that described elsewhere[1,2], except that the cell and laser configurations were modified, so that the laser and spectrometer were at the same height, and the cell mounted with its long axis parallel to the IR-10 entrance slit (Fig. 1). The front and end windows were kept cool by streams of air.

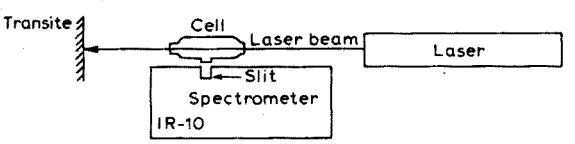


Fig. 1. Schematic diagram of experimental layout.

## RESULTS

Infrared emission spectra were obtained for the thirty-six compounds listed

---

* Present address: Roche Research Unit, Biochemistry Department, Liverpool University, Liverpool L693BX, England.

** Present address: Department of Health, Education and Welfare, Public Health Service, National Center for Air Pollution Control, Cincinnati, Ohio 45227, U.S.A.

TABLE I

| *Compound* | *Principal observed bands* | | *Provisional assignment* | *I.r.*[4-6] *absorption bands* | | *Relative sensitivity* |
|---|---|---|---|---|---|---|
| | $cm^{-1}$ | $\mu m$ | | $cm^{-1}$ | $\mu m$ | |
| Cyclohexane | 1460–1440 | 6.85–6.95 | $CH_2$ def. | 1460 | 6.85 | 17 |
| (J. T. Baker) | 1370 | 7.30 | | | 7.92 | |
| | 1230 | 8.14 | | 1265 | | |
| | 1120 | 8.94 | | 1042, 1020 | 9.6–9.82 | |
| Cyclopentene | 1650 | 6.06 | C=C str. | 1640 | 6.10 | 11 |
| (Matheson, Coleman | 1440 | | $-CH_2$ bend (sym.) | 1471–1450 | 6.80–6.90 | |
| and Bell) | 1340–1200 | 7.46–8.34 | | | | |
| | 1060–1030 | 9.44–9.71 | | 1045, 965 | 9.58, 10.38 | |
| | 930–870 | 10.77–11.50 | | 904 | 11.05 | |
| Cyclohexene | 1525 | 6.56 | | | | 16 |
| (Eastman) | 1450–30 | 6.90–7.00 | $CH_2$ bend (asym.) | 1436 | 6.96 | |
| | 1270 | 7.88 | $CH_2$ bend (sym.) | 1319 | 7.59 | |
| | 1115 | 8.98 | | 1263 | 7.92 | |
| | | | | 1135 | 8.82 | |
| | | | | 1038 | 9.65 | |
| | 900 | 11.11 | | 914 | 10.95 | |
| | | | | 874 | 11.44 | |
| 1-Octene | ~1600 | 6.25 | Includes $-CH_2$ bend | 1634 | 6.12 | 23 |
| (Aldrich) | ~140 –1240 | 6.95–8.07 | | 1465 | 6.84 | |
| | ~985 | 10.17 | Resolution insufficient | 998 | 10.08 | |
| | | | | 906 | 11.02 | |
| 1,3-Butadiene | 1845 | 5.43 | Possible overtone | 1808 | 5.54 | 19 |
| (Matheson) | 1610 | 6.29 | C=C str. (conjugated system) | 1605 | 6.24 | |
| | 1385 | 7.23 | $=CH_2$ bend | 1380 | 7.25 | |
| | 1290 | 7.76 | =CH bend | 1280 | 7.82 | |
| | 1010 | 9.91 | $=CH_2$ out of plane def. | 1017 | 9.85 | |
| | 925 | 10.81 | =CH | 914 | 11.04 | |
| Toluene | 1600 | 6.25 | CH bend | 1592 | 6.28 | 26 |
| (Fisher) | | | | 1489 | 6.72 | |
| | 1470 | 6.80 | C=C str. | 1458 | 6.86 | |
| | | | | 1079 | 9.27 | |
| | | | | 1028 | 9.74 | |
| | 715–680 | 14.0–14.71 | C–H def. ($\gamma$) | 894 | 11.20 | |
| | | | | 728 | 13.75 | |
| | | | | 694 | 14.43 | |
| Thiophene | 1850 | 5.41 | | 1808 | 5.54–5.66 | 17 |
| (Matheson, | 1630 | 6.14 | C=C str. | 1768 | | |
| Coleman and Bell) | 1595 | 6.27 | | 1588 | 6.30 | |
| | 1420 | 7.05 | | 1394 | 7.18 | |
| | 1265–1250 | 7.91–8.00 | | 1248 | 8.02 | |
| | 1110 | 9.01 | | 1077 | 9.30 | |
| | 1055 | 9.48 | | 1031 | 9.70 | |
| | 780 | 12.82 | C–S str. or C–H rock. | 831 | 12.04 | |
| | | | | 712 | 14.06 | |

TABLE 1 (*continued*)

| *Compound* | *Principal observed bands* | | *Provisional assignment* | *I.r.*[4-6] *absorption bands* | | *Relative sensitivity* |
|---|---|---|---|---|---|---|
| | $cm^{-1}$ | $\mu m$ | | $cm^{-1}$ | $\mu m$ | |
| Pyridine | 1650–1600 | 6.06–6.25 | C=C str., C=N str. | 1582 | 6.31 | 24 |
| J. T. Baker) | 1430 | 7.00 | C–H bend | 1218 | 8.22 | |
| | 1320 | 7.58 | | 1147 | 8.74 | |
| | 1230 | 8.14 | Ring vibration, C–H def. | 1068 | 9.38 | |
| | 1075 | 9.31 | | 1030 | 9.72 | |
| | | | | 994 | 10.08 | |
| | 830 | 12.07 | | 749 | 13.39 | |
| | | | | 700 | *ca.* 14.3 | |
| Ethyl ether | 1475–1350 | 6.79–7.41 | $CH_3$, $CH_2$ bend | 1450 | 6.90 | 4 |
| (Allied Chemicals) | 1285 | 7.79 | | 1390 | 7.20 | |
| | 1190 | 8.41 | | 1298 | 7.72 | |
| | 1085–1055 | 9.24–9.49 | C–O str. | 1147 | 8.74 | |
| | 925 | 10.81 | | 1072 | 9.32 | |
| | 830 | 12.07 | $CH_3$, $CH_2$ rock | 929 | 10.78 | |
| | | | | 844 | 11.88 | |
| Isopropyl ether | 1470 | 6.81 | $CH_3$ bend (asym.) | 1470 | 6.80 | A6 |
| (Fisher) | 1375 | 7.28 | $C(CH_3)_2$ bend (sym.) | 1384, 1370 | 7.22, 7.30 | B3 |
| | | | | 1330 | 7.52 | |
| | 1325 | 7.55 | | 1172 | 8.54 | |
| | | | | 1112 | 8.99 | |
| | 1130 | 8.85 | C–O str. (asym.) | 1018 | 9.84 | |
| | 1005 | 9.96 | $CH_3$ rock | | | |
| | | | CHRO def. ? | 904 | 11.04 | |
| | 925 | 10.81 | $CH_3$ def. ? | 850 | 11.78 | |
| | | | | 796 | 12.57 | |
| Dioxane | 1360 | 7.36 | $CH_2$ bend | 1359 | 7.36 | 13 |
| (Fisher) | 1250 | 8.00 | C–C str. ? | 1282 | 7.80 | |
| | 1135–1125 | 8.82–8.90 | C–O str. | 1250 | 8.00 | |
| | | | | 1020 | 8.00 | |
| | 855 | 11.70 | $CH_2$ bend | 866 | 11.54 | |
| Tetrahydrofuran | 1300 | 7.70 | $CH_2$ bend | 1465 | 6.84 | 8 |
| (Fisher) | 1185 | 8.45 | | 1178 | 8.50 | |
| | 1055 | 9.48 | C–O str. | 1068 | 9.39 | |
| | 920 | 11.89 | | 910 | 11.00 | |
| *n*-Propylamine | 1625 | 6.16 | N–H bend | 1612 | 6.20 | 20 |
| (Matheson, | 1455 | 6.88 | $CH_2$ bend | 1468 | 6.81 | |
| Coleman and Bell) | 1385 | 7.23 | $CH_3$ bend | 1385 | 7.22 | |
| | 1070 | 9.35 | C–N str. | 1076 | *ca.* 9.30 | |
| | 760 | 13.18 | | 902 | *ca.* 11.10 | |
| | | | | 800 | *ca.* 12.5 | |
| Allylamine | 1610 | 6.22 | N–H bend | 1646–1608 | 6.08–6.22 | 27 |
| | 1480 | 6.76 | $CH_2$ bend | 1423 | 7.02 | |
| | *ca.* 1000 | 10.0 | C=C str. | 996 | 10.02 | |
| | 885 | 11.31 | | 914 | 10.96 | |
| | 730 | 13.70 | N–H rock ? | 827 | 12.2 | |

(*Continued on p.* 164)

TABLE 1 (*continued*)

| *Compound* | *Principal observed bands* | | *Provisional assignment* | *I.r.*[4-6] *absorption bands* | | *Relative sensitivity* |
|---|---|---|---|---|---|---|
| | $cm^{-1}$ | $\mu m$ | | $cm^{-1}$ | $\mu m$ | |
| Methanol | 1960 | 5.11 | | 1663 | 6.02 | 11 |
| | 1320 | 7.58 | O–H bend, $C–H_3$ bend (should be multiplet, insufficient resolution) | 1561<br>1370, 1300 | 6.40<br>7.30, 7.70 | |
| | 990 | 10.10 | C–OH str. | 1057, 1039, 1018 | 9.46, 9.64, 9.84 | |
| Ethanol (U.S. Industrial Chemicals) | 1385–1365 | 7.23–7.34 | $C–H_n$ bend + O–H bend | 1459–1406 | 6.86–7.22 | 9 |
| | 1210 | 8.27 | O–H bend | | 9.18 | |
| | 1040 | 9.63 | C–O str. + C–C str. | 1090 | 9.52 | |
| | 855 | 11.70 | $CH_n$ rock | 1051<br>883 | 11.34 | |
| *n*-Propanol (Matheson, Coleman and Bell) | 1520–1400 | 6.58–7.15 | O–H bend + $CH_2$, $CH_3$ bend | 1468 | 6.82 | 14 |
| | 1200 | 8.34 | | 1056 | | |
| | 1070 | 9.35 | C–O str. | 1019 | 9.49 | |
| | | | | | 9.82 | |
| | 950 | 10.52 | $CH_2$, $CH_3$ def. | 969 | 10.32 | |
| Isopropanol (Matheson, Coleman and Bell) | 1465 | 6.84 | $CH_3$ bend (asym.) | 1468 | 6.82 | 16 |
| | 1380 | 7.25 | $CH_3$ bend (sym.) | 1379 | 7.26 | |
| | 1240 | 8.07 | O–H bend | 1310 | 7.64 | |
| | 1140 | 8.78 | C–O str. | 1161 | 8.62 | |
| | 1070–1065 | 9.35–9.40 | C–O str. | 1029 | 8.86 | |
| | 955 | 10.49<br>12.82 | $CH_3$ def. (out of plane) | 950 | 10.52 | |
| | 780 | | $CH_3$ rock | | | |
| | 760 | 13.18 | $CH_2$ rock | 816 | 12.26 | |
| Propionaldehyde (Matheson, Coleman and Bell) | 1760 | 5.69 | C=O str. | 1755 | 5.70 | 24 |
| | 1415 | 7.07 | $CH_2$ bend | 1468, 1410 | 6.82, 7.10, 7.20 | |
| | 1240 | 8.07 | | | | |
| | 1100 | 9.10 | C–C str. | 1109, 1095 | 9.04, 9.14 | |
| | 1020 | 9.81 | | | | |
| | 900 | 11.11 | C(=O)–H def. ? | 860, 850 | 11.62, 11.79 | |
| | 850 | 11.79 | | | | |
| Isobutyraldehyde (Matheson, Coleman and Bell) | 1760 | 5.69 | C=O str. | 1700 | 5.88 | 22 |
| | 1480 | 6.76 | $CH_2$ str. | 1465 | 7.16 | |
| | 1390 | 7.20 | | 1385 | 7.23 | |
| | 1260 | 7.95 | | | | |
| | 1130 | 8.86 | | 1118 | 8.96 | |
| | 920 | 10.88 | C(=O)–H def. ? | 956 | 10.47 | |
| | 820 | 12.20 | $CH_2$ rock | | | |
| | 720 | 13.90 | | 770 | 13.00 | |

TABLE I (*continued*)

| *Compound* | *Principal observed bands* | | *Provisional assignment* | *I.r.*[4-6] *absorption bands* | | *Relative sensitivity* |
|---|---|---|---|---|---|---|
| | $cm^{-1}$ | $\mu m$ | | $cm^{-1}$ | $\mu m$ | |
| Methyl ethyl ketone (Matheson, Coleman and Bell) | 1740 | 5.75 | C=O str. | 1708 | 5.86 | 9 |
| | 1440 | 6.95 | $CH_3$, $CH_2$ bend | 1468–1412 | 6.82–7.08 | |
| | 1340 | 7.46 | | 1359 | 7.36 | |
| | 1170 | 8.55 | | 1168 | 8.56 | |
| | | | | 1124 | 8.90 | |
| | 940 | 10.64 | | 959 | 10.44 | |
| Methyl isopropyl ketone (Matheson, Coleman and Bell) | 1740 | 5.75 | C=O str. | 1720 | 5.82 | 12 |
| | 1530 | 6.54 | | | | |
| | 1470 | 6.81 | $CH_n$ bend | 1412 | 7.08 | |
| | 1360 | 7.36 | | 1365 | 7.34 | |
| | 1240 | 8.07 | | 1169 | 8.56 | |
| | 1190 | 8.41 | | 1097 | 9.12 | |
| | 1135 | 8.81 | | 944 | 10.60 | |
| | 950 | 10.52 | | 760 | 13.18 | |
| Formic acid (Matheson, Coleman and Bell) | 1800 | 5.56 | C=O str. | 1706 | 5.86 | 20 |
| | 1365 | 7.34 | CH bend | 1342 | 7.45 | |
| | 1240–1220 | 8.08–8.20 | O–H bend + C–O str. | 1178 | 8.50 | |
| | 1130–1080 | 8.85–9.26 | C–O str., C–C bend ? | 1062 | 9.42 | |
| | 920 | 10.88 | | | | |
| | | | O–O def. | 658 | 15.20 | |
| Ethyl acetate (J. T. Baker) | 1790–1750 | 5.59–5.72 | C=O str. | 1750 | 5.72 | 22 |
| | 1450 | 6.90 | $CH_3$, $CH_2$ bend | 1382 | 7.24 | |
| | 1270 | 7.89 | | | | |
| | 1210 | 8.28 | C–O str. | 1240 | 8.06 | |
| | 1100 | 9.10 | | 1052 | 9.50 | |
| | 1030 | 9.71 | | 941 | 10.64 | |
| | | | | 849 | 11.80 | |
| Acetonitrile (Fisher Scientific) | 1470–1460 | 6.81–6.86 | $-CH_3$ bend | 1440–1367 | 6.95–7.32 | 21 |
| | 1040 | 9.63 | | 1032 | 9.68 | |
| | 890 | 11.24 | $CH_3$ def. ? | 914 | 10.94 | |
| | | | | 748 | 13.39 | |
| Nitromethane (Matheson, Coleman and Bell) | 1595 | 6.28 | N–O str. (asym.) | 1569 | 6.38 | 16 |
| | 1390 | 7.20 | N–O str. (sym.) | 1408, 1388 | 7.12, 7.22 | |
| | 1090–1060 | 9.19–9.44 | | 1102 | 9.08 | |
| Chloroform (J. T. Baker) | 1210 | 8.27 | C–H bend | 1205 | 8.31 | 21 |
| | 745 | 10.41 | C–Cl str. | 760 | 13.18 | |
| Ethyl bromide (J. T. Baker) | 1440 | 6.95 | $CH_3$, $CH_2$ bend | 1441 | 6.94 | 17 |
| | 1270–1234 | 7.88–8.10 | C–C ? | 1247 | 8.04 | |
| | 960 | | | 967–950 | 10.34–10.54 | |
| | 730 | 13.70 | | 770 | 13.0 | |
| | | | C–Br | 500–600 | | |

(*Continued on p.* 166)

TABLE I (*continued*)

| *Compound* | *Principal observed bands* | | *Provisional assignment* | *I.r.*[4-6] *absorption bands* | | *Relative sensitivity* |
|---|---|---|---|---|---|---|
| | $cm^{-1}$ | $\mu m$ | | $cm^{-1}$ | $\mu m$ | |
| Butyl chloride | 1475–1450 | 6.79–6.90 | $CH_3$, $CH_2$ bend | 1458 | 6.86 | 15 |
| | | | | 1402 | 7.14 | |
| | 1310–1295 | 7.64–7.73 | $CH_2$ def. | 1289 | 7.76 | |
| | 1240 | 8.07 | | 1235 | 8.10 | |
| | 1100 | 9.10 | | 1053 | 9.50 | |
| | 1060 | 9.45 | | 1008 | 9.94 | |
| | | | | 926 | 10.80 | |
| | 1000 | 10.00 | | 873 | 11.48 | |
| | 735 | 13.61 | C–Cl str. | 746 | 13.40 | |
| Tetraethyllead | 1475 | 6.79 | $CH_n$ bend | 1459 | 6.86 | 18 |
| (Ethyl Corporation) | 1350 | 7.41 | | | 8.18 | |
| | 1300 | 7.70 | C–C str. | 1224 | 8.68 | |
| | 1075–1040 | 9.30–9.62 | | 1152 | | |
| | | | | 1018 | 9.84 | |
| | | | | 962 | 10.40 | |
| | 980 | 10.20 | | 934 | 10.72 | |
| | ~670 | 14.92 | | | | |
| Carbon disulfide | 1487 | 6.74 | C=S str. (asym.) | 1523 | 6.56 | |
| (Fisher Scientific) | | | | | | |
| Ammonia | 1720 | 5.82 | N–H bend | | | 6 |
| (Matheson Co., C.P.) | 1627 | 6.15 | N–H bend | 1627.5 | 6.15 | |
| | 1530 | 6.54 | N–H bend | | | |
| | 1140 | 8.78 | | 968 | 10.34 | |
| | 1085 | 9.23 | N–H def. | 931 | 10.74 | |
| | 800 | 1250 | | | | |
| Nitrous oxide | 1255 | 7.97 | N=O str. | 1300, 1279 | 7.70, 7.84 | 24 |
| (Matheson Co., C.P.) | | | | | | |
| Nitric oxide | 1850–1830 | 5.41–5.47 | N=O str. | 1907, 1836 | 5.25, 5.45 | 25 |
| (Matheson Co., C.P.) | 1300 | 7.70 | ? | | | |
| Nitrogen dioxide | 1800 | 5.56 | | 1780 | 5.75 | 24 |
| (Matheson Co., C.P.) | 1590 | 6.30 | N=O str. (asym.) | 1600 | 6.25 | |
| | 1270–1240 | 7.88–8.07 | N=O str. (sym.) | 1259 | 7.95 | |
| Sulfur dioxide | 1310 | 7.64 | S=O str. (asym.) | 1380–1352 | 7.25–7.4 | 6 |
| (Union Carbide | 1120 | 8.94 | S=O str. (sym.) | 1170–1138 | 8.55–8.8 | |
| Corp.) | | | | | | |

in Table I and are shown in Figs. 3–37. Comparison with the infrared absorption spectra shows that the major peaks in the emission spectra occur at similar frequencies. It was, therefore, assumed that the emission peaks could be assigned to the same molecular vibration transitions as those associated with infrared absorption bands. These assignments are given, where possible.

The relative sensitivity refers to the instrumental conditions used. Attenuation on the IR-10 was achieved by use of the SB 100% control. It should be borne in mind that these sensitivity readings reflect the concentration of a particular compound in the

cell (*i.e.* its vapor pressure), as well as the efficiency of interaction with the laser beam and subsequent emission.

Some of the spectra, notably those of compounds containing carbonyl groups (Figs. 21–26), were recorded at high gain settings so as to improve instrumental response. The signals in these spectra, therefore, contain appreciable electronic noise.

At maximum sensitivity in single beam mode, the spectrometer background was extremely nonlinear (Fig. 2A). It was possible to flatten out this profile somewhat at lower sensitivities. In the present work a useable background was achieved by adjustment of the Balance Control. Figure 2B shows a typical background, with the Balance Control settings used for the various spectral regions.

## DISCUSSION

The results described above extend the work already reported for alkanes and

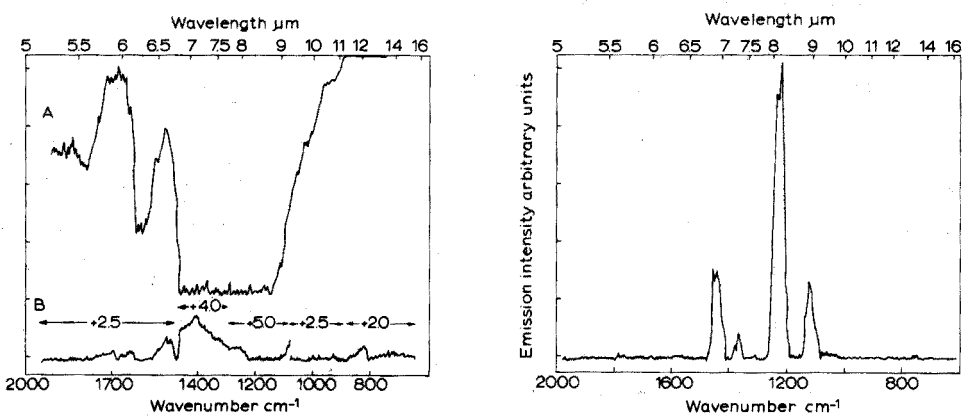


Fig. 2. Background signals for IR-10 spectrometer, no sample present. (A) Slit fully open, SB 100% 10.00, balance +2.5, gain 6; (B) slit fully open, SB 100% 9.96, balance as indicated, gain 5.

Fig. 3. Infrared emission spectrum for cyclohexane.

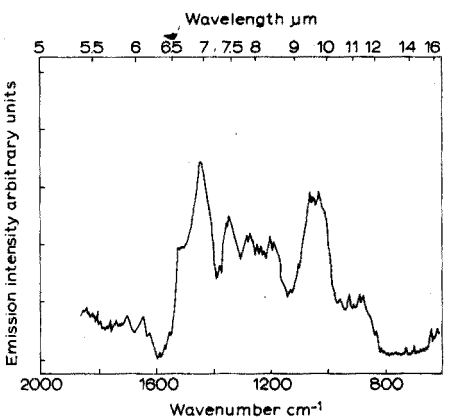


Fig. 4. Infrared emission spectrum for cyclopentene.

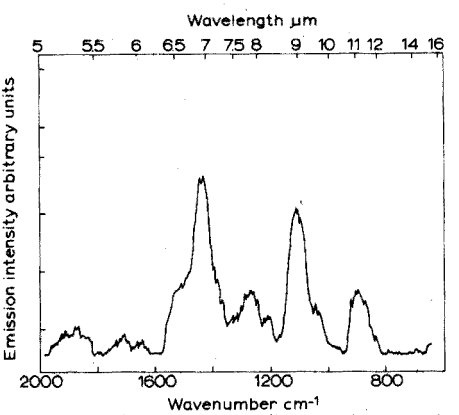


Fig. 5. Infrared emission spectrum for cyclohexene.

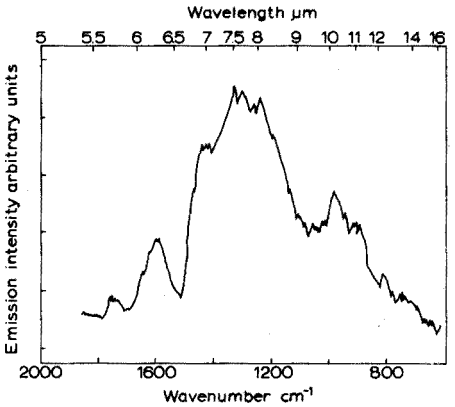


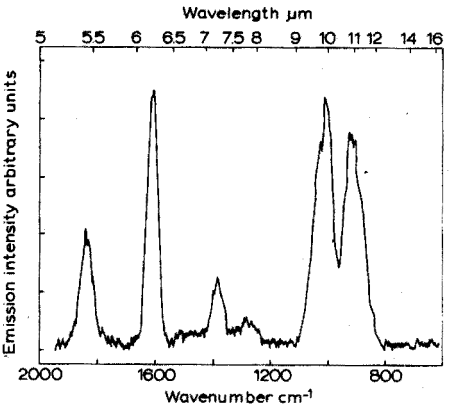


Fig. 6. Infrared emission spectrum for 1-octene.
Fig. 7. Infrared emission spectrum for 1,3-butadiene.

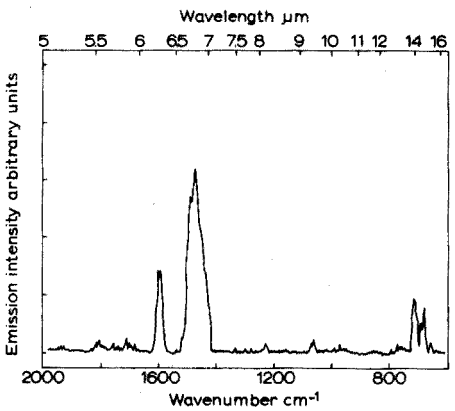


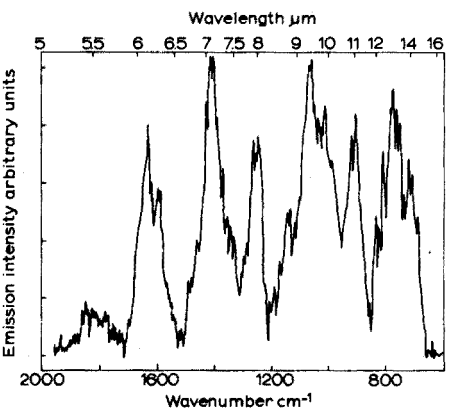


Fig. 8. Infrared emission spectrum for toluene.
Fig. 9. Infrared emission spectrum for thiophene.

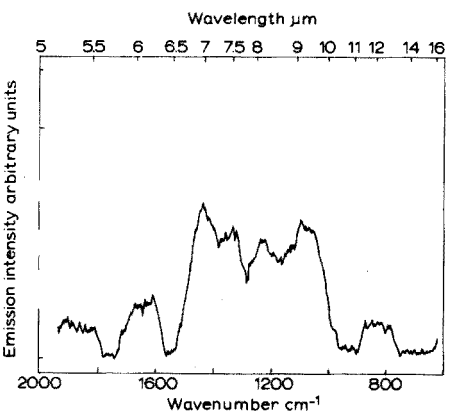


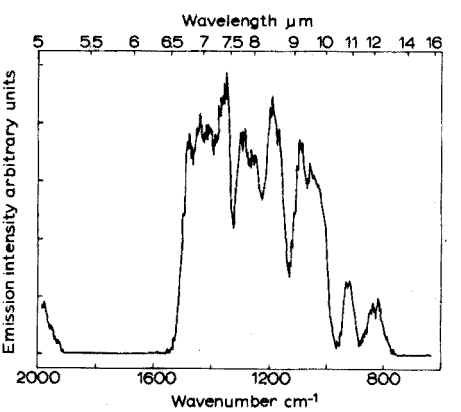


Fig. 10. Infrared emission spectrum for pyridine.
Fig. 11. Infrared emission spectrum for ethyl ether.

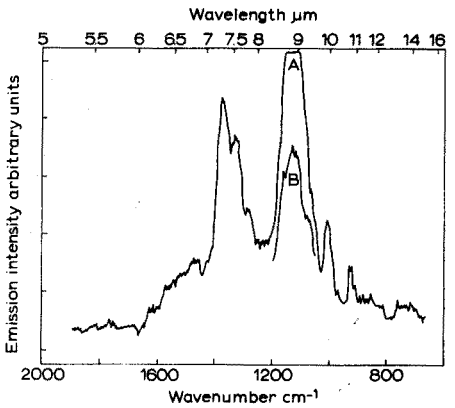


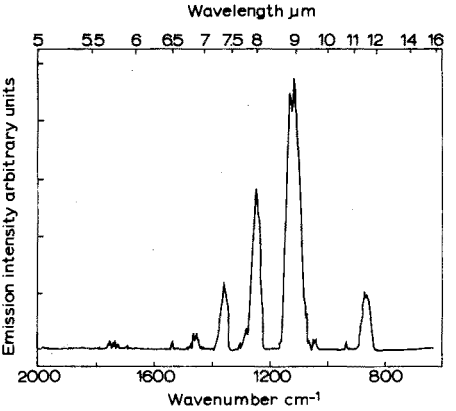


Fig. 12. Infrared emission spectrum for isopropyl ether.
Fig. 13. Infrared emission spectrum for dioxane.

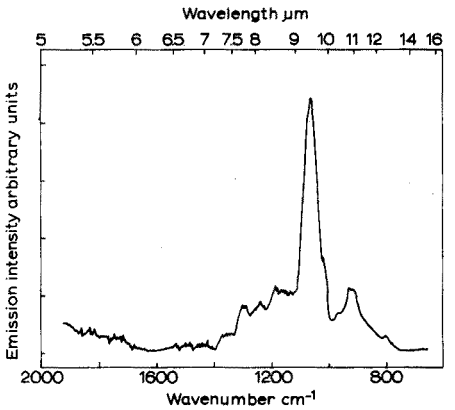


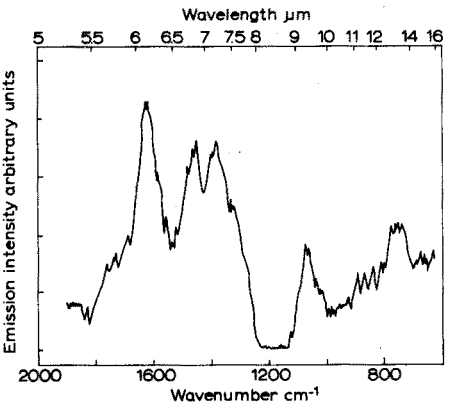


Fig. 14. Infrared emission spectrum for tetrahydrofuran.
Fig. 15. Infrared emission spectrum for propylamine.

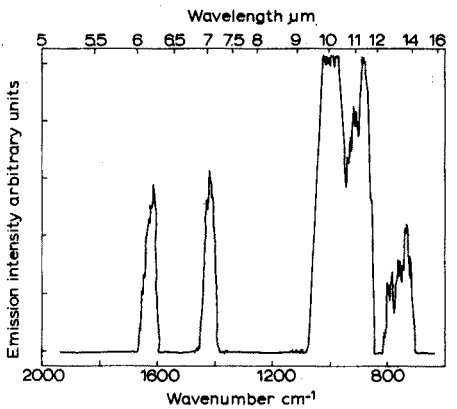


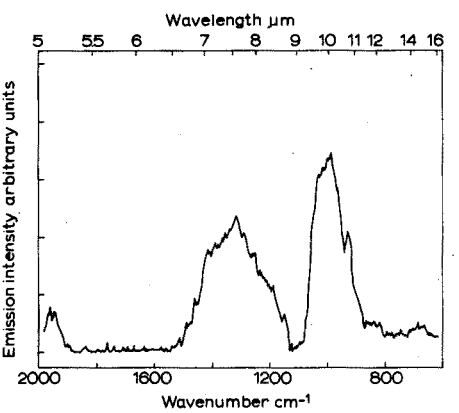


Fig. 16. Infrared emission spectrum for allylamine.
Fig. 17. Infrared emission spectrum for methanol.

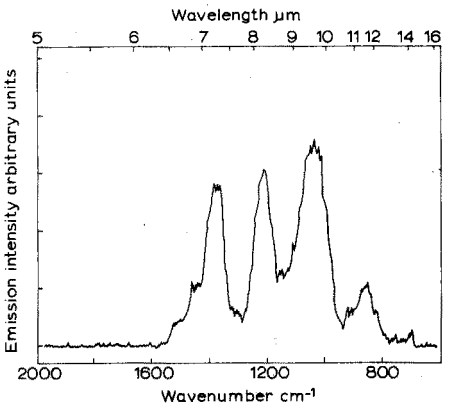


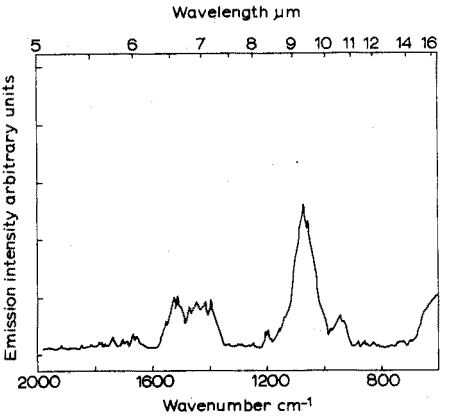


Fig. 18. Infrared emission spectrum for ethanol.
Fig. 19. Infrared emission spectrum for 1-propanol.

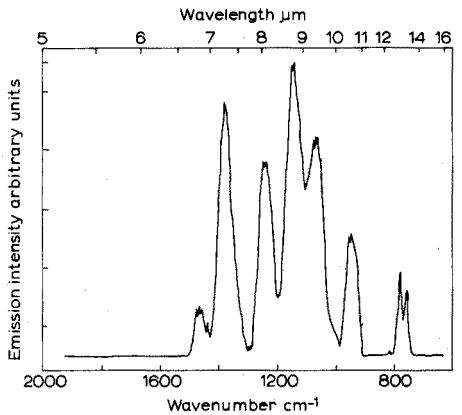


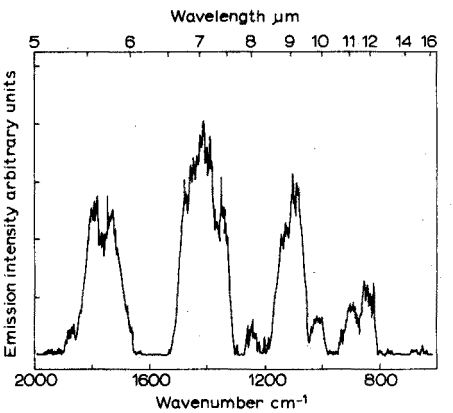


Fig. 20. Infrared emission spectrum for 2-propanol.
Fig. 21. Infrared emission spectrum for propionaldehyde.

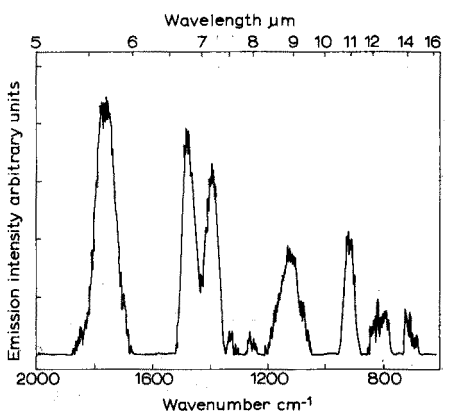


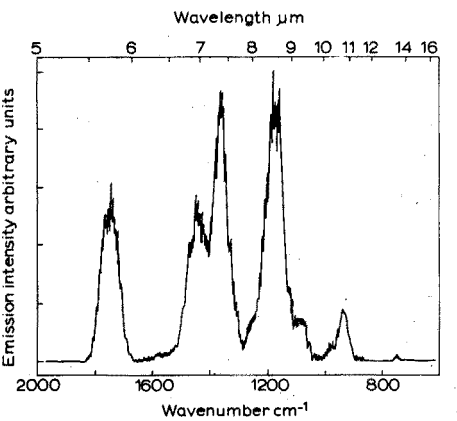


Fig. 22. Infrared emission spectrum for isobutyraldehyde.
Fig. 23. Infrared emission spectrum for methyl ethyl ketone.

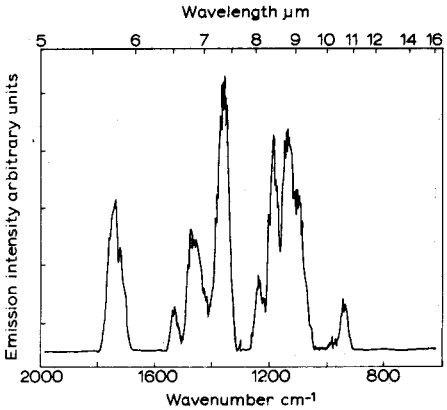


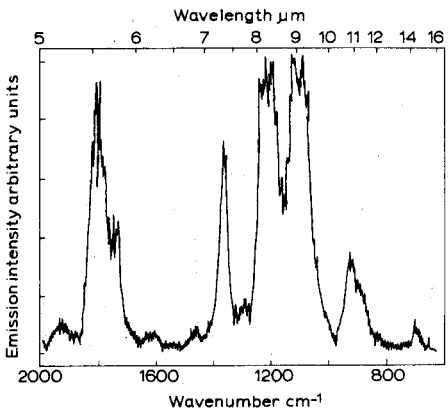


Fig. 24. Infrared emission spectrum for methyl isopropyl ketone.
Fig. 25. Infrared emission spectrum for formic acid.

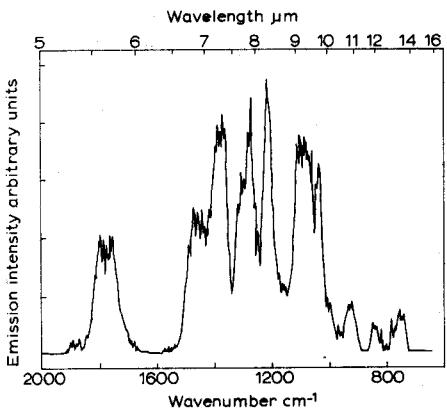


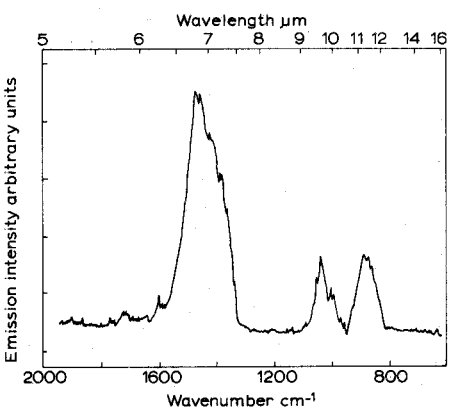


Fig. 26. Infrared emission spectrum for ethyl acetate.
Fig. 27. Infrared emission spectrum for acetonitrile.

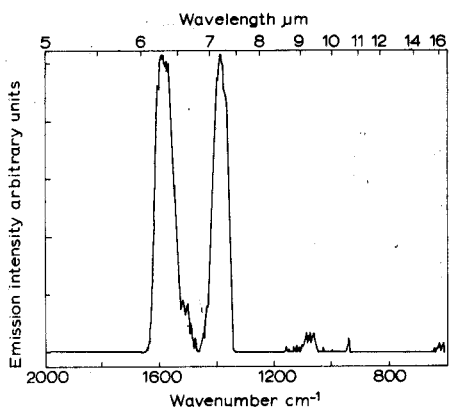


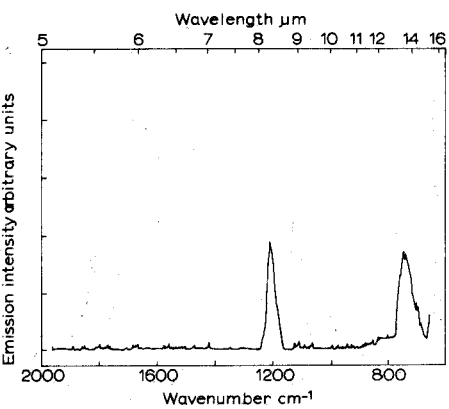


Fig. 28. Infrared emission spectrum for nitromethane.
Fig. 29. Infrared emission spectrum for chloroform.

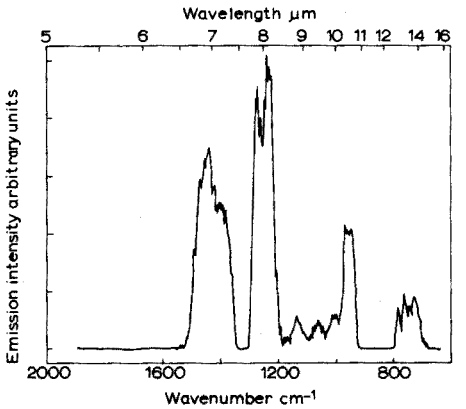


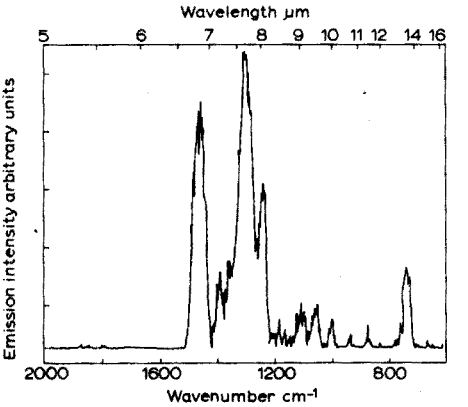


Fig. 30. Infrared emission spectrum for ethyl bromide.
Fig. 31. Infrared emission spectrum for butyl chloride.

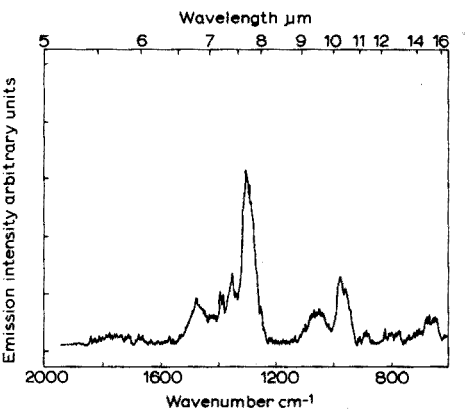


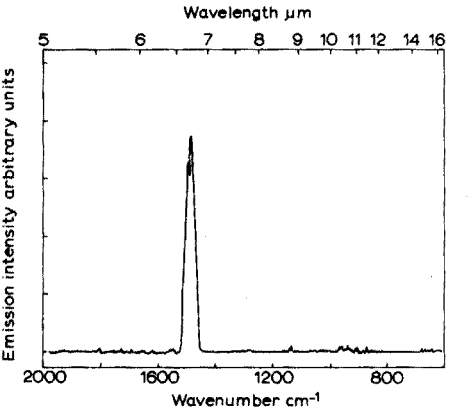


Fig. 32. Infrared emission spectrum for tetraethyllead.
Fig. 33. Infrared emission spectrum for carbon disulfide.

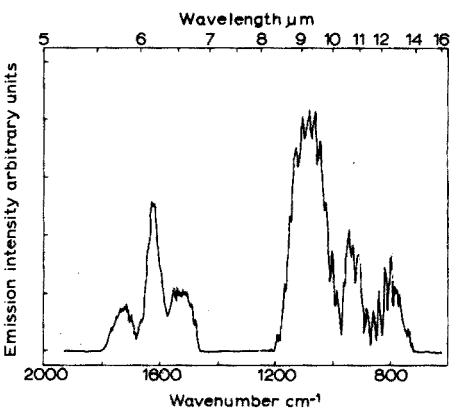


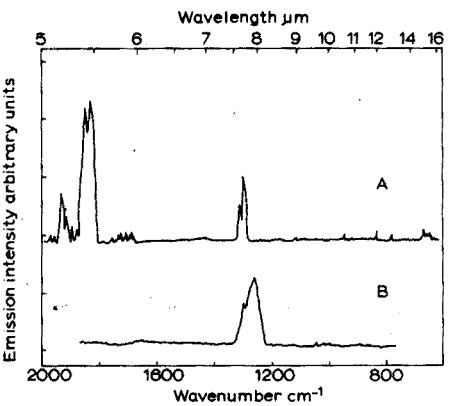


Fig. 34. Infrared emission spectrum for ammonia.
Fig. 35. Infrared emission spectra for (A) nitrous oxide, (B) nitric oxide.

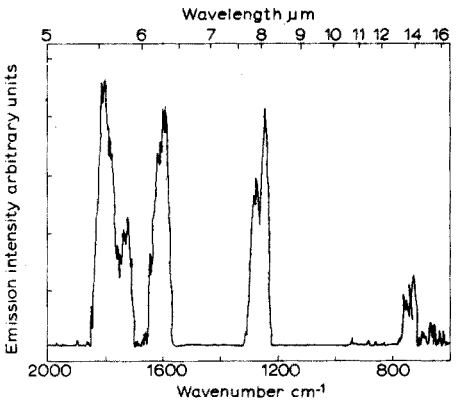


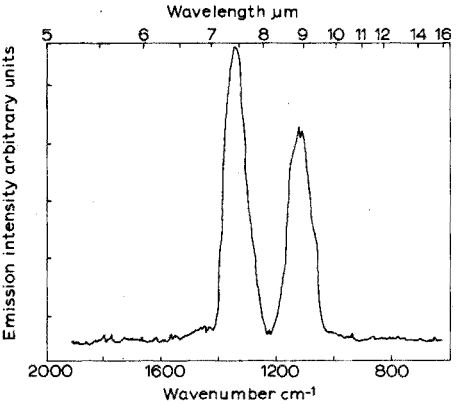


Fig. 36. Infrared emission spectrum for nitrogen dioxide.
Fig. 37. Infrared emission spectrum for sulfur dioxide.

other compounds[2,3], showing that laser-stimulated emission spectra are obtainable from a variety of compounds and bond vibrations. As an analytical technique, therefore, laser-stimulated infrared emission should have wide applicability.

Throughout this work the IR-10 spectrometer was operated with its slits wide open, in order to attain maximal sensitivity. The resulting loss of resolution and slit control programming restrict the depth of interpretation of the spectra beyond the correlations with infrared absorption spectra given above. Nevertheless, certain features of the emission spectra seem worthy of comment.

In several cases (*e.g.* Figs. 28, 29, 33, 35, 37) infrared emission was obtained even when the compound in question absorbed only very weakly, or not at all, at 10.6 μm. Those compounds which did absorb the laser radiation, as expected, gave rise to more intense radiation.

In many of the compounds studied, the observed bands occurred at higher or lower frequencies than the corresponding infrared absorption peaks. These differences (see Table I) were typically of the order of 20–30 $cm^{-1}$. This difference was evidently not totally a result of instrumental deficiencies, as calibration of the spectrometer (polystyrene film) gave maximum discrepancies of only about 10 $cm^{-1}$ (Table II). It seems possible that this shift to different frequencies is a result of fluorescence. It is hoped to further investigate these shifts, using an infrared spectrometer with greatly improved resolution.

Because of the use of an unprogrammed slit, the relative intensities of the emission peaks to each other do not always correspond to intensities in the absorption

TABLE II

CALIBRATION OF IR-10 SPECTROMETER WITH POLYSTYRENE FILM

| *Observed frequency* ($cm^{-1}$) | *True frequency* ($cm^{-1}$) |
|---|---|
| 1601 | 1601.8 |
| 1146 | 1154.6 |
| 1019 | 1028.3 |
| 898 | 906.9 |

spectra. In some cases, however, there are discrepancies in the relative intensities of emission peaks compared to absorption bands which would seem to be greater than expected if caused only by instrumental performance. For example, in Fig. 12, the isopropylether spectrum has a very strong band at 1130 $cm^{-1}$ (8.85 $\mu$m), compared to the 1325 $cm^{-1}$ (7.25 $\mu$m) signal. In the infrared absorption spectrum these peaks are of comparable intensity.

In contrast to earlier results[2], it was not possible in this work to confirm the observation of emission signals in the region 4000–2000 $cm^{-1}$ (3–5 $\mu$m). Strong emission at about 1740 $cm^{-1}$ (5.8 $\mu$m), corresponding to the carbonyl-stretching vibration, was obtained for a number of compounds. No signal was observed for the O–H, NH, and C–H stretching vibrations (3600–2800 $cm^{-1}$, 2.5–3.5 $\mu$m), or for the C=N stretching in acetonitrile (2200 $cm^{-1}$, 4.5 $\mu$m). It appears that these transitions, which must arise from four photon processes, are less probable than was first supposed, and that greater instrumental sensitivity will be required to detect them reproducibly. The excitation of carbonyl bands at 1740 $cm^{-1}$ (5.8 $\mu$m) may be explained by the interaction of three photons or excitons. These unexpected data are being closely examined and excitation mechanism studies are underway.

This investigation was supported by Research Grant AP-01286-01, Air Pollution Control Office, Environmental Protection Agency.

SUMMARY

A catalog has been compiled of laser-stimulated infrared emission spectra from 36 compounds. The spectra are correlated with the appropriate bond vibrations, and other features are discussed. The variety of compounds detected is an indication of the wide applicability of this technique to analytical problems.

RÉSUMÉ

Les auteurs présentent une série de spectres d'émission infra-rouge-laser pour 36 composés. On examine les relations avec les vibrations de liaisons et autres facteurs. La grande variété des composés décelés est une preuve de la large applicabilité de cette technique aux problèmes analytiques.

ZUSAMMENFASSUNG

Es wurde ein Katalog laserangeregter Infrarot-Emissionsspektren von 36 Verbindungen zusammengestellt. Die Spektren werden den zugehörigen Bindungsschwingungen zugeordnet und andere charakteristische Merkmale diskutiert. Die Vielfalt der nachgewiesenen Verbindungen ist ein Hinweis auf die breite Anwendbarkeit dieses Verfahrens auf analytische Probleme.

REFERENCES

1 J. W. Robinson, H. M. Barnes and C. Woodward, *Spectrosc. Lett.*, 1 (1968) 109.
2 J. W. Robinson, C. Woodward and H. M. Barnes, *Anal. Chim. Acta*, 43 (1968) 119.
3 J. W. Robinson, D. M. Hailey and H. M. Barnes, *Talanta*, 16 (1969) 1109.
4 R. H. Pierson, A. N. Fletcher and E. St. C. Gantz, *Anal. Chem.*, 28 (1956) 1218.
5 *Sadtler Catalog of Standard Spectra*, S. P. Sadtler and Son, Inc., Philadelphia, Pa.
6 G. Herzberg, *Infrared and Raman Spectra of Polyatomic Molecules*, Van Nostrand Co., Inc., 1945.

*Analytica Chimica Acta*
Elsevier Publishing Company, Amsterdam
Printed in The Netherlands



# INFRARED FLUORESCENCE SPECTROSCOPY AS AN ANALYTICAL METHOD; QUANTITATIVE STUDIES WITH A LONG PATHLENGTH CELL

D. M. HAILEY*, H. M. BARNES** AND J. W. ROBINSON
*Department of Chemistry, Louisiana State University, Baton Rouge, La. 70803 (U.S.A.)*
(Received 7th May 1971)

In preliminary work with laser-induced infrared emission of organic molecules[1,2] it was shown that the phenomenon applied to a variety of compounds. A catalog of emission spectra has been compiled[3], and illustrates the range of compounds to which this method is applicable. It was shown that the emission intensity was proportional to sample concentration, and sensitivity levels were calculated for hydrocarbons and certain other compounds[2].

From this earlier work, it appeared that infrared fluorescence spectroscopy should provide the basis of a sensitive analytical method. This paper presents quantitative data for several compounds, obtained with a long pathlength (1 m) cell, the use of which has been reported elsewhere[4]. The phenomenon of self-absorption is also considered, and its use as an aid to infrared absorption spectroscopy described.

## EXPERIMENTAL

### *Equipment*

A Perkin-Elmer Model 6200, $CO_2$ gas laser, and a Beckman IR-10 Spectrometer, modified and operated as described previously[1-3], were used.

The sample cell used has been briefly described in a previous communication[4]. It was made from 110-mm, Corning 3340 pyrex tubing, and was 107.5 cm in length. The cell is illustrated in Fig. 1. One end was demountable, having a 103/60 joint, which allowed access to the optical arrangement. The front surfaced concave mirror was mounted on an adjustable brass rod, which was supported by a bored Teflon stopper, fitting into a 24/40 joint at the top of the cell. Two entrance ports were provided for introduction and removal of sample.

Irtran II windows were used, as before, to permit passage of the laser beam. The operating range was therefore restricted to 2–16 $\mu$m. The windows were attached to the cell by mounting in metal camera lens holders which were fastened externally to the cell with adhesive tape. The Irtran windows were held in position in the lens holders by spring clips. This method of mounting eliminated the need for epoxy resin, which

* Present address: Roche Research Unit, Biochemistry Department, Liverpool University, Liverpool L693BX, England.
** Present address: Department of Health, Education, and Welfare, Public Health Service, National Center for Air Pollution Control, Cincinnati, Ohio 45227, U.S.A.

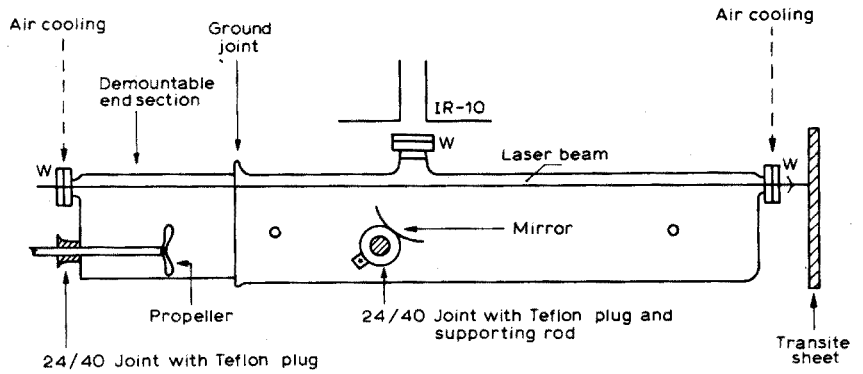


Fig. 1. Long pathlength cell in operational configuration (top view).

was previously used. Use of epoxy resin had two disadvantages. Any slight misalignment of the laser beam resulted in decomposition and introduction of resin pyrolysis products into the cell. Also, removal of the windows required pyrolysis of the resin. In the process the windows invariably became coated with carbonaceous deposits which were difficult to remove.

A problem associated with the operation of the long cell was the dispersion of small gas samples into the cell, the volume of which was almost 10 l. Diffusion-controlled dispersion of the sample throughout the cell took several hours. The detachable front of the cell was therefore adapted to take a 24/40 ground joint. This was filled with a bored Teflon plug through which passed a steel shaft and propeller. The shaft was driven by a cone-type stirrer motor, which was offset from the shaft axis, and could be operated while the laser was on.

This provided more rapid dispersion of the sample throughout the cell, but introduced problems of vibration and sample leakage round the shaft. A more satisfactory solution was to use a magnetic stirrer to drive a paddle mounted on a magnet, positioned about half way down the cell, forward of the mirror. This provided adequate sample dispersion without the problems encountered with the motor-driven propeller.

*Operation of the long pathlength cell*

The mirror was aligned in the cell so that it viewed a pathlength of about 30 cm in front of the IR-10 entrance slit. This was found to give the optimum response. Increasing the viewed pathlength beyond about 45 cm introduced a highly intense background, thought to result from stray radiation from the end window and the glass immediately surrounding it.

The S.B. 100% control on the IR-10 was used for attenuation during the quantitative work. This was not entirely satisfactory, as the instrument response was non-linear, and required careful calibration. The Balance control was used to set the background at a suitable level. The instrument took several minutes to equilibrate after use of this control. As the Balance usually had to be adjusted after each alteration in the S.B. setting, collection of data was rather slow. The IR-10 was normally operated with its slits fully open, and a Gain setting of at least 5.

Quantitative data for liquid samples were obtained by inserting the required

volume of liquid into the cell with a Hamilton syringe or pipette, dispersing with the stirrer, and then scanning the selected analytical peak until the sample was completely dispersed and a constant signal attained. In the case of gas samples, sensitivity data were obtained by diluting the gases with nitrogen, and flowing them through the cell. The flow rates were monitored with rotameters (Brookes Instrument Co.).

## RESULTS

### *Quantitative data for liquid samples*

Plots of emission intensity *vs.* sample size were made for acetone, chloroform, ether, and *n*-propylamine, and are shown in Figs. 2–5. Estimated detection limits are listed in Table I.

TABLE I

QUANTITATIVE DATA FOR LIQUID SAMPLES IN THE LONG PATHLENGTH CELL

| *Compound* | *Line (μm)* | *Band* | *Sample concentration range ($\mu g\ l^{-1}$)* | *Minimum quantity of compound detected*[a] | | *Minimum concentration of compound detected ($\mu g\ l^{-1}$)* |
|---|---|---|---|---|---|---|
| | | | | *μg* | *μmoles* | |
| Acetone | 5.8 | C=O str. | 8–158 | 0.25 | $4.0 \cdot 10^{-3}$ | 10.0 |
| | 8.5 | C–C str. | 8–236 | 0.06 | $1.0 \cdot 10^{-3}$ | 2.3 |
| Chloroform | 13.4 | C–Cl str. | 15–145 | 0.13 | $2.7 \cdot 10^{-3}$ | 10.0 |
| Ether | 9.0 | C–O str. | 7–213 | 0.03 | $3.8 \cdot 10^{-4}$ | 1.1 |
| *n*-Propylamine | 6.0 | N–H | 22–287 | 0.70 | $1.1 \cdot 10^{-2}$ | 45 |

[a] Minimum quantity of compound detected is calculated from that volume occupied by the laser beam which is viewed by the mirror, assuming a pathlength of 30 cm.

*Actone* (8.5-*μm line, C–C stretch*). A linear plot was obtained (Fig. 2) up to a sample concentration of about 95 $\mu g\ l^{-1}$. At larger sample sizes the curve began to flatten out. The points for these higher concentrations were badly scattered, partly because of the limitations of the method for evaporation and dispersion of such large sample sizes.

For the 5.8-μm line (C=O stretch), a linear plot was obtained up to a sample concentration of 157 $\mu g\ l^{-1}$. Data for this line were difficult to gather because of the presence of a spurious signal in the IR-10 background at about 5.6 μm.

*Chloroform* (13.4-*um line, C–Cl stretch*). A linear plot was obtained up to a sample concentration of 120 $\mu g\ l^{-1}$ (Fig. 3).

n-*Propylamine* (6.1-*μm line, N–H stretch*). With this compound, the emission signal decreased very rapidly after evaporation, and it seemed possible that the amine was undergoing a reaction of some sort, either in the laser beam or on the cell walls. A linear relationship between fluorescence intensity and concentration was obtained (Fig. 4) provided that the intensity values obtained just after evaporation of the

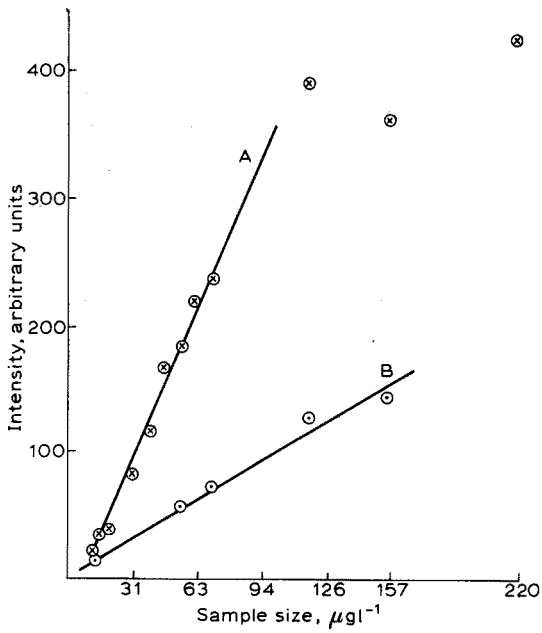


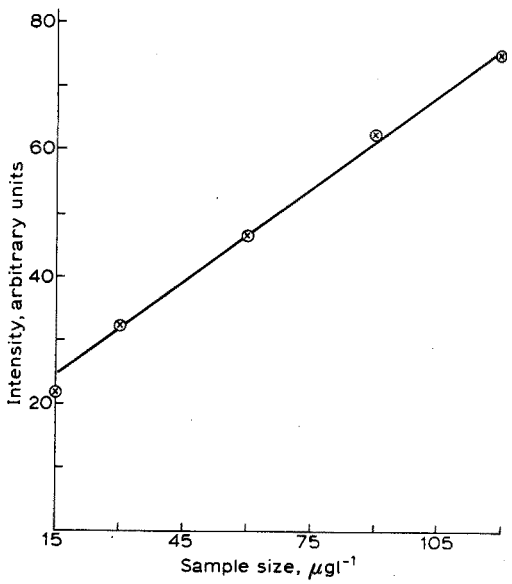


Fig. 2. Intensity–concentration graphs for acetone. (A) 8.5-μm line (C–C stretch); (B) 5.8-μm line (C=O stretch).

Fig. 3. Intensity–concentration graph for chloroform, 13.6-μm line (C–Cl stretch).

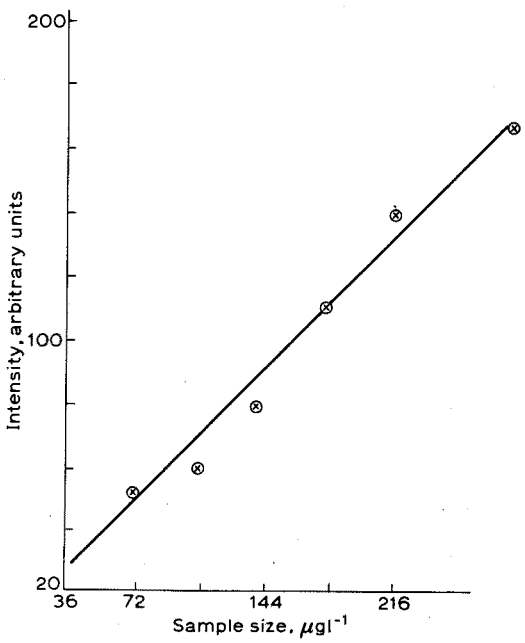


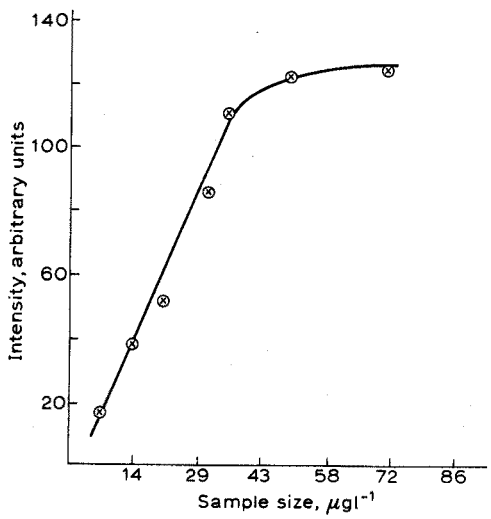


Fig. 4. Intensity–concentration graph for *n*-propylamine, 6.1-μm line (N–H band).

Fig. 5. Intensity–concentration graph for ethyl ether, 9.0-μm line (C–O stretch).

sample were used. As with the 5.8-$\mu$m acetone peak, the varying IR-10 background hindered the measurement of the radiation at 6.1 $\mu$m.

*Diethyl ether* (9.0-$\mu$m *line, C–O stretch*). A linear relationship was obtained up to a sample concentration of about 36 $\mu g\ l^{-1}$, after which the response curve rapidly flattened out (Fig. 5).

*Quantitative data for gas samples*

The results obtained for the gas samples confirmed the trend shown in the work done previously using a short cell[2]. Sensitivity increased in the order methane < ethane < propane < ethylene. The sensitivity towards ethylene was comparable to that for acetone and other polar compounds.

It was noted, with methane as a sample, that the emission intensity did not vary with flow rate. This indicated that the contribution to the signal by indirect heating was negligible. The decreased responses for the hydrocarbons, compared with those found in earlier work[2], also reflect the absence of indirect heating effects. The infrared emission observed in the long cell work therefore originated predominantly from the interaction of the laser beam with the sample rather than thermal excitation.

Sensitivity data were obtained for methane, ethane, propane, ethylene, and sulphur dioxide. The results are given in Table II.

TABLE II

SENSITIVITY DATA FOR GAS SAMPLES

| *Compound* | *Line* ($\mu$m) | *% Sample in nitrogen (vol/vol)* | *Detection limit, minimum quantity of compound detected (30 cm pathlength)* | |
|---|---|---|---|---|
| | | | $\mu g$ | $\mu$moles |
| Methane | 8.0 | 83.5 | 367 | 23 |
| Ethane | 6.9 | 16.7 | 192 | 6.4 |
| Propane | 6.8 | 16.7 | 93 | 2.1 |
| Ethylene | 10.5 | 8.0 | 0.75 | 0.027 |
| Sulphur dioxide | 9.0 | 2.7 | 30 | 0.47 |

DISCUSSION

The results given above show that infrared fluorescence spectroscopy has a good potential as an analytical method for the determination of gas and vapor samples. Greatest sensitivity is exhibited by those compounds with an absorption band in the region of the laser beam wavelength (10.6 $\mu$m).

The long pathlength cell has been shown to be of use in eliminating contributions to infrared emission caused by indirect heating, and in providing more efficient collection of the emitted radiation. While this cell is a definite improvement on the earlier design, it suffers from a number of shortcomings.

1. Even with the mirror aligned and focussed correctly, in the present system only a small solid angle is viewed by the mirror, so that the system collects only a small fraction of the emitted radiation. More efficient collection of the radiation is

obviously required, and should produce a great increase in sensitivity.

2. In our present system the mirror could not be used to view the entire pathlength of laser beam, because with this alignment it would also gather infrared emission originating at the end Irtran window and the surrounding glass.

3. There was considerable dead space in the cell, made up by the section to the rear of the mirror, and the other end of the cell, which was outside the view of the mirror.

It is intended to greatly reduce or eliminate all these deficiencies in future cell designs.

## SELF-ABSORPTION STUDIES

### *Self-absorption in the long pathlength cell*

Spectra obtained by stimulated emission correspond closely to the corresponding infrared absorption spectra[2,4]. In the course of this work several emission lines were observed which appeared not to correlate with absorption lines. During later studies, it was found that at high concentrations the fluorescence bands broadened, and that the center of the band was reabsorbed by non-excited molecules present. The resultant spectra appeared as two separated peaks, which were the wings of the original band. In the emission spectrum of acetone, for example (Fig. 6), there are apparently two anomalous peaks at 9.6 $\mu$m and 5.9 $\mu$m. The 5.9-$\mu$m radiation is in fact caused by line reversal in the emission associated with the 5.8-$\mu$m C=O stretching frequency.

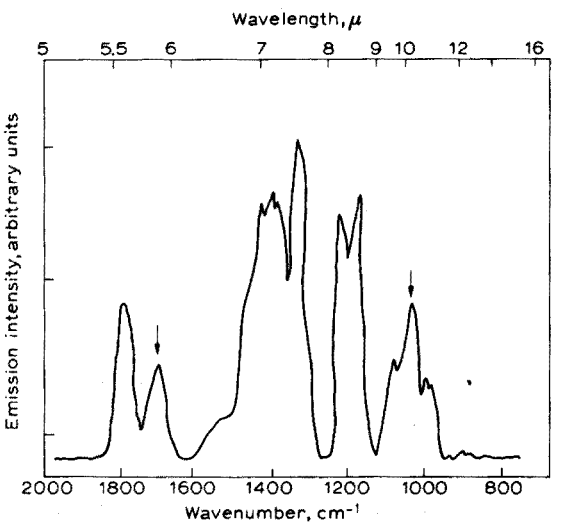


Fig. 6. Emission spectrum of acetone showing anomalous peaks.

At low acetone concentrations a single peak was obtained at 5.8 $\mu$m (Fig. 7). As the concentration of acetone vapor in the cell increased, the top of the peak broadened, and then split into two sections. Reducing the concentration once again caused coalescence into the 5.8-$\mu$m signal. This clearly indicated self-reversal, and showed that

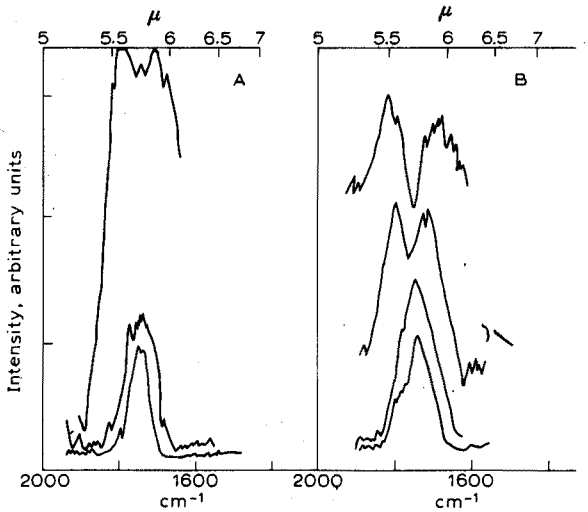


Fig. 7. Effect of self-reversal on the 5.8-$\mu$m line (C=O stretch) of acetone. (A) acetone concentration increasing from bottom to top; (B) acetone concentration decreasing from top to bottom.

the anomalous emission line was one of the unabsorbed portions of the original line.

(The signal at 9.6 $\mu$m may have been caused by a reflection of the incident laser beam inside the cell.)

Self-absorption is also indicated by the shapes of the intensity–concentration graphs for ether and acetone (Figs. 2 and 5), in which the slopes of the corners begin to level off at higher concentrations. Self-reversal of the C–O (9.0 $\mu$m) line for ether was observed at a sample size of 143 $\mu g\ l^{-1}$.

*Self-absorption as an aid to infrared absorption analysis*

In normal infrared absorption studies, the radiation source is usually a Nernst

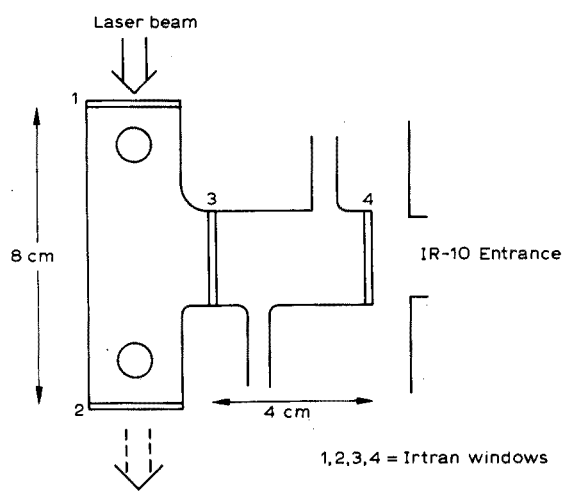


Fig. 8. Double cell used for self-absorption work.

glower or a globar. The radiation is continuous over a wide wavelength range. If molecular infrared fluorescence is used as a source, the radiation appears to be continuous (within an emission band) but is actually made up of numerous lines. A molecule of the same species as that used in the source should absorb at the same narrow lines. The absorption coefficient may be increased by the matching of the fine structure in the source radiation and the absorbing molecules. Significant increases may be useful analytically.

The cell shown in Fig. 8 was used to study this effect. The sample to be irradiated by the laser was placed in section A, and the stimulated emission then passed through section B on the way to the spectrometer monochromator. Acetone, ethanol, and propane were selected as suitable compounds for investigation, because of the number of absorption and emission bands in their infrared spectra.

*Experimental procedure*

After measurement of the background emission level, with air or nitrogen in sections A and B, the sample was introduced into A, and the emission intensity at a fixed wavelength was measured. The instability and fluctuations of the recorded intensity made it necessary to measure the average emission over a period of several minutes to obtain a reasonably reliable value. Section B was then filled with sample, and the resulting reduced emission intensity measured as before. This reduction in intensity could be attributed to absorption of the emission from A by the 4-cm sample pathlength in B. From this it was possible to calculate a value for the absorbance under these conditions.

The results obtained were compared with values of the absorbance measured with the IR-10 nichrome wire glower as a source. The sample was contained in section B, section A being removed, and emission intensities were recorded with the IR-10 in single beam mode.

*Results*

The results of these experiments are summarized in Table III. In all instances,

TABLE III

RESULTS FOR INFRARED ABSORPTION WITH THE TWIN CELL

| *Sample* | *Wavelength* ($\mu m$) | *Absorbance* | |
|---|---|---|---|
| | | *Sample emission as source* | *Continuous source* |
| Acetone | 5.6 | 0.85 | 0.66 |
| | 7.2 | >3 | >3 |
| Ethanol | 7.1 | 0.61 | 0.14 |
| | 7.3 | 0.46 | 0.08 |
| | 8.0 | 0.53 | 0.12 |
| | 8.3 | 0.22 | 0.04 |
| | 9.5 | 0.62 | 0.54 |
| Propane | 7.3 | 0.68 | 0.64 |
| | 8.5 | 0.38 | 0.17 |
| | 8.7 | 0.22 | 0.13 |

the absorbance value was higher when the sample emission was used as a source. This trend is thought to be significant, and indicates a possible means of increasing sensitivity in infrared absorption measurements. The observed increases were small in comparison with those effected with a hollow-cathode source in ultraviolet spectroscopy. However, in the infrared region, where absorbances may be 0.1 or lower, an increase to 0.5 could have practical significance.

This investigation was supported by Research Grant AP-01286-01, Air Pollution Control Office, Environmental Protection Agency.

SUMMARY

Quantitative data are presented for a number of organic compounds, a long pathlength cell being used to measure their laser-induced infrared emission. Self-reversal of emission lines is discussed, and the use of this process as an aid to infrared absorption spectroscopy is described.

RÉSUMÉ

Une étude est effectuée sur les possibilités de la spectroscopie de fluorescence infra-rouge comme méthode d'analyse, pour un certain nombre de composés organiques.

ZUSAMMENFASSUNG

Es werden Zahlenwerte für eine Anzahl organischer Verbindungen vorgelegt, deren laserinduzierte Infrarotemission unter Verwendung einer Küvette mit langem Lichtweg gemessen worden ist. Die Selbstumkehr von Emissionslinien wird diskutiert und die Anwendung dieses Effektes als Hilfsmittel für die Infrarotabsorptionsspektroskopie beschrieben.

REFERENCES

1 J. W. Robinson, H. M. Barnes and C. Woodward, *Spectrosc. Lett.*, 3 (1968) 109.
2 J. W. Robinson, C. Woodward and H. M. Barnes, *Anal. Chim. Acta*, 43 (1968) 119.
3 D. M. Hailey, C. Woodward, H. M. Barnes and J. W. Robinson, *Anal. Chim. Acta*, 56 (1971) 161.
4 J. W. Robinson, D. M. Hailey and H. M. Barnes, *Talanta*, 16 (1969) 1109.

*Analytica Chimica Acta*
Elsevier Publishing Company, Amsterdam
Printed in The Netherlands



# CHELATE VON β-DICARBONYLVERBINDUNGEN UND IHREN DERIVATEN

## TEIL XXI.[1] DIE VERWENDUNG VON THIODIBENZOYLMETHAN ZUR EXTRAKTIONS-PHOTOMETRISCHEN BESTIMMUNG VON KUPFERSPUREN

E. UHLEMANN, B. SCHUKNECHT, K. D. BUSSE UND V. POHL
*Sektion Chemie/Biologie, Pädagogische Hochschule Potsdam, Potsdam-Sanssouci (Deutsche Demokratische Republik)*

(Eingegangen den 15. April 1971)

Aus der Reihe der Thio-β-diketone sind bisher Thiodibenzoylmethan (I)[2-4] und Thiothenoyltrifluoraceton (II)[5-8] als Reagentien zur extraktionsphotometrischen Metallbestimmung vorgeschlagen worden. Von Ihnen besitzt Thiothenoyltrifluoraceton wohl günstige Extraktionseigenschaften[9], zeigt aber gegenüber Lichtein-

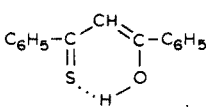

I

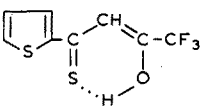

II

flüssen im kristallinen Zustand und in Lösung nur eine beschränkte Haltbarkeit. Weiterhin ist die Darstellung der Substanz in grösseren Mengen relativ aufwendig. Im Gegensatz dazu ist Thiodibenzoylmethan aus einfachen Ausgangsstoffen leicht zugänglich und in kristalliner Form praktisch unbegrenzt haltbar. Daher erscheint die Substanz als extraktionsphotometrisches Reagens bestens geeignet, wobei vor allem ihre Eignung für die Simultanbestimmung mehrerer Metalle von Interesse ist. Unter diesem Gesichtspunkt wurde die Anwendung von Thiodibenzoylmethan zur extraktionsphotometrischen Bestimmung von Kupfer untersucht.

Zur photometrischen Bestimmung von Metallen mit Thiodibenzoylmethan muss der überschüssige Ligand mit Natronlauge aus der organischen Phase reextrahiert werden. Dabei ist die Alkalibeständigkeit der vorliegenden Metallchelate eine wichtige Voraussetzung. Uneingeschränkt ist diese Bedingung nur bei den Chelaten des Kupfers, Nickels, Kobalts und der Platinmetalle erfüllt, eine relativ hohe Stabilität gegenüber Alkalien wurde ausserdem noch bei den Komplexen mit Cadmium und Quecksilber festgestellt. Für analytische Anwendungen des Thiodibenzoylmethans bieten sich daher vor allem diese Metalle an; dabei können zahlreiche Störelemente durch Reextraktion mit Natronlauge unschädlich gemacht werden.

Über die Bestimmung von Kupfer von Thiothenoyltrifluoraceton wurde kürzlich von anderer Seite[5] berichtet, jedoch wird das angegebene Verfahren bereits durch Anwesenheit geringer Mengen an Nickel und Kobalt gestört. Mit Thiodibenzoylmethan kann die Bestimmung neben einer Vielzahl von Fremdionen, vor allem

auch in Gegenwart von Nickel und Kobalt, vorgenommen werden.

Der Kupferkomplex des Thiodibenzoylmethans weist eine intensive Absorptionsbande bei 410 nm ($\varepsilon = 23700$) auf, im gleichen Spektralbereich absorbieren aber auch die entsprechenden Chelate mit Kobalt und Nickel (vgl. Fig. 1). Zur Durchführung der photometrischen Kupferbestimmung muss also die Mitextraktion dieser Metalle unbedingt vermieden werden. Nach Lage der Extraktionskurven[2] kann Kupfer durch Thiodibenzoylmethan bei sehr niedrigem pH ohne Störung durch Kobalt und Nickel extrahiert werden. Eine solche Extraktion erfordert aber einen Zeitaufwand, der analytisch nicht vertretbar ist. Die Zeitabhängigkeit der Kupferextraktion bei verschiedenen pH-Werten ist in Fig. 2 dargestellt. Erhöhung des pH-Wertes erbringt zwar eine Verkürzung der Extraktionszeit, zieht aber die Mitextraktion von Kobalt nach sich. Bei pH 2.5 wird Kupfer in Gegenwart eines 1000fachen

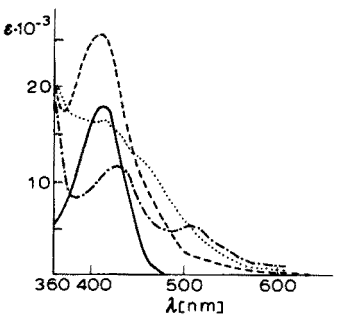


Fig. 1. Absorptionsspektren einiger Chelate von Thiodibenzoylmethan. (——) Ligand; (----) Cu; (–·–·–) Ni; (···) Co.

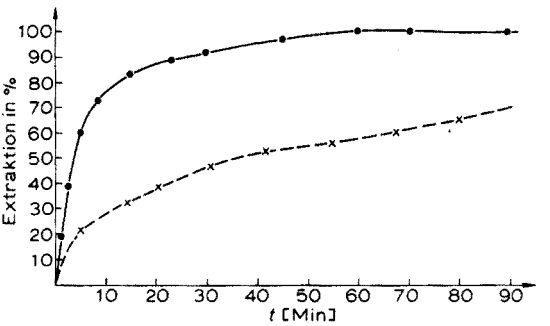


Fig. 2. Zeitabhängigkeit der Kupferextraktion mit Thiodibenzoylmethan. (——) Bei pH 2.55; (----) bei pH 2.00.

Überschusses an Nickel spezifisch extrahiert. Anwesendes Kobalt lässt sich bis zum 100fachen Überschuss durch Salicylaldoxim maskieren. Die Extraktionsdauer beträgt 60 Min. Durch Erhöhung des pH-Wertes auf 4.75 wird die Kupferextraktion bereits nach 10 Min quantitativ, aber Kobalt stört die Bestimmung. Es kann nicht mehr mit Salicylaldoxim maskiert werden, da ein Teil des Kupfers ebenfalls mit dem Maskierungsmittel reagiert. Erst in alkalischer Lösung können Bedingungen eingestellt werden, bei denen Kupfer quantitativ extrahiert, die Mehrzahl der anderen Metalle aber maskiert wird. Zur Maskierung ist in diesem Bereich vor allem EDTA gut geeignet; aus seinem EDTA-Komplex lässt sich Kupfer nach Reduction mit Thiosulfat leicht durch Thiodibenzoylmethan extrahieren.

## EXPERIMENTELLES

### *Reagenzien und Geräte*

Thiodibenzoylmethan wurde nach den Angaben der Literatur[10] dargestellt und zeigte nach zweimaligem Umkristallisieren einen Schmelzpunkt von 83–84°.

Das verwendete *n*-Hexan (p.a.-Qualität) wurde durch Destillation gereinigt. Auch alle sonstigen Chemikalien waren von analytischer Reinheit. Alle Lösungen

wurden mit bidestilliertem Wasser bereitet. Zur Herstellung der Kupferstandardlösung diente der Testal-Bezugstiter 0.1 *M* $CuSO_4 \cdot 5\ H_2O$ (Fa. Feinchemie K. H. Kallies K.G., Sebnitz).

Zur Durchführung der photometrischen Messungen stand das Spektralkolorimeter Spekol des VEB Carl Zeiss Jena zur Verfügung, die pH-Messungen wurden am pH-Meter OP 204 mit Einstab-Glaselektrode der Fa. Radelkis, Budapest durchgeführt. Die Dosierung kleiner Flüssigkeitsmengen erfolgte mit Hilfe von Kolbenbüretten.

Für die statistische Auswertung der Analysenergebnisse kam der Digitalrechner SER 2 zum Einsatz.

*Bestimmung der Extraktionskurven*

Die Extraktionskurven wurden in Abhängigkeit vom pH-Wert der wässrigen Phase und von der Anwesenheit anderer Komplexbildner bestimmt. Zur Durchführung der Messung wurden 10 ml 0.3 m*M* Kupfersulfatlösung nach Zugabe von Pufferlösung (pH 7 bis pH 12) mit 10 ml $10^{-3}$ *M* Lösung von Thiodibenzoylmethan in *n*-Hexan 5 Min geschüttelt. Um überschüssigen Liganden zu zerstören, wurde die organische Phase anschliessend zweimal 1 Min mit 20 ml 0.1 *M* Natronlauge geschüttelt. Die Messung der Extinktion erfolgte bei 410 nm und 1 cm Schichtdicke gegen eine analog behandelte Blindlösung (siehe Fig. 3, Kurve I). Ein vollkommen andersartiger Kurvenverlauf wird bei Zusatz von 5 ml 1 *M* Natriumthiosulfatlösung erhalten (siehe Fig. 3, Kurve II). Ein Ersatz des Thiosulfats durch andere Reduktionsmittel führt zum gleichen Ergebnis. Die Gegenwart von Maskierungsmitteln z.B. EDTA, Jodid, Triäthanolamin, bleibt auf die Extraktion des Kupfers aus stark alkalischer Lösung ohne Einfluss, wenn die organische Phase vor dem Messen filtriert wird.

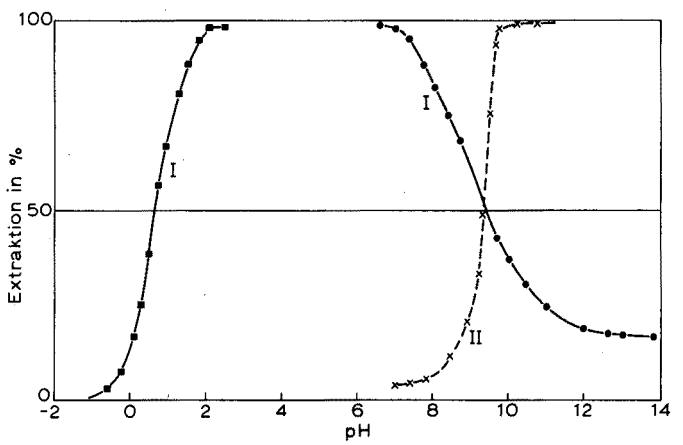


Fig. 3. Extraktion von Kupfer mit Thiodibenzoylmethan in Abhängigkeit vom pH-Wert und zugesetzten Reduktionsmitteln. (——) Normale Extraktionsbedingungen; (----) in Gegenwart von Thiosulfat.

*Extraktionsphotometrische Kupferbestimmung*

In einem Schütteltrichter gibt man zu *a* ml Kupferstandardlösung ($a = 0.5$, 1, 2, 3, 4, 5) je 5 ml 1 *M* Natriumthiosulfatlösung, 5 ml 0.1 *M* EDTA-Lösung, 5 ml 1 *M*

Natronlauge und 10 ml 0.001 *M* Reagenslösung und schüttelt 3 Minuten. Nach der Phasentrennung wird die organische Phase zweimal mit je 20 ml 0.1 *M* Natronlauge 1 Min geschüttelt. Die Extraktion der organischen Phase misst man bei 410 nm in einer 1 cm-Küvette gegen eine kupferfreie Blindlösung.

Die Testung des Verfahrens wurde im angegebenen Arbeitsbereich von 0.05–0.5 μmol Kupfer nach der von Gottschalk[11] angegebenen Methode durchgeführt. Einige Kenngrössen der Methode sind in Tabelle I zusammengefasst. Das Lambert–Beer'sche Gesetz ist im getesteten Bereich erfüllt. Als praktischer Extinktionskoeffizient wurde der Wert $\varepsilon_{410} = 23.7 \cdot 10^3$ l mol$^{-1}$cm$^{-1}$ gefunden. Die Berechnung der in der Probe gefundenen Kupfermenge erfolgte nach der Beziehung $c = E \cdot [\omega]$, wobei die Verfahrenskonstante $[\omega] = 0.042$ mol cm$^{-3}$ beträgt.

TABELLE I

KENNGRÖSSEN DER PHOTOMETRISCHEN KUPFERBESTIMMUNG MIT THIODIBENZOYLMETHAN

| | |
|---|---|
| Arbeitsbereich | 0.05–0.5 μmol Cu |
| Standardabweichtung $S_K$ | ±0.0078 μmol |
| Variationskoeffizient $V$ ($b_o$–$b_u$) | ±(0.15–1.5) Rel. % |
| Fehlerbereiche $T$ ($S$ = 99 %) | ±0.0022 μmol |
| $T$ ($S$ = 99.9 %) | ±0.0029 μmol |
| Bestimmungsgrenze $b_N$ | 0.003 μmol |

*Einfluss von Fremdionen*

Zur Untersuchung des Einflusses von Fremdionen wurden Lösungen ihrer p.a.-Salze zu Kupferlösungen der unteren und oberen Arbeitsbereichsgrenze zugesetzt und dann die Kupferbestimmung durchgeführt. Das Fremdion stört, wenn das Ergebnis der Kupferbestimmung ausserhalb des absoluten Fehlerbereiches $T$ ($S$ = 99.0 %) liegt. Von den untersuchten Begleitsubstanzen stören bis zum 1000fachen Überschuss nicht: Alkali- und Erdalkalimetalle, Bor, Aluminium, Gallium, Indium, Thallium, Blei, Kobalt, Nickel, Mangan, Ammoniak, Tartrat, Citrat, Salicylaldoxim.

Bis zum 100fachen Überschuss stören nicht: Silber, Quecksilber, Antimon, Wismut, Zink, Cadmium, Eisen, Chrom, Thioharnstoff, Thioglykolsäure.

Komplexbildende Anionen wie Fluorid, Jodid, Thiocyanat und Nitrit dürfen auch in 10000fachem Überschuss zugegen sein.

Durch die Anwesenheit von Palladium und Cyanid im Verhältnis 1:1 wird die Bestimmung gestört.

Dem VEB Jenapharm, Laborchemie Apolda, danken wir für die grosszügige Unterstützung und gute Zusammenarbeit.

ZUSAMMENFASSUNG

Kupferspuren lassen sich unter Verwendung von Thiodibenzoylmethan hochselektiv und mit sehr guter Reproduzierbarkeit extraktionsphotometrisch bestimmen. Der molare Absorptionskoeffizient beträgt $23.7 \cdot 10^{-3}$ bei 410 nm. Untersucht wurde der Einfluss von Fe, Co, Ni, Cr, Mn, Zn, Cd, Pb, Bi, Sb, Ga, In, Tl, Hg, Ag, Pd, B, Al, Alkalimetallen, Erdalkalimetallen, Jodid, Fluorid, Ammoniak, Tartrat, Citrat, Cyanid, Thiocyanat, Nitrit, Thioharnstoff, Thioglykolsäure und Salicylaldoxim.

SUMMARY

Traces of copper can be extracted and determined spectrophotometrically by means of thiodibenzoylmethane. The determination is highly selective, with a molar absorptivity of $23.7 \cdot 10^3$ at 410 nm. There is no interference from 1000-fold amounts of Na, K, Ca, Mg, Sr, B, Al, Ga, In, Tl, Pb, Co, Ni, Mn, ammonia, citrate, tartrate, or salicylaldoxime; from 100-fold amounts of Fe, Zn, Cd, Bi, Hg, Ag, Sb, Cr, thiourea, or thioglycolic acid; or from 10000-fold amounts of iodide, fluoride, thiocyanate or nitrate. Cyanide or palladium in equal amounts interfere.

RÉSUMÉ

On propose une méthode de dosage du cuivre, à l'état de traces, par spectrophotométrie, au moyen de thiodibenzoylméthane. Elle est très sélective et présente une très bonne reproductibilité. Coefficient d'extinction molaire $23.7 \cdot 10^3$, à 410 nm. On examine l'influence de nombreux cations et anions.

LITERATUR

1 XX. Mitt.: E. UHLEMANN UND U. ECKELMANN, *Z. Anorg. Allgem. Chem.*, 383 (1971) 321.
2 E. UHLEMANN UND H. MÜLLER, *Anal. Chim. Acta*, 41 (1968) 311.
3 E. UHLEMANN UND H. MÜLLER, *Anal. Chim. Acta*, 48 (1969) 115.
4 H. TANAKA, N. NAKANASHI, Y. SUGIURA UND A. YOKOYAMA, *Japan Analyst*, 17 (1968) 1428.
5 V. M. SHINDE UND S. M. KHOPKAR, *Anal. Chem.*, 41 (1969) 342.
6 A. V. RANGNEKAR UND S. M. KHOPKAR, *Chem. Ind.*, (1969) 293.
7 H. HASHITANI UND K. KATSUYAHA, *Japan Analyst*, 19 (1970) 355.
8 K. IZUKI UND H. KOMURO, *Japan Analyst*, 19 (1970) 1214.
9 E. UHLEMANN UND H. MÜLLER, *Z. Chem.*, 8 (1968) 185.
10 E. UHLEMANN UND H. MÜLLER, *Angew. Chem.*, 77 (1965) 172.
11 G. GOTTSCHALK, *Statistik in der Quantitativen Chemischen Analyse*, Enke-Verlag, Stuttgart, 1962.

*Analytica Chimica Acta*
Elsevier Publishing Company, Amsterdam
Printed in The Netherlands



# SPECTROPHOTOMETRIC DETERMINATION OF MICROAMOUNTS OF PLUTONIUM IN THE PRESENCE OF URANIUM

TADASHI YAMAMOTO, HIROSHI MUTO, SORIN KIHARA AND KENJI MOTOJIMA
*Japan Atomic Energy Research Institute, Tokai-mura, Ibaraki-ken (Japan)*

(Received 11th February 1971)

Several reagents have been reported[1,2] for the spectrophotometric determination of plutonium. Among them, arsenazo III seems to be the most sensitive reagent. However, uranium interferes with the determination of plutonium, and must be removed before the colour development of the plutonium complex.

The purpose of this investigation was to develop a rapid method for the determination of plutonium in the presence of a large quantity of uranium. Solvent extraction with thenoyltrifluoroacetone (TTA) is well-known[3,4] to separate plutonium effectively from many elements. Plutonium(IV) is extracted with TTA from dilute nitric acid solution, and the distribution ratio decreases as the concentration of nitric acid increases. Plutonium(IV) also forms a stable coloured complex with arsenazo III in solutions of high acidity[5]. If plutonium is back-extracted from the organic phase into a definite volume of acid solution containing arsenazo III, a rapid and simple procedure for determining plutonium can be evolved. Based on the same principle, methods for the determination of uranium have been developed[6,7].

Plutonium (IV) is usually determined with arsenazo III in 4–7 *M* nitric acid[5]. For the back-extraction from the organic phase, arsenazo III–nitric acid solution was first tried, but fading of the plutonium(IV) complex occurred frequently. Hydrochloric acid medium has been proposed[8], but was avoided because of glove box corrosion. Perchloric acid medium was found to be suitable for the determination of plutonium.

## EXPERIMENTAL

### *Reagents and apparatus*

*Standard plutonium solution.* A stock solution was prepared by dissolving 0.500 g of pure plutonium metal (U.S. NBS standard reference material 949b) in 20 ml of 6 *M* hydrochloric acid. The solution was diluted to 100 ml with 0.3 *M* hydrochloric acid. An aliquot was taken and evaporated almost to dryness. The residue was dissolved with concentrated nitric acid solution. After evaporation almost to dryness, the residue was dissolved with 1 *M* nitric acid. A solution containing 2 $\mu$g ml$^{-1}$ was obtained by dilution with 1 *M* nitric acid.

*Uranium solution.* A solution containing 0.1 g of uranium per ml was obtained by dissolving uranyl nitrate (Baker & Adamson, reagent grade) in water.

*Arsenazo III* (0.008%)*–perchloric acid* (5.0 *M*) *solution.* Mix 8 ml of aqueous 0.1% arsenazo III solution and 4 ml of 1% urea solution with 83 ml of 6.0 *M* perchloric acid in a 100-ml volumetric flask and dilute to volume with water.

Arsenazo III and TTA (Dojindo Co., Kumamoto-shi, Japan) were used without further purification. All other reagents were of analytical-reagent grade.

Absorbance measurements were made with a modified Shimadzu QB 50 spectrophotometer (1-cm cells) attached to a glove box. A horizontal reciprocal-type shaker made in the Workshop Section of this Institute was used for the extraction. All the manipulations were carried out in glove boxes.

*Recommended procedure*

Place a sample containing 2–15 $\mu$g of plutonium in a 50-ml beaker and evaporate almost to dryness. Dissolve the residue with 20 ml of 0.5 *M* nitric acid. Add 0.5 ml of 0.5 *M* hydroxyammonium chloride and heat for 30 min on a steam bath. After cooling, add 2 ml of 1 *M* potassium nitrite. Transfer the resultant solution to a 50-ml separating funnel. Rinse the beaker with 0.5 *M* nitric acid and adjust the aqueous volume to 40 ml with 0.5 *M* nitric acid. Add 10 ml of 0.2 *M* TTA in carbon tetrachloride and shake vigorously for 20 min. Transfer the organic phase to another separating funnel. Add 20 ml of 0.5 *M* perchloric acid to the second funnel and shake vigorously for 10 min. Transfer the organic phase to a third funnel and shake for 5 min with 10.0 ml of arsenazo III–perchloric acid solution. Measure the absorbance of the aqueous phase at 660 nm against a reagent blank. Determine the plutonium content from a calibration curve, prepared with known amounts (2–15 $\mu$g) of plutonium.

## RESULTS AND DISCUSSION

*Spectrophotometric determination of plutonium*

*Absorption spectra.* Plutonium(IV) forms a green complex with arzenazo III in perchloric acid solution. The absorption spectra of the complex and the reagent blank in 5.0 *M* perchloric acid solution are shown in Fig. 1. The complex has two absorbance peaks at 610 and 660 nm, and the latter wavelength was used for the determination.

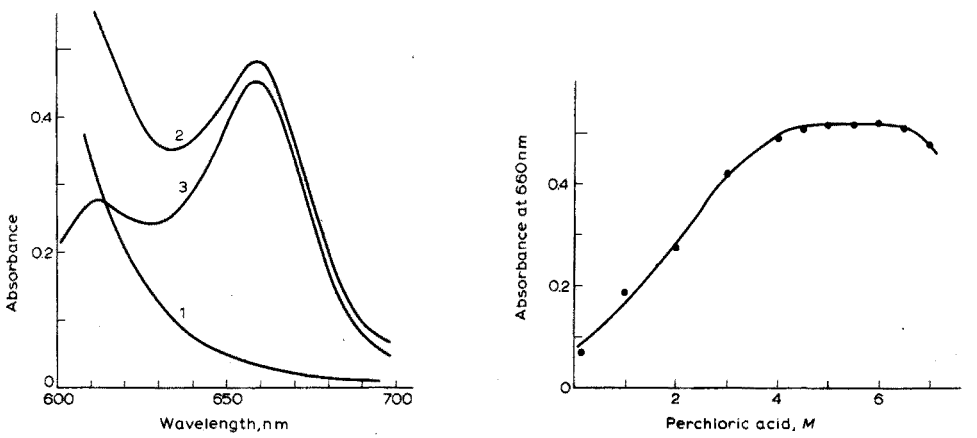


Fig. 1. Absorption spectra of plutonium(IV)–arsenazo III complex. (1) Blank *vs.* water; (2) 0.8 $\mu$g Pu ml$^{-1}$ *vs.* water; (3) 0.8 $\mu$g Pu ml$^{-1}$ *vs.* blank.

Fig. 2. Effect of acidity on absorbance. 1 $\mu$g Pu ml$^{-1}$ *vs.* blank.

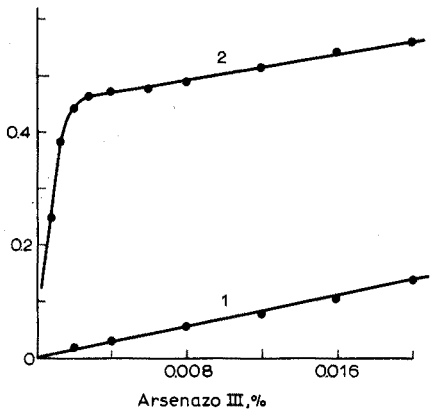


Fig. 3. Effect of reagent concentration. (1) Blank *vs.* water; (2) 0.8 $\mu$g Pu ml$^{-1}$ *vs.* water.

*Effect of acidity.* The dependence of complex formation on the acidity was examined by measuring the absorbance of solutions that were 1 to 8 *M* in perchloric acid. As shown in Fig. 2, the absorbance of the plutonium complex is almost constant at acidities in the range 4.5–6.0 *M*; 5 *M* was used in further investigations.

*Effect of arsenazo III concentration.* The absorbances of solutions that were 0–0.02% in arsenazo III and 5.0 *M* in perchloric acid were measured. Figure 3 shows that the absorbance of the complex *vs.* the reagent blank is constant when the arsenazo III concentration is greater than 0.004%. A concentration of 0.008% was chosen for the determination.

*Effect of time.* The plutonium(IV)–arsenazo III complex develops immediately in 5.0 *M* perchloric acid, but the absorbance decreases slowly in the presence of oxidizing substances such as nitrite ion. When urea is present at a concentration greater than 0.04% in the final solution, the absorbance does not change for at least 2 h at room temperature.

*Molar absorptivity.* A series of solutions containing varying amounts of plutonium, 2 ml of 0.1% arsenazo III and 1 ml of 1% of urea in 25 ml of 5.0 *M* perchloric acid was prepared. The absorbances of these solutions were measured at 660 nm against a reagent blank and plotted against plutonium concentration. The results showed that Beer's law is obeyed over the range 0.1–1.5 p.p.m. of plutonium. The molar absorptivity was $13.0 \cdot 10^4$ at 660 nm, and this value is similar to the case of nitric acid solution[5].

*Extraction and back-extraction of plutonium*

TTA has been used as the extractant for plutonium, and the extraction behaviour was investigated by $\alpha$-activity measurements in almost all previous papers. In the present work, nitric acid solution was selected as the aqueous phase for the first extraction, because it is widely used to dissolve and separate plutonium in the field of nuclear fuels. Carbon tetrachloride was chosen as the solvent for TTA because of its stability, low solubility in water and density. The only detailed report on the extraction behaviour of microgram amounts of plutonium in the TTA–carbon tetrachloride–nitric acid system is that of Cunninghame and Miles[3]. A further study

was made in order to choose the optimal conditions for the determination of plutonium by means of back-extraction and absorption spectrophotometry.

Plutonium in the organic phase was back-extracted with a definite volume of 0.008% arsenazo III–5.0 *M* perchloric acid solution, and determined by measuring the absorbance of the aqueous phase at 660 nm. The absorption spectra of the aqueous phase through back-extraction were similar to that of the 0.008% arsenazo III–5.0 *M* perchloric acid solution containing the same quantity of plutonium. It was confirmed by α-counting techniques that plutonium was transferred rapidly and quantitatively to the aqueous phase by back-extraction.

*Effect of nitric acid concentration on the first extraction*

Plutonium (10 μg) was extracted from 40 ml of 0.1–3 *M* nitric acid solution by shaking with 10 ml of 0.2 *M* TTA–carbon tetrachloride for 20 min. The plutonium content in organic phase was determined by back-extraction with 10.0 ml of 0.008% arsenazo III–5.0 *M* perchloric acid and absorbance measurement. The absorbance of the plutonium complex was found to be constant in the range 0.1–2 *M* nitric acid and then decreased rapidly at higher acidities.

*Effect of TTA concentration.* The concentration of TTA in carbon tetrachloride was varied from 0.02 *M* to 0.3 *M* to examine the effect of TTA concentration on the recovery of plutonium from 0.5 *M* nitric acid solution and the absorbance of the plutonium–arsenazo III complex. The absorbance of the complex was constant in the range 0.1–0.3 *M* of TTA. In the proposed procedure, a concentration of 0.2 *M* was selected.

*Effect of shaking time.* Cuninghame and Miles[3] reported that the distribution ratio for the extraction of traces of plutonium reached a maximum after shaking for 30 min. However, the present work showed that 10 min of shaking was enough to attain equilibrium in the first extraction.

Only plutonium(IV) is extracted as the TTA-complex from dilute nitric acid solution, and it is important to adjust the oxidation state before the extraction. An established method[4], *i.e.*, reduction with hydroxyammonium chloride and oxidation with nitrite ion, was adopted for the procedure.

*Determination of plutonium by the proposed procedure*

A series of solutions containing various amounts of plutonium was prepared and plutonium was determined by the proposed procedure. The absorbance of the final aqueous phase was measured at 660 nm. The results showed that Beer's law is followed between 1.0 and 16 μg of plutonium in 10 ml of final solution. The absorbance per μg of plutonium is 0.051–0.052, and the molar absorptivity is about $12.3 \cdot 10^4$. This values is a little less than that obtained from calibration curves without the extraction and back-extraction ($13.0 \cdot 10^4$). The main reason for the difference is the recovery of plutonium in the first TTA extraction. The absorbance of the plutonium complex does not change within 1 h, but the absorbance of solutions containing more than 10 μg of plutonium decreases after a longer period of time. The absorbance caused by 16 μg of plutonium decreased by 50% after 15 h, and that of 12 μg by 20%.

*Effect of uranium and other elements*

Uranium(VI) forms an arsenazo III complex in 5.0 *M* perchloric acid solu-

TABLE I

RESULTS OF DETERMINATION OF PLUTONIUM IN THE PRESENCE OF URANIUM

| *Pu added* (*μg*) | *U added* (*mg*) | *Absorbance at 660 nm vs. blank*[a] | | *Pu found* (*μg*) | | *Relative error* (%) | |
|---|---|---|---|---|---|---|---|
| — | 1000 | −0.003 | 0.003 | — | — | — | — |
| — | 2000 | 0.035 | 0.039 | (0.7) | (0.8) | — | — |
| 4.0 | — | 0.208 | 0.210 | — | — | — | — |
| 10.0 | — | 0.529 | 0.516 | — | — | — | — |
| 4.0 | 200 | 0.209 | 0.202 | 4.0 | 3.9 | 0 | −3.3 |
| | | 0.199 | 0.212 | 3.8 | 4.05 | −4.8 | +1.3 |
| 10.0 | 1000 | 0.546 | 0.489 | 10.4 | 9.4 | +4.0 | −6.0 |
| | | 0.538 | | 10.3 | | +3.0 | |

[a] Mean absorbance of blank was 0.030.

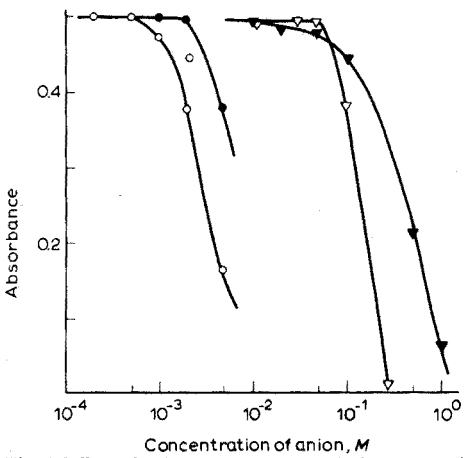


Fig. 4. Effect of anions on extraction. (○) Oxalate; (●) fluoride; (▽) phosphate; (▼) sulphate. 1 μg Pu $ml^{-1}$.

tion[7], though it is less sensitive than the uranium(IV) complex. Uranium(VI) is not extracted with TTA–carbon tetrachloride from dilute nitric acid solution, but occasionally small amounts of uranium are carried over into the organic phase. Washing the organic phase with 0.5 *M* perchloric acid eliminates uranium. The results of the determination of plutonium in the presence of uranium are shown in Table I, and it is seen that microgram amounts of plutonium in the presence of several hundred milligrams of uranium can be determined with a relative error of 5%. The method was specifically designed for the separation and determination of plutonium in uranium. However, in view of the fact that other metals (except zirconium) do not interfere, the method may be applicable to a wide variety of samples containing plutonium. Molybdenum(VI), yttrium, lanthanum and samarium (at the 1-mg level) do not interfere with the determination of plutonium. Cerium(IV) and thorium at the 1-mg level show some absorbance in the final solution but they can be masked completely by addition of 1 ml of 0.04 *M* sodium fluoride to the sample solution before addition of hydroxylamine. Zirconium interferes seriously, and must be removed by a suitable method. The effect of anions is shown in Fig. 4.

The authors wish to thank Dr. H. Onishi for his helpful discussion.

SUMMARY

A rapid spectrophotometric method has been developed for the determination of plutonium in the presence of uranium. Plutonium is extracted with 0.2 *M* thenoyltrifluoroacetone in carbon tetrachloride from 0.5 *M* nitric acid solution. After washing the organic phase with 0.5 *M* perchloric acid solution, plutonium is back-extracted with a definite volume of 0.008% arsenazo III–5.0 *M* perchloric acid solution. The absorbance of the aqueous phase is measured at 660 nm. By this method, 10 $\mu$g of plutonium can be determined in the presence of 1 g of uranium. The effect of diverse ions has been studied.

RÉSUMÉ

Une méthode spectrophotométrique est décrite pour le dosage rapide du plutonium, en présence d'uranium. On procède à une extraction du plutonium, à l'aide de thénoyltrifluoroacétone, dans le tétrachlorure de carbone, en milieu acide nitrique 0.5 *M*. Après lavage de la phase organique au moyen d'acide perchlorique 0.5 *M*, le plutonium est extrait en retour avec un volume déterminé d'arsenazo III à 0.008% en solution acide perchlorique 5.0 *M*. On mesure l'absorption de la phase aqueuse à 660 nm. On peut doser ainsi 10 $\mu$g de plutonium, en présence d'un gramme d'uranium. L'influence de divers ions est examinée.

ZUSAMMENFASSUNG

Für die Bestimmung von Plutonium in Gegenwart von Uran ist eine schnelle spektrophotometrische Methode entwickelt worden. Das Plutonium wird aus 0.5 *M* Salpetersäure mit 0.2 *M* Thenoyltrifluoraceton in Tetrachlorkohlenstoff extrahiert. Nach dem Waschen der organischen Phase mit 0.5 *M* Perchlorsäure wird das Plutonium mit einem definierten Volumen einer Lösung von 0.008% Arsenazo III in 5.0 *M* Perchlorsäure zurückextrahiert. Die Extinktion der wässrigen Phase wird bei 660 nm gemessen. Nach dieser Methode können 10 $\mu$g Plutonium in Gegenwart von 1 g Uran bestimmt werden. Der Einfluss verschiedener Ionen wurde untersucht.

REFERENCES

1 M. S. MILYUKOVA, N. I. GUSEV, I. G. SENTYURIN AND I. S. SKLYARENKO, *Analytical Chemistry of Plutonium*, Israel Program for Scientific Translations, Jerusalem, 1967, p. 125.
2 S. B. SAVVIN AND M. S. MILYUKOVA, *Zh. Analit. Khim.*, 21 (1966) 1075.
3 J. G. CUNINGHAME AND G. L. MILES, *J. Inorg. Nucl. CFem.*, 3 (1956) 54.
4 R. A. SCHNEIDER AND K. M. HARMON, *U.S.A.E.C. report HW-53368*, 1957.
5 A. A. NEMODRUK AND N. E. KOCHETKOVA, *Zh. Analit. Khim.*, 18 (1963) 333.
6 P. N. PALEI, A. A. NEMODRUK AND A. V. DAVYDOV, *Radiokhimiya*, 3 (1961) 181.
7 K. MOTOJIMA, T. YAMAMOTO AND Y. KATO, *Bunseki Kagaku (Japan Analyst)*, 18 (1969) 208.
8 A. A. NEMODRUK, P. N. PALEI AND N. E. KOCHETKOVA, *Radiokhimiya*, 5 (1963) 335.

*Analytica Chimica Acta*
Elsevier Publishing Company, Amsterdam
Printed in The Netherlands



# ÉTUDE DE LA DITHIZONE ET DU DITHIZONATE MERCURIQUE DANS LA N-MÉTHYLPYRROLIDONE

C. BUISSON ET Mme M. BRÉANT
avec la collaboration technique de Mme A. ZANDANEL

*Laboratoire de Chimie Industrielle et Analytique, Institut National des Sciences Appliquées, 20, avenue Albert Einstein, 69-Villeurbanne (France)*

*et*

*Centre de Chimie Analytique, Faculté des Sciences de Lyon, 43, bd. du 11 Novembre 1918, 69-Villeurbanne (France)*

(Reçu le 10 mars 1971)

Dans le cadre d'études sur les propriétés chimiques et électrochimiques dans les amides[1,2] nous nous sommes intéressés aux propriétés de la dithizone et du dithizonate mercurique dans la N-méthylpyrrolidone (NMP). Les propriétés de ce solvant dipolaire, aprotique et dissociant ont été passées en revue dans une mise au point récente[2].

La dithizone (diphénylthiocarbazone, $H_2Dz$) est soluble dans la NMP: les solutions sont vertes en milieu acide et roses en présence de pipéridine.

Le remplacement des hydrogénes mobiles peut se faire par de nombreux cations métalliques et, en particulier, par les ions mercuriques dont l'addition en milieu acide dans la NMP provoque le virage au rouge d'une solution de dithizone initialement verte.

Par comparaison avec les résultats obtenus dans d'autres solvants[3,4], on peut supposer que les équations qui traduisent les réactions décrites ci-dessus sont:
pour les propriétés acide–base de la dithizone:

$$H_2Dz \rightleftharpoons HDz^- + H^+ \qquad (1)$$

pour la formation du complexe mercurique:

$$H_2Dz + Hg^{2+} \rightleftharpoons Hg(HDz)_2 + 2H^+ \qquad (2)$$

Nous nous sommes proposé d'analyser ces deux réactions.

## PROPRIÉTÉS DE LA DITHIZONE DANS LA N-MÉTHYLPYRROLIDONE

### *Propriétés acide–base*

Nous avons suivi la neutralisation d'une solution de dithizone $10^{-3}$ *M* en milieu $LiClO_4$ 0.1 *M* par la pipéridine $10^{-1}$ *M*, soit à l'aide d'une électrode de verre à remplissage aqueux, immergée depuis cinq mois dans la NMP, soit à l'aide d'une électrode à remplissage de mercure[5]. L'électrode de référence est constituée par le système $Hg/Hg(SCN)_4^{2-}$ $10^{-2}$ *M*, $KSCN_{sat}$ obtenu par oxydation d'une nappe de mercure au contact d'une solution saturée de thiocyanate dans la NMP. Cette électrode est reproductible à $\pm$ 5mV près; son potentiel décroit de 5 mV par semaine.

Les différences de potentiel ont été mesurées à l'aide d'un millivoltmètre Solea U8 ou S6. Les courbes obtenues correspondent au dosage d'un acide faible par une base faible.

Considérons les transformées $\log (x/1-x) = f(pH)$ où $x$ représente le quotient du volume $v$ de réactif titrant en un point de la courbe par le volume $V$ de réactif nécessaire pour atteindre le point équivalent : ce sont des droites de pente moyenne 0.82 à l'électrode de verre à remplissage aqueux, et 1.03 à l'électrode à remplissage de mercure.

Ces valeurs, voisines de l'unité, signifient[6] d'une part que la courbe de dosage correspond à l'échange d'un seul proton, réaction (1), d'autre part que les associations entre les molécules $H_2Dz$ et les anions $HDz^-$ restent négligeables. Dans ce cas, lorsque $x=0.5$, le pH est égal à $pK'_A$, $K'_A$ étant la constante d'acidité apparente du couple $H_2Dz/HDz^-$ à force ionique 0.1.

Nous obtenons ainsi : $pK'_A = 6.3 \pm 0.4$.

La deuxième fonction acide de la dithizone qui correspondrait à la formation de l'anion $Dz^{2-}$ est trop faible pour que nous puissions la doser par la pipéridine.

*Caractéristiques spectrophotométriques*

Les mesures d'absorption ont été effectuées avec un spectrophotomètre Beckman DBG.

Les solutions de dithizone ($2.5 \cdot 10^{-5}$ $M$) en milieu acide perchlorique $10^{-2}$ $N$ présentent deux maxima d'absorption à 450 et 620 nm ; en présence de pipéridine, on n'observe plus qu'un seul pic à 510 nm.

Nous avons examiné à 620 nm, la validité de la loi de Beer. Nous obtenons effectivement une droite dont nous déduisons le coefficient d'extinction molaire : $\varepsilon_{620\ nm} = 38.500$.

Nous avons suivi, en fonction du temps, l'évolution de l'absorption des solutions : elle décroît de 8% en 1 h. Toutes nos mesures ont donc été faites dans la demi-heure suivant la mise en solution de la dithizone.

## ÉTUDE DU DITHIZONATE MERCURIQUE

*Caractéristiques spectrophotométriques*

Lorsqu'on ajoute progressivement des ions mercure(II) à une solution acide (pH 2) de dithizone, le spectre de la solution évolue selon le faisceau de courbes reproduit Fig. 1. La présence de points isosbestiques (455 et 545 nm) confirme l'existence d'un équilibre en solution.

L'addition d'un excès d'ions mercure(II) ne modifie plus le spectre observé (courbe 6) dont le maximum à 490 nm se révèle caractéristique du dithizonate mercure (II).

A cette longueur d'onde, l'absorption de la solution suit la loi de Beer et nous calculons : $\varepsilon_{490\ nm} = 77{,}000$.

L'absorption des solutions décroît de 2% par heure. Le dithizonate est donc plus stable que la dithizone.

*Vérification de la formule et détermination de la constante de dissociation du complexe*

Les deux composés colorés présents en solution (dithizone et dithizonate)

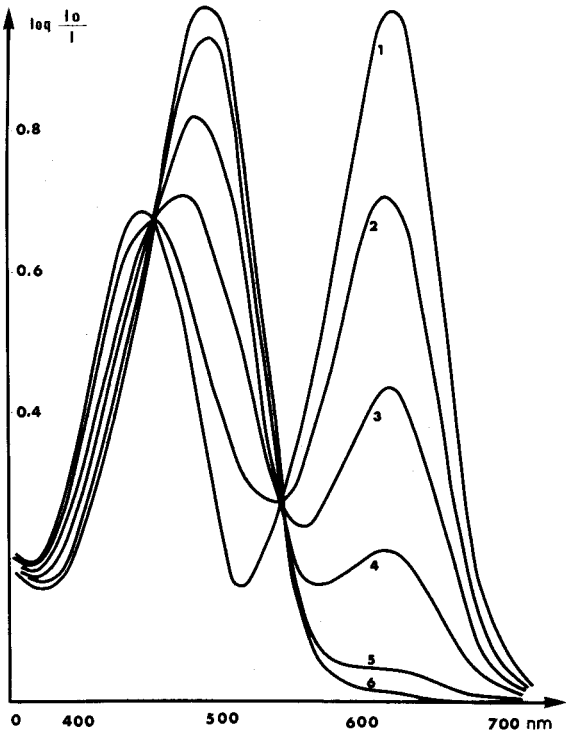


Fig. 1. Evolution du spectre d'absorption de la dithizone $2.5 \cdot 10^{-5}$ *M* en fonction de l'addition d'ions mercure(II). (1) $Hg^{2+} = 0$; (2) $Hg^{2+} = 0.35 \cdot 10^{-5}$ *M*; (3) $Hg^{2+} = 0.70 \cdot 10^{-5}$ *M*; (4) $Hg^{2+} = 1.00 \cdot 10^{-5}$ *M*; (5) $Hg^{2+} = 1.25 \cdot 10^{-5}$ *M*; (6) $Hg^{2+} = 1.50 \cdot 10^{-5}$ *M*.

obéissent à la loi de Beer ; nous pouvons donc suivre leurs concentrations par mesure des absorptions à leur maximum d'absorption.

Nous avons alors examiné la formation du dithizonate par deux méthodes classiques d'analyse des réactions : la méthode des courbes de dosage linéaires[7] et la méthode des variations continues (méthode de Job)[8]. Ces procédés d'analyse, mis au point pour l'étude des équilibres à trois termes, peuvent être facilement appliqués au cas d'équilibres à quatre termes : il suffit de maintenir constante l'une des concentrations en solution. Pour l'étude de l'équilibre (2), il est facile de fixer le pH du milieu à une valeur déterminée.

*La méthode des courbes de dosage linéaires* revient à suivre par spectrophotométrie l'apparition du complexe ou la disparition de l'agent complexant au cours du dosage de la dithizone par les ions mercuriques. Nous employons une cuve à circulation Beckman, reliée à une cellule reproduite Fig. 2. La solution à doser est introduite dans la cellule et la circulation du liquide est assurée par un courant d'azote sec.

Le réactif est introduit par une burette automatique de faible débit ($3 \cdot 10^{-2}$ ml $min^{-1}$), condition imposée par le fait que la formation du complexe n'est pas instantanée et que la solution doit circuler de la cellule à la cuve. Nous avons vérifié que le débit utilisé était satisfaisant en arrêtant l'addition de réactif au cours d'un dosage : l'absorbance reste constante.

En jouant sur la valeur du pH imposé à la solution, il est possible d'obtenir une réaction plus ou moins quantitative. Ce phénomène est mis en évidence par les

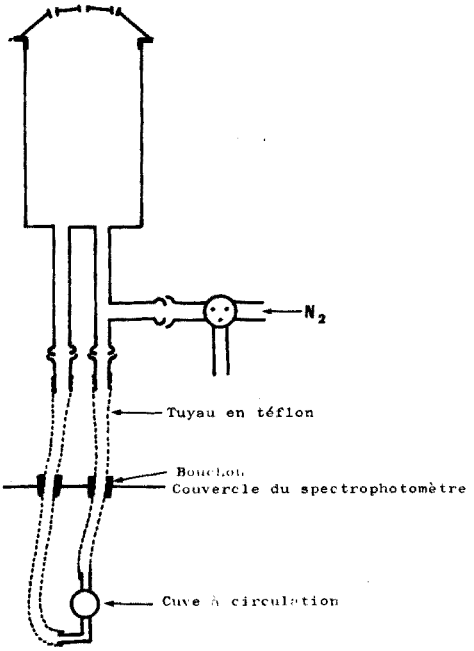


Fig. 2. Bécher et cuve à circulation.

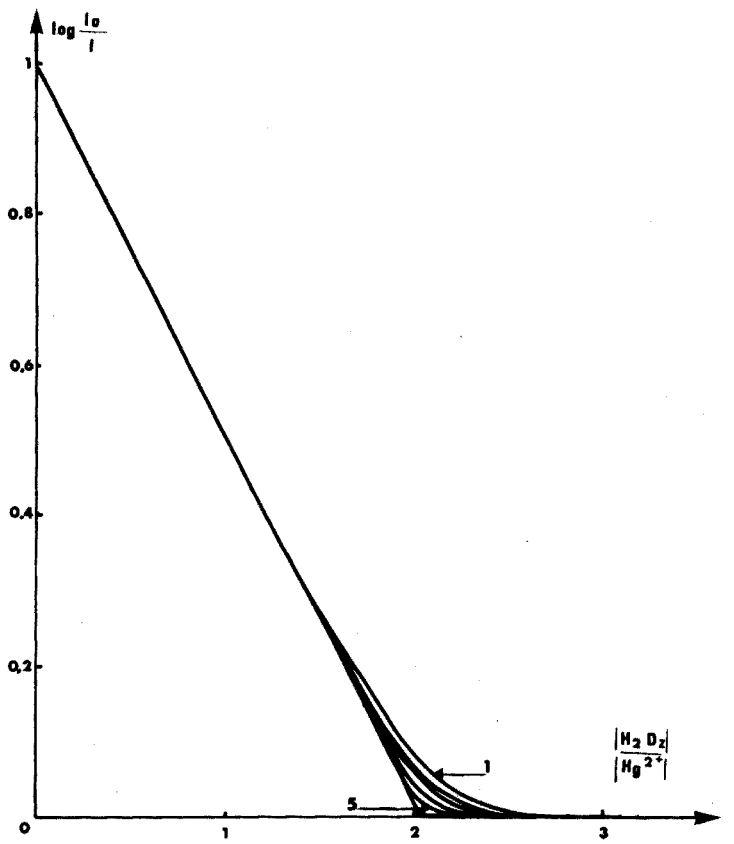


Fig. 3. Courbes de titrage de la dithizone par les ions mercure(II) à 620 nm. (1) pH = 1 ; (2) pH = 2 ; (3) pH = 2.3 ; (4) pH = 3 ; (5) pH = 4.

courbes de la Fig. 3 qui représentent la disparition de l'agent complexant au cours du dosage.

Nous constatons que la fraction $\alpha$ de dithizone non complexée est d'autant plus grande que le pH est plus acide; au point équivalent nous déterminons:

| pH | 1 | 2 | 2.3 | 3 | 4 |
|---|---|---|---|---|---|
| $\alpha$ | 0.135 | 0.10 | 0.08 | 0.05 | 0.03 |

A pH 4, nous pouvons considérer que la réaction est quantitative. Le point équivalent, défini avec précision, correspond à la neutralisation d'un ion $Hg^{2+}$ par 2.03 molécules de dithizone.

Ce résultat confirme la formule $Hg(HDz)_2$ proposée pour le dithizonate mercure(II). A pH 2, la réaction de formation n'est plus quantitative et la valeur $\alpha$ obtenue est suffisamment précise pour calculer la constante de l'équilibre (2).

$$K = \frac{[Hg(HDz)_2][H^+]^2}{[H_2Dz]^2[Hg^{2+}]} = \frac{(1-\alpha)[H^+]^2}{\alpha^3 C_0^2}$$

$C_0$ étant la concentration initiale en dithizone.

Nous calculons ainsi: $pK' = -8.1 \pm 0.5$ à force ionique 0.1.

La constante de dissociation du complexe:

$$K'_c = \frac{[Hg^{2+}]\,[HDz^-]^2}{[Hg(HDz)_2]}$$

peut être obtenue facilement à partir de $K'$ et de $K'_A$, première constante d'acidité de la dithizone. En effet:

$$K'_c = K'^2_A / K'$$

d'où $pK'_c = 2pK'_A - pK' = 12.6 + 8.1 = 20.7$ et $pK'_c = 20.7 \pm 1.3$ à force ionique 0.1.

Pour appliquer *la méthode des variations continues*, nous mélangeons deux solutions de même titre, l'une de dithizone, l'autre d'ions mercure(II) de telle façon que:

$$[Hg^{2+}]_{total} + [H_2Dz]_{total} = C_0$$

et nous mesurons l'absorption au maximum d'absorption du dithizonate (490 nm) en fonction de $a$, fraction de dithizone dans le mélange.

Comme pour la méthode des courbes de dosage linéaires, la formule du complexe est vérifiée sans ambiguïté lorsque la réaction est quantitative tandis que la constante ne peut être déterminée avec précision que dans le cas contraire.

En fait, nous avons constaté, par le tracé des courbes de dosage de la Fig. 3 qu'en opérant à pH 2 il était possible de tracer sans ambiguïté les droites correspondant à une réaction quantitative tout en conservant une bonne précision sur la détermination de $\alpha$. Nous avons donc opéré dans ces conditions de pH. Nous constatons alors que les tangentes à la courbe $\log I_0/I = f(a)$ se coupent pour $a = 0.64$, ce qui confirme de nouveau la formule $Hg(HDz)_2$ attribuée au complexe (Fig. 4).

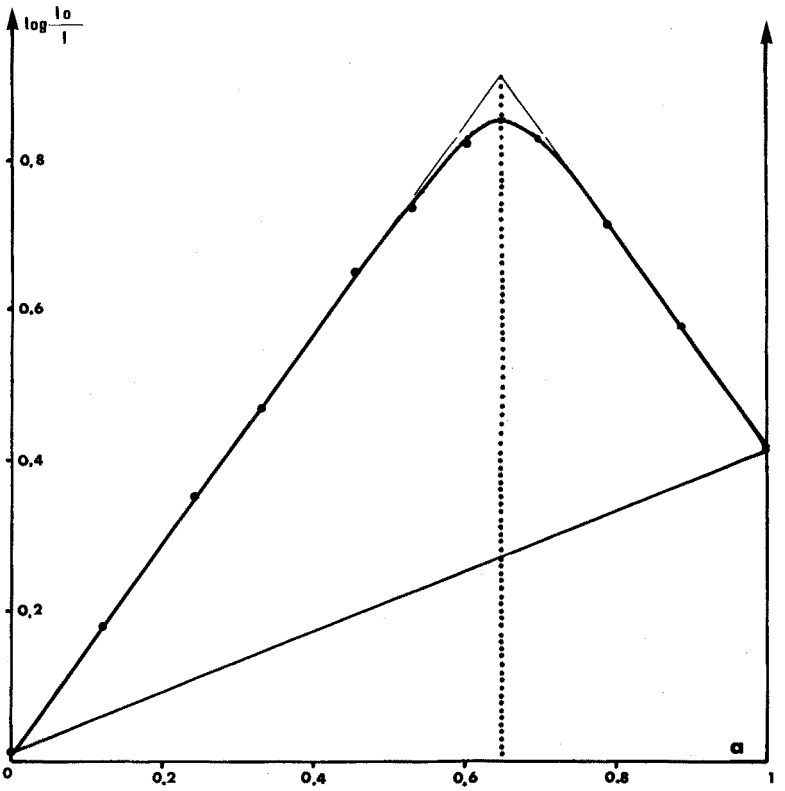


Fig. 4. Courbe obtenue par la méthode des variations continues de Job.

La valeur $\alpha$ est égale à 0.094, ce qui donne pour la constante de l'équilibre (2):

$pK' = -8.3 \pm 0.5$ à force ionique 0.1

et, pour la constante de dissociation du complexe:

$pK'_c = 20.9 \pm 1.3$ à force ionique 0.1

Nous constatons que les valeurs obtenues par la méthode des courbes de dosage linéaires d'une part, par celle des variations continues d'autre part, sont très concordantes.

## DISCUSSION DES RÉSULTATS

Nous avons rassemblé dans le Tableau I les valeurs de constantes que nous avons déterminées et celles précédemment obtenues dans le diméthylformamide[3,9]. Nous constatons que les composés examinés dans ce mémoire se comportent de façon analogue dans la NMP et dans le DMF, le dithizonate étant toutefois plus stable dans le premier solvant.

La méthode des courbes de dosage linéaires, dans les conditions où nous l'avons employée peut être transposée immédiatement au dosage des ions mercure(II) par la dithizone et vice-versa.

TABLEAU I

CARACTÉRISTIQUES DE LA DITHIZONE ET DU DITHIZONATE MERCURE(II) DANS LA N-MÉTHYLPYRROLIDONE ET LE DIMÉTHYLFORMAMIDE

| *Cation* | $\lambda_{max}$ *en milieu acide (nm)* | $\varepsilon_{\lambda_{max}}$ | *Formule* | *pK'* | $pK'_a$ *et* $pK'_c$ |
|---|---|---|---|---|---|
| $H^+$ NMP | 450 | — | $H_2Dz$ | — | $6.3 \pm 0.4$ |
| | 620 | 38,500 | | | |
| DMF | 450 | 21,500 | $H_2Dz$ | — | $6.65 \pm 0.1$ |
| | 620 | 32,000 | | | |
| $Hg^{2+}$ NMP | 490 | 77,000 | $Hg(HDz)_2$ | $-8.2 \pm 0.5$ | $20.7 \pm 1.3$ |
| DMF | 485 | 52,500 | $Hg(HDz)_2$ | $-4.2 \pm 0.3$ | $17.5 \pm 0.5$ |

RÉSUMÉ

Nous avons déterminé la première constante d'acidité de la dithizone dans la N-méthylpyrrolidone: $pK_A = 6.3 \pm 0.4$ à force ionique 0.1, puis la formule $Hg(HDz)_2$ et la constante de dissociation du dithizonate mercurique dans ce solvant: $pK_c = 20.7 \pm 1.3$ à force ionique 0.1. Cette étude a également permis de mettre en évidence les caractéristiques spectrophotométriques des deux composés étudiés.

SUMMARY

The first acidity constant of dithizone in N-methylpyrrolidone was found to be $pK_A = 6.3 \pm 0.4$ at ionic strength 0.1. The complex formed with mercury(II) in this solvent was shown to have the formula $Hg(HDz)_2$, the dissociation constant being $pK = 20.7 \pm 1.3$ at ionic strength 0.1. The spectrophotometric characteristics of the two compounds studied are discussed.

ZUSAMMENFASSUNG

Die Bestimmung der ersten Aciditätskonstante von Dithizon in N-Methylpyrrolidon ergab den Wert $pK_A = 6.3 \pm 0.4$ bei Ionenstärke 0.1. Es wurde gezeigt, dass der mit Quecksilber(II) in diesem Lösungsmittel gebildete Komplex die Formel $Hg(HDz)_2$ hat; die Dissoziationskonstante bei Ionenstärke 0.1 ist $pK = 20.7 \pm 1.3$. Die Spektrophotometrischen Eigenschaften der beiden untersuchten Verbindungen werden diskutiert.

BIBLIOGRAPHIE

1 M. BRÉANT ET G. DEMANGE-GUERIN, *Bull. Soc. Chim. France*, (1969) 2935.
2 M. BRÉANT, *Bull. Soc. Chim. France*, (1971) 725.
3 M. BRÉANT, *Bull. Soc. Chim. France*, (1967) 3081.
4 P. LE GOFF ET B. TRÉMILLON, *Bull. Soc. Chim. France*, (1964) 350.
5 M. BRÉANT, M. DUPIN ET J. P. TERRAT, *Journées d'Electrochimie Organique*, Clermont-Ferrand, 28–29 mai 1970.
6 J. DESBARRES, *Bull. Soc. Chim. France*, (1962) 2103.
7 G. CHARLOT, *Les Méthodes d'Analyse des Réactions en Solution*, Masson, Paris, 1951.
8 P. JOB, *Ann. Chim. (Paris)*, 9 (1928) 133.
9 M. BRÉANT, *Compt. Rend.*, 262 (1966) 346.

*Analytica Chimica Acta*
Elsevier Publishing Company, Amsterdam
Printed in The Netherlands



# STUDIES WITH DITHIZONE

## PART XXV*. THE DETERIORATION OF STOCK SOLUTIONS AND THE IDENTIFICATION OF TWO OXIDATION PRODUCTS

H. M. N. H. IRVING, A. M. KIWAN, D. C. RUPAINWAR AND S. S. SAHOTA
*Department of Inorganic and Structural Chemistry, University of Leeds, Leeds 2 (England)*
(Received 1st April 1971)

It is notoriously difficult to prepare and preserve pure solid samples of dithizone (3-mercapto-1,5-diphenylformazan, $H_2Dz$) and the deterioration of its stock solutions in organic solvents such as chloroform and carbon tetrachloride has plagued the analyst since this reagent was introduced in 1925. Careful purification of the organic solvent[1] reduces the rate of deterioration which is certainly accelerated by traces of heavy metals, by light and air, by alkali and oxidants, and by rise of temperature[2].

Helmuth Fischer was the first to examine deteriorated solutions of dithizone spectrophotometrically[3] and he reported that what he described as the "yellow oxidation product" has its maximum absorption at *ca.* 400 nm with lower absorption at higher wavelengths where dithizone absorbs strongly (at 450 and 620 nm in carbon tetrachloride). Iwantscheff[4] reported three peaks at 390, 305 and 260 nm (with $\varepsilon_{max}$ = 8800, 8000 and 8500, respectively) but he warns that this substance, which he refers to as the "intermediate oxidation product", may vary in composition according to the way it has been prepared. This "intermediate oxidation product" is certainly not the same as the substance first obtained by Fischer and Besthorn[5] by treating an alkaline solution of dithizone with manganese dioxide and formulated by him (incorrectly) as diphenylthiocarbadiazone (I), for it absorbs at *ca.* 470 nm in the visible but has an intense absorption band in the ultraviolet ($\lambda_{max}$ 265 nm, $\varepsilon_{max}$ 17,400). Weber[6] resported that dithizone in carbon tetrachloride is oxidised by a solution of hydrogen perioxide in dilute (1 : 100) ammonia to a yellow product with $\lambda_{max}$ 410 nm and $\varepsilon_{max}$ 8000 but commented that these parameters were not constant, for on standing a certain amount of dithizone was reformed. Yellow solutions have also been reported from the use of oxidants such as iron(III) salts[7], nitric acid[6] and chloramine-T[8], though bromine gives rise to nuclear-brominated dithizones[8]. These products must be distinguished from another yellow compound of definite characteristics ($\lambda_{max}$ 375; $\varepsilon_{max}$ 19,300: broad shoulder at *ca.* 305 nm) formed when a solution of dithizone in chloroform is exposed to bright sunlight. This is the heterocyclic compound 5-phenylazo-3-phenyl-1,3,4-thiadiazole-2-one (II) formed by condensation of dithizone with phosgene produced by photochemical oxidation of the solvent[9].

* *Anal. Chim. Acta*, 54 (1971) 55 is regarded as Part XXIV of this paper.

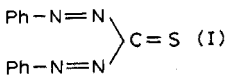


(I)

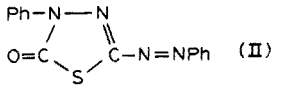


(II)

The literature contains many recipes for minimising the loss of titre of dithizone solutions during storage. For example, solutions in carbon tetrachloride overlaid with 10% of their volume of 0.1 *M* sulphurous acid are said to retain their strength indefinitely if stored in the dark and kept cool[10]. With chloroform solutions the use of sulphurous acid or other holding reductants such as hydroxylamine or sodium thiosulphate proved less effective than the use of a purified solvent[1] containing 1% of ethanol and storage in the dark at 40°F[10]. A significant observation is that yellow solutions of deteriorated dithizone could sometimes be reconverted to dithizone by treatment with sulphurous acid, sometimes completely and sometimes only partially[10]. Clearly there is no reason to suppose that solutions containing the "yellow oxidation product" are not mixtures, and there are no grounds for assuming that the same substances will be formed in different organic solvents. Indeed, it has recently been shown that small amounts of aldehydes or ketones present as impurities can give rise to yellow solutions. Thus dithizone readily condenses with acetaldehyde formed by the acid hydrolysis of 2-methyldioxalane, often present up to 1% in commercially pure dioxan, to give the red heterocyclic compound 2-methyl-3-phenyl-5-phenylazo-1,3,4-thiadiazoline[11].

Clearly, the yellow colour of a deteriorated solution of dithizone could originate from a variety of causes. Furthermore, the almost black products obtained by removing the solvent from deteriorated solutions in chloroform or carbon tetrachloride have been found by chromatography to be complex mixtures. An essential preliminary to their investigation would seem to be the preparation and characterisation of single pure oxidation products obtained from dithizone under carefully controlled and reproducible conditions.

Since dithizone can exist both as a thioketone, PhN:N·CS·NH·NHPh, and in the tautomeric thiol form, PhN:N·C(SH):N·NHPh, (III), it seemed likely that mild oxidation would yield a disulphide (IV) since this is a characteristic reaction of thiols. Indeed when the yellow solution of primary silver dithizonate (Ag(HDz); $\lambda_{max}$ 470 nm) in chloroform was treated with an equivalent amount of iodine there was an immediate precipitation of silver iodide according to the equation

$$I_2 + 2\,Ag(HDz) \rightarrow 2\,AgI + (HDz)_2 \qquad (1)$$

and a change of spectrum to give a new species with $\lambda_{max}$ 420 nm (Fig. 1, curves 1 and 2)[12]. With less than the equivalent amount of iodine a composite spectrum of unreacted silver dithizonate and the new species was observed. With more than the equivalent of iodine there were further changes which will be described later. However, the most surprising result was that shortly after the initial reaction (eqn. 1) had been completed the spectrum began to change towards that of free dithizone (Fig. 1, curves 3 and 4). The rate of formation of dithizone increased with the concentration of reactants and with the temperature, but quantitative measurements showed that even after several hours the amount formed was never more than half that originally present as the silver complex. An exactly similar sequence of changes was observed when primary mercury(II) dithizonate was treated with iodine[12].

At this point it was decided to reinvestigate the interaction of dithizone with

elementary iodine, since this is also commonly used to oxidise thiols to disulphides. By using concentrated solutions of the components in chloroform this reaction had previously been shown to yield a sparingly soluble black adduct, $H_2DzI_2$, from which the dithizone could be quantitatively recovered by treatment with aqueous sodium thiosulphate. When, however, more dilute solutions were used in the presence of water the green colour of the dithizone immediately changed to red and hydriodic acid appeared in the aqueous phase in stoicheiometric agreement with eqn. (2):

$$2\,H_2Dz + I_2 \rightarrow 2\,HI + (HDz)_2 \qquad (2)$$

Here again, a deficiency of iodine gave rise to a mixed spectrum and an excess caused further changes. On standing, the band at 420 nm decreased in intensity and the green colour and the spectrum of dithizone reappeared[12] (Fig. 2, curves 1, 2 and 3) and there was a distinct isosbestic point at 488 nm. On shaking the organic phase again with fresh iodine (and water) the whole sequence of changes could be repeated; but each time the total amount of dithizone regenerated became smaller.

These observations could be fully explained by the initial formation of a disulphide (IV) and its spontaneous thermal fission into equimolecular amounts of dithizone (III; only the thiol form is shown here, but rapid tautomeric equilibration with the thione form will take place) and a compound containing two fewer hydrogen atoms which does not absorb in the visible region. We have shown that this second component is the meso-ionic compound (V).

The plausibility of this hypothesis[12] was supported by the discovery of similar cases in the early literature although the rate of fission was often very slow at room temperature. For example, Busch[13] found in 1895 that the series of disulphides (VI) derived from the thiols (VII) decomposed to give equimolecular amounts of (VII)

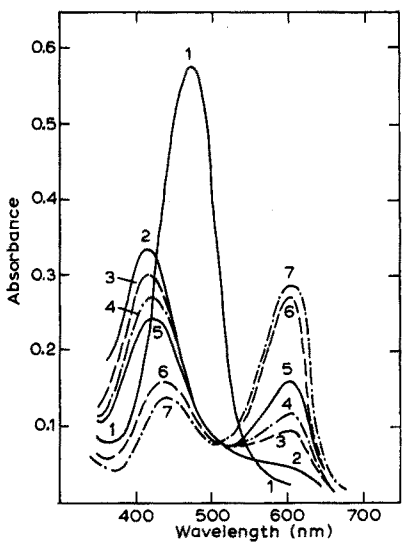


Fig. 1. The oxidation of a solution of primary silver dithizonate in chloroform by iodine. (1) $1.9 \cdot 10^{-5}$ *M* solution of silver dithizonate in chloroform; (2) spectrum of reaction product obtained by treating this with a slight excess of iodine dissolved in moist chloroform; (2, 3, 4, 5, 6 and 7) taken after the lapse of 5, 30, 45, 75, 180 and 2880 min respectively.

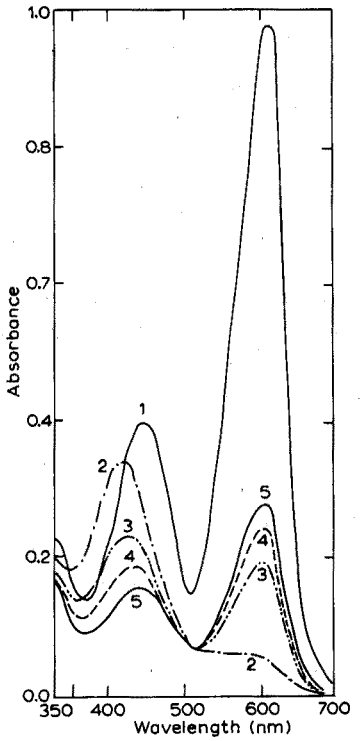


Fig. 2. The oxidation of dithizone by aqueous iodine. (1) $2.45 \cdot 10^{-5}$ *M* solution of dithizone in chloroform; (2) spectrum after shaking with iodine (dissolved in chloroform) and water; (3, 4 and 5) spectra of the organic phase after 0.5, 1.0 and 1.5 h.

and compounds with two fewer hydrogen atoms which he formulated as (VIII) but which would nowadays, following Baker *et al.*[14] be represented as meso-ionic compounds analogous to (V).

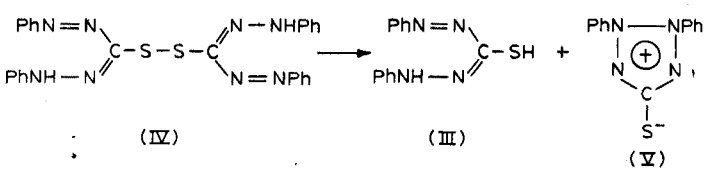


The reaction with the disulphide (VI; R = H) took 15–20 h in chloroform solution at room temperature. With another disulphide (VI; $R = CH_3$) no change was detected under these conditions and heating in a sealed tube at 100° for a short time was required. For solutions of a phenyl derivative (VI; $R = C_6H_5$) fission was slow even at 100° and heating for 2 h at 110–120° proved necessary.

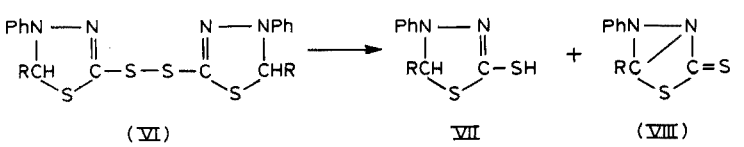

The possibility that the interaction of iodine with dithizone had given rise to a free radical $C_{13}H_{11}N_4S$ rather than the disulphide (IV) was first disproved by examining a solution of the primary product with a Varian 4500 Electron Spin Resonance Spectrometer with 100 Hz modulation. The absence of free radicals during the fission process (IV) → (III) + (V) was established in the same way.

Since in this case and in the decomposition of (VI), the meso-ionic compounds (V) or (VIII) are strongly polar, theory predicts that the rate of thermal fission should depend on the polarity of the solvent, decreasing as it becomes less polar. Indeed, when the oxidation of dithizone by iodine was carried out in carbon tetrachloride the rate of regeneration of dithizone was noticeably slower and by using a suitable non-polar solvent (cyclohexane) it proved possible to isolate a pure sample of bis-1,5-diphenylformazan-3-yl-disulphide (IV) after chromatography on silica gel as deep reddish-black crystals (m.p. 107° decomp.) which had the correct molecular weight and analysis[15].

By using solutions of this pure disulphide, we have studied the kinetics of the reaction (IV) → (III) + (V) in a variety of solvents and have shown that it provides a unique example of a first-order heterolytic fission. Enthalpies and entropies of activation have been reported for this and the thermal fission of the disulphide (VI; R = H)[15]. The effect of solvent polarity is very marked and $t_{\frac{1}{2}}$ at 25° for the disulphide (IV) increased from 10.5 min (alcohol or acetone) to 86 min with chloroform and 77 days for cyclohexane, *n*-hexane or isooctane. The rate of fission decreases in the order ethanol ≦ acetonitrile < acetone < chloroform < 1,2-dichloroethane ≪ carbon tetrachloride < diethylether < cyclohexane ≦ *n*-hexane ≦ isooctane which parallels the order of their respective polarity parameters[15].

The disulphide (IV) gives yellow solutions with one strong absorption band at 410–428 nm (see Table I), and two in the ultraviolet region, one at *ca.* 303 nm attributable to the –S–S– bond and another at still shorter wavelength due to the aromatic rings. The molecular extinction coefficient varies with the solvent and ranges from 49,000 in *n*-hexane to 18,400 in methanol in the visible region and 30,000 to 16,000 in the ultraviolet. The effective value of $\varepsilon_{max}$ *per dithizone residue* (24,250 at 415 nm in carbon tetrachloride) should be compared with the values $\varepsilon_{max} = 20{,}000$ at 450 nm for the thiol form of dithizone itself, suggesting that the chromophoric group has remained essentially unchanged in the oxidation product.

The infrared spectrum of the disulphide (Table II) showed a medium band at 504 $cm^{-1}$ which may be attributable to the S–S stretching frequency. Similar assignments (470–520 $cm^{-1}$) are reported in the literature for a number of organic disulphides[16–18]. The strong band at 712 $cm^{-1}$ in the spectrum of dithizone which can be assigned to the >C=S stretching frequency has disappeared from the spectrum of (IV). The strong band at 1220 $cm^{-1}$ shown by nickel dithizonate and assigned by Freiser *et al.*[19] to the presence of a thiocarbonyl group is also absent from the infrared spectrum of the disulphide (IV). But since this strong band also appears in the infrared spectra of 2-phenylazo-benzo-1,3,4(4H)-thiadiazine (X)[20] and in that of 1,5-diphenyl-3-nitroformazan[21], in which there are certainly no >C=S groupings, the assignment of the >C=S stretch to 712 $cm^{-1}$ seems more reliable and it is supported by the shift to a lower frequency, *viz.* 705 $cm^{-1}$, when sulphur is replaced by selenium[22].

Freshly prepared solutions of the disulphide (IV) are readily reduced back to dithizone by sulphurous acid and sulphites, by sodium thiosulphate, by hypophos-

TABLE I

OPTICAL CHARACTERISTICS OF BIS-1,5-DIPHENYLFORMAZAN-3-YLDISULPHIDE (IV) IN ORGANIC SOLVENTS

| *Solvent* | $\lambda_{max}$ | $\lambda_{min}$ | $\lambda_{max}$ | $\lambda_{min}$ | $\lambda_{max}$ |
|---|---|---|---|---|---|
| *n*-Hexane | 410 (49.0)[a] | 335 (19.1) | 303 (22.0) | | |
| Carbon tetrachloride | 415 (48.5) | 338 (15.8) | 302 (21.0) | 286 (20.0) | |
| Cyclohexane | 415 (38.9) | 332 (13.7) | 303 (16.7) | 283 (14.5) | 253 (24.6) |
| Diethyl ether | 416 (40.0) | 338 (13.5) | 307 (16.7) | 284 (15.2) | 252 (26.2) |
| Chloroform[b] | 420 (42.0) | 349 (16.9) | 305 (18.9) | 285 (18.0) | 257 (29.6) |
| Acetone[b] | 424 (38.4) | 345 (15.7) | | | |
| Ethanol[c] | 428 (27.4) | 342 (10.0) | | | 256 (30.0) |
| Methanol[c] | 420 (18.4) | 335 (5.4) | | | 254 (16.1) |
| Nitromethane | 420 (36.2) | | | | |

[a] Values of $10^{-3}$ $\varepsilon_{max}$ are given in parentheses.
[b] Thermal fission was rapid in these solvents and results were obtained by extrapolation to zero time.
[c] With ethanol there is an additional band at $\lambda_{max}$ 206 (32.4) with $\lambda_{min}$ 224 (16.6).

TABLE II

INFRARED SPECTRA OF DITHIZONE (III), BIS-1,5-DIPHENYLFORMAZAN-3-YL-DISULPHIDE (IV), 2,3-DIPHENYL-2,3-DIHYDROTETRAZOLIUM-5-THIOLATE (V), 1,5-DIPHENYLFORMAZAN-3-SULPHONIC ACID (IX) AND 2-PHENYL-AZO-BENZO-1,3,4(4H)-THIADIAZINE (X)
(s = strong; m = medium; w = weak; vw = very weak; sh = shoulder. The infrared spectra of 3-methyl-mercapto-1,5-diphenylformazan (S-methyldithizone) and 3-nitro-1,5-diphenylformazan are reported and discussed in D.C. Rupainwar's *D.Phil. Dissertation*, Leeds, 1969).

| (*III*) | (*IV*) | (*V*) | (*IX*) | (*X*) |
|---|---|---|---|---|
| 297 m | | 307 m | | |
| | 384 w sh | 351 s | | |
| | | 392 m | | |
| | | 413 w | 410 vw | 415 vw |
| 440 w | | | 439 w | |
| 448 s | | | | 460 m |
| 495 s | | 498 s | 482 s | |
| 505 w | 504 m | | | |
| 520 w | 530 vw | | | 521 m |
| 541 w | | 563 s | 553 w | 555 w |
| 572 m | 596 w | 592 s | 605 w | |
| 603 w | | 620 w | 628 s | 629 m |
| | | 640 m | | 653 w |
| 678 s | | 680 s | 679 s | 682 s |
| | 685 s | 690 s | | |
| | 704 w sh | | | |
| 711 s | | | 713 w | |
| 749 s | 750 s | | 742 s | 748 s |
| 760 w | 768 m | 765 s | 756 s | 768 s |
| 774 m | | | 779 m | 772 sh s |
| | | | 818 m | |
| 828 w | 830 w | 832 s | 830 m | 835 w |
| | 850 w | | | 851 w |
| 872 w | 870 w | | 867 m | |
| 890 s | 890 m | 885 w | | |
| 901 w | | 911 s | | |
| 960 w | 920 w | 920 s | 960 vw | 920 s |
| | | 945 m | 972 vw | |

TABLE II (*continued*)

| (*III*) | (*IV*) | (*V*) | (*IX*) | (*X*) |
|---|---|---|---|---|
| 993 w | 1000 w | 980 s | 987 vw | |
| 1020 w | 1019 w | 1008 m | 1001 w | 1000 w |
| | | 1027 s | 1038 s | 1030 m |
| 1070 m | 1070 m | 1070 s | 1072 vw | 1072 s |
| 1095 s | 1121 s | 1118 s | 1118 w | 1120 sh m |
| 1143 s | 1150 m | 1160 s | 1160 m | 1130 s |
| 1171 s | 1170 w | 1175 s | 1170 m | |
| | 1190 w | 1197 m | 1182 s | 1182 m |
| 1217 s | 1210 vw | 1242 s | 1208 s | 1220 s |
| 1250 m | 1257 s | | 1248 s | 1252 s |
| | | 1270 s | | 1282 s |
| | | | 1290 s | 1292 s |
| 1314 s | 1307 w | 1310 s | 1310 s | 1305 s |
| | | 1330 s | 1330 sh m | |
| 1360 m | | 1365 s | | 1362 s |
| 1380 m | | 1375 s | | |
| | 1398 s | 1400 s | | |
| 1437 s | 1435 m | | 1453 m | 1431 m |
| 1457 s | 1458 m | 1460 s | 1462 m | 1468 s |
| 1481 s | 1480 sh | 1483 s | 1485 w | 1489 m |
| 1495 s | | | | 1508 s |
| | 1520 s | | 1532 m | 1545 m |
| | | 1582 s | | 1571 s |
| 1589 s | 1600 s | 1590 s | 1595 m | 1590 s |
| | | | | 1665 m |
| 2960 mw | | | 2910 w | 2965 w |
| | | 3008 w | 3010 w | 3010 w |
| 3030 sh w | 3050 w | 3055 m | 3060 m | 3185 s |
| 3045 m | 3260 w | | | 3270 s |
| 3430 m | 3440 w | | | |

phites and by diethylthiocarbamic acid[23]. These reactions appear to be quantitative but the yield of dithizone in particular cases may be less than 100% if the meso-ionic compound (V) has been formed to any extent by the spontaneous thermal fission process since the meso-ionic compound is unaffected by these reducing agents.

Cleavage of disulphides by reactions of the type

$$R\text{–}S\text{–}S\text{–}R + HgCl_2 \rightarrow RSHgCl + RSCl \qquad (3)$$

are well known, although the composition of the mercury complex finally obtained varies according to the disulphide taken[24]. When a solution of the disulphide (IV) in cyclohexane is shaken with excess of an aqueous solution of mercury(II) chloride, primary mercury(II) dithizonate, $Hg(HDz)_2$, and the meso-ionic compound (V; meso) are formed in equivalent amounts. The former remains in the organic phase while the latter enters the aqueous phase as the complex cation $Hg(meso)_2^{2+}$ whose composition[12], properties and analytical applications will be reported elsewhere. This reaction may be represented as follows

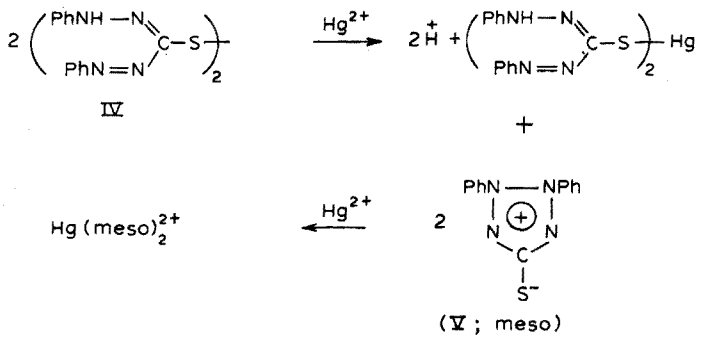


The sulphur–sulphur bond is similarly cleaved by other cations *e.g.* $Zn^{2+}$, $Cd^{2+}$, $Cu^{2+}$, $Pd^{2+}$ and $PhHg^{+}$ to give the corresponding metal dithizonate and an equivalent amount of the meso-ionic compound (V).

The disulphide (IV) can be produced from dithizone by oxidants other than iodine. The behaviour of selenium dioxide in concentrated mineral acid has already been reported[23] although the results are unfortunately at variance with those of Starý and Růžička who claim the formation of selenium(IV) dithizonate under these

TABLE III

OXIDATION PRODUCTS OF DITHIZONE FORMED UNDER DIFFERENT CONDITIONS

(+ + + Major product; + + Product in smaller amount; + Product detected (*ca.* 5%))

| *Oxidant and conditions* | *Solvent for dithizone*[a] | *Products* | | | |
|---|---|---|---|---|---|
| | | *(IV)* $C_{26}H_{22}N_8S_2$ | *(V)* $C_{13}H_{10}N_4S$ | *(IX)* $C_{13}H_{12}N_4O_3S$ | *(X)* $C_{13}H_{10}N_4S$ |
| $I_2$ in aqueous solution | | | | | |
| (i) $[H_2Dz] : [I_2] \geqq 1 : 1$ | A | + +[b] | + + + | — | — |
| (ii) $[H_2Dz] : [I_2] = 1 : 0.5$ | B | + + +[c] | + + | — | — |
| 1 mol $H_2O_2$/1 : 100 | A | — | + + + | — | — |
| aqueous ammonia | C | + + + | + + | — | — |
| Excess $H_2O_2$/0.5 *M* alkali | D | — | + | + + + | — |
| Air bubbled into solution in concd. alkali | D | — | + + + | — | — |
| Amyl nitrite | B | — | + + + | — | — |
| $MnO_2$/alkali | D | — | + + + | — | — |
| $KMnO_4$/alkali | Water | — | + + + | — | — |
| $K_3Fe(CN)_6/K_2CO_3$ | A | — | + + + | — | — |
| $PhICl_2$ | A | — | + + | + | — |
| $Ph_2I^+Cl^-$ | C | + + + | — | — | — |
| $HOOC \cdot C_6H_4 \cdot IO$ | C | + + + | — | — | — |
| $FeCl_3$/dil. alkali | A | — | + + + | — | — |
| $Tl^{3+}$/0.1 *M* $HClO_4$ | A | — | + + + | — | — |
| Air/hot concd. acetic acid | | — | — | — | + + + |

[a] A = chloroform; B = diethylether; C = carbon tetrachloride; D = 0.5 *M* NaOH.

[b] The disulphide is the initial product and the proportion of (V) increases if the reaction mixture is left to stand.

[c] The proportion of meso-ionic compound (V) increases if the disulphide is not isolated quickly.

conditions[25]. We have now found the disulphide to be the main product when dithizone is oxidised by *o*-iodosobenzoic acid or by the diphenyliodonium cation. The former reagent is said to be specific for the oxidation of thiols to disulphides[26] but the latter often behaves as a phenylating agent. On the other hand, treatment of dithizone with iodobenzenedichloride, $PhICl_2$, gave the meso-ionic compound (V). In many cases a mixture of products was obtained and some of the results are summarised in Table III.

Ogilvie and Corwin[27] were the first to suggest the meso-ionic structure (V) for the orange crystalline "dehydrodithizone" obtained by oxidising dithizone with potassium hexacyanoferrate(III). This superseded the thiocarbodiazone structure (I) ascribed by Fischer and Besthorn[5] to the product obtained by treating a solution in potash with manganese dioxide, and the tetrazolium betaine structure proposed by Bamberger *et al.*[28] for the product obtained by aerial oxidation or by the action of amyl nitrite in ether solution. Although the identity of these products has been assumed by previous workers, we have repeated each of these preparations and confirmed the identity of the products by ultimate analysis and by their spectra both in the visual and infrared region. Some confusion was caused initially by the apparent discrepancies between the electronic absorption spectra of different samples which had been measured in different solvents. It was later realised that the electronic absorption spectra of the meso-ionic compound (V) were unusually sensitive to the solvent used. For example, in water $\lambda_{max} = 380$ nm, $\varepsilon_{max} = 1640$, whereas in ethyl acetate the corresponding values are 480 nm and 1365. This phenomenon, which can be correlated systematically with the polarity of the solvent, has been thoroughly studied[15,29].

Ogilvie and Corwin[27] have already noted the nucleophilic displacement of halogens from methyl iodide and chloroacetic acid leading to the formation of 5-methylmercapto-2,3-diphenyltetrazolium iodide and 5-carboxymethylmercapto-2,3-diphenyltetrazolium chloride, respectively. During studies on the action of excess of iodine on dithizone, it was found that iodine would add on to the meso-ionic compound (V) to give a red crystalline solid (m.p. 186° ; $C_{13}H_{10}N_4SI_2$) which must clearly be 5-iodomercapto-2,3-diphenyltetrazolium iodide. On treatment with aqueous sodium thiosulphate the meso-ionic compound (V) was recovered.

The meso-ionic compound is also formed from dithizone when other oxidising agents are used, *e.g.* iodine in aqueous solution, hydrogen peroxide in dilute ammonia, iron(III) chloride and thallium(III) cations. In several cases, it is accompanied by the disulphide (IV) but under other conditions (Table III) the sulphonic acid (IX)[30] or

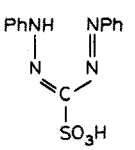


(IX)

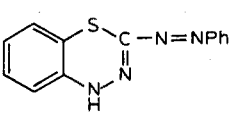


(X)

the "purple compound" (X)[20] may be the main products.

To assist in identifying the components of possible mixtures occurring in oxidation reactions, the behaviour of each well characterised product was studied by thin layer chromatography. The results are summarised in Table IV. Comparison of

TABLE IV

$R_F$ VALUES FOR DITHIZONE AND RELATED COMPOUNDS

| *Compound* | *Average $R_F$ value* | | | | | | |
|---|---|---|---|---|---|---|---|
| | *Ether* | *Benzene* | *Hexane* | *Ethanol* | *Acetone* | *Chloroform* | *Carbon tetrachloride* |
| Dithizone | | | | | | | |
| (a) green spot | 0.76 | 0.24 | 0.01 | 0.90 | 0.73 | 0.68 | 0.12 |
| (b) brown spot[a] | 0.89 | — | — | 0.85 | — | 0.76 | — |
| S-Methyldithizone[b] | 0.89 | 0.48 | 0.02 | 0.86 | 0.81 | 0.71 | 0.34 |
| Disulphide(IV) | | | | | | | |
| (a) brown spot | 0.89 | 0.55 | 0.01 | 0.85 | 0.78 | 0.75 | 0.14 |
| (b) green spot[a] | — | 0.34 | — | 0.90 | — | 0.67 | — |
| Meso-ionic compound (V) | 0.0 | 0.0 | 0.0 | 0.77 | 0.67 | 0.05 | 0.0 |
| Sulphonic acid (IX) | 0.0 | 0.0 | 0.0 | 0.85 | 0.36 | 0.0 | 0.0 |
| Purple compound (X) | 0.78 | 0.15 | 0.02 | 0.86 | 0.77 | 0.42 | 0.03 |

[a] Spots due to decomposition of the parent substance during chromatography.
[b] 3-Methylmercapto-1,5-diphenylformazan.

the results for dithizone and for the disulphide (IV) show clearly that the green spot caused by the former appears during the chromatography of the latter, especially when a polar solvent such as chloroform or ethanol is used. Similarly, the appearance of the brown spot caused by disulphide in the chromatography of pure dithizone is a clear indication of its sensitivity towards oxidation when in solution and exposed in a thin film to air. As expected S-methyldithizone travels faster than dithizone itself in all solvents, whereas the highly polar substances (V) and (IX) have conspicuously low $R_F$ values except in ethanol and acetone. Compounds (IX) and (X), both of which are purple coloured, are readily distinguished and separated. On the other hand, although the purification of dithizone by paper chromatography with benzene as an eluent[31] is likely to remove any coexisting disulphide, pretreatment with a suitable reducing agent would be desirable.

Our general experience suggests that whereas mild oxidants may produce the disulphide or meso-ionic compound or an admixture, the sulphonic acid is only formed under drastic oxidising conditions in strongly alkaline solution. The disulphide may well be an intermediate in the formation of the sulphonic acid (IX) although this may be formed directly from the thiol form of dithizone or from the dithizonate ion[32]. The meso-ionic compound (V) is doubtless produced by oxidative cyclisation of a dithizonate ion since many 3-substituted formazans are known to undergo

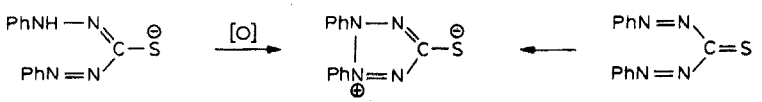


(III − H⁺) (V; one canonical form) (I)

aerial oxidation (often catalysed by light) to give the corresponding tetrazolium

salts[33]. We have not been able to produce an authentic sample of diphenylthiocarbadiazone (I) and it seems not improbable that, should it be formed, it would quickly isomerise to the meso-ionic compound (V) or, under the influence of acid to the "purple compound" (X)[20].

*The interaction of primary silver dithizonate with iodine*

Silver dithizonate was prepared by shaking $3 \cdot 10^{-5}$ *M* dithizonate in chloroform (20 ml) with an equal volume of $3 \cdot 10^{-5}$ *M* silver nitrate in 0.5 *M* nitric acid. The organic layer was found absorptiometrically to be $0.69 \cdot 10^{5}$ *M*.
solution ($1.5 \cdot 10^{-5}$ *M*) and distilled water (10 ml) when the colour changed from yellow to orange. After shaking for 5 min the organic phase was separated from suspended silver iodide and kept overnight in a stoppered tube, when the spectrum of dithizone appeared and achieved a concentration of $0.70 \cdot 10^{-5}$ *M* based on the absorbance at 605 nm. After this dithizone had been stripped by equilibration with dilute aqueous ammonia (1 : 100), the concentration of meso-ionic compound (V) remaining in the organic layer was found absorptiometrically to be $0.69 \cdot 10^{-5}$ *M*.

When exactly equivalent amounts of iodine and silver dithizonate (both $3 \cdot 10^{-5}$ *M*) were allowed to interact as above for 20 min the yield of meso-ionic compound was 97.3% and no dithizone was regenerated on keeping the organic solution overnight.

*The interaction of dithizone and iodine in solution*

A $2.45 \cdot 10^{-5}$ *M* solution of dithizone in chloroform (20 ml) was added to a $1.23 \cdot 10^{-5}$ *M* solution of iodine in the same solvent (20 ml) and shaken with distilled water (30 ml) for 2 min. The colour of the organic layer changed from green to yellow. After 5 min it was separated and dried over anhydrous sodium sulphate, and the spectrum was recorded at intervals (Fig. 2). After about 10 h there was no further change and the absorbance corresponded to 50% of the dithizone originally taken. At this stage dithizone was stripped by shaking with dilute (1 : 100) aqueous ammonia, when the meso-ionic compound (V) was left in the organic phase. By absorptiometry at 266 nm its concentration was found to be 48.5% of that of the dithizone originally taken.

In a second experiment solutions of 0.01 *M* dithizone (30 ml) and 0.005 *M* iodine (30 ml) in chloroform were mixed and shaken with deionised water (30 ml) for 2 min. The phases were then separated. Hydriodic acid in a 10-ml aliquot portion of the aqueous phase was titrated with 0.01 *M* sodium hydroxide (found : 0.010 *M*; calc. 0.0100 *M*). The concentration of iodide ions in a second 10-ml aliquot portion was determined by Andrew's method (found : 0.0098 *M*; calc. 0.0100 *M*).

*The reaction between the meso-ionic compound (V) and iodine. Formation of 5-iodomercapto-2,3-diphenyltetrazolium iodide*

Iodine (0.3 g) in chloroform (50 ml) was added to a solution of (V) (0.3 g) in chloroform (50 ml); the colour changed from reddish-orange to deep yellow. On allowing the solvent to evaporate at room temperature, a red solid separated which formed bright red crystals of 5-iodomercapto-2,3-diphenyltetrazolium iodide from hot ethanol (m.p. 186° ; yield 75–80%). (Found : C, 31.1 ; H, 1.9 ; N, 11.15 ; S, 6.2 ; I, 49.55. $C_{13}H_{10}N_4SI_2$ requires C, 30.7 ; H, 2.0 ; N, 11.0 ; S, 6.3 ; I, 49.95%.)

*Identification of the disulphide (IV) in a deteriorated solution of dithizone. Its reaction with diethyldithiocarbamic acid*

An impure sample of dithizone (0.1 g) dissolved in carbon tetrachloride (100 ml) was extracted with dilute isopiestic ammonia (1 : 100) until the organic phase was a clear yellow. This solution was diluted to give an absorbance in the range 0.8–0.9. When 8 ml of this stock solution was diluted to 10 ml with pure carbon tetrachloride, the spectra recorded on a Unicam SP700 had $\lambda_{max}$ 420 and 622 nm with a shoulder at 540 nm. The ratio of the absorbances at 420 and 622 nm was 0.750 : 0.048 = 15.6.

An aliquot portion (8 ml) of the stock solution was made up to 10 ml by adding 2 ml of a solution of diethyldithiocarbamic acid in carbon tetrachloride which had been freshly prepared by shaking together an aqueous *ca.* $10^{-3}$ *M* solution of sodium diethyldithiocarbamate (BDH AnalaR ; 50 ml) with carbon tetrachloride (50 ml) and adding 0.5 *M* sulphuric acid dropwise until the pH was between 2 and 3. The organic layer was separated, dried over anhydrous sodium sulphate, protected from light and used immediately. The spectrum taken immediately on mixing had $A$ (420) = 0.590 and $A$ (622) = 0.850. After 5 min this had changed to $A$ (622) = 1.02 and after 15 min the absorbance at $\lambda_{max}$ = 622 nm was 1.08. There was a subsidiary maximum at 448 nm.

*The reaction between bis-1,5-diphenylformazan-3-yl disulphide and metal ions*

A $3.2 \cdot 10^{-5}$ *M* solution of the disulphide (IV) in cyclohexane (10 ml) was shaken with an equal volume of aqueous mercury(II) chloride (excess) when there was an immediate change in colour. The phases were separated and primary mercury-(II) dithizonate was identified in the organic phase by its spectrum and reactions. From the absorbance at 490 nm the concentration was calculated to be $1.45 \cdot 10^{-5}$ *M* (90.6% of the theoretical). The aqueous phase was separated and shaken with excess of a slightly acidic solution of potassium iodide (2% w/v) containing about 1% of sodium thiosulphate to complex all the mercury(II) ions and to reduce any free iodine that might appear since this would interfere with subsequent spectrophotometry. The aqueous solution was then shaken with chloroform for 5 min, after which the presence of extracted meso-ionic compound (V) was established by its characteristic absorption spectrum with $\lambda_{max}$ 467, $\lambda_{min}$ 360 and $\lambda_{max}$ 266 nm, and $\varepsilon_{max}$ 1170 and 19,700, respectively. The amount formed corresponded to 94% of the theoretical.

In similar experiments with $Zn^{2+}$, $Cu^{2+}$, $Pb^{2+}$, $Cd^{2+}$ and $PhHg^{+}$ the quantitative formation of primary metal dithizonate was established spectrophotometrically.

*Formation of the disulphide (IV) by oxidation of dithizone with o-iodosobenzoic acid*

A $1.807 \cdot 10^{-5}$ *M* dithizone solution in carbon tetrachloride (20 ml) was shaken with an equal volume of the same concentration of *o*-iodosobenzoic acid in a buffer of pH 7.3 for 2 min, during which the colour changed from green to yellow. After 5 min the layers were separated. The spectrum of an aliquot portion of the organic phase showed a single peak at 410 nm, which established the presence of the disulphide (IV) as the main product which could be reverted to dithizone by shaking with sulphurous acid.

Precisely similar results were obtained when the oxidation of dithizone was effected with an equimolar solution of a diphenyliodonium salt.

*Preparation of the meso-ionic compound (V)*

(*a*) *With amyl nitrite.* Following Bamberger *et al.*[28], amyl nitrite was added dropwise to a solution of dithizone (4 g) in warm chloroform (200 ml) until the colour began to change from green to red, when it was rapidly cooled to 0°. Unchanged dithizone was removed by washing with dilute aqueous alkali and, after being dried over anhydrous potassium carbonate, the solvent was removed *in vacuo* from the separated organic phase. The red residue was dissolved in boiling acetone (animal charcoal) and filtered. Addition of light petroleum precipitated (V) as orange crystals (0.5 g; m.p. 173° decomp.) which were recrystallised from ethanol until the spectra of successive fractions in chloroform were identical. (Found: C, 61.3; H, 4.15; N, 22.3. M (isopiestic in chloroform[34]) 258. Calcd. for $C_{13}H_{10}N_4S$: C, 61.4; H, 4.0; N, 22.0; S, 12.6%. M = 254.3.) The same product was obtained when the oxidation was carried out in ethereal solution[28] but the yield was lower.

(*b*) *With manganese(IV) oxide.* Freshly prepared manganese(IV) oxide was added to a vigorously stirred solution of dithizone (3 g) in alcoholic potash (100 ml of 5% w/v) at 50° until the colour changed from red to orange. After filtration the filtrate deposited red crystals of (V) on cooling and a further amount was obtained by extracting the solid residue with hot ethanol. The total yield (10%) gave orange red crystals (m.p. 172° decomp.) from ethanol and the adsorption spectrum was indistinguishable from the above (Found: C, 61.5; H, 4.1; N, 21.95%.)

(*c*) *With potassium permanganate.* Potassium permanganate (3 g) in distilled water (200 ml) was added dropwise to a vigorously stirred solution of dithizone (3 g) in 0.5 *M* sodium hydroxide (300 ml). The solid was collected and extracted with boiling ethanol from which (V) separated on cooling (0.9 g; 30%) as orange red crystals (m.p. 173° decomp.). (Found: C, 61.6; H, 4.25; N, 21.75; S, 12.9%.)

(*d*) *With potassium hexacyanoferrate(III).* A solution of dithizone (1 g) in chloroform (300 ml) was stirred mechanically (2 h) with a solution of potassium hexacyanoferrate(III) (3.2 g) and potassium carbonate (3 g) in water (100 ml). The organic layer was removed and the solvent allowed to evaporate at room temperature. The residue of (V) (0.5–0.6 g; 50–60%), gave orange-red crystals (m.p. 172° decomp.) from hot ethanol. For details of this preparation based on J. Reinheimer's Dissertation (John Hopkins University, 1948), we are indebted to Prof. A. H. Corwin.

(*e*) *With iodine.* Dithizone (1 g) and iodine (1.05 g) in chloroform (300 ml) were stirred mechanically for 90 min with sodium carbonate solution (200 ml of 2% w/v). The organic phase was removed and evaporation of the solvent gave (V) (0.6 g; 60%; m.p. 173° decomp.) from hot ethanol.

(*f*) *With iodobenzenedichloride.* Iodobenzenedichloride dissolved in pyridine can selectively oxidise a large number of aliphatic, aromatic and heterocyclic sulphides to the corresponding sulphoxides[35].

A solution of freshly prepared iodobenzenedichloride (0.55 g) in anhydrous pyridine (3 ml) was added dropwise to a stirred solution of dithizone (0.51 g) in aqueous pyridine (7 ml of 20% w/v). The temperature was kept below 20° and direct light was excluded. After 2 h the reaction mixture was diluted with chloroform (30 ml) and the pyridine removed by washing with dilute sulphuric acid. The chloroform was washed with water, dried over anhydrous sodium sulphate and the solvent removed in a current of air. Chromatography of the crude product or alumina gave unreacted dithizone (~62%), meso-ionic compound (V) (~12%), the sulphonic acid (IX) (~5%)

and unidentified material.

(*g*) *With thallium(III) perchlorate.* A solution of 0.015 *M* thallium(III) in 0.1 *M* perchloric acid was added dropwise to a mechanically stirred solution of pure dithizone (0.5 g) in chloroform (150 ml) until the colour had changed from green through red to brown. The organic layer was then separated and the solvent removed at room temperature. The brown residue on recrystallisation from hot ethanol gave 0.3 g (60%) of the meso-ionic compound (V) (m.p. 172° decomp.).

(*h*) *With iron(III) perchlorate.* Spectrophotometric studies of the reaction between an aqueous $1.76 \cdot 10^{-5}$ *M* solution of iron(III) perchlorate and a $1.45 \cdot 10^{-5}$ *M* dithizone solution in chloroform showed that there was no reaction below pH 3 but that the meso-ionic compound (V) was formed in small amounts after 20-min shaking. The yield was increased when the iron(III) salt was present in large (30–150 fold) excess.

*Thin layer chromatography*

A slurry of neutral silica gel (Kieselgel G nach Stahl) in water was used with a Desaga TLC applicator to prepare plates (20 × 20 cm) of uniform thickness (200 μm). These were dried first in air and then in an oven at 110° for 20 min. $R_F$ values were calculated from the results of at least 3 separate runs where the solvent ran up to the 10.0-cm mark.

Exploratory work on the oxidation of dithizone was carried out by several Part (II) students at Oxford and we express our gratitude in particular to J.M. Crewe (1954), W. R. Cross (1958) and M. J. Eastwood (1958). One of us (A.M.K.) acknowledges financial support from the University of Leeds. We are indebted to Dr. P. B. Ayscough for the E.S.R. measurements.

## SUMMARY

The deterioration of solutions of dithizone in organic solvents is reviewed and shown to be due to a multiplicity of photochemical and oxidative reactions. Bis-1,5-diphenylformazan-3-yl disulphide has been isolated and characterised as a product of the action (*inter alia*) of aqueous iodine upon dithizone or silver dithizonate. Its spontaneous thermal cleavage to give an equimolar mixture of a meso-ionic compound 2,3-diphenyl-2,3-dihydrotetrazolium-5-thiolate and dithizone is shown to explain the partial regeneration of deteriorated solutions of dithizone when treated with reducing agents. The reactions of the disulphide towards a variety of reducing agents and to cleavage by metal cations is reported. The identity of Fischer's diphenylthiocarbazide, Bamberger's tetrazolium betaine and Ogilvie and Corwin's dehydrodithizone with the orange meso-ionic compound obtained from dithizone by using such oxidants as hydrogen peroxide, potassium permanganate, iodobenzene-dichloride and iron(III) or thallium(III) was established by ultimate analysis and visual and infrared spectrometry.

The behaviour of S-methyldithizone, dithizone, and its known oxidation products towards thin-layer chromatography with a range of solvents is described and the significance of the $R_F$ values discussed.

RÉSUMÉ

Une étude est effectuée sur les facteurs d'instabilité des solutions de dithizone dans des solvants organiques: réactions photochimiques et d'oxydo–réduction. Diverses substances de décomposition sont identifiées par spectrométrie dans le visible et dans l'infrarouge. On examine le comportement de la S-méthyldithizone, de la dithizone et de ses produits d'oxydation connus, par chromatographie sur couche mince, avec divers solvants. Une discussion est présentée sur la signification des valeurs $R_F$.

ZUSAMMENFASSUNG

Die Zersetzung von Dithizonlösungen in organischen Lösungsmitteln wurde überprüft und als Ursache eine Vielfalt von photochemischen und oxidativen Reaktionen festgestellt. Es wurde Bis-1,5-diphenylformazan-3-yl-disulfid isoliert und u.a. als ein Produkt der Einwirkung von wässrigem Jod auf Dithizon oder Silberdithizonat charakterisiert. Seine spontane thermische Spaltung in ein äquimolares Gemisch einer mesoionischen Verbindung 2,3-Diphenyl-2,3-dihydrotetrazolium-5-thiolat und von Dithizon erklärt die teilweise Regenerierung von zersetzten Dithizonlösungen bei Behandlung mit Reduktionsmitteln. Es wird über Reaktionen des Disulfids mit verschiedenen Reduktionsmitteln sowie Spaltung durch Metallkationen berichtet. Durch Elementaranalyse sowie Spektrometrie im Sichtbaren und Infrarot wurde die Identität von Fischers Diphenylthiocarbazid, Bambergers Tetrazoliumbetain sowie Ogilvies und Corwins Dehydrodithizon mit der orangefarbenen mesoionischen Verbindung festgestellt, die aus Dithizon bei Verwendung von Oxidationsmitteln wie Wasserstoffperoxid, Kaliumpermanganat, Jodbenzoldichlorid und Eisen(III) oder Thallium(III) erhalten wird. Es wird das Verhalten von S-Methyldithizon, Dithizon und dessen bekannten Oxidationsprodukten bei der Dünnschichtchromatographie mit einer Reihe von Lösungsmitteln beschrieben und die Bedeutung der $R_F$-Werte diskutiert.

REFERENCES

1 D. A. BIDDLE, *Ind. Eng. Chem., Anal. Ed.*, 8 (1936) 99.
2 H. IRVING, S. J. H. COOKE, S. C. WOODGER AND R. J. P. WILLIAMS, *J. Chem. Soc.*, (1949) 541.
3 H. FISCHER AND W. WEYL, *Wiss. Veröffentl. Siemens-Werken*, 14 (1935) 41.
4 G. I. IWANTSCHEFF, *Dithizon und seine Anwendung in der Mikro- und Spurenanalyse*, GMBH Weinheim, 1958.
5 E. FISCHER AND E. BESTHORN, *Ann.*, 212 (1878) 316.
6 O. WEBER, *Dissertation*, Zagreb, 1956.
7 E. C. DAWSON, *Analyst*, 73 (1948) 618.
8 H. IRVING AND R. S. RAMAKRISHNA, *J. Chem. Soc.*, (1961) 1272, 2118.
9 H. M. N. H. IRVING AND D. C. RUPAINWAR, *Anal. Chim. Acta*, 48 (1969) 187.
10 P. A. CLIFFORD, *J. Assoc. Offic. Agr. Chemists*, 21 (1938) 695.
11 H. M. N. H. IRVING AND U. S. MAHNOT, *Chem. Ind. (London)*, (1967) 193; *Talanta*, 15 (1968) 811.
12 S. S. SAHOTA, *Ph. D. Thesis*, Leeds University, 1964.
13 M. BUSCH, *Ber.*, 28 (1895) 2635; *J. Prakt. Chem.*, (2) 60 (1899) 25.
14 W. BAKER, W. OLLIS, A. PHILLIPS AND T. STRAWFORD, *J. Chem. Soc.*, (1949) 307; (1951) 289.
15 A. M. KIWAN AND H. M. N. H. IRVING, *Chem. Commun.*, (1970) 928; *J. Chem. Soc., B* (1971) 901.

16 N. SHEPPARD, *Trans. Faraday Soc.*, 46 (1950) 429.
17 J. CYMERAMAN AND J. B. WILLIS, *J. Chem. Soc.*, (1951) 1332.
18 Y. MINOURA AND T. MORIYOSHI, *Trans. Faraday Soc.*, 59 (1963) 1504.
19 H. FREISER, Q. FERNANDO AND K. S. MATH, *Anal. Chem.*, 36 (1964) 1762.
20 H. M. N. H. IRVING, U. S. MAHNOT AND D. C. RUPAINWAR, *Anal. Chim. Acta*, 49 (1970) 261.
21 D. C. RUPAINWAR, *D. Phil. Thesis*, University of Leeds, 1969, where a fuller discussion is given.
22 R. S. RAMAKRISHNA AND H. M. N. H. IRVING, *Chem. Ind. (London)*, (1969) 325; *Anal. Chim. Acta*, 48 (1969) 251.
23 R. S. RAMAKRISHNA AND H. M. N. H. IRVING, *Chem. Commun.*, (1969) 1356; *Anal. Chim. Acta*, 49 (1970) 9.
24 L. F. LINDON, *Coordination Chem. Rev.*, 4 (1969) 41.
25 J. STARÝ AND J. RŮŽIČKA, *Talanta*, 15 (1968) 505; J. STARÝ AND J. MAREK, *Chem. Commun.*, (1970) 519 (*cf.* H. M. N. H. IRVING).
26 L. HELLERMAN, F. P. CHINARD AND P. A. RAMSDELL, *J. Amer. Chem. Soc.*, 63 (1941) 2551.
27 J. W. OGILVIE AND A. H. CORWIN, *J. Amer. Chem. Soc.*, 83 (1961) 5023.
28 E. BAMBERGER, R. PADOVA AND F. ORMEROD, *Ann.*, 446 (1926) 260.
29 A. M. KIWAN AND H. M. N. H. IRVING, *J. Chem. Soc., B* (1971) 898.
30 H. M. N. H. IRVING, D. C. RUPAINWAR AND S. S. SAHOTA, *Anal. Chim. Acta*, 45 (1969) 249.
31 H. G. C. KING AND G. PRUDEN, *Analyst*, 96 (1971) 146.
32 W. E. SAVIGE AND J. A. MACLAREN, in N. KHARASCH AND C. Y. MEYBRS, *The Chemistry of Organic Sulphur Compounds, Vol. 2*, Pergamon Press, 1966, p. 367.
33 A. W. NINEHAM, *Chem. Rev.*, 55 (1955) 380.
34 J. E. MORTON, A. D. CAMPBELL AND T. S. MA, *Analyst*, 78 (1953) 722.
35 G. BARBIERI, M. CINQUINI, S. COLONNA AND F. MONTANARI, *J. Chem. Soc.*, C (1968) 659.

*Analytica Chimica Acta*
Elsevier Publishing Company, Amsterdam
Printed in The Netherlands



# BISMUTH–DITHIZONE EQUILIBRIA AND HYDROLYSIS OF BISMUTH ION IN AQUEOUS SOLUTION*

TERRY F. BIDLEMAN**
*School of Chemistry, University of Minnesota, Minneapolis, Minn. (U.S.A.)*
(Received 11th March 1971)

Dithizone (diphenylthiocarbazone, $H_2Dz$) is one of the most popular organic reagents for the separation and determination of traces of metals. Extraction equilibrium data have been obtained for several metal–dithizone reactions and have been compiled by Sandell[1] and Iwantscheff[2]. Such information allows the analyst to predict suitable separation and determination conditions by a few simple calculations.

Although a number of studies of the bismuth–dithizone system have been made[3-7], there is disagreement among various workers' values for the extraction equilibrium constant. Also the hydrolysis of bismuth ion in dilute ($< 10^{-4}$ *M*) aqueous solution has not been well studied. In this work the equilibrium constants for the bismuth–dithizone system and the formation constants of the species $BiOH^{2+}$, $Bi(OH)_3$, and $Bi(OH)_4^-$ have been determined.

## EXPERIMENTAL

### *Reagents*

Carbon tetrachloride and dithizone were purified by Mathre and Sandell's method[8]. The dithizone purity, as determined by photometric titration with silver, was 99.4%. Water having a heavy metal content of 0.0015 p.p.m. (as lead) was prepared by twice distilling from borosilicate glass apparatus the distilled water supplied to the laboratory. Pure aqueous ammonia solution was prepared by isothermal distillation from 15 *M* ammonia liquor. Carbonate-free solutions of sodium hydroxide were obtained by diluting a saturated solution with deaereated water. A solution of sodium perchlorate was prepared by neutralizing sodium carbonate with perchloric acid and boiling to remove carbon dioxide. Heavy metals were removed from the solution by dithizone extraction. Standard bismuth solutions were prepared from the reagent-grade metal (99.8% purity). All other chemicals were of reagent-grade quality.

Bismuth dithizonate was prepared as follows. A solution of 0.003 *M* bismuth in 0.01 *M* perchloric acid was shaken with an equal volume of 0.12% dithizone in chloroform. The extract was washed twice with aqueous 2 *M* ammonia to remove unreacted dithizone. 1 l of extract was reduced to 125 ml by heating to 40° and passing dry nitrogen through the solution. Carbon tetrachloride (75 ml) was added and the evaporation was continued to a volume of about 30 ml. Another 10-ml portion of

* From the Ph.D. thesis of T.F.B., Univ. of Minn. 1970.
** Present address: Department of Chemistry, Dalhousie University, Halifax, Nova Scotia, Canada.

carbon tetrachloride was added and solution was evaporated to a small volume. After cooling in ice, the crystals were collected and washed with carbon tetrachloride. The product was recrystallized by dissolving in 2:1 chloroform–carbon tetrachloride, evaporating to a small volume, adding carbon tetrachloride, again evaporating to a volume of a few milliliters, and cooling in ice. The crystals were vacuum-dried at 80° for two days. They had a metallic green lustre but became orange-red when powdered.

The product was analyzed for bismuth by EDTA titration after decomposing a sample by heating with perchloric–sulfuric acid. A carbon tetrachloride solution of the complex was shaken with 1.0 *M* hydrochloric acid and the liberated dithizone was determined spectrophotometrically. Calculated for $Bi(HDz)_3$: 21.44% Bi, 78.56% $HDz^-$; found: 21.12% Bi, 78.6% $HDz^-$; solubility ($CCl_4$, 25°) $= 5.4 \cdot 10^{-4}$ *M*; m.p. 211°.

*Apparatus*

Beckman DU and Cary 15 spectrophotometers were used. Path lengths of spectrophotometer cells were checked with an alkaline chromate solution[9].

Measurements of pH were made with a Corning Model 7 pH meter equipped with a Corning single-probe glass–Ag/AgCl reference electrode. Buffers for pH meter standardization were prepared according to the directions given by Bates[10].

Borosilicate glass separatory funnels having Teflon stopcocks were used for extraction work involving acidic solutions. Polypropylene separatory funnels were used for extractions from basic solutions as adsorption losses of bismuth were found to be less than on glass funnels of similar size.

*Molar absorptivities of dithizone and bismuth dithizonate*

Stock solutions of dithizone and bismuth dithizonate were prepared by dissolving weighed quantities of the pure solids in carbon tetrachloride which had been bubbled with nitrogen to remove dissolved oxygen. Quantitative dilutions of the stock solutions were made and the absorbances were measured at 25°. Solutions of dithizone in aqueous ammonia were used to determine the molar absorptivity of primary dithizonate ion, $HDz^-$. Beer's law is obeyed at the measured wavelengths. The visible spectra of dithizone and bismuth dithizonate in carbon tetrachloride are shown in Fig. 1; the molar absorptivities are listed in Table I.

TABLE I

MOLAR ABSORPTIVITIES OF DITHIZONE, BISMUTH DITHIZONATE, AND PRIMARY DITHIZONATE ION

| | *Conc. range* ($M \cdot 10^5$) | *Solvent* | $\varepsilon$ ($l\ mole^{-1}\ cm^{-1} \cdot 10^{-4}$) | | | |
|---|---|---|---|---|---|---|
| | | | 620 *nm* | 490 *nm* | 475 *nm* | 450 *nm* |
| $H_2Dz$ | 0.25–2.8 | $CCl_4$ | 3.25 | 1.13 | | 1.93 |
| $Bi(HDz)_3$ | 0.14–1.2 | $CCl_4$ | 0.21 | 7.92 | | |
| $HDz^-$ | 0.73–2.9 | $H_2O$ | | | 2.24 | |

COMPOSITION OF THE EXTRACTED BISMUTH SPECIES

Spectrophotometric titration of $2.5 \cdot 10^{-4}$ mmole of bismuth with dithizone

was carried out by extracting from pH 7.5 acetate buffer and pH 9.3 ammonia–ammonium perchlorate buffer. The reacting ratios of dithizone: bismuth in these experiments were 2.88/1.00 and 2.92/1.00, respectively, indicating that the extracted complex is the primary dithizonate, $Bi(HDz)_3$.

Secondary dithizonates, *i.e.* complexes of the $Dz^{2-}$ anion, have been reported for several of the dithizone-reacting metals[1,2]. Early work by Reith and Van Dijk[3] suggested the formation of secondary bismuth dithizonate, $Bi_2Dz_3$. Their evidence was based on titration data at pH 7.5 (acetate buffer). Koroleff[4] later claimed to have confirmed Reith and Van Dijk's findings.

In order to verify further the composition of the extracted dithizonate, two experiments were carried out.

1. A solution of dithizone in carbon tetrachloride ($10^{-4}$ *M*) was shaken with a 10-fold excess of bismuth in pH 10.8 ammonia–ammonium perchlorate buffer.

2. A solution of the primary dithizonate, prepared by dissolving the solid product in carbon tetrachloride, was shaken with a 10-fold excess of bismuth at pH 9.8

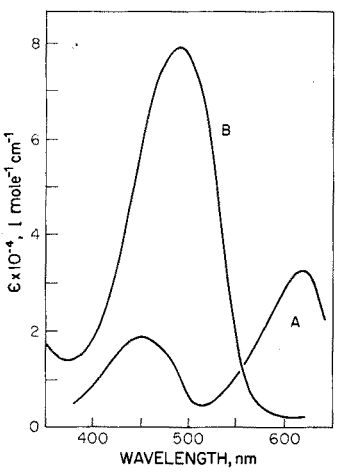


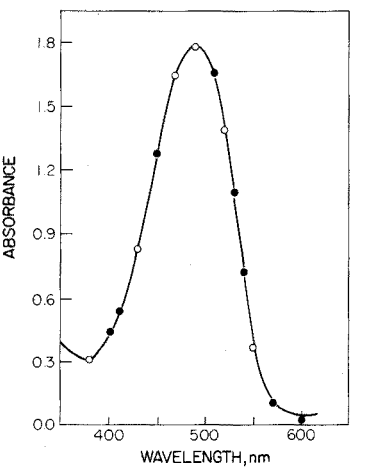


Fig. 1. Visible spectra of dithizone and bismuth dithizonate in carbon tetrachloride. (A) Dithizone; (B) $Bi(HDz)_3$.

Fig. 2. Visible spectra of $2.2 \cdot 10^{-5}$ *M* $Bi(HDz)_3$ in carbon tetrachloride (1-cm cell). (○) Prepared by extracting dithizone with a 10-fold excess of bismuth from pH 10.8 ammonia–ammonium perchlorate buffer. (●) A solution of $Bi(HDz)_3$, prepared by dissolving the solid in $CCl_4$, shaken with a 10-fold excess of bismuth in pH 9.8 ammonia–ammonium perchlorate buffer. (——) Solid $Bi(HDz)_3$ dissolved in $CCl_4$.

These conditions of high pH and excess metal are those which normally favor the formation of secondary dithizonates. The spectra of the extracts are compared to that of the primary complex in Fig. 2. In order to facilitate comparison of these spectra, the absorbances of the extracted product at all wavelengths were mathematically adjusted by application of Beer's law to correspond to a concentration of $2.2 \cdot 10^{-5}$ *M*. There appears to be no difference in the spectra, further indicating that the secondary dithizonate is not formed under these conditions.

The equilibrium constant for the extraction reaction

$$Bi^{3+} + 3\{H_2Dz\}_o \rightleftharpoons \{Bi(HDz)_3\}_o + 3\,H^+ \quad (1)$$

is the *extraction constant*, $K_{ext} = [Bi(HDz)_3]_o[H^+]^3/[Bi^{3+}][H_2Dz]_o^3$. The subscript o refers to a species in the carbon tetrachloride phase; w or no subscript indicates an aqueous species. The extraction coefficient is defined as the ratio of the analytical concentration of bismuth in the organic phase to that in the aqueous phase. If $Bi^{3+}$ predominates in the aqueous phase and if only $Bi(HDz)_3$ is extracted,

$$E = \frac{[Bi(HDz)_3]_o}{[Bi^{3+}]} = \frac{K_{ext}[H_2Dz]_o^3}{[H^+]^3} \quad (2)$$

If hydrolyzed bismuth species are present in addition to free bismuth ion, the expression for $E$ is of the form:

$$E = \frac{K_{ext}[H_2Dz]_o^3}{[H^+]^3(1+\Sigma\beta_n[OH^-]^n)} \quad (3)$$

or

$$E = \frac{K'_{ext}[HDz^-]^3}{1+\Sigma\beta_n[OH^-]^n} \quad (4)$$

where $\beta_n$ is the notation for cumulative formation constants of the form $\beta_n = [Bi(OH)_n^{3-n}]/[Bi^{3+}][OH^-]^n$. In eqn. (4), $K'_{ext} = K_{ext} \cdot P_{dz}^3/K_{dz}^3$. The quantities $P_{dz}$ and $K_{dz}$ are the partition coefficient and dissociation constant of dithizone, respectively, and are defined by $P_{dz} = [H_2Dz]_o/[H_2Dz]_w$ and $K_{dz} = [H^+][HDz^-]/[H_2Dz]_w$. Equations (3) and (4) further assume that the concentration of $Bi(HDz)_3$ in the aqueous phase is negligible compared to the other forms of bismuth, that no complexing agents other than dithizone and hydroxide ion are present, and that no association or polynucleation of bismuth species occurs in either phase.

*Determination of $K_{ext}$ and $\beta_1$*

In the pH range where $Bi^{3+}$ and $BiOH^{2+}$ are the major bismuth species in aqueous solution, eqn. (3) reduces to

$$E = \frac{K_{ext}[H_2Dz]_o^3}{[H^+]^3(1+\beta_1[OH^-])} \quad (5)$$

Introducing $K_w = [H^+][OH^-]$ and rearranging:

$$\frac{[H_2Dz]_o^3}{E[H^+]^3} = \frac{\beta_1 K_w}{K_{ext}[H^+]} + \frac{1}{K_{ext}} \quad (6)$$

A plot of the left side of eqn. (6) *vs.* $1/[H^+]$ should be linear and $K_{ext}$ and $\beta_1$ may be evaluated from the slope and intercept.

Aqueous solutions of bismuth containing perchloric acid and sodium perchlorate ($\mu = 0.1$) were shaken with carbon tetrachloride solutions of dithizone at 25°. Equilibrium was established within 2 min, contrary to reports of other workers[6] who claimed that longer shaking times were required. Dithizone and bismuth dithizonate

in the organic layer were determined spectrophotometrically by measuring the absorbances at 490 and 620 nm. Bismuth in the aqueous phase was determined spectrophotometrically after quantitative extraction with dithizone. The hydrogen ion concentration was determined by titration with standard base.

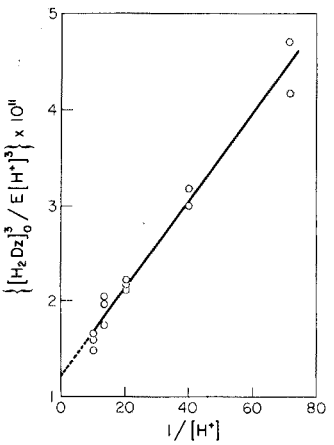


Fig. 3. Determination of $\beta_1$ and $K_{ext}$ ($\mu=0.1$); slope (least sq.) $=4.56\cdot10^{-13}$, intercept $=1.22\cdot10^{-11}$.

Figure 3 shows a plot of $[H_2Dz]_o^3/E[H^+]^3$ *vs.* $1/[H^+]$. The values of the extraction coefficient were independent of the concentration of bismuth in either phase in the ranges $\Sigma[Bi]_w = 1.7\cdot10^{-6}$–$1.7\cdot10^{-5}$ and $\Sigma[Bi]_o = 9\cdot10^{-6}$–$1.4\cdot10^{-5}$, thus disproving the possibility of associated or polynuclear bismuth complexes in either phase. Calculations based on Olin's constants[11] indicated that polynuclear bismuth species in the aqueous phase were not to be expected under these conditions. From the slope and intercept, $K_{ext} = (8.2\pm0.9)\cdot10^{10}$ and $\beta_1 K_w = 0.037\pm0.004$ ($\mu=0.1$). (Precision in this paper is reported as the standard deviation of a single determination.)

TABLE II

BISMUTH–DITHIZONE EXTRACTION CONSTANT AT $\mu=1.0$

| *Shaking time (min)* | $[H^+]$ | $[H_2Dz]_o \cdot 10^4$ | $\Sigma[Bi]_o \cdot 10^6$ | $\Sigma[Bi]_w \cdot 10^6$ | $E$ | $K_{ext} \cdot 10^{-10}$ |
|---|---|---|---|---|---|---|
| 1.0 | 0.998 | 2.94 | 8.08 | 6.38 | 1.27 | 5.0 |
| 1.5 | 0.994 | 1.42 | 3.28 | 24.4 | 0.143 | 5.2 |
| 2.0 | 1.006 | 2.88 | 4.43 | 3.17 | 1.40 | 6.0 |
| 2.0 | 1.006 | 1.21 | 1.07 | 14.8 | 0.072 | 4.2 |
| 2.0 | 0.994 | 1.31 | 2.97 | 24.6 | 0.121 | 5.3 |
| 2.5 | 0.998 | 2.97 | 4.11 | 2.35 | 1.75 | 6.6 |
| 2.5 | 0.994 | 1.42 | 3.78 | 24.8 | 0.153 | 5.2 |
| 3.0 | 1.000 | 2.65 | 6.80 | 7.70 | 0.885 | 4.8 |
| 3.0 | 0.987 | 2.22 | 6.93 | 9.90 | 0.706 | 6.2 |
| 3.0 | 0.975 | 3.68 | 7.07 | 2.59 | 2.73 | 5.1 |
| 4.0 | 0.998 | 2.94 | 7.79 | 6.48 | 1.20 | 4.7 |
| 5.0 | 0.994 | 1.40 | 3.62 | 24.3 | 0.149 | 5.3 |
| 5.0 | 0.998 | 4.36 | 6.84 | 1.19 | 5.75 | 6.9 |

For $K_w^0 = [H^+][OH^-](f_{H^+})(f_{OH^-}) = K_w(f_{H^+})(f_{OH^-}) = 1.008 \cdot 10^{-14}$, $f_{H^+} = 0.83$ and $f_{OH^-} = 0.76$, $\beta_1 = [BiOH^{2+}]/[Bi^{3+}][OH^-] = (2.3 \pm 0.2) \cdot 10^{12}$. The value of $\beta_1 K_w$ determined in this work may be compared with Olin's result[11] of 0.027 as to order of magnitude only, since his work was done at an ionic strength of 3.0.

The extraction constant was also determined at an ionic strength of 1.0 by extracting bismuth from 1.0 *M* perchloric acid. At this acidity less than 4% of the bismuth is hydrolyzed and $K_{ext}$ is easily determined by measuring the other quantities in eqn. (2). Thirty-two determinations gave a mean value of $(5.8 \pm 0.9) \cdot 10^{10}$ for the extraction constant at $\mu = 1.0$; a sample of the data is given in Table II.

The values of $K_{ext}$ found in this work are larger than those reported by Busev and Bazhanova[6] ($9.4 \cdot 10^9$, $\mu = 0.2$) and Koroleff[4] ($5.6 \cdot 10^9$), but are in reasonable agreement with those of Pilipenko[5] ($3.7 \cdot 10^{10}$, $\mu = 0.5$) and Brock[7], another worker in this laboratory ($4.4 \cdot 10^{10}$, $\mu = 0.5$). The small difference between the values of $K_{ext}$ at ionic strengths 0.1 and 1.0 seems to indicate that bismuth ion is not strongly complexed by perchlorate.

*The partition coefficient of bismuth dithizonate*

The partition coefficient of bismuth dithizonate, $P_{Bi} = [Bi(HDz)_3]_o/[Bi(HDz)_3]_w$, was determined as follows. Portions (10 ml) of approximately saturated solutions of bismuth dithizonate in carbon tetrachloride containing varying concentrations of dithizone were shaken with 800-ml volumes of 0.1 *M* sodium perchlorate at pH 2 for 1–2 h at 25°. The phases were separated by centrifugation followed by filtration of the aqueous phase through a plug of glass wool. Two experiments in which the aqueous phase was unfiltered or filtered through filter paper yielded results which were the same as for the glass wool-filtered samples. An aliquot of the aqueous phase was analyzed spectrophotometrically for bismuth after dithizone extraction; dithizone and bismuth dithizonate in the organic phase were determined spectrophotometrically.

Eight determinations of the partition coefficient gave a mean value of $(2.5 \pm 0.3) \cdot 10^4$. The experimental values of the extraction coefficient were independent of the dithizone concentration in the range $[H_2Dz]_o = 8.0 \cdot 10^{-4}$–$2.0 \cdot 10^{-3}$ *M*, indicating that the maximum value had been reached, *i.e.* $E = P_{Bi}$. Furthermore, a calculation of the concentrations of the other bismuth species present ($Bi^{3+}$ and $BiOH^{2+}$) using the equilibrium constants determined in this work showed that they were at least $10^3$ times smaller than the experimental $\Sigma[Bi]_w$, and therefore $\Sigma[Bi]_w = [Bi(HDz)_3]_w$.

*Determination of $\beta_3$*

If only one hydrolyzed bismuth species, $Bi(OH)_n^{3-n}$, predominates in a given pH range, eqn. (4) reduces to

$$E = \frac{K'_{ext}[HDz^-]^3}{\beta_n[OH^-]^n} \tag{7}$$

or

$$\log E - 3 \log [HDz^-] = n \cdot pOH + \log K'_{ext}/\beta_n \tag{8}$$

A plot of the left side of eqn. (8) *vs.* pOH allows the determination of $n$ and $\beta_n$.

Ammonia–ammonium perchlorate solutions of bismuth were shaken with

dithizone in carbon tetrachloride; equilibrium was established within 1 min. The extraction coefficient and dithizonate ion concentration were determined spectrophotometrically. The pH was measured with a glass electrode; borate (pH 9.18), carbonate (pH 10.00), and saturated calcium hydroxide (pH 12.45) buffers were used to standardize the pH meter. In several experiments the bismuth was added as the dithizonate in carbon tetrachloride. In some cases the basic bismuth solutions were allowed to stand for 24–48 h before extraction in order to determine whether the hydrolysis was time-dependent.

TABLE III

EXTRACTION OF BISMUTH FROM AMMONIA–AMMONIUM PERCHLORATE SOLUTIONS, $\mu = 0.1$

| *pOH* | $[HDz^-]$ $\cdot 10^5$ | $\Sigma[Bi]_o$ $\cdot 10^6$ | $\Sigma[Bi]_w$ $\cdot 10^6$ | *E* | $K'_{ext}/\beta_{3a}$ $\cdot 10^{-5}$ | *Method of Bi addition*[a] |
|---|---|---|---|---|---|---|
| 2.72 | 4.09 | 2.02 | 2.20 | 0.918 | 0.93 | D |
| 2.73 | 2.95 | 2.33 | 4.67 | 0.499 | 1.25 | D |
| 3.01 | 3.20 | 12.8 | 1.75 | 7.31 | 2.08 | A |
| 3.09 | 1.00 | 1.33 | 3.43 | 0.388 | 2.07 | B |
| 3.09 | 1.27 | 2.68 | 3.38 | 0.793 | 2.07 | C |
| 3.11 | 0.991 | 1.26 | 3.20 | 0.394 | 1.90 | B |
| 3.15 | 2.44 | 8.61 | 1.60 | 5.38 | 1.32 | D |
| 3.20 | 1.78 | 7.38 | 1.75 | 4.22 | 1.88 | A |
| 3.45 | 1.89 | 11.8 | 1.08 | 10.9 | 0.73 | D |
| 3.53 | 0.916 | 3.95 | 0.909 | 4.35 | 1.46 | A |
| 3.55 | 0.903 | 3.93 | 0.909 | 4.32 | 1.32 | A |
| 3.99 | 0.573 | 15.5 | 0.603 | 25.7 | 1.47 | D |
| 4.08 | 0.295 | 12.5 | 1.86 | 6.72 | 1.51 | A |

[a] A = Bi solution, pH 3, made basic immediately before extraction. B = Bi solution, pH 10.9, allowed to stand 24 h before extraction. C = Bi solution, pH 10.9, allowed to stand 48 h before extraction. D = Bi added as $Bi(HDz)_3$ in carbon tetrachloride.

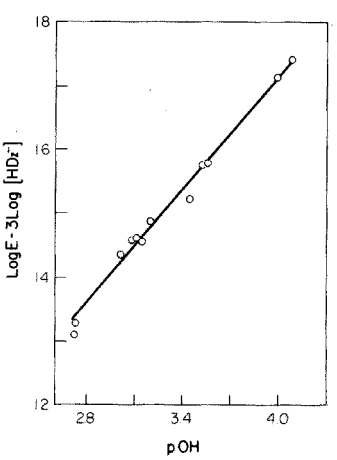


Fig. 4. Extraction of bismuth from ammonia–ammonium perchlorate solution ($\mu = 0.1$); slope (least sq.) = 2.99.

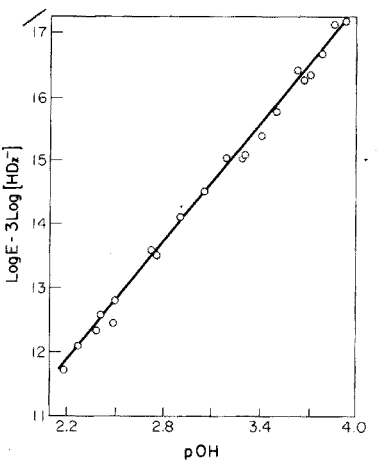


Fig. 5. Extraction of bismuth from ammonia–ammonium perchlorate solution ($\mu = 1.0$); slope (least sq.) = 3.08.

Table III and Figs. 4 and 5 give the results of a series of experiments carried out at ionic strengths 0.1 and 1.0. From the slopes of 3, the principal bismuth species in aqueous solutions is $Bi(OH)_3$. The average values of $K'_{ext}/\beta_{3a}$ at ionic strengths 0.1 and 1.0 are $(1.5 \pm 0.4) \cdot 10^5$ and $(2.1 \pm 0.6) \cdot 10^5$ respectively, and are independent of the concentrations of bismuth in either phase within the experimental limits (Figs. 6 and 7). Therefore only mononuclear complexes are present in both phases. The accuracy of the value of $K'_{ext}/\beta_{3a}$ obtained at $\mu = 1.0$ is questionable because of the uncertainty in the pH measurements caused by the residual liquid junction potential (the buffers used to standardize the pH meter had ionic strengths $\leqslant 0.1$). For Sandell's value[12] of $K_{dz}/P_{dz} = 1.4 \cdot 10^{-9}$ ($\mu = 0.1$), and $K_{ext} = 8.2 \cdot 10^{10}$, $\beta_{3a} = [Bi(OH)_3]/[Bi^{3+}](a_{OH^-})^3 = (2.0 \pm 0.6) \cdot 10^{32}$ ($\mu = 0.1$). With a value for $f_{OH^-} = 0.76$, $\beta_3 = [Bi(OH)_3]/[Bi^{3+}][OH^-]^3 = (8.8 \pm 2.6) \cdot 10^{31}$.

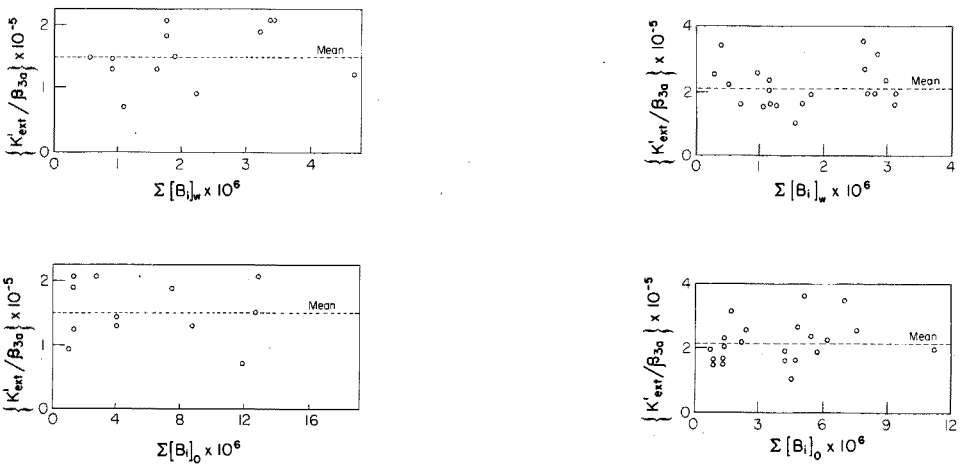


Fig. 6. Constancy of $K'_{ext}/\beta_{3a}$ with variations in the analytical concentration of bismuth in each phase, $\mu = 0.1$.

Fig. 7. Constancy of $K'_{ext}/\beta_{3a}$ with variations in the analytical concentration of bismuth in each phase, $\mu = 1.0$.

*The Solubility of α-$Bi_2O_3$ in Sodium Hydroxide Solutions and Determination of $\beta_4$*

The solubility of $Bi_2O_3$ in strongly basic solutions may be described by the equations:

$$Bi_2O_3(s) + 3\,H_2O \rightleftharpoons 2\,Bi(OH)_3 \tag{9}$$

$$Bi_2O_3(s) + 3\,H_2O + 2\,OH^- \rightleftharpoons 2\,Bi(OH)_4^- \qquad K_s = \frac{[Bi(OH)_4^-]}{[OH^-]} \tag{10}$$

$$S = [Bi(OH)_3]_{sat} + [Bi(OH)_4^-] = [Bi(OH)_3]_{sat} + K_s[OH^-] \tag{11}$$

A plot of the solubility $S$ *vs.* $[OH^-]$ should have a slope of $K_s$ and an intercept of $[Bi(OH)_3]_{sat}$, the intrinsic solubility of bismuth hydroxide. Schumb and Rittner[13] reported the solubility of α-$Bi_2O_3$ in 0.5–2.5 *M* sodium hydroxide; a plot of their data gives a value for $K_s$ of $4.8 \cdot 10^{-5}$ and an intrinsic solubility of $4 \cdot 10^{-6}$ *M*. The rather long extrapolation introduces uncertainty in the latter value, and the ionic strength

was not held constant in their work. Therefore the solubility of $\alpha$-$Bi_2O_3$ was determined at lower hydroxide concentrations and at a constant ionic strength of 1.0.

Weighed quantities of $Bi_2O_3$ (0.1–1.0 g) were equilibrated with sodium hydroxide–sodium perchlorate solutions ($\mu = 1.0$) for 2–9 days. The oxide was confirmed to be the $\alpha$-form by obtaining the X-ray diffraction pattern and comparing it with that published by the National Bureau of Standards[14]. Equilibrations were done in polyethylene ampoules having a 30–40 ml capacity. The ampoules were constructed from low-density polyethylene tubing and rod and heat sealed by the method of Ehmann and McKown[15]. The ampoules were rotated end-over-end in a thermostated water bath at $25.0 \pm 0.2°$. Before analysis the tubes were centrifuged and cut open, and the supernatant solution was filtered through a medium-porosity glass frit. A Tyndall beam passed through a portion of the filtered solution appeared to be the same as that passed through distilled water, so it is unlikely that the filtered solutions contained colloids. The bismuth content was determined spectrophotometrically with dithizone; the sodium hydroxide concentration was determined by titrating with standard acid.

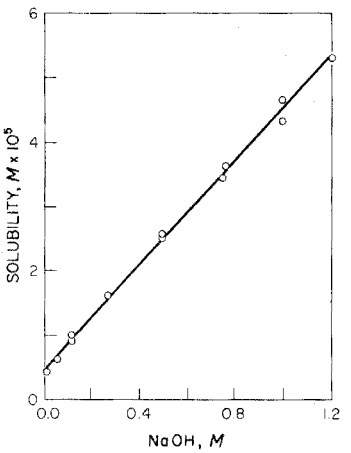


Fig. 8. Solubility of $\alpha$-$Bi_2O_3$ in sodium hydroxide–sodium perchlorate solution, $\mu = 1.0$ (except [NaOH] = 1.22 $M$); slope (least sq.) = $4.04 \cdot 10^{-5}$, intercept = $4.52 \cdot 10^{-6}$.

A linear relationship between solubility and hydroxide concentration was obtained (Fig. 8). The solubility was independent of the weight of oxide taken and equilibrium was established in 2–5 days. The value of $K_s$ obtained is $4.04 \cdot 10^{-5}$; the extrapolated intrinsic solubility is $4.52 \cdot 10^{-6}$ $M$. For the reaction

$$Bi(OH)_3 + OH^- \rightleftharpoons Bi(OH)_4^-$$

$K_4 = [Bi(OH)_4^-]/[Bi(OH)_3][OH^-] = K_s/[Bi(OH)_3]_{sat} = 8.96$ ($\mu = 1.0$). The solubility data do not distinguish between mononuclear $Bi(OH)_4^-$ and a polynuclear species having the general formula $Bi_n(OH)_{3n+1}^-$. However, basic bismuth solutions are mononuclear at least up to the intrinsic solubility of $Bi(OH)_3$, as shown in the preceding section. By combination of $\beta_3$ and $K_4$, $\beta_4 = [Bi(OH)_4^-]/[Bi^{3+}][OH^-]^4 = \beta_3 K_4 = (7.9 \pm 2.3) \cdot 10^{32}$. This value is somewhat uncertain because it involves the combination of two constants determined at different ionic strengths. However $K_4$

will be less subject to ionic strength changes because of the partial cancelling of the activity coefficients of $OH^-$ and $Bi(OH)_4^-$. From the value of $\beta_3$ and the intrinsic solubility, $K_{sp}=[Bi^{3+}][OH^-]^3=[Bi(OH)_3]_{sat}/\beta_3=(5.1\pm1.5)\cdot10^{-38}$ (solid phase $=\alpha$-$Bi_2O_3$).

The author wishes to thank Dr. E. B. Sandell for his many helpful suggestions and criticisms during the course of this work.

SUMMARY

The reaction of bismuth with dithizone and the hydrolysis of bismuth ion in dilute solution were studied. Bismuth is extracted from aqueous solutions with carbon tetrachloride solutions of dithizone as the primary complex, $Bi(HDz)_3$; the molar absorptivities of dithizone and bismuth dithizonate have been determined. The extraction constant of the bismuth–dithizone system, $K_{ext}=[Bi(HDz)_3]_o[H^+]^3/[Bi^{3+}][H_2Dz]_o^3$, has values of $8.2\cdot10^{10}$ and $5.8\cdot10^{10}$ at ionic strengths 0.1 and 1.0 respectively. The partition coefficient of bismuth dithizone, $P_{Bi}=[Bi(HDz)_3]_o/[Bi(HDz)_3]_w$, between carbon tetrachloride and water is $2.5\cdot10^4$ ($\mu=0.1$). In dilute solution, bismuth ion hydrolysis results in the formation of the mononuclear species $BiOH^{2+}$...$Bi(OH)_4^-$. The cumulative formation constants for three of these species at 25° are: $\beta_1=2.3\cdot10^{12}$ ($\mu=0.1$), $\beta_3=8.8\cdot10^{31}$ ($\mu=0.1$), and $\beta_4=7.9\cdot10^{32}$ ($\mu=$ variable), where $\beta_n \triangleq [Bi(OH)_n^{3-n}]/[Bi^{3+}][OH^-]^n$. The formation of $Bi(OH)_2^+$ was not studied. No evidence for the formation of polynuclear species in bismuth solutions $\leqslant 10^{-5}$ $M$ was found.

RÉSUMÉ

Une étude est effectuée sur la réaction du bismuth avec la dithizone et l'hydrolyse de l'ion bismuth en solution diluée. Le bismuth est extrait en solution aqueuse á l'aide de solutions de dithizone dans la tétrachlorure de carbone, sous forme de $Bi(HDz)_3$. La constante d'extraction du système bismuth–dithizone est de $8.2\cdot10^{10}$ et $5.8\cdot10^{10}$, aux forces ioniques de 0.1 et 1.0 respectivement. Le coefficient de partage du dithizonate de bismuth entre tétrachlorure de carbone et eau est de $2.5\cdot10^4$ ($\mu=0.1$). En solution diluée, il y a hydrolyse et formation de particules mononucléaires $BiOH^{2+}$...$Bi(OH)_4^-$. Des particules polynucléaires dans des solutions de bismuth $\leqslant 10^{-5}M$ n'ont pas été décelées.

ZUSAMMENFASSUNG

Die Reaktion von Wismut mit Dithzon und die Hydrolyse von Wismutionen in verdünnter Lösung wurden untersucht. Wismut wird aus wässrigen Lösungen mit Tetrachlorkohlenstofflösungen von Dithizon als primärer Komplex $Bi(HDz)_3$ extrahiert; die molaren Extinktionskoeffizienten von Dithizon und Wismutdithizonat wurden bestimmt. Die Extraktionskonstante des Wismut–Dithizon-Systems, $K_{ext}=[Bi(HDz)_3]_o[H^+]^3/[Bi^{3+}][H_2Dz]_o^3$, hat die Werte $8.2\cdot10^{10}$ bzw. $5.8\cdot10^{10}$ bei Ionenstärken von 0.1 und 1.0. Der Verteilungskoeffizient von Wismutdithizonat, $P_{Bi}=[Bi(HDz)_3]_o/[Bi(HDz)_3]_w$, zwischen Tetrachlorkohlenstoff und Wasser ist

$2.5 \cdot 10^4$ ($\mu = 0.1$). In verdünnter Lösung hydrolysieren Wismutionen zu den einkernigen Spezies $BiOH^{2+}$...$Bi(OH)_4^-$. Die kumulativen Bildungskonstanten für drei dieser Spezies bei 25° sind: $\beta_1 = 2.3 \cdot 10^{12}$ ($\mu = 0.1$), $\beta_3 = 8.8 \cdot 10^{31}$ ($\mu = 0.1$) und $\beta_4 = 7.9 \cdot 10^{32}$ ($\mu$ = variabel), wobei $\beta_n = [Bi(OH)_n^{3-n}]/[Bi^{3+}][OH^-]^n$. Die Bildung von $Bi(OH)_2^+$ wurde nicht untersucht. Hinweise auf die Bildung mehrkerniger Spezies in Wismutlösungen $\leqslant 10^{-5} M$ wurden nicht gefunden.

## REFERENCES


1 E. B. SANDELL, *Colorimetric Determination of Traces of Metals*, 3rd Edn., Interscience, New York, 1959.
2 G. IWANTSCHEFF, *Das Dithizon und seine Anwendung in der Mikro- und Spurenanalyse*, Verlag Chemie, 1958.
3 J. REITH AND C. VAN DIJK, *Chem. Weekblad*, 36 (1939) 343.
4 F. KOROLEFF, *Thesis*, Univ. of Helsingfors, Helsinki, Finland, 1950.
5 A. PILIPENKO, *Zh. Analit. Khim.*, 8 (1953) 256.
6 A. BUSEV AND L. BAZHANOVA, *Russ. J. Inorg. Chem., English Transl.*, 6 (1961) 1128.
7 D. BROCK, Univ. of Minnesota, unpublished results, 1969.
8 O. MATHRE AND E. B. SANDELL, *Talanta*, 11 (1964) 295.
9 G. HAUPT, *J. Res. Natl. Bur. Std.*, 48 (1952) 414.
10 R. BATES, *Determination of pH, Theory and Practice*, J. Wiley, New York, 1964.
11 A. OLIN, *Acta Chem. Scand.*, 11 (1957) 1445.
12 E. B. SANDELL, *J. Amer. Chem. Soc.*, 72 (1950) 4660.
13 W. SCHUMB AND E. RITTNER, *J. Amer. Chem. Soc.*, 65 (1943) 1055.
14 NATIONAL BUREAU OF STANDARDS, *Standard X-ray Diffraction Powder Patterns*, 3 (1968) 16.
15 W. EHMANN AND D. MCKOWN, *Anal. Chem.*, 40 (1968) 1758.

*Analytica Chimica Acta*
Elsevier Publishing Company, Amsterdam
Printed in The Netherlands



# SPECTROPHOTOMETRIC DETERMINATION OF TRACES OF NITRITE BY CONCENTRATION OF AZO DYE ON AN ANION-EXCHANGE RESIN

## APPLICATION TO SEA WATERS*

EITARO WADA AND AKIHIKO HATTORI
*Ocean Research Institute, University of Tokyo, Nakano, Tokyo (Japan)*

(Received 10th March 1971)

Information on the distribution of nitrite and its seasonal and regional variation is very useful for analyzing the dynamics of the nitrogen cycle in the sea. The diazotization method as described by Bendschneider and Robinson[1] and Barnes and Folkards[2] is sensitive and reliable, and is commonly used for the analysis of sea waters. Unfortunately, however, the concentrations of nitrite occurring in sea waters are very often lower than 0.05 $\mu$g-at. $NO_2^-$–N per liter, the limit of precision of this method. The detailed pattern of nitrite distribution in the sea has thus been left unexplored except for that in well-known nitrite maximum layers.

In this report a new method for the determination of small concentrations of nitrite is described. A large volume of the sample, of which the nitrite content is less than 0.1 $\mu$g-at. N per liter, is treated with sulfanilic acid and N-(1-naphthyl)ethylenediamine dihydrochloride[3]. The azo dye produced is then concentrated by collection on a Dowex 1-X8 column and eluted with a small volume of 60% acetic acid with almost 100% recovery. Concentrations as low as 1 ng-at. N per liter, can be detected. The salts contained in sea water do not interfere with the determination. Sulfanilic acid can be successfully replaced with sulfanilamide. The present paper also includes some data on nitrite content in deep waters of Suruga Bay measured on shipboard by the proposed method.

## EXPERIMENTAL

### *Column*

The column unit used (Fig. 1) consists of three parts: sample reservoir (A), column (B) and discharge device (C), silicone rubber tubing being used to join them together. Through a three-way stopcock (D), the effluent from the column is led either to a drain (E) or to a discharge tip (F).

The column was prepared as follows. Place about 4–7 ml of Dowex 1-X8 exchange resin (50–100 mesh), which has been washed thoroughly with deionized water, in a pyrex glass tube, 1 cm in diameter and 20 cm in length. Plug the bottom end of the tube with 1 cm of glass wool. Wash the column with 20–30 ml of 60% acetic acid and then with *ca.* 50 ml of nitrite-free water. Carefully remove air bubbles with the aid of a glass rod. Units of 5 columns were set on a rack and used both on shipboard

* This work was supported by a grant (No. 8814) from the Ministry of Education.

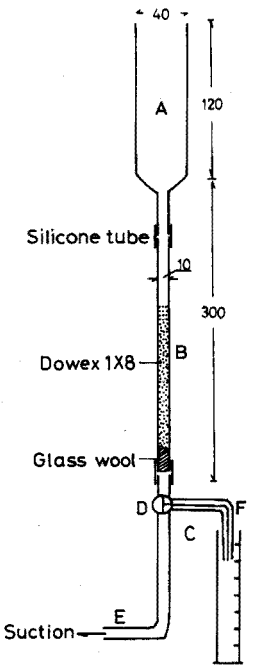


Fig. 1. Column used for collecting azo dye compound (dimensions are given in mm).

and in the laboratory. After each run, the used columns were regenerated by washing with 60% acetic acid and water as described above.

*Reagents*

*Nitrite-free water.* Dissolve 1 ml of concentrated hydrochloric acid in 1 l of deionized water and boil for more than 30 min.

*Sulfanilic acid solution (Reagent A).* Dissolve 6.0 g of sulfanilic acid in a solution of 200 ml of glacial acetic acid and 800 ml of nitrite-free water. This solution is stable for several months when stored in a brown bottle.

*N-(1-Naphthyl)ethylenediamine solution (Reagent B).* Dissolve 3.0 g of N-(1-naphthyl)ethylenediamine dihydrochloride in 500 ml of nitrite-free water, and store in a brown bottle. This solution is stable for several weeks.

*Acetic acid solution.* Dilute glacial acetic acid with deionized water to give 60% (v/v).

*Nitrite standard.* Dissolve 0.690 g of sodium nitrite (dried for 1 h at 110°) in nitrite-free water and dilute to 1 l; 1 ml of this solution contains 10.0 $\mu$g-at. $NO_2^-$–N. Prepare two series of standard solutions over the range of 0.001–0.100 $\mu$g-at. $NO_2^-$–N per liter, just before use; one of the series must contain 3.2% sodium chloride. A CSK standard of nitrite, which was provided by the courtesy of Dr. K. Sugawara, Sagami Chemical Research Center, was simultaneously used as a reference standard.

*Procedure*

Add 20 ml of Reagent A and 2 ml of Reagent B to 500 ml of the sample and mix

thoroughly. During this process, it is necessary to keep the sample away from exposure to direct sunlight. After standing for 30 min, pour the sample solution into the reservoir (A in Fig. 1) and pass through the column with gentle suction by an aspirator at a flow rate of 15–50 ml $min^{-1}$. The azo dye is retained at the top of the column to form a red band of 1–2 cm. Air bubbles formed during the process do not reduce the yield of the dye. After washing the column with about 50 ml of deionized water, elute the azo dye with 60% acetic acid without suction. First, place several separate drops of 60% acetic acid gently on the top of the column so as to prevent the back-diffusion of the azo dye. After the upper end of the colored zone has moved down about 5 mm, add 5 ml of 60% acetic acid, and then elute at a rate of 1–2 ml $min^{-1}$. Collect the first 15–25 ml of effluent and measure the absorbance at 550 nm by a Hitachi 101 spectrophotometer in cells of 5 cm optical path. Use 60% acetic acid as the reference. When necessary, dilute the effluent appropriately with 60% acetic acid.

## RESULTS AND DISCUSSION

### *Effects of concentrations of reagents and time course of color development*

The effects of concentration of the diazotizing (A) and coupling (B) reagents are shown in Fig. 2. Maximal and consistent development of color was observed

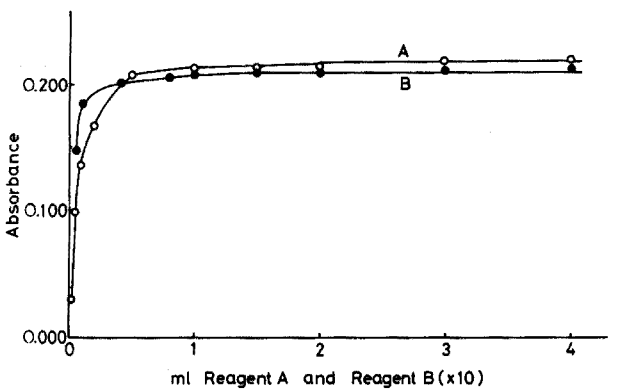


Fig. 2. Effects of concentration of sulfanilic acid and N-(1-naphthyl)ethylenediamine on color development. 25 ml of standard solution containing 1.6 μg-at. $NO_2^-$–N $l^{-1}$ and 64.0 g NaCl $l^{-1}$ was made up to 50 ml before the absorbance was measured. Curve A: Indicated amounts of Reagent A were added before addition of 0.20 ml of Reagent B. Curve B: Indicated amounts of Reagent B were added in the presence of 2.0 ml of Reagent A.

when more than 0.5 ml of Reagent A and 0.05 ml of Reagent B were present. On the basis of these data, 20 ml of Reagent A and 2 ml of Reagent B were used for 500 ml of the sample.

The time course of the color development was also measured. More than 30 min were needed to achieve maximal color development.

### *Effects of pH and flow rate*

Both the color development and the recovery of the azo dye by the column

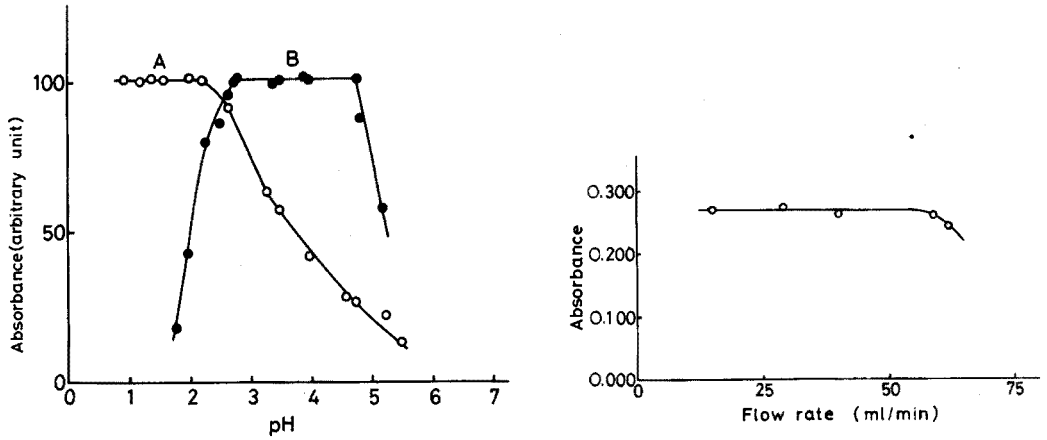


Fig. 3. Effect of pH on color intensity and yield of azo dye in column procedure. Curve A: Effect of pH on color intensity. 50 ml of standard solution containing 1.60 $\mu$g-at. $NO_2^-$-N $l^{-1}$ and 3.2% NaCl was used. Curve B: Effect of pH on recovery of azo dye by column treatment. 500 ml of standard solution containing 0.080 $\mu$g-at. $NO_2^-$-N $l^{-1}$ and 3.2% NaCl was concentrated by the column to give a final volume of 25 ml.

Fig. 4. Effect of flow rate on yield of azo dye in the column procedure. 500 ml of 3.2% NaCl solution containing 0.080 $\mu$g-at. $NO_2^-$-N $l^{-1}$ was made up to 25 ml by the column procedure. pH: 3.25. Flow rate was controlled by changing aspiration.

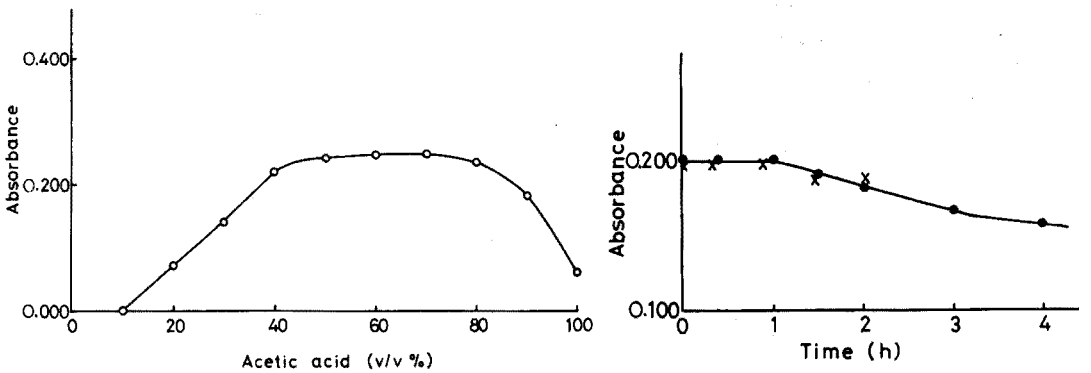


Fig. 5. Effect of concentration of acetic acid upon elution of azo dye from the column. 20 ml of standard solution containing 1.6 $\mu$g-at. $NO_2^-$-N $l^{-1}$ was placed on the column. Elution was made with 25 ml of solutions containing the indicated amounts of acetic acid.

Fig. 6. Effect of time interval between collection and elution of azo dye and the elution yield. 20 ml of 1.5 $\mu$g-at. $NO_2^-$-N $l^{-1}$ (●) and 500 ml of 0.060 $\mu$g-at. $NO_2^-$-N $l^{-1}$ (×) were made up to 25 ml by the column procedure. The end of running of the sample was taken as zero time.

treatment were considerably influenced by pH (Fig. 3). The color intensity was highest in the pH range 1–2, and decreased with increase in pH. On the other hand, maximal and quantitative recovery of the azo dye was accomplished when the pH of the sample was maintained between 3.0 and 4.5. At lower pH values, the retention of the azo dye

on the column was reduced to a great extent. Therefore, the pH of the sample was adjusted to 3.0–4.0 before the solution was applied to the column. The elution of the dye with 60% acetic acid lowered the pH and resulted in the complete restoration of the color.

Figure 4 shows the effect of flow rate. The retention of the azo dye was satisfactory when the sample was run at rates of 15–50 ml $min^{-1}$.

*Effects of concentration of acetic acid and time interval between collection of azo dye on column and its elution*

The effect of acetic acid concentration on the elution yield of the azo dye is shown in Fig. 5. The yield was almost constant over a concentration range between 40 and 80%, but at concentrations lower than 50%, the effluent sometimes became an emulsion; 60% acetic acid solution was thus selected as the eluting solvent. The flow rate during elution was arbitrarily chosen between 1 and 2 ml $min^{-1}$.

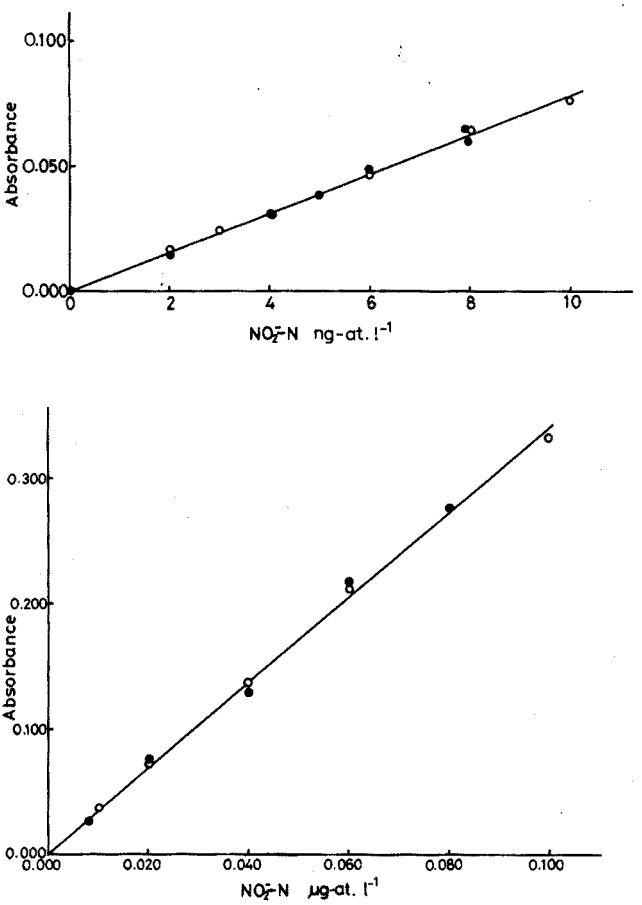


Fig. 7. Calibration curve in the presence (●) and absence (○) of sodium chloride. a: 500 ml of standard solution was made up to 15 ml. b: 500 ml of standard solution was made up to 25 ml.

If the azo dye was left for several hours on the column, its elution yield decreased with time (Fig. 6). Some chemical reaction must occur between dye and resin, the nature of which is unknown.

*Calibration curve and reproducibility of the proposed method*

Figure 7 shows calibration curves obtained by the proposed method. The absorbances are proportional to the nitrite concentrations over the range 0.001–0.100 $\mu$g-at. $NO_2^-$–N per liter. No significant difference was observed between the water standard and the sodium chloride standard. The reproducibility of the method was

TABLE I

THE REPRODUCIBILITY OF THE PROPOSED METHOD

| $NO_2^-$–N $\mu$g-at. N per liter | 0.0040[a] | 0.030[b] | 0.080[b] |
|---|---|---|---|
| Average absorbance | 0.032 | 0.114 | 0.267 |
| Standard deviation | 0.002 | 0.002 | 0.003 |
| Standard deviation (%) | 6.6 | 1.8 | 1.1 |

[a] 500-ml sample was made up to 15 ml.

[b] 500-ml sample was made up to 25 ml.

examined with the nitrite standard (Table I). The standard deviations for 5 samples at each level were 6.6., 1.8 and 1.1% for concentrations of 0.0040, 0.030 and 0.080 $\mu$g-at. $NO_2^-$–N per liter respectively.

*Blank determinations*

Two possible sources of nitrite contamination must be considered. One is nitrite induced in the reagents used, and the other is the introduction of atmospheric nitrogen oxides. The amount of the latter is expected to change from one place to another. The blank was estimated as follows. Varied volumes (50–500 ml) of deionized water, 3.2% sodium chloride solution or deep waters from the open ocean were treated simultaneously with equal amounts of Reagent A and Reagent B. The sodium chloride solution was treated in advance with hydrochloric acid to remove nitrite. The samples were further processed as described above, and the absorbances thus obtained were plotted against sample volumes and extrapolated to zero volume. The blank value measured in this way was of the order of 0.040 in 5-cm cells when 15 ml of effluent was used.

*Retention of azo dye*

When acetic acid was replaced with various concentrations of hydrochloric acid or sulfanilic acid, the yield of the azo dye was always very poor. Cation-exchange resins, silica gel and aluminosilicate could be used to collect the azo dye, but no quantitative recovery of the dye was achieved with acetic acid or any other of the acids so far examined.

Sulfanilic acid could be successfully replaced with sulfanilamide if acetic acid (20%) was used instead of hydrochloric acid for the preparation of the sulfanilamide solution.

*Distribution of nitrite in deep waters of Suruga Bay*

During the KT-69-3 Cruise of the R.V. Tansei Maru, sea-water samples from 0–1500 m depths were obtained at two stations in Suruga Bay. The determination of nitrite was made immediately after sampling by using 500-ml aliquots of the sea-water samples (Fig. 8). The nitrite concentrations of intermediate and deep waters ranged

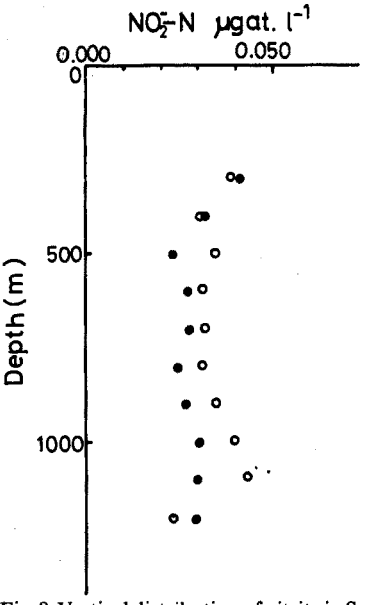


Fig. 8. Vertical distribution of nitrite in Suruga Bay. 15th March, 1969. (●) 35°01′N, 138°40′E; (○) 34°55′N, 138°39′E.

between 0.020 and 0.040 μg-at. $NO_2^-$–N per liter. The content was approximately ten times higher than those observed in deep waters of the central Pacific Ocean (unpublished data).

SUMMARY

A sensitive and accurate method for the determination of 0.001–0.100 μg-at. $NO_2^-$–N per liter in sea water is described. The sample (500–1000 ml) is treated with sulfanilic acid and N-(1-naphthyl)ethylenediamine, and drawn through a column of Dowex 1-X8 resin. The azo dye collected on the column is then eluted with 10–25 ml of 60% acetic acid and the absorbance is determined at 550 nm. The effects of the amounts of reagents, pH, flow rate and eluting solvents are discussed. Data are presented on the nitrite content in deep waters of Suruga Bay which have been measured by the proposed method.

RÉSUMÉ

On décrit une méthode sensible et précise pour le dosage de 0.001–0.100 μg-at. de nitrite dans l'eau de mer. L'échantillon á analyser (500–1000 ml) est traité par l'acide

sulfanilique et la N-(1-naphtyl) éthylènediamine et envoyé sur une colonne de résine Dowex 1-X8. Le colorant retenu sur la colonne est élué au moyer d'acide acétique á 60% (10 à 25 ml). L'absorption est mesurée à 550 nm. On examine l'influence de divers paramètres: pH, vitesse d'écoulement, solvants d'élution.

ZUSAMMENFASSUNG

Es wird eine empfindliche und genaue Methode für die Bestimmung von 0.001–0.100 μg-Atom $NO_2^-$–N pro Liter in Meerwasser beschrieben. Die Probe (500–1000 ml) wird mit Sulfanilsäure und N-(1-Naphthyl)-äthylendiamin behandelt und durch eine Kolonne mit dem Austauscherharz Dowex 1-X8 gesaugt. Der auf der Kolonne gesammelte Azofarbstoff wird dann mit 10–25 ml 60%iger Essigsäure eluiert und die Extinktion bei 550 nm ermittelt. Die Einflüsse von Reagenzienmengen, pH-Wert, Fliessgeschwindigkeit und Elutionsmitteln werden diskutiert. Nach der vorgeschlagenen Methode erhaltene Ergebnisse über den Nitritgehalt von Tiefwasserproben der Suruga Bay werden vorgelegt.

REFERENCES

1 K. BENDSCHNEIDER AND R. J. ROBINSON, *J. Marine Res.*, 11 (1952) 87.
2 H. BARNES AND A. R. FOLKARD, *Analyst*, 76 (1951) 559.
3 B. E. SALTZMAN, *Anal. Chem.*, 26 (1955) 1949.

*Analytica Chimica Acta*
Elsevier Publishing Company, Amsterdam
Printed in The Netherlands



# ANION EXCHANGE IN ACETIC ACID SOLUTIONS

P. VAN DEN WINKEL*, F. DE CORTE** AND J. HOSTE
*Institute for Nuclear Sciences, Ghent University, Ghent (Belgium)*
(Received 10th May 1971)

Systematic surveys of the behaviour of elements on a strongly basic anion-exchange resin have been reported for most mineral acids and acid mixtures[1]. Numerical data on the distribution of inorganic ions in mineral acid–organic solvent systems are also available[2]. Up to now little attention has been paid to media involving aqueous solutions of a single organic acid. In a previous paper[3] the applicability of aqueous oxalic acid solutions to the chromatographic separation of metals has been pointed out. A preliminary study[4] showed the usefulness of acetic acid in the elution chromatography of inorganic ions involving the strongly basic anion exchanger Dowex 1-X8.

A rather broad survey of adsorbabilities of the elements in acetic acid solutions has now been completed and the results are given in the present paper. The adsorption functions show that both individual and group separations, useful for instance in radioactivation analysis, are possible.

## EXPERIMENTAL

A quaternary ammonium base polysterene–divinylbenzene resin of average cross-linkage and bead size (Dowex 1-X8, 100–200 mesh) was used. The conversion of the anion exchanger, available in the chloride form, into the acetate form was achieved by washing a resin bed with anhydrous acetic acid until the effluent was free of chloride, followed by thorough rinsing with water. The resin was dried at 60° to constant weight.

The adsorbabilities are expressed as weight distribution coefficients $K_d$ (amount of ion per g of dry resin/amount of ion per ml of solution). They were determined by column elution or batch equilibration techniques[5].

Elution chromatography was used for the measurements of small ($< 10$) $K_d$ values. The $K_d$ values were calculated by means of the following expression

$$K_d = \rho\left(\frac{V_{max}}{V} - i\right) \quad (1)$$

where $\rho$ = specific volume of the resin in ml per g of dry resin; $i$ = void fraction of the

* Research Associate of the I.I.K.W.
** Research Associate of the N.F.W.O.

column; $V_{max}$ = peak elution volume in ml; $V$ = total volume of the column in ml.

The determination of the specific volume $\rho$ and the interstitial fraction $i$ were carried out as described earlier[3]. In Fig. 1 the bed volume of Dowex 1-X8 as a function of the acetic acid molarity is represented. The void fraction of the resin was found to be 0.40.

For the measurements of larger distribution coefficients weighed amounts of resin were agitated with known volumes of solution until equilibrium was reached. Thereafter the concentration of the ion under investigation was determined in the aqueous phase. All experiments were carried out at 25°. The adsorption data were obtained under conditions of low loading (less than 1%). The concentration range of acetic acid was chosen from 2 $M$ up to 17.4 $M$ (anhydrous acetic acid). Some $K_d$ *versus*

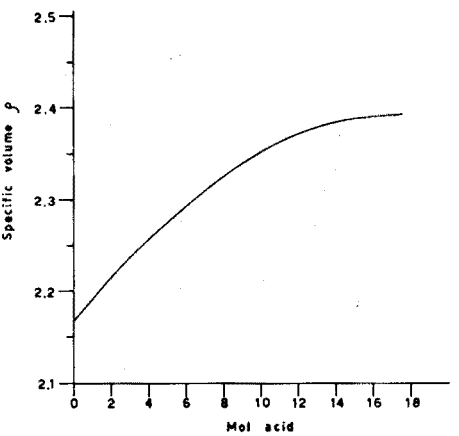


Fig. 1. Specific volume $\rho$ of Dowex 1-X8 as a function of molarity HAc.

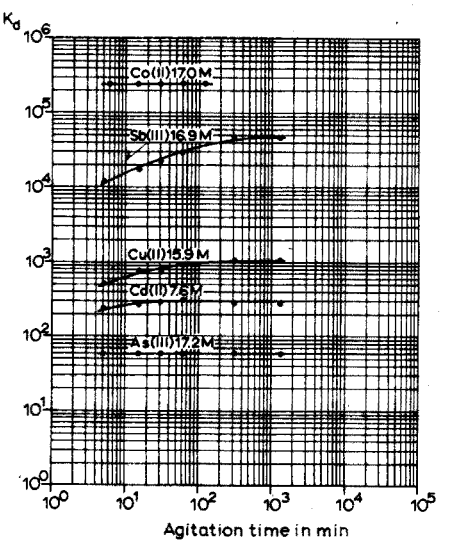


Fig. 2. $K_d$ *versus* time curves for Co(II), Sb(III), Cu(II), Cd(II) and As(III).

time curves are given in Fig. 2. An equilibrium time of 15 h (overnight) was found to be sufficient in all cases.

*Analytical methods and radioactive tracers*

Most analyses were carried out radiometrically. Counting of $\gamma$-emitting nuclides was performed by integral counting in a NaI(Tl) well-type detector. When more than one tracer was present, or in the analysis of mother–daughter pairs, Ge(Li) or NaI(Tl) $\gamma$-spectrometry was used for identification and determination. In the case of transient equilibria ($^{99}$Mo–$^{99m}$Tc, $^{109}$Pd–$^{109m}$Ag, $^{115}$Cd–$^{115m}$In, $^{113}$Sn–$^{113m}$In, $^{140}$Ba–$^{140}$La) the counting was carried out after establishment of the mother–daughter equilibrium, according to the relation:

$$t_{eq} = \frac{1}{\lambda_1 - \lambda_2} \cdot \ln \frac{\lambda_1}{\lambda_2} \qquad (2)$$

where $\lambda_1$ = decay constant of the mother nuclide, and $\lambda_2$ = decay constant of the daughter nuclide.

The analysis of the low energetic $\gamma$-ray of $^{210}Pb$ (46.5 keV) was done by means of a low-energy photon detector, coupled to a 4000-channel analyzer. For the determination of $\beta$-emitting nuclides either liquid scintillation counting or $\beta$-spectrometry by means of a plastic scintillator detector coupled to a 4096-channel analyzer was applied. In the case of $^{210}Bi$, which is a high-energy $\beta$-emitter, counting of the bremstrahlung by means of a well-type NaI(Tl) detector was preferred. The 5.305-MeV $\alpha$-radiation of $^{210}Po$ was measured by means of a ZnS(Ag) detector after deposition of the polonium on a silver foil[6].

Most tracers were obtained by neutron irradiation of appropriate target materials in the BR-2 reactor in Mol or in the Thetis reactor in Ghent, operating at fluxes of, respectively, $10^{14}$ and $10^{12}$ n cm$^{-2}$ sec$^{-1}$.

The tracers $^{137}Cs$, $^{210}Pb$–$^{210}Bi$ and $^{54}Mn$ were obtained as carrier-free solutions from U.K.A.E.A. (Amersham). The $^{210}Bi$ was separated from $^{210}Pb$ by anion exchange in nitric acid medium[11].

The $^{101+102+102m}Rh$ tracer was obtained from François[12] who prepared it by 18-MeV deuteron bombardment of natural ruthenium.

$^{234}Th$ tracer was isolated as the natural daughter from uranium by anion exchange in hydrochloric acid medium[7]. Further purification was achieved by TBP extraction from 14 *M* nitric acid[13], followed by back-extraction with 0.1 *M* nitric acid.

In Table I, the data for the preparation of solutions of tracers, obtained by irradiation in BR-2 or Thetis, are summarized. In the first column the elements together with their initial oxidation state are listed. When the target compound (column 2) was not soluble in acetic acid, it was treated with one or more adequate solvents (column 4), evaporated to dryness or near dryness and subsequently dissolved in acetic acid.

For cesium and manganese, acetic acid solutions were prepared by evaporating small aliquots of the stock solutions, after the addition of suitable amounts of carriers, and taking up the residues in acetic acid. $^{210}Bi$ tracer was obtained by evaporating the 0.25 *M* nitric acid eluate to dryness and dissolution of the residue in acetic acid. For rhodium, the hydrochloric acid solution was gently evaporated under an infrared lamp and the residue redissolved in acetic acid. The same holds for $^{234}Th$. This tracer was finally present in concentrated acetic acid in the presence of $2 \cdot 10^{-3}$ *M* hydrofluoric acid.

Because of the rather unfavourable conditions for radiometric determinations, titanium, vanadium and niobium were determined spectrophotometrically by the hydrogen peroxide method[14]. Stock solutions of titanium(IV) and vanadium(III) were prepared by dissolving titanium sponge and $V_2O_3$ in hydrochloric acid. Titanium was then oxidized by addition of a few drops of nitric acid. The solution was carefully taken to dryness and the residue redissolved in acetic acid. The solution of vanadium (IV) was prepared by dissolution of $VOSO_4 \cdot 5\ H_2O$ in acetic acid. The niobium (V) solution was prepared by dissolving $Nb_2O_5$ in hydrofluoric–nitric acid mixture, whereafter 100 $\mu$l of this solution were diluted with acetic acid.

The fluoride, calcium(II) and lithium(I) solutions were obtained by dissolving $NH_4F$, $CaCO_3$ and $LiAc \cdot 2H_2O$ in acetic acid. The measurements of fluoride were

*Anal. Chim. Acta*, 56 (1971) 241–259

TABLE I

PREPARATION AND DISSOLUTION OF RADIOACTIVE TRACERS

| *Element + oxidation state* | *Target compound* | *Isotope measured* | *Mode of dissolution* | *Element + oxidation state* | *Target compound* | *Isotope measured* | *Mode of dissolution* |
|---|---|---|---|---|---|---|---|
| Na(I) | $Na_2CO_3$ | $^{24}Na$ | HAc | Ag(I) | $AgNO_3$ | $^{110m}Ag$ | HAc |
| Mg(II) | $MgCO_3$ | $^{27}Mg$ | HAc | Cd(II) | CdO | $^{115}Cd \rightarrow$ $^{115m}In$ | HAc |
| P(V) | $(NH_4)_2HPO_4$ | $^{32}P$ | HAc | In(III) | $In_2O_3$ | $^{116m}In$ | HCl; HAc |
| $Cl^-$ | $NH_4Cl$ | $^{38}Cl$ | HAc | Sn(IV) | Sn metal | $^{113}Sn \rightarrow$ $^{113m}In$[e] | HCl; HAc |
| K(I) | $K_2CO_3$ | $^{42}K$ | HAc | | | | |
| Sc(III) | $Sc_2O_3$ | $^{46}Sc$ | $HNO_3$; HAc | Sb(III) | $Sb_2O_3$ | $^{122}Sb$ | HCl; HAc |
| Cr(III) | $K_2CrO_4$ | $^{51}Cr$ | $H_2O + NH_2OH$; HAc | Sb(V) | $Sb_2O_3$ | $^{122}Sb$ | A.R.; HAc |
| | | | | Te(IV) | $TeO_2$ | $^{127m}Te$ | $HNO_3$; HAc |
| Cr(VI) | $K_2CrO_4$ | $^{51}Cr$ | HAc | $I^-$ | $NH_4I$ | $^{128}I$ | HAc + $NaHSO_3$ [f] |
| Fe(III) | Fe sponge | $^{59}Fe$ [a] | $HCl + H_2O_2$; HAc | Ba(II) | $UO_3$(n, f) | $^{140}Ba \rightarrow$ $^{140}La$ | |
| Co(II) | $Co_2O_3$ | $^{60}Co$ | $HNO_3$; HAc | La(III) | $La_2O_3$ | $^{140}La$ | $HNO_3$; HAc |
| Ni(II) | $NiCO_3 \cdot 2Ni(OH)_2 \cdot 4aq$ | $^{65}Ni$ | HAc | Eu(III) | $Eu_2O_3$ | $^{152m}Eu$ | $HNO_3$; HAc |
| | | | | Lu(III) | $Lu_2O_3$ | $^{177}Lu$ | $HNO_3$; HAc |
| Cu(II) | CuO | $^{64}Cu$ | $HNO_3$; HAc | Hf(IV) | $HfO_2$ | $^{180m}Hf$ | HF : HAc[c] |

| | | | | | | | |
|---|---|---|---|---|---|---|---|
| Zn(II) | ZnO | $^{65}Zn$ | $HNO_3$; HAc | Ta(V) | $Ta_2O_5$ | $^{182}Ta$ | HF; $H_3BO_3$; HAc[g] |
| Ga(III) | $Ga_2O_3$ | $^{72}Ga$ | HF; $HNO_3$; HAc | | | | |
| Ge(IV) | $GeO_2$ | $^{77}Ge$ | HCl; HAc[b] | W(VI) | $WO_3$ | $^{187}W$ | $NH_4OH$; HAc |
| As(III) | $As_2O_3$ | $^{76}As$ | $NH_4OH$; HAc | Re(VII) | $NH_4ReO_4$ | $^{188}Re$ | HAc |
| As(V) | $As_2O_3$ | $^{76}As$ | $NH_4OH$; A.R.; HAc | Os(IV) | $(NH_4)_2OsCl_6$ | $^{193}Os$ | HAc |
| | | | | Ir(IV) | $(NH_4)_2IrCl_6$ | $^{194}Ir$ | HAc |
| Se(IV) | $SeO_2$ | $^{75}Se$ | $HNO_3$; HAc | Pt(IV) | Pt metal | $^{197}Pt$ | A.R.; HCl; HAc |
| $Br^-$ | $NH_4Br$ | $^{82}Br$ | HAc | | | | |
| Rb(I) | RbCl | $^{86}Rb$ | HAc | Au(III) | Au metal | $^{198}Au$ | A.R.; HCl; HAc |
| Sr(II) | $Sr(Ac)_2$ | $^{87m}Sr$ | HAc | | | | |
| Y(III) | $Y_2O_5$ | $^{90}Y$ | HCl; HAc | Hg(II) | HgO | $^{197}Hg$ | $HNO_3$; HAc |
| Zr(IV) | $ZrO_2$ | $^{97}Zr$ | HF; HAc[c] | Tl(III) | $Tl_2O_3$ | $^{204}Tl$ | $HNO_3$; HAc |
| Mo(VI) | $(NH_4)_2Mo_7O_{24}\cdot 4aq.$ | $^{99}Mo \rightarrow ^{99m}Tc$ | HAc | Po(IV) | Bi metal | $^{210}Po$ | [h] |
| | | | | Pa(V) | $Th(NO_3)_4$ | $^{233}Pa$ | HAc |
| Tc(VII) | $(NH_4)_2Mo_7O_{24}\cdot 4aq.$ | $^{99m}Tc$ | [d] | U(VI) | $UO_2(Ac)_2$ | $^{239}Np$[i] | HAc |
| Ru(III) | $(NH_4)_2Ru(H_2O)Cl_5$ | $^{105}Ru$ | HAc | Np(VI) | $UO_2(Ac)_2$ | $^{239}Np$ | HAc |
| Pd(II) | $PdCl_2$ | $^{109}Pd \rightarrow ^{109m}Ag$ | HBr; HAc | | | | |

[a] The $^{59}Fe$ was purified from $^{54}Mn$, formed by the reaction $^{54}Fe(n, p)^{54}Mn$, by anion exchange in HCl medium[7]. [b] Under pressure; formation of $GeCl_4$. [c] Final HF concentration $< 10^{-2}$ *M*. [d] The $^{99m}Tc$ was separated from the Mo matrix on an anion-exchange column[8]. The Tc eluate (4 *M* $HNO_3$) was evaporated to dryness and the residue taken up in glacial acetic acid. [e] The Sn tracer was purified from $^{125}Sb$, formed by the reaction $^{124}Sn(n, \gamma, \beta^-)^{125}Sb$, by spontaneous deposition of Sb on Fe foil[9]. [f] The $^{140}Ba$ tracer was separated as $BaCl_2\cdot aq$ according to Minkkinen[10]. The precipitate was redissolved in acetic acid. [g] The HF solution was treated with excess $H_3BO_3$ to volatilize the fluoride as $BF_3$. The residual solution was taken up in a large volume of acetic acid. [h] The $^{210}Po$ was obtained from De Boeck, who described its preparation[6]. [i] Irradiation after batch experiments.

done by means of a fluoride-sensitive lanthanum fluoride electrode at constant ionic strength[15]. The $K_D$ values for calcium(II) were obtained from potentiometric titrations with EGTA using a mercury–mercury–EDTA indicator electrode[16]. Finally, lithium was determined by atomic absorption.

## ADSORPTION FUNCTIONS

The adsorption functions of the elements are described below. The data are classified according the groups of the periodic system. It should be noted that "no adsorption" means that the $K_d$ value is smaller than or equal to unity. In batch experiments, the lower limits of the adsorbability of strongly adsorbed elements were calculated from the detection limit for activity measurements, according to the convention of Currie[17].

*Alkali metals*

The alkali metals lithium through cesium (and presumably francium) show no adsorption over the whole acetic acid molarity range. However, a slight increase of the $K_d$ values was observed with increasing acid concentration.

*Alkaline earths*

The behaviour of Mg(II), Ca(II), Sr(II), Ba(II) and probably Be(II) and Ra(II) was found to be similar to that of the alkali metals.

*Scandium(III), yttrium(III) and the rare earths (Fig. 3)*

These trivalent elements show similar, sharply increasing adsorption functions, positioned in the high molarity region (above 13 *M*). Considering the sequence Sc(III), Y(III) and Eu(III) at a given concentration of acetic acid, the $K_d$ values for the heavier elements are markedly larger. For increasing atomic numbers, the $K_d$ functions are shifted towards lower acetic acid concentration.

The adsorption function of the lightest and heaviest rare earth, lanthanum(III) and lutetium(III), apparently define the region of adsorbability of the rare earths. For the three rare earths studied, La(III), Eu(III) and Lu(III), almost parallel, adjacent adsorption curves were found.

*Titanium(IV), zirconium(IV), hafnium(IV) and thorium(IV) (Fig. 4)*

The adsorbability of titanium(IV) was found to be negligible above 8 *M* acetic acid. Below this concentration colloidal solutions were obtained. Zirconium(IV) is strongly adsorbed, $K_d$ slowly decreasing with increasing acid molarity. At concentrations higher than 12 *M*, precipitation occurs.

For hafnium(IV) a lower adsorption limit of $5 \cdot 10^4$ was calculated. This value holds for 2 *M* to 17.5 *M* acetic acid.

Thorium(IV) shows a constants adsorption up to 14 *M*, whereafter the $K_d$ increases rapidly.

*Vanadium(III) and (IV), niobium(V), tantalum(V) and protactinium(V) (Fig. 5)*

The anion-exchange behaviour of vanadium(III) is similar to that of other trivalent cations, such as scandium(III), yttrium(III) and some others, as chromium-

(III) and iron(III), which will be discussed later. For vanadium(IV) no stable solutions were obtained above 16.5 *M* acetic acid. The adsorption of the vanadyl cation is negligible below 13 *M*. From 13 *M* up to 16.5 *M* a straight line adsorption function is obtained, the slope of which is smaller than that of the vanadium(III) adsorption isotherm. Attempts to prepare vanadium(V) solutions in acetic acid resulted in the precipitation of vanadium pentoxide.

Concerning niobium(V), no stable acetic acid solutions could be obtained even in the presence of small amounts of fluoride. For tantalum(V) solutions prepared as described in Table I, no hydrolysis phenomena were observed. Batch experiments allowed the lower adsorption limit to be evaluated as $5 \cdot 10^5$.

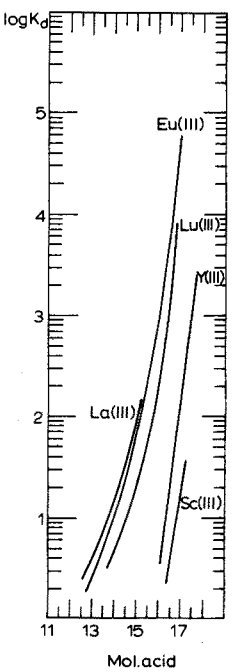


Fig. 3. Adsorption curves for Sc(III), Y(III), La(III), Eu(III) and Lu(III).

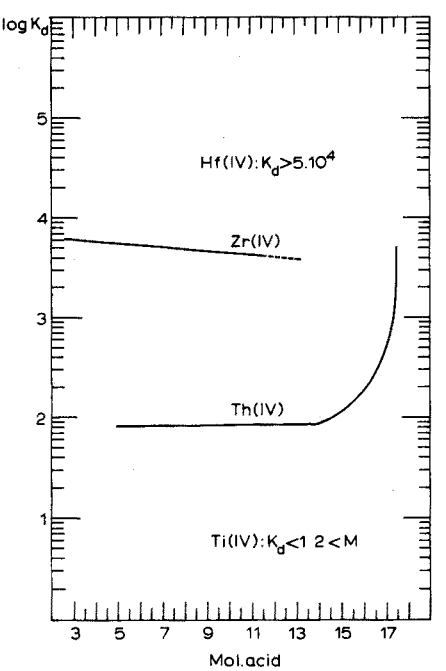


Fig. 4. Adsorption curves for Ti(IV), Zr(IV), Hf(IV) and Th(IV).

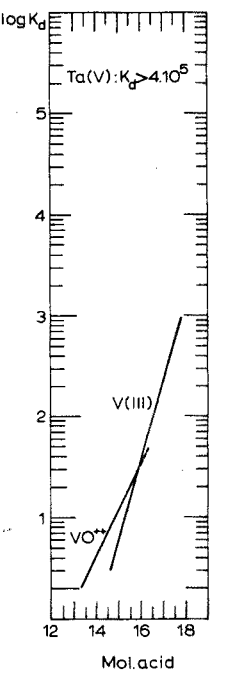


Fig. 5. Adsorption curves for V(III) and (IV) and Ta(V).

For protactinium(V) irreproducible results were obtained, probably owing to the tendency of protactinium to deposit on the walls of glass vessels[18]. The order of magnitude of the $K_d$ value was established as being $10^2$.

*Chromium(III) and (VI), molybdenum(VI), tungsten(VI) and uranium(VI) (Fig. 6)*

Both chromium(III) and chromium(VI) show rectilinear adsorption. Chromium(III) behaves similarly to vanadium(III), as can be expected from their chemical analogy, though the adsorption is less pronounced. The adsorbability of chromate is independent of the acetic acid concentration. As distinct from the results of a former

investigation in oxalic acid medium[3], equilibrium was reached after a reasonable time. Indeed, results from 1-h and 15-h batch experiments were identical.

Molybdenum(VI) and tungsten (VI) are very strongly adsorbed. For molybdenum(VI), a slight increase of $K_d$ with acetic acid molarity was found. The adsorbability of tungsten(VI) first decreases with increasing acidity to a shallow minimum near 8 *M* and then increases slowly.

Uranium(VI), present as the complexed uranyl ion, shows a small decrease of $K_d$ up to 11 *M* (minimum). Above 11 *M* the adsorbability increases quite rapidly.

*Manganese(II), technetium(VII), rhenium(VII) and neptunium(VI) (Fig. 7)*

Manganese(II) and neptunium(VI), the latter presumably present as $NpO_2^{2+}$,

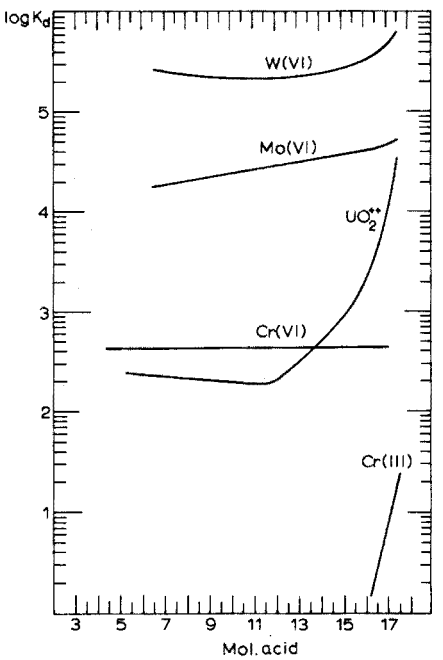


Fig. 6. Adsorption curves for Cr(III) and (VI), Mo(VI), W(VI) and U(VI).

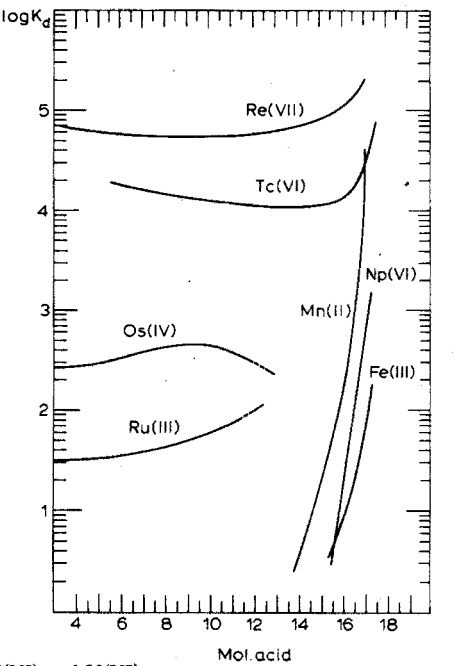


Fig. 7. Adsorption curves for Mn(II), Tc(VII), Re(VII), Np(VI), Fe(III), Ru(III) and Os(IV).

show similar behaviour. Both are adsorbed at $M > 14$, $K_d$ rapidly increasing with acid concentration.

High $K_d$ values were found for typical anionic species as $TcO_4^-$ and $ReO_4^-$. The adsorption functions have a shallow minimum at 12 *M* and 10 *M*, respectively.

*Iron(III), ruthenium(III) and osmium(IV) (Fig. 7)*

Iron(III) shows the typical adsorption behaviour of the trivalent metals, as mentioned above.

The $K_d$ values for ruthenium(III) and osmium(IV), originally present as $Ru(H_2O)Cl_5^{2-}$ and $OsCl_6^{2-}$, increase slowly up to *ca.* 12 *M* and 10 *M* acetic acid,

respectively. From 10 to 12 $M$ a slight decrease of $K_d$ was observed for osmium(IV). Results for both elements above 12 $M$ are doubtful owing to precipitation reactions, observed when the acetic acid molarity of a diluted solution is increased.

*Cobalt(II), rhodium(III) and iridium(IV) (Fig. 8)*

Cobalt(II) is adsorbed above 14 $M$, the $K_d$ value increasing very rapidly to $10^6$ in anhydrous acetic acid.

The adsorption function for rhodium(III) is reminiscent of that for iridium(IV), but is an order of magnitude lower. In both cases $K_d$ increases slowly with $M$. Above 12 $M$ results for iridium(IV) are doubtful because of precipitation reactions.

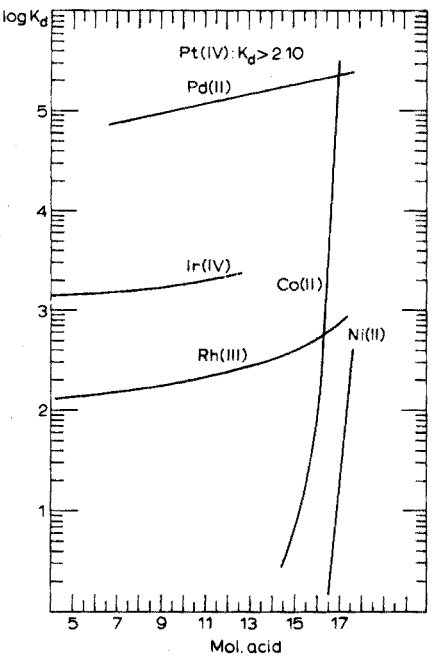


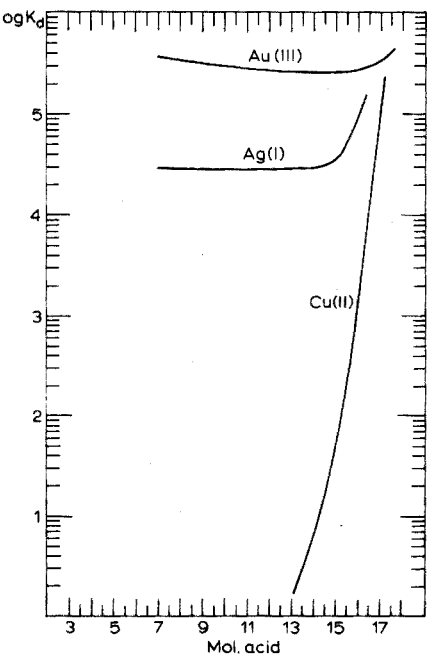


Fig. 8. Adsorption curves for Co(II), Rh(III), Ir(IV), Ni(II), Pd(II) and Pt(IV).

Fig. 9. Adsorption curves for Cu(II), Ag(I) and Au(III).

*Nickel(II), palladium(II) and platinum(IV) (Fig. 8)*

Nickel(II) is only adsorbed at very high acetic acid concentrations ( $>16.5$ $M$) and shows an extremely steep adsorption curve.

Palladium(II) and platinum(IV) are very strongly adsorbed over the whole molarity scale. For palladium(II) a straight line is obtained through the points $K_d = 3.7 \cdot 10^4$ at 2 $M$ and $K_d = 2.2 \cdot 10^5$ at 17.4 $M$. For platinum(IV) $K_d$ was larger than $2 \cdot 10^5$ at all acid concentrations.

*Copper(II), silver(I) and gold(III) (Fig. 9)*

The adsorption of copper(II) above 13 $M$ acetic acid is quite similar to that of other divalent elements such as Co(II) and Ni(II).

For silver(I) a constant $K_d$ value of $3 \cdot 10^4$ up to 14 *M* acetic acid was established, followed by a fairly slow increase at higher acid concentrations.

The adsorption function of gold(III) shows a very small bend. The minimal $K_d$ value is $2.7 \cdot 10^5$ at 14 *M*.

*Zinc(II), cadmium(II) and mercury(II) (Fig. 10)*

Zinc(II), cadmium(II) and mercury(II) show linearly increasing adsorption functions, the slope of which decreases with increasing atomic number. The adsorbability at a given acetic acid molarity increases in the same sequence.

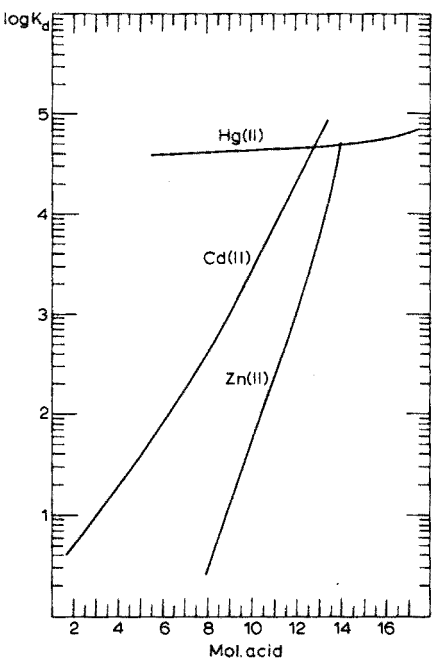


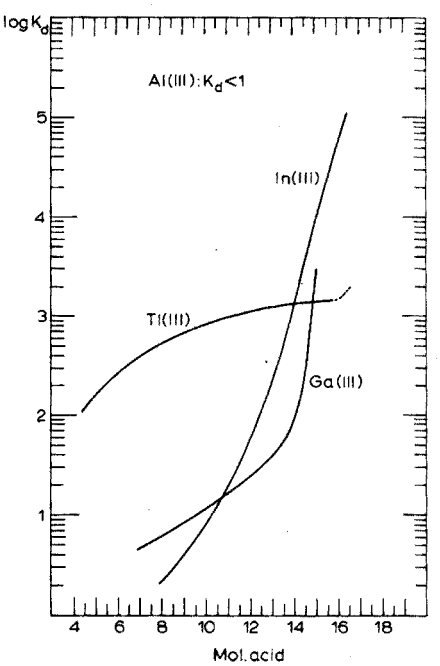


Fig. 10. Adsorption curves for Zn(II), Cd(II) and Hg(II).

Fig. 11. Adsorption curves for Al(III), Ga(III), In(III) and Tl(III).

*Aluminum(III), gallium(III), indium(III) and thallium(III) (Fig. 11)*

Adsorption of aluminum(III) was found to be negligible over the whole acetic acid molarity range.

The adsorption behaviour of gallium(III) and indium(III) looks similar. Both are adsorbed above 8 *M* acetic acid. The $K_d$ values rise respectively to $1.1 \cdot 10^5$ and $9.9 \cdot 10^4$ at 16.5 *M*.

The adsorption function of thallium(III) differs from most others in the way that it is convex to the abscissa. The results at acid concentrations above 16 *M* (dotted line) are in doubt because of the possibility of reduction of Tl(III) to Tl(I) by the resin.

*Germanium(IV), tin(IV) and lead(II) (Fig. 12)*

Adsorption of germanium(IV) occurs above 15 *M* acetic acid. The adsorption line increases linearly with a moderate slope.

The results for tin(IV) are reliable only above 10 *M* acetic acid, because of its tendency to hydrolyze at lower acid concentrations.

The adsorption of lead(II) follows a straight line through the points $K_d = 2.1$ at 10 *M* and $K_d = 4.6 \cdot 10^4$ at 16.5 *M*.

*Phosphate, arsenic(III) and (V), antimony(III) and (V) and bismuth(III) (Fig. 13)*

Phosphate shows the typical behaviour of the other oxy-anions ($CrO_4^{2-}$,

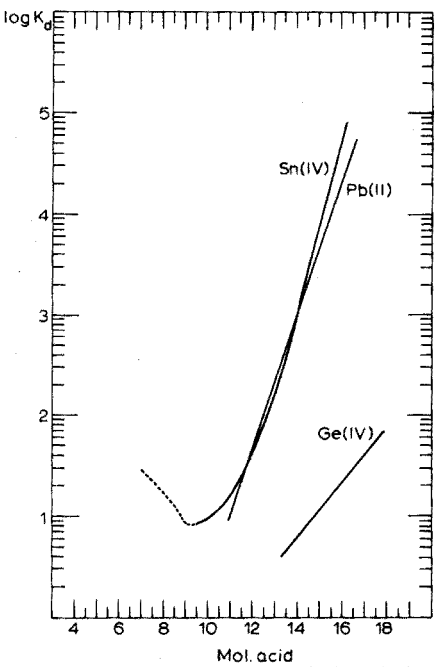


Fig. 12. Adsorption curves for Ge(IV), Sn(IV) and Pb(II).

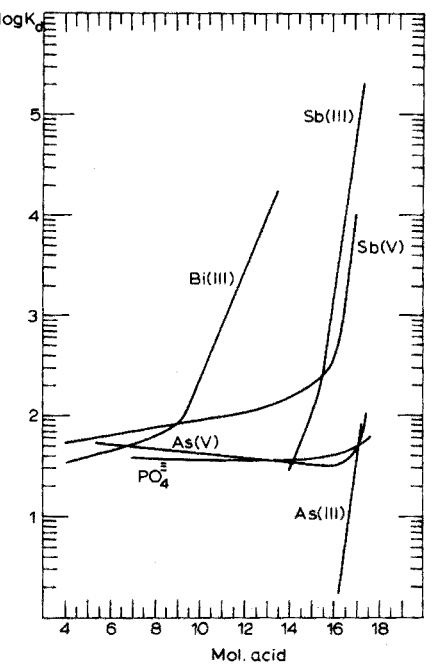


Fig. 13. Adsorption curves for $PO_4^{3-}$, As(III) and (V), Sb(III) and (V) and Bi(III).

$TcO_4^-$, $ReO_4^-$, etc.) though $K_d$ is much lower ($K_d = 37$ for $3 < M < 16$). Above 16 *M*, $K_d$ increases very slowly.

The $K_d$ functions of arsenic(III) and antimony(III) are similar to those of other trivalent elements. Antimony(III) tends to be more strongly adsorbed than arsenic(III). In the case of antimony(III) irreproducible results were obtained from batch experiments below 14 *M* acetic acid, probably because of an hydrolytic reaction.

Arsenic(V) and antimony(V) behave like typical anions. The slope of their adsorption isotherms is smaller than that of their trivalent state.

For bismuth(III) a straight-line adsorption was found above 10 *M* acetic acid. Below this molarity the adsorption isotherm is curved. Bismuth is the most strongly adsorbed element of the fifth group.

*Selenium(IV), tellurium(IV) and polonium(IV)* (*Fig.* 14)

Selenium(IV) is weakly adsorbed near 8 *M* acetic acid, $K_d$ being equal to 2.1. The adsorption increases slowly to $K_d = 26$ at $M = 16.5$.

The adsorption of tellurium(IV) remains nearly constant up to 12 *M* ($K_d = 95$), whereafter a moderate increase is established.

The shape of the adsorption function of polonium(IV) is peculiar and looks like that of thallium(III). Here again the curve is convex.

*Halogens* (*Fig.* 15)

At a given acetic acid concentration, the halides are adsorbed more strongly

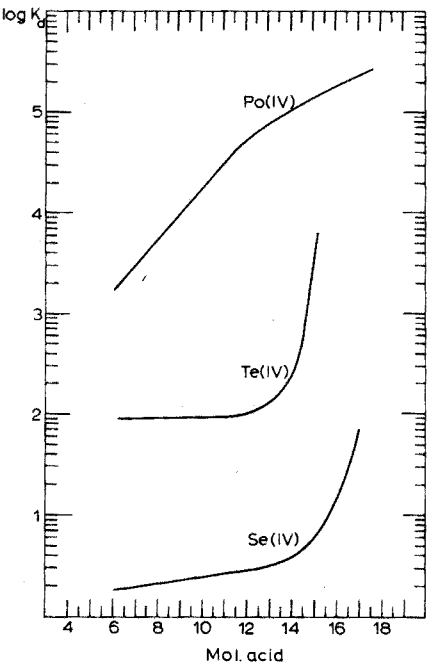


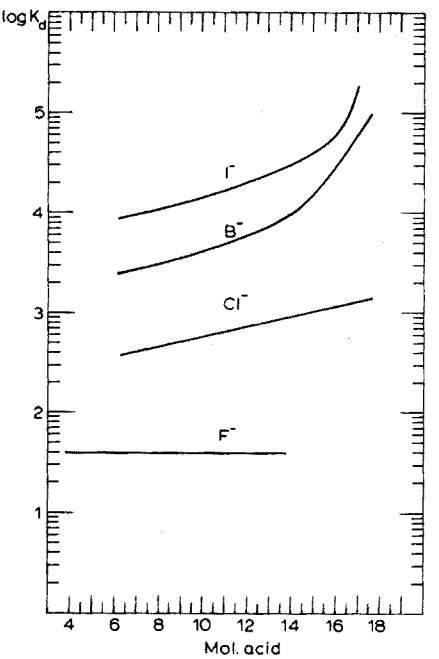


Fig. 14. Adsorption curves for Se(IV), Fe(IV) and Po(IV).

Fig. 15. Adsorption curves for $F^-$, $Cl^-$, $Br^-$ and $I^-$.

in the sequence $F^- < Cl^- < Br^- < I^-$. The adsorption of fluoride is not influenced by acid concentration up to 14 *M*, whereas the other halides show $K_d$ values increasing with *M*. At the highest acid concentrations, both bromide and iodide are much more stronger adsorbed than would be expected from their linear isotherms at lower concentration.

## SEPARATIONS

The results obtained allow the elements to be classified into three main groups, namely:

(1) *Non-adsorbed elements* ($K_d < 1$ *for* $2 < M < 17.4$)
These are: (*a*) the alkali metals: Li, Na, K, Rb, Cs, (Fr).
(*b*) the alkaline earths: (Be), Mg, Ca, Sr, Ba, (Ra).
(*c*) Al(III) and Ti(IV).

(2) *Adsorbed and elutable* ($K_d < 10$ *at* $M = 2$, $K_d \gg 10$ *for* $M > 2$)
Sc(III), V(III), V(IV), Cr(III), Mn(II), Fe(III), Co(II), Ni(II), Cu(II), Zn(II), Ga(III), Ge(IV), As(III), Se(IV), Y(III), Cd(II), In(III), Sn(IV), Sb(III), R.E.(III), Pb(II) and Np(VI).

(3) *Strongly adsorbed* ($K_d \gg 10$ *for* $2 < M < 17.4$)
$F^-$, $PO_4^{3-}$, $Cl^-$, Cr(VI), As(V), $Br^-$, Zr(IV), Mo(VI), Tc(VI), Ru(III), Rh(III), Pd(II), Ag(I), Sb(V), Te(IV), $I^-$, Hf(IV), Ta(V), W(VI), Re(VII), Os(IV), Pt(IV), Au(III), Hg(II), Tl(III), Bi(III), Po(IV), Th(IV) and U(VI).

In view of this classification, the applicability of anion exchange in acetic acid to separations of elements may be stated as follows:

1. group or individual separations involving elements of the first, second and third group mentioned above;

2. mutual separations of the elements of the second group, due to the different slope and intersection point with the abscissa of their adsorption function.

A few illustrations of separations are described below.

*Group separation* (*Fig.* 16)

A group separation useful in the activation analysis of oligo-elements in biological samples has been described by one of us [19]. It allows the separation of the matrix elements bromine, potassium and sodium from the trace elements Ag, As, Au, Co, Cu, Mn, Mo, Sc and Zn.

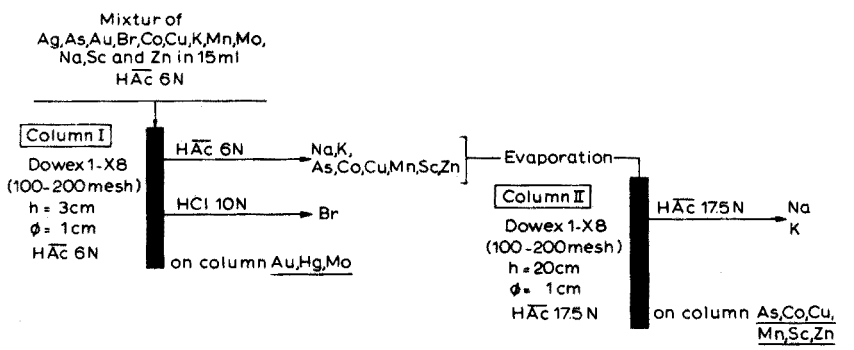


Fig. 16. Group separation in acetic acid medium on Dowex 1-X8.

Microgram amounts of $^{76}As$, $^{198}Au$, $^{82}Br$, $^{64}Cu$, $^{197+203}Hg$, $^{42}K$, $^{54}Mn$, $^{99}Mo$–$^{99m}Tc$, $^{24}Na$, $^{46}Sc$ and $^{65}Zn$ were adsorbed from 15 ml of 6 *M* acetic acid on column I. Upon washing with 20 ml of 6 *M* acetic acid, the eluate, containing the elements of group 1 and 2, was evaporated to about 5 ml without loss of arsenic(III) (eluate A). The elements adsorbed (group 3) were further separated as given in Fig. 16. $^{198}Au$, $^{99}Mo$–$^{99m}Tc$ and $^{197+203}Hg$, remaining on the column, were determined by

means of Ge(Li) $\gamma$-spectrometry. To the eluate A one drop of acetic anhydride was added and the solution was adsorbed on column II. Sodium and potassium (group 1) were removed by washing with anhydrous acetic acid. The isotopes $^{76}As$, $^{60}Co$, $^{64}Cu$, $^{54}Mn$, $^{46}Sc$ and $^{65}Zn$ (group 2) can be measured on the resin or after elution with 2 *M* acetic acid.

*Elution of zinc(II) from Dowex 1-X8 (Fig. 17)*

In Fig. 17 the eluting power of acetic acid is compared to that of the usual eluting agents for zinc(II), originally adsorbed from 6 *M* hydrochloric acid. Zinc was eluted with 1 *M* acetic acid, 1 *M* sodium hydroxide, 0.004 *M* hydrochloric acid and a mixture of α-hydroxyisobutyric acid (α-HIBA) and 0.13 *M* ammonia solution.

Although tailing occurs to some extent, the eluting power of acetic acid was found to be equivalent to or even better than that of the common eluting agents.

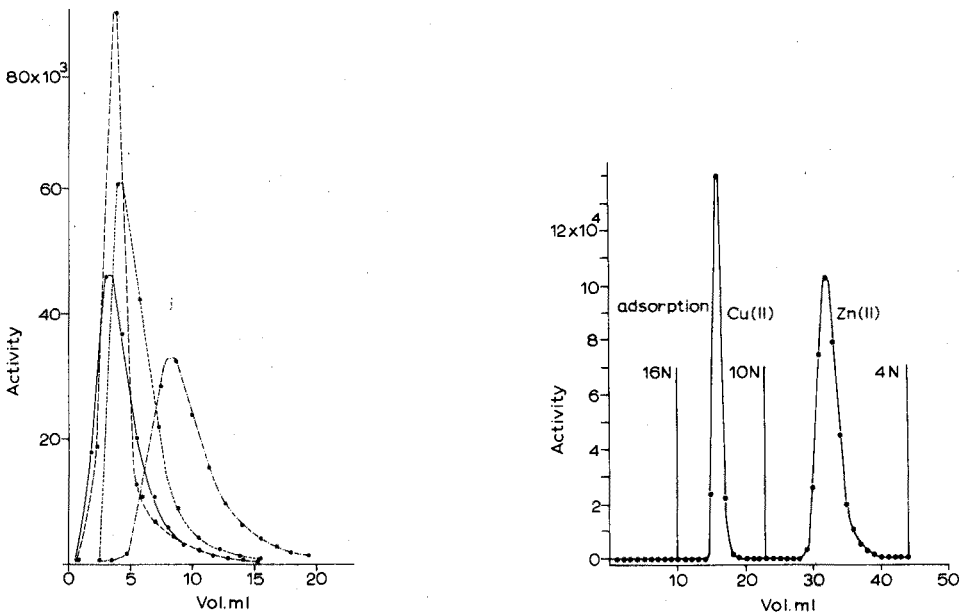


Fig. 17. Elution of Zn(II) from Dowex 1-X8 with different eluting agents. (——) 1 *M* HAc; (----) 1 *M* NaOH; (·····) 0.004 *M* HCl; (–·–·–) 0.5 *M* α-HIBA + 0.13 *M* $NH_4OH$.

Fig. 18. Separation of Cu(II) and Zn(II) on Dowex 1-X8.

*Separation of Cu and Zn (Fig. 18)*

The tracers $^{64}Cu$ and $^{65}Zn$ were adsorbed from 1 ml of 16 *M* acetic acid on a column pretreated with the same acetic acid molarity. The column size was 7 mm × 130 mm. After rinsing with 9 ml of 16 *M* acetic acid, copper(II) was eluted with 13 ml of 10 *M* acetic acid and zinc(II) with 20 ml of 4 *M* acetic acid. The yields were quantitative.

*Separation of Mn, Cu and Zn (Fig. 19)*

The tracers $^{54}Mn$, $^{64}Cu$ and $^{65}Zn$ were adsorbed from 5 ml of 16 *M* acetic acid

on a column of the same size as mentioned above. Mn(II), Cu(II) and Zn(II) were successively eluted with 14.5 *M*, 10 *M* and 1 *M* acetic acid. The elution yields were quantitative.

*Separation of Na, As and Cu (Fig. 20)*

The tracers $^{24}Na$, $^{76}As$ and $^{64}Cu$ were adsorbed from 1 ml of anhydrous acetic acid on a column (7 mm diam. × 240 mm height), pretreated with 17.4 *M* acetic acid. Na(I), As(III) and Cu(II) were successively eluted with 17.4 *M*, 15.5 *M* and 6.0 *M* acetic acid. In all cases the elution yields were better than 99.5%.

*Separation of the mother–daughter pair $^{239}U$–$^{239}Np$*

About 0.5 g of irradiated uranyl acetate was dissolved in a small amount of 2.06 *M* acetic acid and the solution passed through a column (9 mm diam. × 150 mm

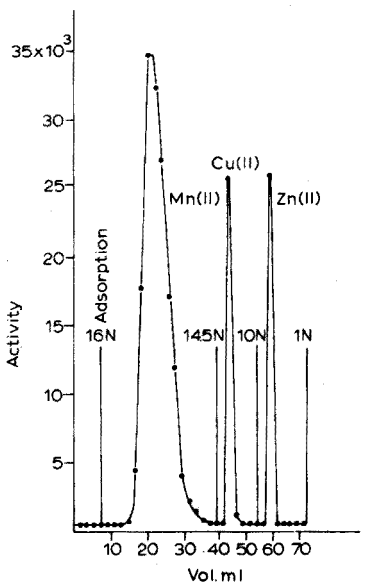


Fig. 19. Separation of Mn(II), Cu(II) and Zn(II) on Dowex 1-X8.

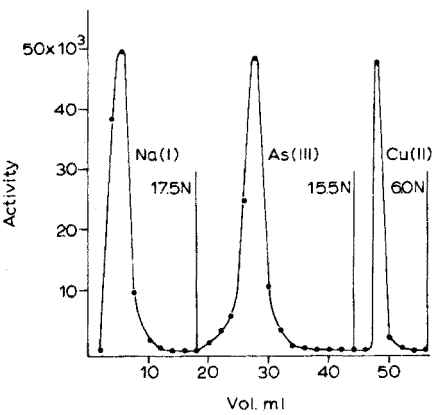


Fig. 20. Separation of Na(I), As(III) and Cu(II) on Dowex 1-X8.

height) pretreated with the same acetic acid molarity. The elution was performed with 2.06 *M* acetic acid.

Qualitative analysis of the eluate by addition of potassium hexacyanoferrate(II) showed uranyl ion to be absent in the effluent. Ge(Li) $\gamma$-spectrometry of both eluate and resin, showed that the neptunium was quantitatively collected in the eluate.

## CONCLUSIONS

From anion-exchange data of 65 elements in acetic acid solutions (Fig. 21) it appeared to be possible to classify the elements into three groups with respect to their behaviour, namely:

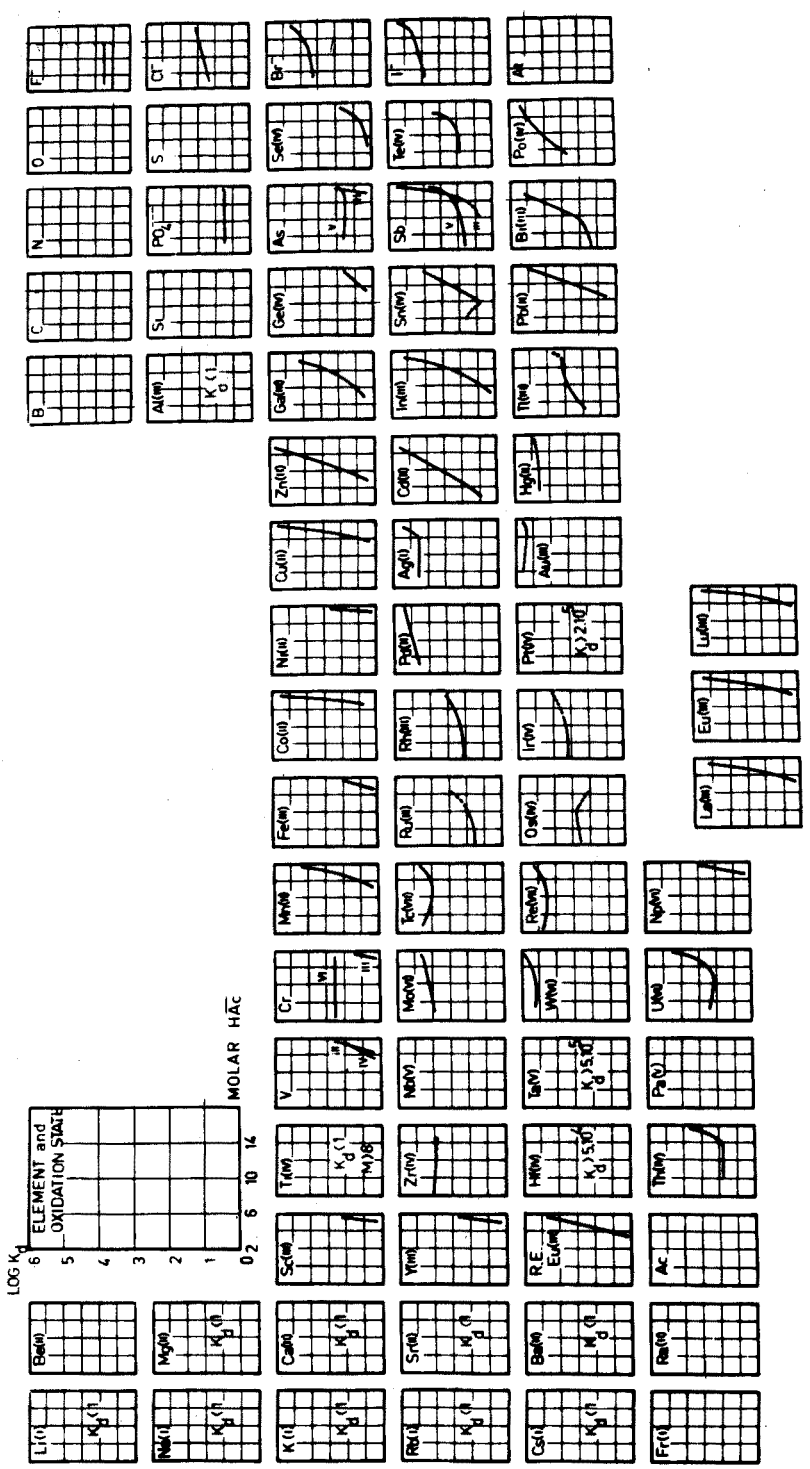


Fig. 21. Adsorption of the elements from acetic acid solutions by an anion-exchange resin.

1. elements with essentially no adsorption from 2 *M* to 17.4 *M* acetic acid;
2. elements that are strongly adsorbed from 2 *M* up to 17.4 *M* acid;
3. elements with steeply increasing distribution functions.

The elements of the first group obviously form no anionic complexes with acetate in acetic acid and so are excluded from the resin by the Donnan potential. Examples are the alkali metals, the alkaline earths and aluminum and titanium.

A qualitative interpretation for the behaviour of the elements of groups 2 and 3 can be given on the basis of two effects:

1. addition of acetic acid lowers the dielectric constant $\varepsilon$ of the medium ($\varepsilon_{H_2O}=80.36$; $\varepsilon_{HAc}=6.2$) thereby increasing the attraction between ions. Therefore ion association and complex formation are favored.

2. Selective solvation, the elements tending to be retained in the solution, may play an important role, especially at high acetic acid concentrations.

Assuming that the selectivity scale of Dowex 1-X8 is valid in moderate or even concentrated acetic acid solutions, the behaviour of some elements can be explained. The strongly adsorbed elements of the second group are in all probability present as anionic species. They can be subdivided in three groups.

(*a*) *The halides*, where the well-known selectivity scale is followed: $F^- < Cl^- < Br^- < I^-$. The slow increase of $K_d$ with acetic acid molarity may be attributed to the growth of attraction forces between the anions and the fixed cationic $-N(CH_3)_3^+$ groups, owing to the lowering of $\varepsilon$. The horizontal adsorption function of fluoride may be explained by compensation of the former effect by competition. Indeed, in aqueous solutions acetate shows a stronger affinity for the resin than fluoride.

(*b*) *The oxy-anions*, chromate, molybdate, tungstate, technetate, perrhenate, phosphate, arsenate, antimonate, selenite, tellurite and probably pollonite, where apart from coulombic forces and polarisation, the strong adsorption may be attributed to weak solvation. In agreement with Chu *et al.*[20], these oxy-anions which are the largest and have the smallest charge, are most strongly adsorbed. As a matter of fact, when $K_d$ curves for the divalent $CrO_4^{2-}$ and $Mo_7O_{24}^{2-}$ anions are compared, the larger and thus less solvated molybdate anion is more strongly adsorbed. The same holds for the sequences $PO_4^{3-} < AsO_4^{3-} < SbO_4^{3-}$ and $SeO_3^{2-} < TeO_3^{2-} < PoO_3^{2-}$. Evenso, chromate is more strongly adsorbed than phosphate, the trivalent phosphate being more strongly solvated than the divalent chromate.

(*c*) *Anions formed from the preparation of tracer solutions* (*Table I*). The noble metals Ru(III), Rh(III), Os(IV), Ir(IV), Pt(IV), Au(III) and Pd(II) were originally present as chloro, chloro-aquo or bromide complexes. Zr(IV), Hf(IV) and Ta(V) were undoubtedly present as fluoride complexes, whereas Tl(III) and Bi(III) were added as their nitrates. Therefore their affinity for the resin may be attributed to the adsorption of their halide or nitrate complexes, stabilized by a low $\varepsilon$ value.

For Ag(I), Hg(II), Th(IV) and U(VI), the formation of highly stable acetate complexes must be responsible for their marked adsorption.

The third class consists of elements showing a nearly rectilinear distribution function, intersecting the abscissa and steeply rising with increasing acetic acid molarity. The elements are Sc(III), V(III), V(IV), Cr(III), Mn(II), Fe(III), Co(II), Ni(II), Cu(II), Zn(II), Ga(III), Ge(IV), As(III), Y(III), Cd(II), In(III), Sn(IV), Sb(III), R.E.(III), Pb(II) and Np(IV). Since the association between ions of unlike charge increases very rapidly below a certain critical value of the dielectric constant, which

depends on the charges and the radii of the ions, the formation of adsorbable acetate complexes must occur above a well-defined acetic acid concentration. This is in agreement with the results obtained. At higher acid concentrations, the reduced solvation and the enhanced attraction forces between the anionic complexes and the positively charged trimethylammonium groups of the resin, cause the increased adsorption.

If at present a physico-chemical interpretation of the results is still uncertain, the usefulness of acetic acid for group and individual separations is well defined. From the distribution curves it is obvious that apart from the few examples given many other interesting applications are possible, as for instance Co–Ni, Pb–Bi–Po, As–Sb and Zn–Cd–Hg separations.

The authors wish to thank the "Interuniversitair Instituut voor Kernwetenschappen" and the "Nationaal Fonds voor Wetenschappelijk Onderzoek" for financial support. The authors are highly indebted to Mr. T. De Wispelaere, R. Smits, M. Waegemans and P. Van Cauwenberge, for helpful technical assistance. Thanks are also due to Mr. G. De Bruyckere for his measurements of fluoride by means of the $LaF_3$ electrode.

SUMMARY

The adsorbabilities of 65 elements in water–acetic acid medium on the anion-exchanger Dowex 1-X8 have been investigated in the region 2–17.4 *M* acetic acid. Examples of possible individual separations of elements are given, namely: Cu–Zn, Mn–Cu–Zn, Na–As–Cu and U–Np. A separation of the elements Ag, As, Au, Br, Co, Cu, K, Mn, Mo, Na, Sc and Zn into four groups is described. A qualitative interpreta- of the adsorption properties is proposed.

RÉSUMÉ

Une étude est effectuée sur le comportement de 65 éléments, en milieu eau-acide acétique, sur échangeur d'anions Dowex 1-X8. Des exemples de séparations individuelles possibles sont donnés, notamment: Cu–Zn; Mn–Cu–Zn; Na–As–Cu et U–Np. On décrit également une séparation en quatre groupes des éléments Ag, As, Au, Br, Co, Cu, K, Mn, Mo, Na, Sc et Zn. On propose une interprétation qualitative des propriétés d'adsorption.

ZUSAMMENFASSUNG

Die Adsorption von 65 Elementen am Anionenaustauscher Dowex 1-X8 in Wasser–Essigsäure-Medium wurde im Bereich 2–17.4 *M* untersucht. Es werden Beispiele für individuelle Trennungen von Elementen vorgelegt, und zwar: Cu–Zn; Mn–Cu–Zn; Na–As–Cu und U–Np. Eine Trennung der Elemente Ag, As, Au, Br, Co, Cu, K, Mn, Mo, Na, Sc und Zn in vier Gruppen wird beschrieben. Es wird eine qualitative Deutung der Adsorptionseigenschaften vorgeschlagen.

REFERENCES

1 W. RIEMAN AND H. F. WALTON, *Ion Exchange in Analytical Chemistry*, Pergamon Press, 1970, p. 153.
2 B. TRÉMILLON, *Les Séparations par les Résines Echangeuses d'Ions*, Gauthier-Villars, Paris, 1965, p. 362.
3 F. DE CORTE, P. VAN DEN WINKEL, A. SPEECKE AND J. HOSTE, *Anal. Chim. Acta*, 42 (1968) 67.
4 P. VAN DEN WINKEL, F. DE CORTE, A. SPEECKE AND J. HOSTE, *Anal. Chim. Acta*, 42 (1968) 340.
5 K. A. KRAUS AND F. NELSON, *Symposium on Ion Exchange and Chromatography in Analytical Chemistry*, Am. Soc. Testing Materials, Spec. Publ. No. 195, June 1956.
6 R. DE BOECK, F. ADAMS AND J. HOSTE, *J. Radioanal. Chem.*, 1 (1968) 397.
7 K. A. KRAUS AND F. NELSON, *Proc. Intern. Conf. Peaceful Uses At. Energy, Geneva, 1955*, 7 (1956) 113.
8 E. H. HUFFMAN, R. L. OSWALT AND L. A. WILLIAMS, *J. Inorg. Nucl. Chem.*, 3 (1956) 49.
9 F. DE CORTE, A. SPEECKE AND J. HOSTE, *J. Radioanal. Chem.*, in press.
10 C. O. MINKKINEN, *Collected Radiochemical Procedures*, Los Alamos, Report L.A. 1721, Jan. 1958.
11 F. NELSON AND K. A. KRAUS, *J. Amer. Chem. Soc.*, 76 (1954) 5916.
12 J. P. FRANÇOIS, R. GIJBELS AND J. HOSTE, *J. Radioanal. Chem.*, 5 (1970) 251.
13 D. F. PEPPARD, G. W. MASSON AND J. L. MAIER, *J. Inorg. Nucl. Chem.*, 3 (1956) 215.
14 E. B. SANDELL, *Colorimetric Determinations of Traces of Metals*, Interscience, London, 1959.
15 *Instruction Manual of the Fluoride Electrode*, Orion Research Incorporation.
16 D. MONNIER, G. DELPIN AND W. HAERDI, *Anal. Chim. Acta*, 35 (1966) 231.
17 L. CURRIE, *Anal. Chem.*, 40 (1968) 587.
18 H. W. KIRBY, *The Radiochemistry of Protactinium*, NAS-NS 3016, 1959.
19 P. VAN DEN WINKEL, De Bepaling van Sporenelementen in Biologisch Materiaal door Neutronen-activeringsanalyse, *Verhandel. Koninkl. Vlaam. Akad. Wetenschap. Belg., Kl. Wetenschap.*, 114 (1970) 106.
20 B. CHU, D. C. WHITNEY AND R. M. DIAMOND, *J. Inorg. Nucl. Chem.*, 24 (1962) 1405.

*Analytica Chimica Acta*
Elsevier Publishing Company, Amsterdam
Printed in The Netherlands



# EXTRACTION PAR LES SELS D'AMMONIUM QUATERNAIRE A HAUT POIDS MOLECULAIRE, DE L'ACIDE HYDROXYETHYLETHYLENEDIAMINETRIACETIQUE ET DE SES COMPLEXES AVEC LES LANTHANIDES ET LES ACTINIDES TRIVALENTS

## TOME I. EXTRACTION DU COMPLEXANT

N. ZAMAN*, E. MERCINY ET G. DUYCKAERTS
*Laboratoire de Chimie Analytique et Nucléaire, Université de Liège au Sart Tilman, B-4000 Liège (Belgique)*
(Reçu le 14 mai 1971)

La formation, entre l'acide hydroxyéthyléthylènediaminetriacétique (HEDTA) et les lanthanides ou les actinides trivalents, de complexes chargés négativement est prouvée par de nombreux résultats expérimentaux[1-6]. On relève pourtant certaines divergences de vue en ce qui concerne la stoechiométrie et la charge de ces complexes; pour delle Sitte et Baybarz[5], les complexes formés répondent aux formules $Me_2Y_3^{3-}$ et $MeY_2^{3-}$; Merciny *et al.*[6], par contre, interprètent leurs résultats expérimentaux en attribuant à ces complexes la formule $MeY_2H_{3-m}^{m-}$ dans laquelle $m$ peut être égal à 1, 2 ou 3 selon la nature du métal et le pH du milieu.

Nous avons résolu d'étudier ce problème par extraction liquide–liquide dans le double but de préciser leur formule et leur charge, d'une part, et, d'autre part, de trouver des conditions favorables de séparation des lanthanides et surtout des actinides trivalents.

Les résultats expérimentaux rapportés dans cette première partie du travail concernent l'extraction, par les sels d'ammonium quaternaire, du complexant lui-même.

### CONDITIONS EXPÉRIMENTALES

*Purification des réactifs*

Nous utilisons, comme phase organique, une solution, dans le benzène, de chlorure de tricaprylméthylammonium (TCMACl ou Aliquat 336; General Mills). Le produit commercial est souillé par des quantités importantes d'alcool caprylique, des traces de HCl et quelques impuretés solubles dans l'eau. On le purifie tout d'abord par chauffage sous vide à 90° pendant 4 jours. Il est ensuite dissous dans le benzène et lavé plusieurs fois à l'eau. Après élimination du benzène et des traces d'eau par chauffage modéré sous vide, on titre l'amine. Sa pureté est évaluée à plus de 99%.

Le HEDTA utilisé est fourni par la firme Fluka. On le purifie par une double cristallisation dans l'eau tridistillée.

---

* Boursier O.C.D. du Pakistan.

*Dosage des réactifs dans les deux phases*

*Titrage direct de HEDTA en phase organique.* On prépare une solution ammoniacale de cuivre en ajoutant goutte à goutte de l'ammoniaque concentrée à une solution de $CuCl_2$ jusqu'à redissolution complète du précipité de $Cu(OH)_2$. On pipette une partie aliquote de la phase organique et on titre par la solution de cuivre ammoniacal en présence de murexide comme indicateur. Différents tests ont montré que les résultats ne sont influencés ni par la teneur de la phase organique en sel d'ammonium quaternaire, ni par le pH de la phase aqueuse d'équilibration. La reproductibilité des résultats est de 0.05%. Le HEDTA en phase aqueuse est titré par la même méthode.

*Titrage du chlorure d'ammonium quaternaire en phase organique*[7]. Deux méthodes ont été utilisées pour titrer l'amine en phase organique : la première consiste à diluer un volume connu de phase organique par un mélange d'acide acétique et d'anhydride acétique et de titrer par une solution d'acide perchlorique dans du dioxane anhydre. Le titrage est suivi potentiométriquement grâce à une électrode de verre conditionnée dans l'acide acétique glacial et une électrode de référence au calomel.

La seconde méthode est une modification de la méthode de dosage des chlorures de Volhard: à un volume connu de phase organique, on ajoute un très large excès d'alcool méthylique dont le rôle sera de maintenir une seule phase pendant le titrage; on ajoute encore de l'acide nitrique à 50% et un excès de nitrate d'argent afin de précipiter la totalité des ions chlors.

L'excès de nitrate d'argent est déterminé par titrage au sulfocyanate de potasse en présence d'alun ferrique comme indicateur.

Les résultats obtenus par ces deux méthodes sont identiques.

Les chlorures en phase aqueuse sont titrés par la méthode classique de Volhard.

*Conditions expérimentales de l'extraction*

Dans des tubes en Pyrex à fermeture hermétique, on introduit un volume égal (15 ml) de chacune des deux phases suivantes: phase organique, solution de TCMACl dans le benzène, phase aqueuse, solution de HEDTA dans l'eau tridistillée.

On laisse équilibrer pendant au moins 6 h, à 25°, sous agitation constante. Les deux phases sont ensuite séparées par centrifugation; on détermine, à l'équilibre, la teneur en HEDTA et en chlorures des deux phases ainsi que le pH de la phase aqueuse.

Le HEDTA est un acide tribasique dont les trois p$K$ valent respectivement 2.64, 5.33 et 9.74. Les fonctions de distribution des différentes formes ioniques du complexant montrent qu'à pH égal à 4, l'acide est essentiellement sous forme $H_2Y^{2-}$ (91%); à pH 7, il est entièrement sous forme binégative $HY^{2-}$ et, à pH 11, entièrement sous forme trinégative $Y^{3-}$. Afin de simplifier l'interprétation des résultats, nous avons conduit les extractions de façon à ce que le pH à l'équilibre soit toujours égal à 4, 7 ou 11 respectivement. On peut ainsi admettre qu'une seule forme ionique de $H_3Y$ participe à l'extraction, les autres pouvant être négligées.

## RÉSULTATS

*Influence de la concentration en HEDTA et en $Cl^-$ en phase aqueuse*

On peut imaginer une équation générale représentant l'extraction de HEDTA

en phase organique et écrire:

$$m(R_3R'NCl)_o + (H_{3-m}Y^{m-})_w \overset{K_m}{\rightleftharpoons} [(R_3R'N)_mH_{3-m}Y^{m-})]_o + m(Cl^-)_w \quad (1)$$

Cette relation ne tient pas compte d'une éventuelle polymérisation de l'amine en phase organique ou du complexant en phase aqueuse et suppose, à priori, que l'extraction de HEDTA en phase organique est uniquement due à une réaction d'échange ionique.

Si cette hypothèse est valable, on voit que:

$$[H_3Y]_o = m[Cl^-]_w \quad (2)$$

où $m$ peut être égal à 1, 2 ou 3 suivant la valeur du pH à l'équilibre, $[H_3Y]_o$ représentant $[(R_3R'N)_mH_{3-m}Y^{m-}]_o$, c'est-à-dire la concentration totale en HEDTA dans la phase organique. La relation (2) mise sous forme logarithmique est l'équation d'une droite de pente 1 dont l'ordonnée à l'origine est égale à log $m$.

Une série d'expériences d'extraction a été réalisée en maintenant constante la concentration de l'amine en phase organique (0.5 $M$) et en faisant varier soit la concentration en HEDTA, soit la concentration en $Cl^-$ en phase aqueuse aux 3 pH habituels de 4, 7 et 11. Les résultats sont représentés sur la Fig. 1.

*pH* 11. Le graphique de log $[H_3Y]_o$ en fonction de log $[Cl^-]_w$ est une droite de pente égale à 1. Log $m$ est égal à 0.47, $m$ vaut par conséquent 3.

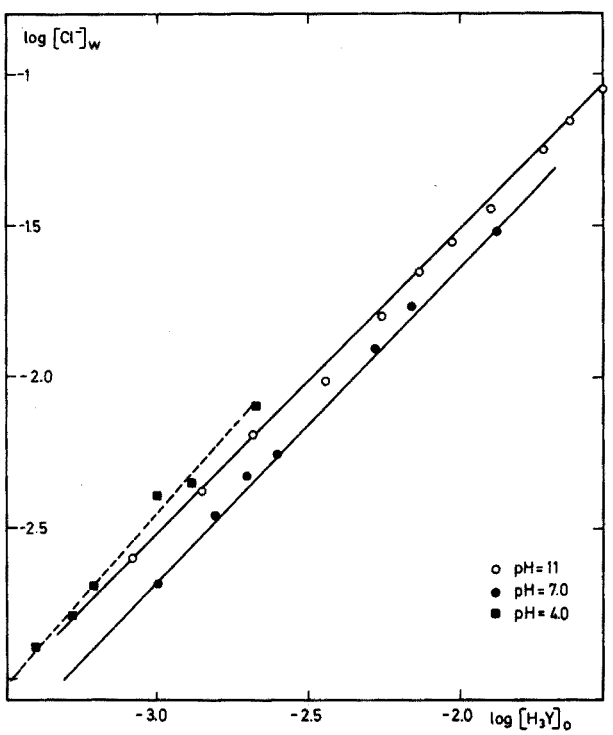


Fig. 1. Relation entre la concentration en HEDTA en phase organique et la concentration en ions $Cl^-$ en phase aqueuse pour trois pH: 11, 7 et 4. $[TCMACl]_o = 0.5$ $M$ dans le benzène. Température: 25°.

*pH* 7. La pente de la droite log $[H_3Y]_o$ en fonction de log $[Cl^-]_w$ est aussi égale à 1 et on trouve pour *m* une valeur de 2.09.

Ainsi, pour ces deux pH à l'équilibre, les résultats expérimentaux semblent prouver la validité de l'équation proposée. Le mécanisme de l'extraction semble bien être une réaction d'échange ionique et le HEDTA se comporte comme un monomère en phase aqueuse.

On peut d'ailleurs représenter ces résultats d'une autre façon; en appliquant la loi d'action des masses à l'éqn. (1), on obtient:

$$\log [H_3Y]_o/[H_3Y]_w = m \log [Cl^-]_o/[Cl^-]_w + \log K_m \quad (3)$$

avec $[H_3Y]_w = [H_{3-m}Y^{m-}]_w$ et $[Cl^-]_o = [R_3R'NCl]_o$.

Ainsi, en portant en graphique le log du coefficient de distribution du complexant en fonction de log $[Cl^-]_o/[Cl^-]_w$, on doit obtenir respectivement une droite de pente 3 à pH 11 et de pente 2 à pH 7. Les résultats expérimentaux sont rassemblés dans le Tableau I et représentés sur la Fig. 2. Ils confirment, une fois de plus, l'hypothèse émise.

TABLEAU I

INFLUENCE DE LA CONCENTRATION EN HEDTA ET EN KCl EN PHASE AQUEUSE

| $[Cl^-]_o(M\ l^{-1})$ | $[Cl^-]_w(M\ l^{-1})$ | $\log \frac{[Cl^-]_o}{[Cl^-]_w}$ | $[H_3Y]_{initial}$ | $\log (D_c)_{HEDTA}$ |
|---|---|---|---|---|
| *pH* = 7 | | | | |
| $5.00 \cdot 10^{-1}$ | $3.00 \cdot 10^{-2}$ | 1.20 | $2.5 \cdot 10^{-2}$ | 0.02 |
| $4.70 \cdot 10^{-1}$ | $3.50 \cdot 10^{-2}$ | 1.12 | $5.0 \cdot 10^{-2}$ | −0.48 |
| $5.00 \cdot 10^{-1}$ | $1.00 \cdot 10^{-1}$ | 0.70 | $5.0 \cdot 10^{-2}$ | −1.16 |
| $5.00 \cdot 10^{-1}$ | $5.00 \cdot 10^{-1}$ | 0.00 | $5.0 \cdot 10^{-2}$ | −2.42 |
| $4.60 \cdot 10^{-1}$ | 1.00 | −0.3 | $5.0 \cdot 10^{-2}$ | −3.02 |
| $5.00 \cdot 10^{-1}$ | $6.00 \cdot 10^{-2}$ | 0.88 | $1.0 \cdot 10^{-1}$ | −0.577 |
| $4.90 \cdot 10^{-1}$ | $1.00 \cdot 10^{-1}$ | 0.70 | $1.0 \cdot 10^{-1}$ | −1.22 |
| $5.00 \cdot 10^{-1}$ | $5.00 \cdot 10^{-1}$ | 0.00 | $1.0 \cdot 10^{-1}$ | −3.05 |
| $5.00 \cdot 10^{-1}$ | $4.00 \cdot 10^{-2}$ | 1.08 | $5.0 \cdot 10^{-1}$ | −0.30 |
| $3.00 \cdot 10^{-1}$ | $2.50 \cdot 10^{-2}$ | 1.08 | $2.5 \cdot 10^{-2}$ | −0.25 |
| *pH* = 11 | | | | |
| $4.45 \cdot 10^{-1}$ | $5.40 \cdot 10^{-2}$ | 0.92 | $2.5 \cdot 10^{-2}$ | 0.41 |
| $4.53 \cdot 10^{-1}$ | $7.00 \cdot 10^{-2}$ | 0.79 | $5.0 \cdot 10^{-2}$ | 0.08 |
| $4.75 \cdot 10^{-1}$ | $1.30 \cdot 10^{-1}$ | 0.56 | $5.0 \cdot 10^{-2}$ | −0.67 |
| $4.30 \cdot 10^{-1}$ | $5.00 \cdot 10^{-1}$ | −0.07 | $5.0 \cdot 10^{-2}$ | −2.29 |
| $4.2 \cdot 10^{-1}$ | $1.00 \cdot 10^{-1}$ | 0.62 | $1.0 \cdot 10^{-1}$ | −0.45 |
| $4.1 \cdot 10^{-1}$ | $9.00 \cdot 10^{-2}$ | 0.64 | $1.0 \cdot 10^{-1}$ | −0.37 |
| $4.6 \cdot 10^{-1}$ | $1.40 \cdot 10^{-1}$ | 0.52 | $1.0 \cdot 10^{-1}$ | −0.82 |
| $5.0 \cdot 10^{-1}$ | $5.00 \cdot 10^{-1}$ | 0.00 | $1.0 \cdot 10^{-1}$ | −2.30 |

*pH* 4. La droite du log $[H_3Y]_o$ en fonction de log $[Cl^-]_w$ a une pente différente de 1 et on ne trouve plus pour *m* la valeur attendue. On peut trouver deux explications à ce fait: il faut d'abord se rappeler qu'à ce pH, 91 % seulement de l'acide se trouve sous forme de $H_2Y^-$, le reste étant réparti entre la forme inactive $H_3Y$ et la forme binégative $HY^{2-}$ qui participe également à l'extraction en tendant à augmenter la

pente de la droite. De plus, à ce pH, il y a formation d'émulsion en phase aqueuse qu'il est impossible de démixer même par centrifugation prolongée. La détermination de la concentration en ions $Cl^-$ libres en phase aqueuse est affectée par la présence d'amine en suspension; il est, par conséquent, difficile d'établir, avec précision, la balance entre le $Cl^-$ en phase aqueuse et le HEDTA en phase organique.

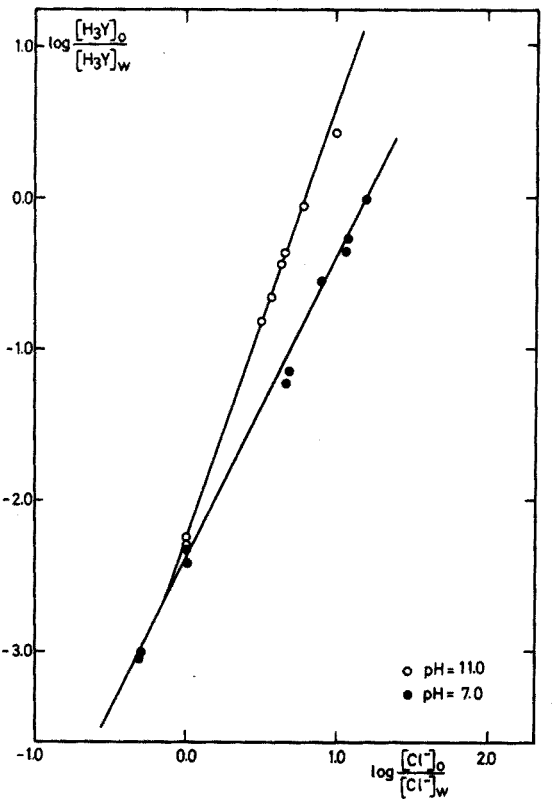


Fig. 2. Influence de la concentration en HEDTA et en $Cl^-$ en phase aqueuse sur le coefficient de distribution de l'acide à pH 11 et 7. Phase organique: 0.5 *M* en TCMACl dans le benzène. Température: 25°.

*Influence de la concentration en amine de la phase organique*

La seconde série d'expériences a été réalisée en maintenant constants tous les paramètres expérimentaux à l'exception, cette fois, de la concentration en amine en phase organique. Les résultats sont résumés dans le Tableau II et représentés graphiquement sur la Fig. 3.

Aux trois pH considérés, la pente de la droite log $[Cl^-]_o/[Cl^-]_w$ en fonction du log $[H_3Y]_o/[H_3Y]_w$ est égale à 1. La relation (1) qui nous a permis d'interpréter quantitativement les premiers résultats est mise en défaut par ces dernières expériences.

On sait, par de nombreux travaux sur le comportement des sels d'ammonium quaternaire en phase organique, que ceux-ci se trouvent en solution sous forme d'agrégats moléculaires, le degré de polymérisation dépendant très fortement des conditions du milieu (solvant, température, concentration ...)[8-10].

TABLEAU II

INFLUENCE DE LA CONCENTRATION EN TCMACl EN PHASE ORGANIQUE
(Phase aqueuse: $2.50 \cdot 10^{-2}$ *M* HEDTA)

| $[Cl^-]_o (M\ l^{-1})$ | $[Cl^-]_w (M\ l^{-1})$ | $\log \frac{[Cl^-]_o}{[Cl^-]_w}$ | $\log (D_c)_{HEDTA}$ |
|---|---|---|---|
| *pH* = 4.0 | | | |
| $5.00 \cdot 10^{-1}$ | $8.60 \cdot 10^{-3}$ | 1.77 | −0.38 |
| $3.20 \cdot 10^{-1}$ | $1.13 \cdot 10^{-2}$ | 1.45 | −0.70 |
| $1.13 \cdot 10^{-1}$ | $7.93 \cdot 10^{-3}$ | 1.15 | −1.0 |
| $5.00 \cdot 10^{-2}$ | $4.30 \cdot 10^{-3}$ | 1.06 | −1.12 |
| $3.00 \cdot 10^{-2}$ | $4.00 \cdot 10^{-3}$ | 0.87 | −1.36 |
| $1.00 \cdot 10^{-2}$ | $2.90 \cdot 10^{-3}$ | 0.55 | −1.36 |
| $8.00 \cdot 10^{-3}$ | $2.03 \cdot 10^{-3}$ | 0.59 | −1.56 |
| $5.00 \cdot 10^{-3}$ | $1.70 \cdot 10^{-3}$ | 0.46 | −1.62 |
| $2.74 \cdot 10^{-3}$ | $1.23 \cdot 10^{-3}$ | 0.34 | −1.75 |
| *pH* = 8.0 | | | |
| $5.40 \cdot 10^{-1}$ | $2.54 \cdot 10^{-2}$ | 1.28 | 0.02 |
| $3.00 \cdot 10^{-1}$ | $3.00 \cdot 10^{-2}$ | 1.00 | −0.26 |
| $1.07 \cdot 10^{-1}$ | $1.35 \cdot 10^{-2}$ | 0.90 | −0.43 |
| $4.50 \cdot 10^{-2}$ | $1.01 \cdot 10^{-2}$ | 0.65 | −0.59 |
| $3.66 \cdot 10^{-2}$ | $9.00 \cdot 10^{-3}$ | 0.60 | −0.77 |
| $9.76 \cdot 10^{-3}$ | $4.80 \cdot 10^{-3}$ | 0.31 | −0.97 |
| $6.90 \cdot 10^{-3}$ | $3.90 \cdot 10^{-3}$ | 0.24 | −1.07 |
| $3.50 \cdot 10^{-3}$ | $2.98 \cdot 10^{-3}$ | −0.05 | −1.20 |
| $1.70 \cdot 10^{-3}$ | $1.81 \cdot 10^{-3}$ | −0.02 | −1.44 |
| *pH* = 11.0 | | | |
| $4.45 \cdot 10^{-1}$ | $5.40 \cdot 10^{-2}$ | 0.92 | 0.41 |
| $2.75 \cdot 10^{-1}$ | $4.30 \cdot 10^{-2}$ | 0.80 | 0.12 |
| $7.40 \cdot 10^{-2}$ | $3.78 \cdot 10^{-2}$ | 0.29 | −0.08 |
| $2.80 \cdot 10^{-2}$ | $2.16 \cdot 10^{-2}$ | 0.11 | −0.34 |
| $1.40 \cdot 10^{-2}$ | $1.63 \cdot 10^{-2}$ | −0.07 | −0.55 |
| $2.50 \cdot 10^{-3}$ | $7.43 \cdot 10^{-3}$ | −0.48 | −0.96 |
| $2.00 \cdot 10^{-3}$ | $6.00 \cdot 10^{-3}$ | −0.48 | −1.05 |
| $7.00 \cdot 10^{-4}$ | $4.29 \cdot 10^{-3}$ | −0.79 | −1.22 |

Nous avons donc tenté d'interpréter nos résultats en modifiant l'équation (1) de façon à tenir compte d'une éventuelle polymérisation du sel d'amine et en admettant qu'un agrégat n'échange qu'un seul ion chlorure.

Tous les résultats expérimentaux, qu'il s'agisse de ceux en fonction de la concentration en HEDTA et en $Cl^-$ ou de ceux en fonction de la concentration en sel d'ammonium se laissent interpréter sur la base de l'équation générale suivante:

$$m(R_3R'NCl)_x + H_{3-m}Y^{m-} \underset{K_m}{\rightleftharpoons} [(R_3R'NCl)_{x-1} \ldots (R_3R'N)]_m\, H_{3-m}Y^{m-} + m\, Cl^- \quad (4)$$

$x$ étant le degré moyen d'agrégation.

Si nous appliquons la loi d'action des masses à cette équation, nous pouvons écrire:

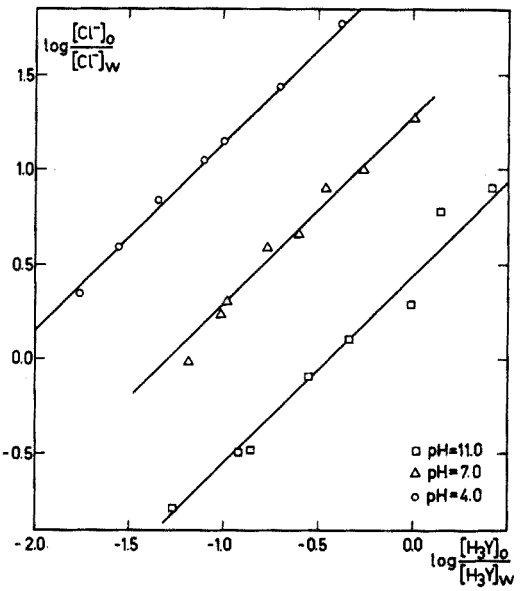


Fig. 3. Influence de la concentration en TCMACl en phase organique (benzène) sur le coefficient de distribution du HEDTA. Phase aqueuse: $2.5 \cdot 10^{-2}$ *M* en HEDTA à pH 11,7 et 4. Température: 25°.

$$\frac{[H_3Y]_o[Cl^-]_w^m}{[H_3Y]_w[(R_3R'NCl)_x]_o^m} = K_m \qquad (5)$$

en admettant qu'aux trois pH considérés, 4, 7 et 11, nous n'avons qu'une espèce ionique du HEDTA en phase aqueuse et organique et que $[H_3Y]_o$ et $[H_3Y]_w$ représentent les concentrations analytiques en HEDTA dans chacune des phases.

*Calcul du degré de polymérisation et de la constante d'extraction*

Nous pouvons, dans l'éqn. (5), remplacer $[(R_3R'NCl)_x]_o$ par

$$\frac{[R_3R'NCl]_i}{x} - m[H_3Y]_o ,$$

si bien que l'on obtient,

$$\frac{[H_3Y]_o[Cl^-]_w^m}{[H_3Y]_w\left[\frac{[R_3R'NCl]_i}{x} - m[H_3Y]_o\right]_o^m}$$

Nous avons vu qu'à pH 11, le HEDTA se trouve entièrement sous forme de $Y^{3-}$, donc $m=3$. Nous pouvons alors utiliser toutes les données expérimentales pour déterminer $K_3$ et $x$; le calcul a été fait par approximations successives.

Le même calcul a été fait à pH 7 où $m=2$; toutefois, à pH 4, nous avons vu que les données expérimentales sont difficilement interprétables à cause des phénomènes secondaires dont nous avons parlé.

Les résultats obtenus à pH 7 et 11 sont repris dans le Tableau III.

TABLEAU III

DEGRÉ DE POLYMÉRISATION MOYEN ET CONSTANTE D'EXTRACTION

| *pH* | *Degré de polymérisation* | *Constante d'extraction K* |
|---|---|---|
| 11 | 2.75 | 0.200 |
| 7 | 2.75 | 0.0316 |

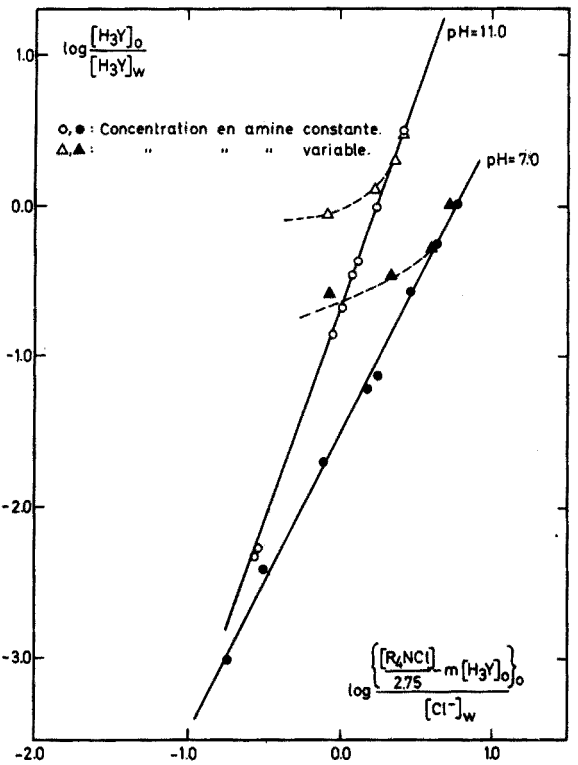


Fig. 4. Interprétation des résultats expérimentaux sur la base de la réaction d'extraction

$$m(R_3R'NCl)_{2.75} + H_{3-m}Y^{m-} \underset{K_m}{\rightleftharpoons} [(R_3R'NCl)_{1.75}(R_3R'N)]_m\, H_{3-m}Y^{m-} + mCl^-$$

Tous les résultats expérimentaux obtenus à pH 7 et 11 ont été recalculés sur la base de la relation (4) en tenant compte de la valeur du degré de polymérisation de 2.75.

La Fig. 4 montre qu'en ce qui concerne les expériences effectuées à concentration en amine constante, la concordance est parfaite entre la théorie et la pratique. Les expériences effectuées en fonction de la concentration en amine en phase organique ne s'interprètent, sur la base de la relation (4), que dans un domaine de concentration en amine allant de 0.1 à 0.5 *M*; les écarts observés en dessous de cette concentration sont vraisemblablement dus à une diminution du degré de polymérisation de l'amine.

Nous remercions l'Institut Interuniversitaire des Sciences Nucléaires et l'Office de la Coopération au Développement pour l'intérêt constant apporté à nos travaux et le soutien financier accordé à notre laboratoire.

RÉSUMÉ

Le chlorure d'ammonium quaternaire est utilisé pour extraire en phase organique l'acide hydroxyéthyléthylènediaminetriacétique (HEDTA). Quel que soit le pH considéré, le passage du HEDTA en phase organique semble s'effectuer par réaction d'échange d'ions. Les résultats de distribution montrent également que l'amine existe en phase organique sous forme d'agrégats moléculaires et qu'à l'intérieur de ces agrégats, un seul ion $Cl^-$ est disponible pour l'échange avec le HEDTA. Le degré moyen d'agrégation trouvé est de 2.75 et les constantes d'équilibre d'extraction ont été déterminées avec l'Aliquat 336.

SUMMARY

The extraction of hydroxyethylethylenediaminetriacetic acid is carried out at different pH values of the aqueous phase with quaternary ammonium chloride in benzene: in all cases, the extraction of HEDTA in the organic phase seems to be an ion-exchange phenomenon. The distribution results show that the quaternary ammonium salt is polymeric in the organic phase and that, per molecule, only one chloride ion is exchanged with the acid molecule. The average polymerisation factor was found to be 2.75. Extraction equilibrium constants are determined with Aliquat 336.

ZUSAMMENFASSUNG

Quaternäre Ammoniumchloride werden zur Extraktion von Hydroxyäthyläthylendiamintriessigsäure (HEDTA) in eine organische Phase benutzt. Bei allen untersuchten pH-Werten scheint sich die HEDTA-Extraktion durch eine Ionenaustauschreaktion zu vollziehen. Die Messungen ergeben weiter, dass das Amin in der organischen Phase als Molekülaggregat vorliegt. Im Inneren dieser Aggregate kann nur ein Chloridion gegen HEDTA ausgetauscht werden. Der mittlere Aggregationsgrad (2.75) und die Gleichgewichtskonstanten der Extraktion wurden für Aliquat 336 bestimmt.

BIBLIOGRAPHIE

1 W. KRAAK ET J. VAN OOYEN, *Final Report on Transplutonium Research*, Euratom Contract 005-61-11, Petten, 1965.
2 F. L. MOORE, *Anal. Chem.*, 36 (1964) 2159.
3 F. L. MOORE, *Anal. Chem.*, 37 (1965) 419.
4 E. MERCINY ET G. DUYCKAERTS, *J. Chromatog.*, 35 (1968) 549.
5 A. DELLE SITTE ET D. R. BAYBARZ, *J. Inorg. Nucl. Chem.*, 34 (1969) 220.
6 E. MERCINY, P. ZUR NEDDEN ET G. DUYCKAERTS, *Anal. Lett.*, 4 (1) (1971) 29.
7 J. KUCHARSKY ET L. SAFARYK, *Titration in Non-Aqueous Solvents*, Elsevier, Amsterdam, 1965.
8 J. VAN OOYEN, *Thèse de doctorat*, Université d'Amsterdam, 1970.
9 M. L. GOOD ET S. C. SRIVASTAVA, *J. Inorg. Nucl. Chem.*, 27 (1965) 2429.
10 Y. G. FROLOVE, A. V. OCHKIN ET V. V. SERGIENSKY, *At. Energy Rev.*, 7 (1969) 71.

*Analytica Chimica Acta*
Elsevier Publishing Company, Amsterdam
Printed in The Netherlands



# EXTRACTION PAR LES SELS D'AMMONIUM QUATERNAIRE A HAUT POIDS MOLECULAIRE, DE L'ACIDE HYDROXYETHYLETHYLENEDIAMINETRIACETIQUE ET DE SES COMPLEXES AVEC LES LANTHANIDES ET LES ACTINIDES TRIVALENTS

## TOME II. EXTRACTION DE L'AMÉRICIUM ET DU CURIUM

N. ZAMAN*, E. MERCINY ET G. DUYCKAERTS
*Laboratoire de Chimie Analytique et Nucléaire, Université de Liège au Sart Tilman, B-4000 Liège (Belgique)*
(Reçu le 14 mai 1971)

Dans la première partie de ce travail[1], nous avons étudié le mécanisme d'extraction des différentes formes ioniques de HEDTA par le chlorure de tricaprylméthylammonium en solution dans le benzène.

Nous voudrions rendre compte, dans cette seconde partie, des résultats obtenus dans l'étude de l'extraction des complexes négatifs de stoechiométrie 1:2 formés entre le HEDTA et les actinides trivalents américium et curium.

Ces expériences ont pour buts de déterminer les constantes de formation des complexes doubles, d'une part, et, d'autre part, de trouver les conditions expérimentales les plus favorables pour une séparation du couple d'actinides considéré.

### CONDITIONS EXPÉRIMENTALES

Des volumes égaux (15 ml) de phase aqueuse contenant l'isotope radioactif en dose traceur et de phase organique sont équilibrés pendant au moins 6 h, à 25°, sous agitation constante. Après séparation des deux phases par centrifugation prolongée, on pipette des volumes égaux (2 ml) de phase aqueuse et de phase organique; la mesure de l'activité de chacune des deux phases permet le calcul du coefficient de distribution du métal.

La distribution du métal est étudiée en fonction du pH; ce dernier est mesuré au moyen d'un pH-mètre Beckman type Expandomatic.

Les expériences sont effectuées dans les conditions suivantes:

1. phase organique 0.5 *M* en TCMACl, saturée au préalable par HEDTA à différents pH; phase aqueuse 0.1 *M* en HEDTA au même pH que celui de saturation de l'amine.

2. phase organique 0.5 *M* en TCMACl sans saturation préalable; phase aqueuse 0.1 *M* en HEDTA à différents pH.

3. phase organique 0.5 *M* en TCMACl sans prétraitement; phase aqueuse 0.1 *M* en HEDTA, 0.1 *M* en KCl à différents pH.

---

* Boursier O.C.D. du Pakistan.

## RÉSULTATS ET DISCUSSION

Les résultats de ces trois séries d'expériences sont résumés dans les Tableaux I, II et III et représentés graphiquement sur les Figs. 1, 2 et 3.

TABLEAU I

EXTRACTION AMÉRICIUM–CURIUM

(Phase organique: $5.0 \cdot 10^{-1}$ *M* TCMACl saturé au préalable par HEDTA; phase aqueuse: $10^{-1}$ *M* HEDTA; $t = 25°$)

| *pH* | $\log (D_c)_{Am}$ | $\log (D_c)_{Cm}$ |
|---|---|---|
| 2.10 | −0.45 | −0.75 |
| 3.00 | −0.20 | −0.15 |
| 4.00 | −0.00 | 0.28 |
| 5.00 | 0.08 | 0.52 |
| 6.00 | 0.00 | 0.58 |
| 7.00 | 0.00 | 0.60 |
| 8.10 | 0.05 | 0.75 |
| 8.30 | 0.07 | 0.76 |
| 9.00 | 0.16 | 0.80 |
| 10.00 | −0.15 | 0.37 |
| 11.00 | −0.26 | 0.00 |

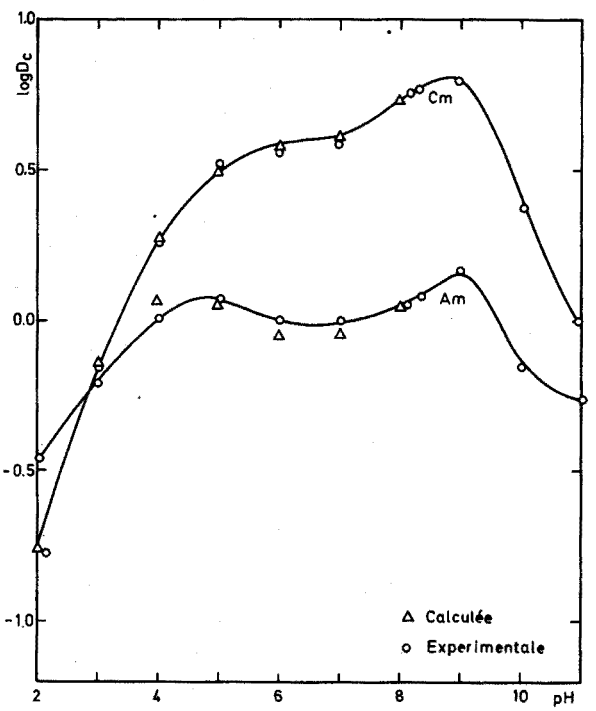


Fig. 1. Extraction de $Am^{3+}$ et $Cm^{3+}$ en dose traceur par TCMACl en solution dans le benzène. Phase organique: 0.5 *M* en TCMACl prétraitée par HEDTA à différents pH. Phase aqueuse: 0.1 *M* en HEDTA. $t = 25°$.

TABLEAU II

EXTRACTION AMÉRICIUM–CURIUM

(Phase organique: $5.0 \cdot 10^{-1}$ *M* TCMACl; phase aqueuse: $10^{-1}$ *M* HEDTA; $10^{-1}$ *M* KCl; $t = 25°$)

| *pH* | $\log (D_c)_{Am}$ | $\log (D_c)_{Cm}$ |
|---|---|---|
| 2.18 | — | −2.20 |
| 3.0 | −2.40 | −1.27 |
| 4.04 | −1.48 | −0.61 |
| 4.48 | −1.39 | −0.78 |
| 5.10 | −1.45 | −0.69 |
| 5.53 | −1.49 | −0.80 |
| 6.33 | −1.34 | −0.61 |
| 8.93 | −1.15 | −0.41 |
| 9.23 | −1.09 | −0.24 |
| 9.42 | −1.12 | −0.46 |
| 9.80 | −1.16 | −0.50 |
| 10.24 | −1.18 | −0.52 |
| 10.62 | −1.26 | −0.59 |
| 10.81 | −1.28 | −0.53 |

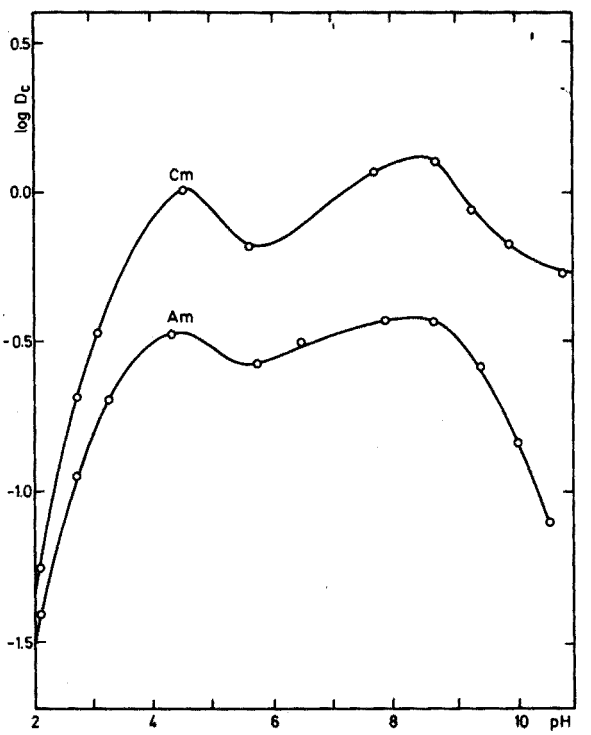


Fig. 2. Extraction de $Am^{3+}$ et $Cm^{3+}$ en dose traceur par TCMACl en solution dans le benzène. Phase organique: 0.5 *M* en TCMACl sans prétraitement. Phase aqueuse: 0.1 *M* en HEDTA. $t = 25°$.

TABLEAU III

EXTRACTION AMÉRICIUM–CURIUM

(Phase organique: $5 \cdot 10^{-1}$ *M* TCMACl; phase aqueuse: $10^{-1}$ *M* HEDTA; $t = 25°$)

| *pH* | $log\ (D_c)_{Am}$ | $log\ (D_c)_{Cm}$ |
|---|---|---|
| 2.10 | −1.42 | −1.24 |
| 2.81 | −0.90 | −0.63 |
| 3.52 | −0.61 | −0.29 |
| 4.76 | −0.48 | −0.04 |
| 5.60 | −0.58 | −0.22 |
| 6.35 | −0.53 | −0.12 |
| 7.72 | −0.43 | −0.06 |
| 9.32 | −0.56 | −0.06 |
| 9.92 | −0.79 | −0.21 |
| 10.25 | −0.84 | −0.31 |
| 11.25 | −1.13 | −0.26 |
| 12.3 | −0.87 | −0.31 |

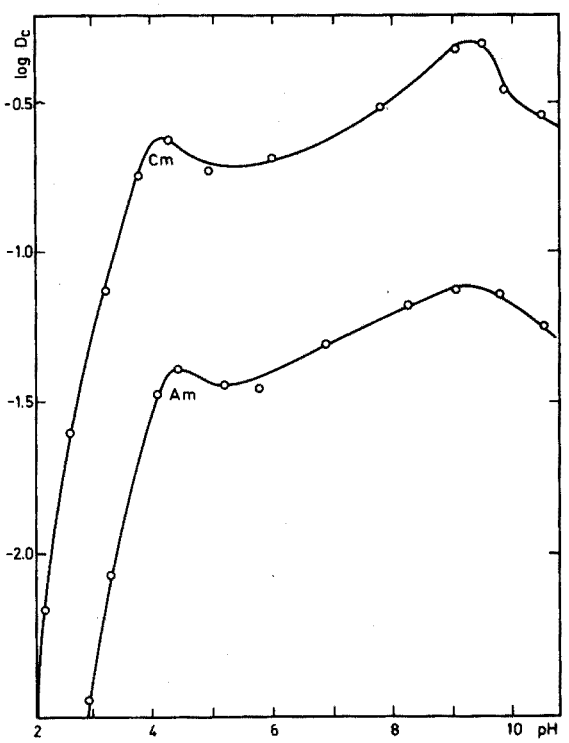


Fig. 3. Extraction de $Am^{3+}$ et $Cm^{3+}$ en dose traceur par TCMACl en solution dans le benzène. Phase organique: 0.5 *M* en TCMACl sans prétraitement. Phase aqueuse: 0.1 *M* en HEDTA et 0.1 *M* en KCl. $t = 25°$.

*Détermination des constantes de formation des complexes doubles*

Les conditions les plus favorables pour la détermination des constantes de stabilité des complexes doubles $MeH_{3-m}Y_2^{m-}$ sont celles où la solution organique d'amine a été préalablement saturée par du HEDTA au même pH et se trouve, par conséquent, déjà en équilibre avec celle où s'effectue l'extraction du métal; en effet, dans ces conditions, on peut considérer que le seul phénomène qui entre en jeu est la distribution du métal entre les deux phases. Ce dernier étant, en outre, en dose traceur, on peut admettre que son passage en phase organique ne modifie en rien la composition du milieu: les concentrations, en phase aqueuse et en phase organique, de HEDTA et de l'amine ne subissent aucune modification.

On peut alors établir une relation qui permet le calcul de la constante de formation du complexe double; en effet:

$$K_c = \frac{[MeY]}{[Me][Y]} \tag{1}$$

et

$$(K'_c)_m = \frac{[MeH_{3-m}Y_2^{m-}]}{[MeY][H_{3-m}Y]} \tag{2}$$

La constante de partage du complexe s'écrit:

$$(P_c)_m = \frac{[MeH_{3-m}Y_2^{m-}]_0}{[MeH_{3-m}Y_2^{m-}]_w} \tag{3}$$

Le coefficient de distribution du métal étant défini par la relation

$$D_c = \frac{\text{concentration totale en métal en phase organique}}{\text{concentration totale en métal en phase aqueuse}}$$

on obtient:

$$D_c = \frac{[MeH_2Y_2^-]_0 + [MeHY_2^{2-}]_0 + [MeY_2^{3-}]_0}{[Me^{3+}]_w + [MeY]_w + [MeH_2Y_2^-]_w + [MeHY_2^{2-}]_w + [MeY_2^{3-}]_w} \tag{4}$$

En tenant compte des relations (1), (2) et (3) et en les introduisant dans la relation (4), on arrive à l'expression:

$$D_c = \frac{[(P_c)_1 (K'_c)_1 \theta_2 + (P_c)_2 (K'_c)_2 \theta_3 + (P_c)_3 \theta_4}{([H_3Y]_w^2 K_c \theta_4)^{-1} + ([H_3Y]_w)^{-1} + (K'_c)_1 \theta_2 + (K'_c)_2 \theta_3 + (K'_c)_3 \theta_4} \tag{5}$$

dans laquelle $\theta_2$, $\theta_3$ et $\theta_4$ sont les fonctions de distribution des différentes formes ioniques du complexant et $[H_3Y]_w$, la concentration analytique en HEDTA en phase aqueuse.

Dans cette relation, la concentration en $[H_3Y]_w$ est connue, de même que la constante de formation du complexe ($K_c$). Les valeurs de $\theta_2$, $\theta_3$ et $\theta_4$ sont aisément calculables si on connait le pH du milieu et $D_c$ est déterminé expérimentalement. On obtient ainsi une équation à 6 inconnues dont la résolution, même par ordinateur, s'avère très difficile.

Afin de simplifier le calcul, on commence par choisir une zône de pH où l'on peut considérer comme négligeable l'une des formes protonées du complexe double; ainsi, au delà de pH = 6, on peut admettre, en première approximation, que la concentration en $MeY_2H_2^-$ est négligeable vis-à-vis de celle des autres formes. $(P_c)_1$ et

$(K'_c)_1$ peuvent être éliminés et on arrive à l'équation à 4 inconnues:

$$D_c = \frac{(P_c)_2\,(K'_c)_2\,\theta_3 + (P_c)_3\,(K'_c)_3\,\theta_4}{\frac{10^{3.204}}{K_c\theta_4} + 10^{1.602} + (K'_c)_2\,\theta_3 + (K'_c)_3\,\theta_4} \qquad (6)$$

Cette équation est résolue, sur ordinateur, par la méthode des déterminants. Les valeurs des $(P_c)_m$ et $(K_c)_m$ sont ensuite réintroduites dans l'éqn. (5) et on détermine les valeurs de $(P_c)_1$ et $(K_c)_1$. A partir des valeurs obtenues par cette méthode, on trace la courbe d'extraction théorique et on la compare à la courbe expérimentale. Les faibles différences obtenues sont corrigées par la méthode par approximations successives.

Le Tableau IV résume les valeurs des constantes de formation obtenues dans ces conditions. La courbe calculée à partir de ces constantes est comparée à la courbe expérimentale sur la Fig. 1.

TABLEAU IV

CONSTANTES DE FORMATION DES COMPLEXES DOUBLES, $(K'_c)_m$ (mole/l)$^{-1}$

| *Eléments* | $MeY_2H_2^-$ | $MeY_2H^{2-}$ | $MeY_2^{3-}$ |
|---|---|---|---|
| Américium | 20 | 10 | 600 |
| Curium | 10 | 660 | $1.3 \cdot 10^4$ |

Les constantes de formation des complexes doubles sont nettement plus élevées pour le curium que pour l'américium. Il faut aussi noter l'inversion entre les valeurs de $(K'_c)_1$ et $(K'_c)_2$ pour l'américium.

On ne trouve, dans la littérature, que très peu de travaux concernant la détermination des constantes de formation des complexes doubles du HEDTA avec les actinides trivalents.

Eberle et Bayat[2], en 1967, publient des valeurs de constantes de formation obtenues par chromatographie sur résine cationique. Ils obtiennent $10^{11.65}$ pour l'américium et $10^{11.27}$ pour le curium pour la réaction $AmY + Y^{3-} \rightleftharpoons AmY_2^{3-}$.

Plus récemment, delle Sitte et Baybarz[3], par une méthode spectrophotométrique, mettent en évidence trois types de complexes entre l'américium et le HEDTA: AmY, $Am_2Y_3^{3-}$ et $AmY_2^{3-}$, ce dernier complexe se formant suivant la réaction:

$$Am_2Y_3^{3-} + HY^{2-} \rightleftharpoons 2\,AmY_2^{3-} + H^+$$

Ils trouvent ainsi une constante de formation de $10^{1.05}$ mais ne donnent pas la valeur de la constante de formation du complexe de stoechiométrie 2:3 si bien qu'il est difficile de comparer leurs valeurs avec les nôtres.

Signalons enfin que Merciny *et al.*[4] ont déterminé, par mesures potentiométriques, les constantes de formation des complexes doubles avec la plupart des lanthanides trivalents. Pour le gadolinium et le terbium, notamment, ils obtiennent les valeurs suivantes:

| | | | |
|---|---|---|---|
| | $(K'_c)_1 = 5.9$ | | $(K'_c)_1 = 2.6$ |
| (Gd) | $(K'_c)_2 = 100$ | (Tb) | $(K'_c)_2 = 145$ |
| | $(K'_c)_3 = 2.1 \cdot 10^3$ | | $(K'_c)_3 = 2.8 \cdot 10^3$ |

Ces constantes sont du même ordre de grandeur que celles que nous obtenons pour le curium, mais sont fort différentes de celles obtenues pour l'américium. De plus, dans aucun cas, les auteurs ne remarquent d'inversion dans les valeurs de $(K'_c)_1$ et $(K'_c)_2$.

Cela revient à dire que, exception faite pour $AmY_2H_2^-$, les complexes $MeY_2H_2^-$ et $MeY_2H^{2-}$ sont respectivement plus acides que $H_2Y^-$ et $HY^{2-}$.

L'américium semble donc se comporter de façon particulière et cela explique le facteur de séparation très élevé que l'on obtient pour les deux actinides.

*Séparation américium–curium*

Les expériences réalisées avec une phase organique non traitée et une phase performances sont obtenues en présence d'une phase aqueuse $10^{-1}$ *M* en KCl.

Il est difficile d'interpréter quantitativement les courbes de distribution étant donné que la variation du pH est accompagnée non seulement d'une variation dans la distribution du métal mais encore dans celle du HEDTA et du chlorure. D'un point de vue pratique, les résultats présentent un très grand intérêt car, comme le montrent les courbes, il est possible d'obtenir un facteur de séparation très important pour les deux actinides.

Les valeurs des coefficients de distribution sont cependant fort faibles surtout à bas pH; la zône la plus intéressante se situe aux environs de pH = 9.5 où l'on obtient un facteur de séparation de 7 entre l'américium et le curium pour des valeurs de log $D_c$ valant respectivement $-1.2$ et $-0.4$.

Les expériences réalisées avec une phase organique non traitée et une phase aqueuse sans KCl fournissent des coefficients de distribution $D_c$ nettement plus élevés; le facteur de séparation est cependant moins important mais conserve encore une valeur fort intéressante de 5.5 au pH égal à 8.5.

Nous remercions l'Institut Interuniversitaire des Sciences Nucléaires et l'Office de la Coopération au Développement pour l'intérêt constant apporté à nos travaux et le soutien financier accordé à notre laboratoire.

RÉSUMÉ

Les complexes de stoechiométrie 1:2 formés entre le HEDTA et les deux actinides trivalents Am et Cm sont extraits en phase organique par une solution benzénique de chlorure de tricaprylméthylammonium. L'étude de la distribution du métal en fonction du pH a permis de déterminer la charge et la constante de formation de ces complexes doubles $MeH_{3-m}Y_2^{m-}$. Dans certaines conditions expérimentales, on peut obtenir un facteur de séparation de 7 pour les deux actinides.

SUMMARY

The extraction of the 1:2 complexes formed between the trivalent actinides, americium and curium, and HEDTA is carried out, at different pH values of the

aqueous phase with tricaprylmethylammonium chloride in benzene. The charge and the stability constants of the 1:2 complexes $MeH_{3-m}Y_2^{m-}$ are determined. In certain experimental conditions, separation factors as high as seven can be obtained for the two actinides.

ZUSAMMENFASSUNG

Die Komplexe, die sich zwischen den dreiwertigen Actiniden Am und Cm und HEDTA im Verhältnis 1:2 bilden, werden durch Tricaprylmethylammoniumchlorid in Benzol extrahiert. Verteilungsmessungen der Metallionen in Abhängigkeit vom pH-Wert ergaben die Ladung und die Bildungskonstante dieser Doppelkomplexe $MeH_{3-m}Y_2^{m-}$. Unter bestimmten Versuchsbedingungen wird für die beiden Actiniden der Trennfaktor 7 erhalten.

BIBLIOGRAPHIE

1 N. ZAMAN, E. MERCINY ET G. DUYCKAERTS, *Anal. Chim. Acta*, 56 (1971)
2 S. H. EBERLE ET I. BAYAT, *Radiochim. Acta*, 7 (4) (1967) 214.
3 A. DELLE SITTE ET R. D. BAYBARZ, *J. Inorg. Nucl. Chem.*, 31 (1969) 2201.
4 E. MERCINY, P. ZUR NEDDEN ET G. DUYCKAERTS, *Anal. Lett.*, 4 (1) (1971) 29.

*Analytica Chimica Acta*
Elsevier Publishing Company, Amsterdam
Printed in The Netherlands



# INVESTIGATION OF SURFACE LAYERS ON ELECTRODE GLASSES FOR pH MEASUREMENT

B. CSÁKVÁRI, Z. BOKSAY AND G. BOUQUET
*Department of General and Inorganic Chemistry, L. Eötvös University, Budapest (Hungary)*

(Received 2nd May 1971)

Since it was established that the composition of a glass electrode mainly determines its properties[1], many attempts have been made to provide a detailed explanation for these properties on the basis of the structure attributed to the glass. In principle, the theories published in the literature can be accepted only if the structure of the surface layer of the electrode is identical to that encountered inside the glass phase far from the surface. The glass electrodes sensitive to alkali ions very probably comply with this requirement[2], but those used for pH measurements do not. The latter show some features which are unexpected on the basis of the structure of the bulk glass, hence it seemed reasonable and promising to investigate their surface layer.

TABLE I

COMPOSITION OF GLASSES IN MOLE PER CENT

| | $Li_2O$ | $Na_2O$ | $Cs_2O$ | $CaO$ | $BaO$ | $La_2O_3$ | $SiO_2$ | *Reference* |
|---|---|---|---|---|---|---|---|---|
| Dole glass | — | 21.4 | — | 6.4 | — | — | 72.2 | 3 |
| Perley glass | 28 | — | 3 | — | — | 4 | 65 | 4 |
| Lithium–barium glass | 24 | — | — | — | 8 | — | 68 | 5 |

The experiments were carried out on McInnes–Dole glass[3] and on two kinds of lithium glasses[4,5]. The composition of the glasses is given in Table I. The surface films of the glass samples were dissolved gradually in hydrofluoric acid solutions. By determining the amounts of alkali and silicon dissolved in these solutions, a picture of the alkali ion distribution in the surface layer, and thus some characteristic information on the structure, were obtained. The principle of this method published elsewhere[6] remained unchanged, but some details had to be improved, as the layers on the glass electrodes in question were thinner than those found on the model glasses investigated earlier.

## EXPERIMENTAL

Rod-shaped samples of 8–10 cm length and 0.3–0.5 cm diameter were leached in water in a polyethylene vessel in order to develop the surface layer. By renewing the leaching water daily, the concentration of alkali ions and silicic acid never exceeded the value of $10^{-5}$ and $10^{-6}$ mole $l^{-1}$, respectively. After the leaching process the

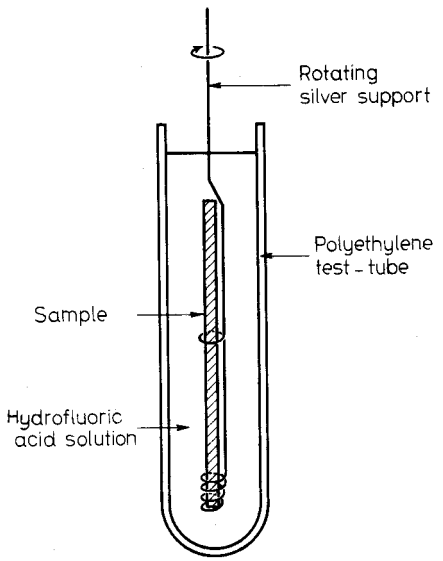


Fig. 1. The rotating silver support with the sample in hydrofluoric acid solution.

sample was placed on a rotating silver support and immersed in a polyethylene test-tube filled with 15 ml of 0.1% hydrofluoric acid solution (Fig. 1). The solution was changed every 3–7 min until the entire surface layer was dissolved.

A portion of 0.8 ml of each solution containing one dissolved fraction of the film was mixed with 2 ml of a solution containing 25 g of ammonium molybdate, $[(NH_4)_6Mo_7O_{24} \cdot 4H_2O]$, 49 g of concentrated sulphuric acid and 24.5 g of boric acid per litre; 9 min after mixing, 1 ml of 4.5% ascorbic acid solution was added while 1 min later 32 ml of 20% sodium carbonate solution were added. The absorbance of the molybdenum-blue was measured with a Hilger spectrophotometer at 740 nm after 1 h. The alkali ion concentration was determined by flame photometry. The minimal thickness of the layer fraction detectable by this method was $2 \cdot 10^{-6}$ cm.

## RESULTS AND DISCUSSION

Samples of McInnes–Dole glass were exposed to water at 20 and 40°, respectively, for 13 days. Figure 2 shows the characteristic profiles of the surface layers, *i.e.* the plot of the relative concentration of sodium ions ($c/c_0$ where $c_0$ is the bulk concentration) *vs.* distance. The values of the distance calculated from the analytical data are consistent with the original volume of the silicate network; in other words, its indeterminate swelling has not and could not be taken into account. The relative concentration of sodium ions increases from a low value at the phase boundary to the final one measured in the bulk glass. The difference in the thickness of the layers developed at 20° and 40°, respectively, can be understood on the basis of the temperature dependence of the rate of formation of the film.

As electrical neutrality must be maintained, it must be supposed that the alkali ions which have left the glass phase are replaced by hydrogen or hydroxonium ions in an ion-exchange process connected with interdiffusion. The whole layer seems to

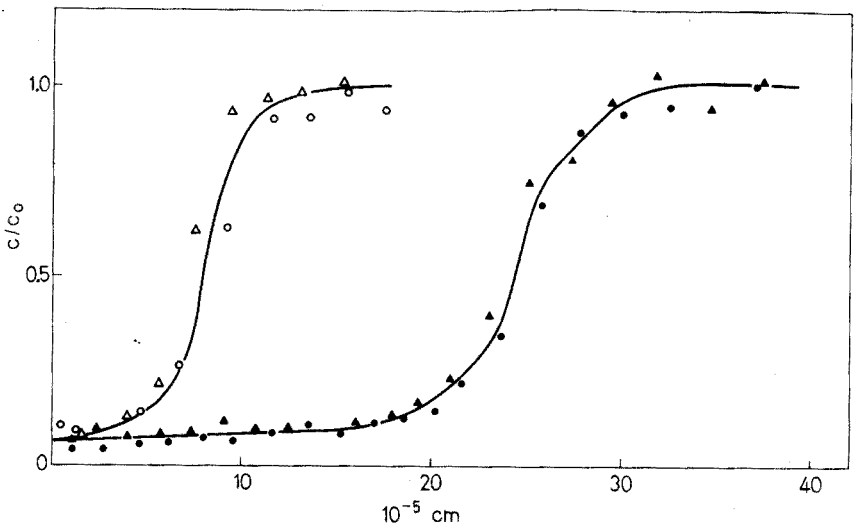


Fig. 2. The distribution of sodium ions in the surface layer of McInnes–Dole glass after 13 days' treatment in water. (△, ○) After leaching at 20°; (▲, ●) after leaching at 40°.

consist of two sections. The present discussion is confined to the outer part only, since it is of greater interest with regard to electrode properties. Earlier it had been ascertained[6] that the low slope (*cf.* Fig. 2) characteristic of the outer part indicates a very high value of the interdiffusion coefficient compared to that found in the bulk glass.

This phenomenon can be explained as follows. The exchange of sodium ion for hydroxonium ions causes a local stress, owing to the difference in the diameters of the ions. The stress is thought to promote the reaction of bridging oxygen atoms and hydroxonium ions. For the sake of simplicity, the parts of the network not involved in the reaction are disregarded and the following reaction is proposed.

$$\equiv Si-O^- + H_3O^+ + \equiv Si-O-Si\equiv \rightarrow 3\equiv Si-O-H$$

On account of such depolymerization processes, the ions in general can migrate more easily than before the reaction. The depolymerization of the silicate network also facilitates the entering of ions and small molecules of different kinds from the solution in contact with the glass electrodes.

First of all the penetration of water molecules and the subsequent formation of hydroxonium ions should be mentioned.

$$\equiv Si-O-H + H_2O \rightarrow \equiv Si-O^- + H_3O^+$$

As far as we know, the equilibrium constant of this reaction has not been determined yet. However, investigations carried out by means of tritiated water proved that the activity coefficient of water depended to a great extent on the concentration of alkali ions[7] in the surface layer. Schwabe and Glöckner[8] gave evidence that the surface layer could also absorb the molecules of hydrochloric and sulphuric acids. It is known from Jordan's work[9] that some bivalent cations present in an alkaline solution are able to cause an unwelcome deviation of the e.m.f. in pH measurements. This fact can be interpreted by taking into consideration the structure of the surface film only, because

the bivalent ions are localized in the original glass structure and thus they can neither leave nor enter it. However, the structure of the surface film being looser, these ions can cross the solution–surface film boundary and thus create the deviation in the e.m.f. function.

The role of the stress produced by hydroxonium ions appears from Fig. 3

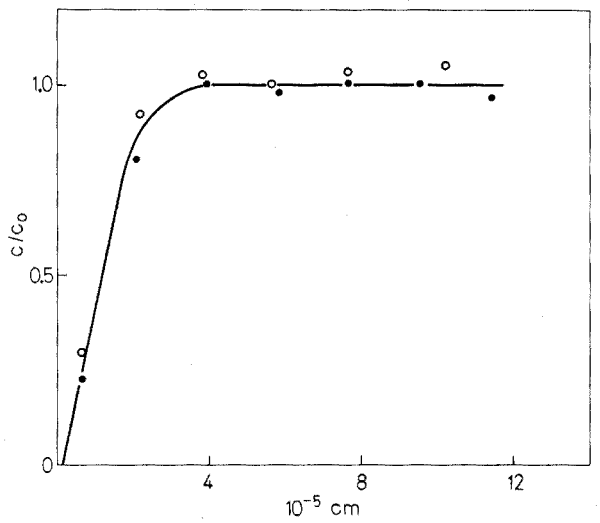


Fig. 3. The distribution of sodium ions in the surface layer of McInnes–Dole glass after 13 days' treatment in commercial pure ethanol at 40°. (○, ●) Individual samples.

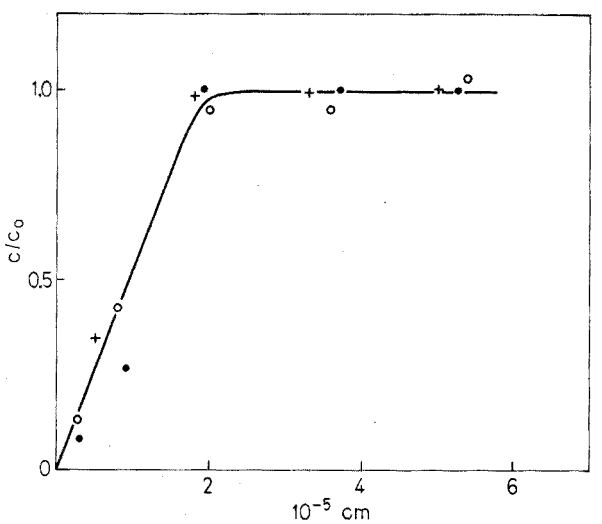


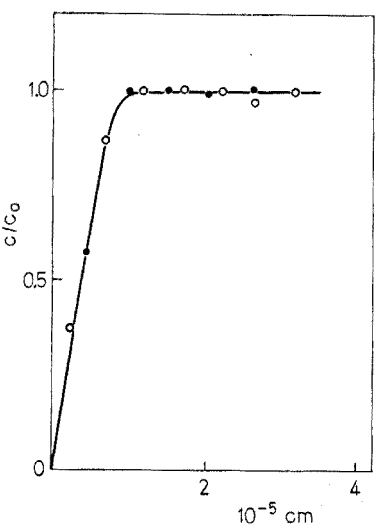


Fig. 4. The distribution of lithium ions in the surface layer of the lithium–barium glass after 13 days' treatment in water at 40°. (○, ●, +) Individual samples.

Fig. 5. The distribution of lithium ions in the surface of Perley glass after 40-h treatment in water at 100° (○, ●) Individual samples.

which shows the surface layer of a sample treated with commercial ethanol. The layer was found to be rather thin and to show no sign of loosened structure, because of the lack of hydroxonium ions in the liquid. The sites of the missing sodium ions were probably occupied by hydrogen ions, originating from sporadic water molecules in the liquid and forming hydroxyl groups in the glass.

$$\equiv Si{-}O^-_{glass} + Na^+_{glass} + H_2O_{liquid} \rightarrow \equiv Si{-}O{-}H_{glass} + Na^+_{liquid} + OH^-_{liquid}$$

As the leaching of lithium glasses at room temperature requires a few months (or even more than one year) to obtain a surface layer suitable for investigation, the layer was developed at elevated temperature. By comparing Figs. 4 and 5, it is apparent that the curves of the lithium–barium glass and the Perley glass, respectively, are similar. Neither of the curves indicates that the structure of the surface layer is loosened. But a structural change of an other type and/or a decrease in the diffusion coefficient in the surface layer cannot be precluded. In fact, Brand and Rechnitz[10] have concluded from electrical investigations that the mass transport of ions across the glass membrane may be rate-limited by the surface film. The absence of a loose layer is expected for structural reasons, as it is known that the holes left by lithium ions are very small and are hardly able to accommodate the larger hydroxonium ions.

The relatively low sodium ion error of electrodes made of lithium glasses is due to the hindered process of the exchange of alkali ions and of hydrogen ions situated in the solution and in the glass, respectively. This explanation can also be applied to potassium ion error. Considering the diameters of the ions, we conclude that the potassium ion error must be lower than the values of the sodium error under the same

TABLE II

THE CONSTANTS OF JORDAN'S EQUATION RELATING TO LITHIUM–BARIUM GLASS[5]

| *Ion in solution* | *A* | *B* | *C* |
|---|---|---|---|
| Lithium | 0.5 | 0.9 | 6.70 |
| Sodium | 0.27 | 0.85 | 4.25 |
| Potassium | 0.13 | 0.60 | 3.20 |

conditions. The constants of Jordan's equation are available (Table II) to prove this conclusion. If the metal ion error is expressed in pH units ($\Delta$ pH), the Jordan equation has the form

$$\log(\Delta \text{ pH}) = A \text{ pH}' + B \log m + C$$

where pH′ is the measured pH, and $m$ is the metal ion concentration in mole $l^{-1}$. It is worth mentioning that for the sodium error of different sodium glasses[11]

$$B = 0.93A,$$

but this equation does not seem to hold for lithium glasses. This deviation has not been explained yet. Bivalent ions in the solutions do not affect the phase boundary potential of lithium glasses, contrary to that of sodium glasses, in accordance with present knowledge of the surface films.

The resistance of lithium glasses against concentrated solutions of acids is generally higher than that of sodium glasses. Thus electrodes made of lithium glasses

show reduced acidic error. Some details on the behaviour of lithium–barium glasses attacked by hydrochloric acid are known, but the kinetics of the process have not been clarified in every respect[12]

SUMMARY

The determination of the alkali distribution in the surface layer of some pH-responsive glass electrodes leads to some conclusions regarding the structure of the layer. The structure of the surface layer is shown to be responsible for the errors of the glass electrodes. The properties and the structure of McInnes–Dole glass and two lithium glasses are discussed in detail.

RÉSUMÉ

Une étude est effectuée sur la nature des couches superficielles des électrodes de verre, pour la mesure du pH. La structure de ces surfaces est responsable des erreurs observées avec des électrodes de verre. On examine en détail le verre McInnes–Dolle et deux verres au lithium.

ZUSAMMENFASSUNG

Die Bestimmung der Alkaliverteilung in der Oberflächenschicht einiger pH-Glaselektroden führte zu Folgerungen hinsichtlich der Struktur der Schicht. Es wird gezeigt, dass die Struktur der Oberflächenschicht für die bei Glaselektroden auftretenden Fehler verantwortlich ist. Die Eigenschaften und die Struktur von McInnes–Dole-Glas und von zwei Lithiumgläsern werden im einzelnen diskutiert.

REFERENCES

1 B. LENGYEL AND E. BLUM, *Trans. Faraday Soc.*, 30 (1934) 461.
2 Z. BOKSAY, B. CSÁKVÁRI, J. HAVAS AND M. PATKÓ, *Hung. Sci. Instr.*, 19 (1970) 31.
3 M. DOLE, *J. Chem. Phys.*, 2 (1934) 862.
4 G. A. PERLEY, *Anal. Chem.*, 21 (1949) 559.
5 B. LENGYEL, B. CSÁKVÁRI, F. TILL AND Z. BOKSAY, *Magy. Kem. Lapja*, 9 (1954) 265 (in Hungarian).
6 G. BOUQUET, S. DOBOS AND Z. BOKSAY, *Ann. Univ. Sci. Budapest., Sect. Chim.*, 6 (1964) 5; Z. BOKSAY, G. BOUQUET AND S. DOBOS, *Phys. Chem. Glasses*, 8 (1967) 140.
7 Z. BOKSAY AND B. CSÁKVÁRI, *Ann. Univ. Sci. Budapest., Sect. Chim.*, 10 (1968) 125.
8 K. SCHWABE AND G. GLÖCKNER, *Z. Elektrochem.*, 59 (1955) 504.
9 D. O. JORDAN, *Trans. Faraday Soc.*, 34 (1938) 1305.
10 M. J. D. BRAND AND G. A. RECHNITZ, *Anal. Chem.*, 41 (1969) 1788; 42 (1970) 304.
11 Z. BOKSAY, G. BOUQUET AND B. CSÁKVÁRI, *Acta Chim. Acad. Sci. Hung.*, 46 (1965) 151.
12 Z. BOKSAY, B. CSÁKVÁRI AND B. LENGYEL, *Z. Phys. Chem.*, 207 (1957) 223.

*Analytica Chimica Acta*
Elsevier Publishing Company, Amsterdam
Printed in The Netherlands



# NEW ENZYME ELECTRODE PROBES FOR D-AMINO ACIDS AND ASPARAGINE

G. G. GUILBAULT AND E. HRABANKOVA

*Department of Chemistry, Louisiana State University in New Orleans, Lakefront Campus, New Orleans, La. 70122 (U.S.A.)*

(Received 2nd April 1971)

Guilbault and co-workers have described electrode probes for urea[1-3] and L-amino acids[4,5] using insolubilized enzymes as the active membrane. The enzymatic reactions produce ammonium ions which are sensed by the cation glass electrode sensor:

$$\text{Substrate} \xrightarrow{\text{enzyme}} NH_4^+$$

In this paper the evaluation of new stable electrodes, suitable for the rapid and direct measurement of D-amino acids and asparagine are described.

The electrodes are prepared by placing a thin layer of D-amino acid oxidase (D-AAO) or asparaginase over a Beckman monovalent cation electrode. The enzyme catalyzes the decomposition of the amino acid to $NH_4^+$ by the reactions

$$R\text{–}CHNH_3^+COO^- + O_2 + H_2O \xrightarrow{\text{D–AAO}} R\text{–}\underset{\underset{O}{\|}}{C}\text{–}COO^- + NH_4^+ + H_2O_2 \qquad (1)$$

$$R\text{–}\underset{\underset{O}{\|}}{C}\text{–}COO^- + H_2O_2 \longrightarrow R\text{–}COO^{\ominus} + CO_2 + H_2O \qquad (2)$$

or

$$\begin{array}{l}CONH_2\\|\\CH_2\\|\\CHNH_2\\|\\COOH\end{array} + H_3O^+ \xrightarrow{\text{asparaginase}} \begin{array}{l}COOH\\|\\CH_2\\|\\CHNH_2\\|\\COOH\end{array} + NH_4^+ \qquad (3)$$

Ammonium ions formed in these reactions are sensed by the electrode described, the steady state potential of which is proportional to the activity of $NH_4^+$ ions in the enzyme layer, *i.e.*, to the concentration of amino acid in the solution.

*Preparation of D-amino acid electrode*

The Beckman monovalent cationic electrode 39137 was used as the sensor of ammonium ions. A nylon netting was placed over the glass bulb and was fixed with

rubber rings. A 1 : 1 mixture of enzyme suspension (preparation II) and polyacrylamide gel (0.58 g of N,N′-methylene bisacrylamide and 5 g of acrylamide per 25 ml of solution, with 3 mg of $K_2S_2O_8$ and riboflavin added as catalyst) was dropped on the netting and polymerized[3] for 1 h (Type I electrode). After polymerization, the electrode was covered with dialysis paper and was stored in $4 \cdot 10^{-4}$ *M* FAD when not in use.

A Type II electrode (liquid membrane electrode) was prepared by soaking a nylon netting with an aqueous solution of D-amino acid oxidase. In the case of crude preparation (preparation I), solutions with 50, 100, 200, 500, 750 and 1000 ml of enzyme per ml were used. The more purified enzyme (preparation II) was used in the form of suspension without any further dilution. For each electrode 0.04 ml of enzyme solution (measured by pipette) was used.

*Preparation of asparagine electrode*

A Type I asparagine electrode was prepared as described above for D-amino acids. A 0.1 ml of gel and 0.1 ml of an asparaginase solution containing 500 units per ml were used. The electrode was stored in triply distilled water between uses.

## EXPERIMENTAL

*Apparatus and solutions*

A standard fibre-junction saturated calomel electrode was used as reference electrode. Millivolt measurements were made with a Beckman research pH meter and Beckman recorder (sensitivity 1 mV/div) in the usual manner. Readings were taken in stirred solutions after allowing sufficient time (1–2 min.) to reach the steady state value. All measurements were carried out in a cell thermostated at $25 \pm 0.1°$.

Stock solutions of amino acids (0.1 *M*) were prepared in TRIS buffer with twice-distilled water. TRIS buffer, 0.1 *M*, pH 6.5–8.5 was used for preparing solutions. A $4 \cdot 10^{-4}$ *M* solution of flavine adenine dinucleotide (FAD, Sigma) was prepared in TRIS buffer, pH 8.0.

D-Amino acid oxidase was obtained from Sigma as a crude preparation from hog kidney (Preparation I, activity 0.02 units $mg^{-1}$— one unit will oxidatively deaminate 1.0 μmole of D-alanine per min at pH 8.3 at 37°) and also as a more purified preparation in the form of a crystalline suspension in 1.8 *M* ammonium sulfate, pH 6.5 (Preparation II, 5 mg protein $ml^{-1}$, 25 units per mg protein).

Asparaginase was obtained from Sigma Chemical Co. (Grade I, chromatographically purified from *E. coli*, 40 units $mg^{-1}$— one unit will liberate 1 μmole of ammonium ion per min at pH 8.6 at 37°).

## RESULTS AND DISCUSSION

*D-Amino acid electrode*

D-Amino acid oxidase catalyzes the oxidation of some D-amino acids selectively in the presence of other D- and L-amino acids according to the equation:

$$R\text{–}CH\underset{\oplus}{NH_3}COO^{\ominus} + O_2 + H_2O \xrightarrow{\text{DAAO}} R\text{–}COO^- + NH_4^+ + CO_2 + H_2O$$

Of the amino acids D-phenylalanine, -alanine, -valine, -methionine, -leucine, -nor-

leucine, and -isoleucine react, and electrodes for these amino acids could be expected. D-proline is deaminated, but $CH_3NH_2$ is formed as product instead of $NH_4^+$ :

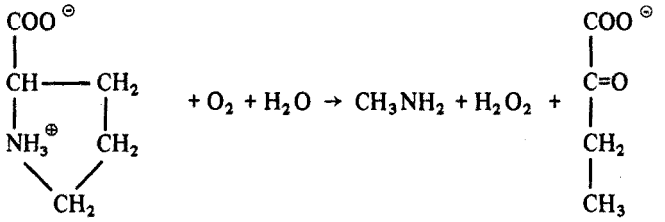

This behavior was observed (Fig. 1), a plot of potential of the D-amino acid electrode *vs.* the log of D-amino acid concentration being linear from $10^{-4}$ to $5 \cdot 10^{-2}$ *M* for these amino acids.

To determine the stability of the electrode, the steady state potential was measured for a definite concentration of substrate at periodic time intervals. The experiments were all performed at a temperature of 25°. Some of the parameters that were found to affect the stability of the electrode were the condition of the storage solution and the concentration of enzyme in the electrode.

All the initial electrodes prepared from pure or crude D-amino acid oxidase in a liquid or polyacrylamide membrane were found to lose activity rapidly. This was surprising in the case of the crude enzyme since aqueous solutions of this enzyme are stable for weeks. It was noted that the electrodes prepared with crude enzyme solutions of high concentration (750 and 1000 mg $ml^{-1}$), which are dark yellow after preparation, became light yellow when stored in buffer solution overnight. The buffer solution itself turned yellow. Charlwood *et al.*[6] found that the bond between protein and coenzyme (FAD) is very weak in D-amino acid oxidase and that FAD can be easily removed by dialysis against buffer without FAD. The FAD content is decreased from 1 mole FAD in a basic molecular weight of 45,000 to 0.5 mole of FAD, and the

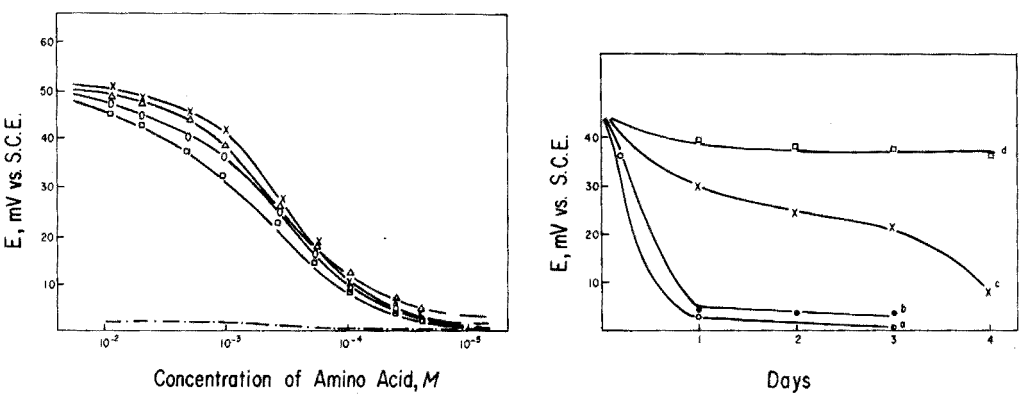


Fig. 1. Concentration curves for different amino acids using the Type I D-amino acid electrode, pH 8.2. (×) D-phenylalanine; (△) D-alanine; (0) D-valine; (□) D-methionine, D-leucine, D-norleucine, D-isoleucine; (—·—) D-proline.

Fig. 2. Stability of the Type I D-amino acid electrode as a function of the FAD solution used for storing the electrode. (a) 0 *M* FAD; (b) $2 \cdot 10^{-6}$ *M* FAD; (c) $5 \cdot 10^{-5}$ *M* FAD; (d) $2.5 \cdot 10^{-4}$ *M* FAD.

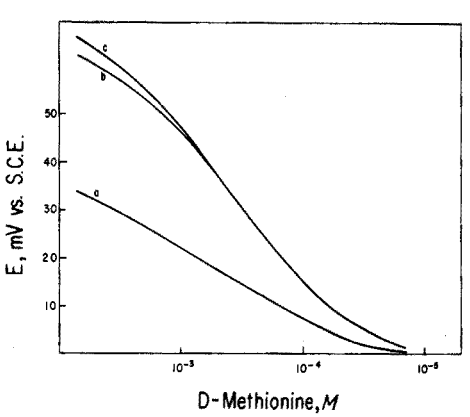


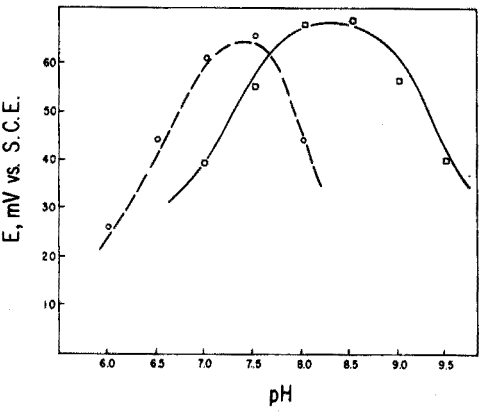


Fig. 3. Influence of increasing enzyme concentration on calibration curves of D-methionine (pH 8.2). (a) 500 mg enzyme/mg; (b) 750 mg enzyme/mg; (c) 1000 mg enzyme/mg.

Fig. 4. Influence of pH on electrode response. Type II L-AAO electrode and Type I D-AAO electrode. L- or D-methionine = $10^{-3}$ *M*. (○) L-Amino acid oxidase; (□) D-amino acid oxidase.

loss is accompanied by a polymerization of the enzyme to tetramer and octamer[7]. A study of the u.v.–visible spectrum of the enzyme proved this observation. Hence, an attempt was made to improve the stability of the Type I enzyme electrode by storing it in FAD solutions between use (Fig. 2). The optimal FAD concentration was found to be $4 \cdot 10^{-4}$ *M* in TRIS buffer, pH 8.0. Under these storage conditions the electrode is stable for at least 21 days. The FAD solutions should be protected from light and changed at least every week.

The stability and response of the electrodes were tested as a function of the concentration of enzyme in the gel layer. Some typical response curves for the Type I electrode are shown in Fig. 3 for 500, 750 and 1000 mg of D-amino acid oxidase per mg of gel. Electrodes with the higher enzyme concentrations were more stable and exhibited a more Nernstian response.

The liquid membrane electrodes (Type II) were much less stable than the polyacrylamide-immobilized electrodes (Type I), the latter being stable for at least 21 days.

The rate of enzymatic reaction is dependent on the pH of the solution. The optimal pH range for the D-amino acid oxidase reaction is 8–8.5 (best 8.2), compared to an optimal pH range of 7–7.5 for the L-amino acid oxidase (Fig. 4). Calibration curves for D-methionine at pH 7–9.5 were compared (Fig. 5), optimal results being obtained at 8–8.5.

The electrode response to different concentrations of D-methionine was measured at temperatures of 25, 30, 35, 37 and 40°. Only very small effects of elevated temperatures were observed, although the theoretical Nernstian slope is 61.74 mV at 37°.

Also, high concentrations of oxygen in the solution (by bubbling oxygen through the solution) did not increase the electrode response.

*Asparagine electrode*

Asparaginase is an enzyme which is specific for L-asparagine. Enzyme solutions are unstable, although the crystalline enzyme is stable at $-10°$.

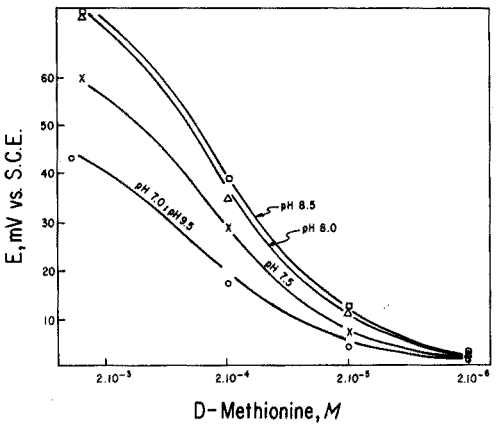


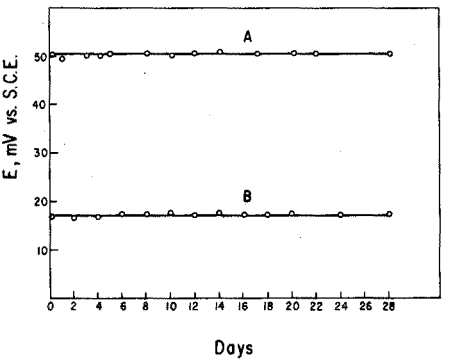


Fig. 5. Influence of pH on electrode response. Type I electrode; TRIS buffer solutions of different pH.

Fig. 6. Stability of the asparagine electrode. Potential of electrode to A = $2 \cdot 10^{-3}$ *M* asparagine or B = $2 \cdot 10^{-4}$ *M* asparagine measured each day. pH 8.0.

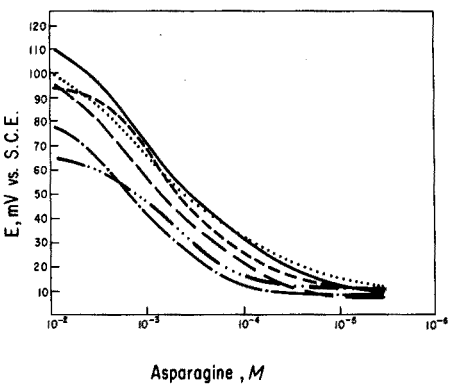


Fig. 7. Influence of pH on electrode response. Type I electrode; TRIS buffer solutions of different pH. pH: (—···—) 7.0; (···) 7.5; (——) 8; (----) 8.5; (—··—) 9.0; (—·—) 9.5.

Liquid membrane electrodes prepared gave a good response, but the stability of the electrodes was not good. All the electrodes lost about half of their response in 4 days. To obtain an electrode with better stability, the immobilization of asparaginase in polyacrylamide gel was tried. The results (Fig. 6) show that immobilization improved the electrode stability and made the electrode quite stable for more than 3 weeks.

The electrode response also improved with increasing concentration of enzyme in the gel, reaching a maximum at about 500 units $ml^{-1}$ of solution used (0.1 ml or 5 units in the gel).

The influence of pH on the response of the electrode to varying concentrations of asparagine is shown in Fig. 7. The optimal pH range observed, 7.5–8.5, was the same as that observed in solution. Most measurements were made at a pH of 8.

As in the case of the D-amino acid electrode bubbling oxygen through the solution did not increase the electrode response.

The financial assistance of the National Science Foundation, Grant No. GB-12669, is gratefully acknowledged.

SUMMARY

Enzyme electrode probes suitable for the assay of D-phenylalanine, D-alanine, D-valine, D-methionine, D-leucine, D-norleucine, D-isoleucine and asparagine are described. These electrodes are prepared by covering a Beckman cation-sensitive glass electrode with a layer of insolubilized D-amino acid oxidase or asparaginase. The electrodes are stable for at least 1 month. Various parameters affecting the stability and sensitivity of the electrode are discussed as are the effect of pH, temperature, oxygen, enzyme and substrate on the response of the probe.

RÉSUMÉ

De nouvelles électrodes-sondes á enzymes sont décrites pour D-phénylalanine, D-alanine, D-valine, D-méthionine, D-leucine, D-norleucine, D-isoleucine et asparagine. Elles sont préparées à l'aide d'enzymes insolubles comme membrane active. Ces électrodes sont stables pendant un mois au moins. On examine divers paramètres pouvant affecter la stabilité et la sensibilité de l'électrode: pH, température, oxygène, enzyme et substrat.

ZUSAMMENFASSUNG

Es werden Enzymelektrodensonden beschrieben, die sich für die Bestimmung von D-Phenylalanin, D-Alanin, D-Valin, D-Methionin, D-Leucin, D-Norleucin, D-Isoleucin und Asparagin eignen. Diese Elektroden werden hergestellt, indem eine kationenempfindliche Beckman-Glaselektrode mit einer Schicht unlöslich gemachter D-Aminosäureoxidase oder Asparaginase bedeckt wird. Die Elektroden sind mindestens 1 Monat beständig. Verschiedene Parameter, die die Stabilität und Empfindlichkeit der Elektrode beeinflussen, z.B. der Einfluss von pH, Temperatur, Sauerstoff, Enzym und Substrat, werden diskutiert.

REFERENCES

1 G. G. GUILBAULT AND J. MONTALVO, *J. Amer. Chem. Soc.*, 91 (1969) 2164.
2 G. G. GUILBAULT AND J. MONTALVO, *J. Amer. Chem. Soc.*, 92 (1970) 2533.
3 G. G. GUILBAULT AND E. HRABANKOVA, *Anal. Chim. Acta*, 52 (1970) 287.
4 G. G. GUILBAULT AND E. HRABANKOVA, *Anal. Letters*, 3 (1970) 53.
5 G. G. GUILBAULT AND E. HRABANKOVA, *Anal. Chem.*, 42 (1970) 1779.
6 P. A. CHARLWOOD, G. PALMER AND R. BENNETT, *Biochim. Biophys. Acta*, 50 (1961) 17.
7 V. MASSEY, G. PALMER AND R. BENNETT, *Biochim. Biophys. Acta*, 48 (1961) 1.

*Analytica Chimica Acta*
Elsevier Publishing Company, Amsterdam
Printed in The Netherlands



# POTENTIOMETRIC DETERMINATION OF THIOUREA WITH A SULPHIDE-SELECTIVE MEMBRANE ELECTRODE

M. K. PÁPAY, K. TÓTH AND E. PUNGOR
*Institute for General and Analytical Chemistry, Technical University, Budapest (Hungary)*
(Received 11th May 1971)

The development of sulphide-selective electrodes has made possible selective, highly sensitive and rapid determinations of sulphide ions by means of the direct potentiometric method or potentiometric titration[1-4]. Determinations have usually been made in alkaline solution (1 *M* or 0.1 *M* in sodium hydroxide) in the presence of an antioxidant such as ascorbic acid[5].

The field of application of the sulphide-selective electrode has been considerably extended by the use of the electrode for the determination of various compounds containing sulphur[6]. In the present paper, the extension of the method to the potentiometric determination of thiourea is described in detail.

## EXPERIMENTAL

The measurements were made with a Radelkis Precision pH meter Model OP-205 (Radelkis, Budapest). A Radelkis sulphide-selective OP-S-711 membrane electrode was used as the indicator electrode, and a saturated calomel electrode as the reference electrode. Electrical contact between the sample solution and the reference electrode was ensured with an agar–agar potassium nitrate salt bridge.

All reagents used were of analytical grade.

Thiourea solution (0.1 *M*) was prepared by dissolving the appropriate amount of thiourea in 1 *M* sodium hydroxide solution. Standard solutions ($10^{-2}$–$10^{-8}$ *M*) were prepared from the stock by dilution with 1 *M* sodium hydroxide solution.

Thiourea solutions which were 0.1 *M* in sodium hydroxide were prepared similarly.

## RESULTS

### *Potentiometric titration of thiourea*

Figures 1 and 2 show the curves of the potentiometric titration of $10^{-1}$, $10^{-2}$, $10^{-3}$ and $10^{-4}$ *M* thiourea with silver nitrate standard solution in 1 *M* and 0.1 *M* sodium hydroxide, respectively. Similar titration curves were obtained when the titrations were done in solutions which were 0.1 *M* in ammonia. Titrations of thiourea in 1 *M* sodium hydroxide with standard mercury(II) nitrate solution were also satisfactory (Fig. 3).

The reverse titration of silver nitrate with thiourea–1 *M* sodium hydroxide solution is shown in Fig. 4.

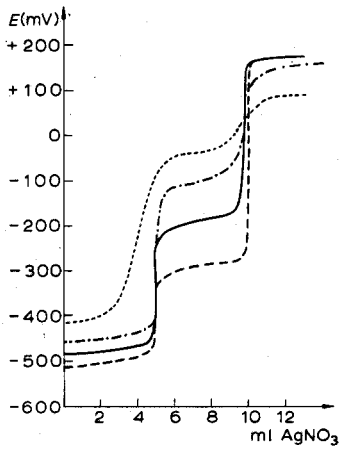


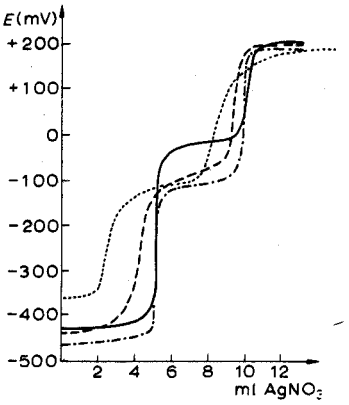


Fig. 1. Potentiometric titration of $10^{-1}$–$10^{-4}$ *M* thiourea solutions with standard silver nitrate solution, in 1 *M* sodium hydroxide. (---) $10^{-1}$ *M*; (——) $10^{-2}$ *M*; (·—·—·) $10^{-3}$ *M*; (------) $10^{-4}$ *M*.

Fig. 2. Potentiometric titration of thiourea solutions in 0.1 *M* sodium hydroxide with standard silver nitrate solution. (·—·—·) $10^{-1}$ *M*; (——) $10^{-2}$ *M*; (---) $10^{-3}$ *M*; (------) $10^{-4}$ *M*.

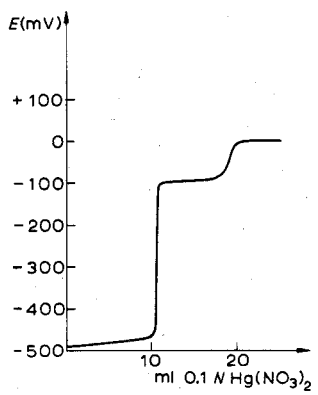


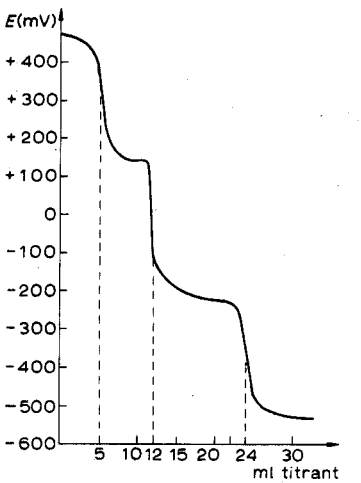


Fig. 3. Potentiometric titration of 0.1 *M* thiourea with 0.1 *M* mercury(II) nitrate standard solution in 1 *M* sodium hydroxide.

Fig. 4. Titration of 50 ml of 0.1 *M* silver nitrate with 0.1 *M* thiourea dissolved in 1 *M* sodium hydroxide solution.

### *Direct determination of thiourea*

The results of direct measurements of thiourea in 0.1 *M* and 1 *M* sodium hydroxide solutions, are presented in Fig. 5.

## DISCUSSION

As shown by the titration curves presented in Figs. 1–3, thiourea can be titrated with standard silver nitrate solution in the concentration range of $10^{-1}$–$10^{-3}$

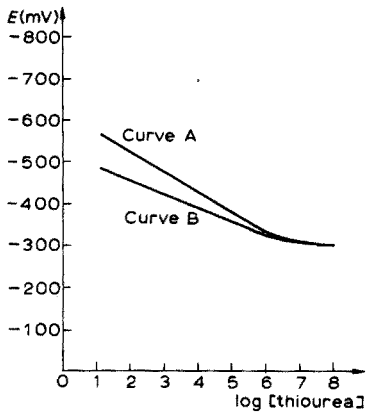


Fig. 5. Direct potentiometric measurement of thiourea in 1 *M* (curve A) and 0.1 *M* sodium hydroxide (curve B).

*M*, in the presence of 1 *M* sodium hydroxide. The reactions that occur rapidly during the titration can easily be followed by the sulphide-selective electrode. Titrations can also be carried out at $10^{-4}$ *M* concentrations, but the titration then requires a longer period of time, since in very dilute solutions the electrode potential attains equilibrium relatively slowly.

There are two jumps on the titration curve of thiourea, either of which can be used to evaluate the amount of thiourea. At the first end-point the equivalent weight of thiourea is half the molecular weight, and at the second one a quarter of the molecular weight. As can be seen from Figs. 1–3, the sum of the potential changes at the first and second jump of the titration curve was always the same. In the titration of low thiourea concentrations, the potential change at the first step of the titration increased with increasing concentration, whereas that in the second step decreased. This phenomenon has not yet been completely elucidated.

In $10^{-1}$ *M* sodium hydroxide, thiourea can be determined with silver nitrate solution only in the concentration range $10^{-1}$–$10^{-2}$ *M*. In more dilute solutions the potential reaches equilibrium slowly, and the potential jump occurs at a smaller volume of titrant than the theoretical value.

Thiourea can also be titrated in 1 *M* ammonia solution, and again either of the jumps in the titration curve can be utilized for the determination of thiourea.

In the titration of thiourea with mercury(II) nitrate solution, two potentiometric jumps again occurred, but the ratio of the heights of the two steps differed from that in the titration with silver nitrate.

In the reverse titration, *i.e.* when silver nitrate solution was titrated with thiourea dissolved in 1 *M* sodium hydroxide solution (Fig. 4), three potential jumps were observed. Before the first end-point silver hydroxide precipitated by reaction with the sodium hydroxide present in the titrant. Thiourea then participates in a precipitate exchange reaction with the silver hydroxide, so causing the second and third potential jumps.

The results of the direct measurement of thiourea showed (Fig. 5) that the *E vs.* log $c_{\text{thiourea}}$ plot is linear in the concentration range $10^{-1}$–$10^{-6}$ *M* in the presence

of 1 *M* or 0.1 *M* sodium hydroxide. The slopes of the calibration curves are 50 and 30 mV, respectively.

The standard deviation of the titration of 0.1 *M* thiourea in 1 *M* sodium hydroxide with silver(I) solution was found to be 0.06 ml.

*Identification of the products of the titration*

The precipitates obtained in the first and second steps of the titration were separated and analyzed. The results obtained were: 86.84% Ag and 12.87% S, the theoretical values for $Ag_2S$ being 87.06% and 12.94%, respectively. The precipitate was therefore proved to be $Ag_2S$.

The filtrate was titrated further until the second potential jump, during which titration a new precipitate was formed. This was also filtered off and analyzed. The results obtained were: 83.84% Ag, 10.80% N, and 4.79% C; required for $Ag_2NCN$, 84.35% Ag, 10.95% N and 4.70% C. Accordingly, the second precipitate was $Ag_2NCN$.

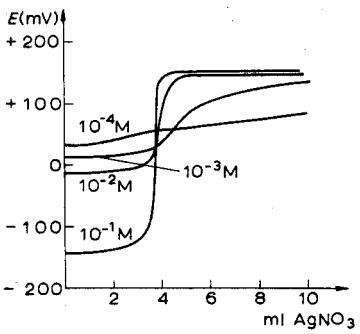


Fig. 6. Potentiometric titration of different amounts of cyanamide with silver nitrate solution in 1 *M* sodium hydroxide.

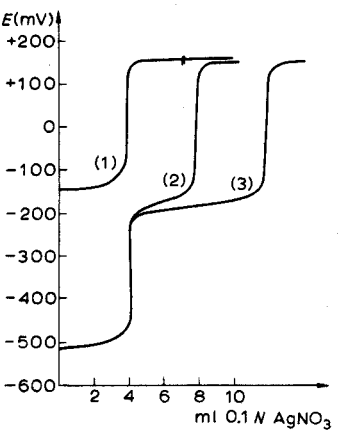


Fig. 7. Titration of (1) cyanamide, (2) thiourea, and (3) cyanamide + thiourea with silver nitrate solution in 1 *M* sodium hydroxide.

As further proof, various amounts of cyanamide were titrated in 1 *M* sodium hydroxide with silver nitrate (Fig. 6). The potentials measured in the initial and titrated solution corresponded to the values measured at the beginning and end of the second step in the titration of thiourea, and the consumption of silver nitrate was stoicheiometric, one mole of cyanamide reacting with two moles of silver nitrate.

Figure 7 shows the titration curves obtained when cyanamide alone (curve 1), thiourea alone (curve 2) and a mixture of the two compounds (curve 3) were titrated with silver(I) solution. The consumption of titrant in the second step of the titration of the mixture increased by an amount of titrant equivalent to the cyanamide present.

As reflected by these curves, the reaction between thiourea and silver nitrate proceeds in two steps. In the first step, sulphur splits off to form silver sulphide and cyanamide is also formed:

$$S{=}C\begin{matrix}NH_2\\NH_2\end{matrix} + 2\,AgNO_3 \rightarrow Ag_2S + H_2N{-}C{\equiv}N + 2\,HNO_3$$

The produced cyanamide reacts with a further two moles of silver nitrate to form a precipitate of silver cyanamide.

$$H_2N{-}C{\equiv}N + 2\,AgNO_3 \rightarrow Ag_2N{-}C{\equiv}N + 2\,HNO_3$$

*Investigation of the products of titration by infrared spectroscopy*

The products of titration ($Ag_2S$ and $Ag_2N{-}C{\equiv}N$) were separated from the titrated solution by filtration and their infrared spectra were measured. For comparison, the spectra of pure cyanamide and thiourea were also recorded.

The infrared spectra of the various precipitates obtained in the titrations, and of the pure compounds, are shown in Fig. 8.

The spectra in Fig. 8 B, D and F, exhibit a strong band between 2000 and 2200 $cm^{-1}$ which is characteristic of the cyanide group. The spectra seem to support the assumption that in the course of the titration of thiourea in alkaline medium first silver sulphide is precipitated and cyanamide is formed; the cyanamide can then be titrated with silver nitrate.

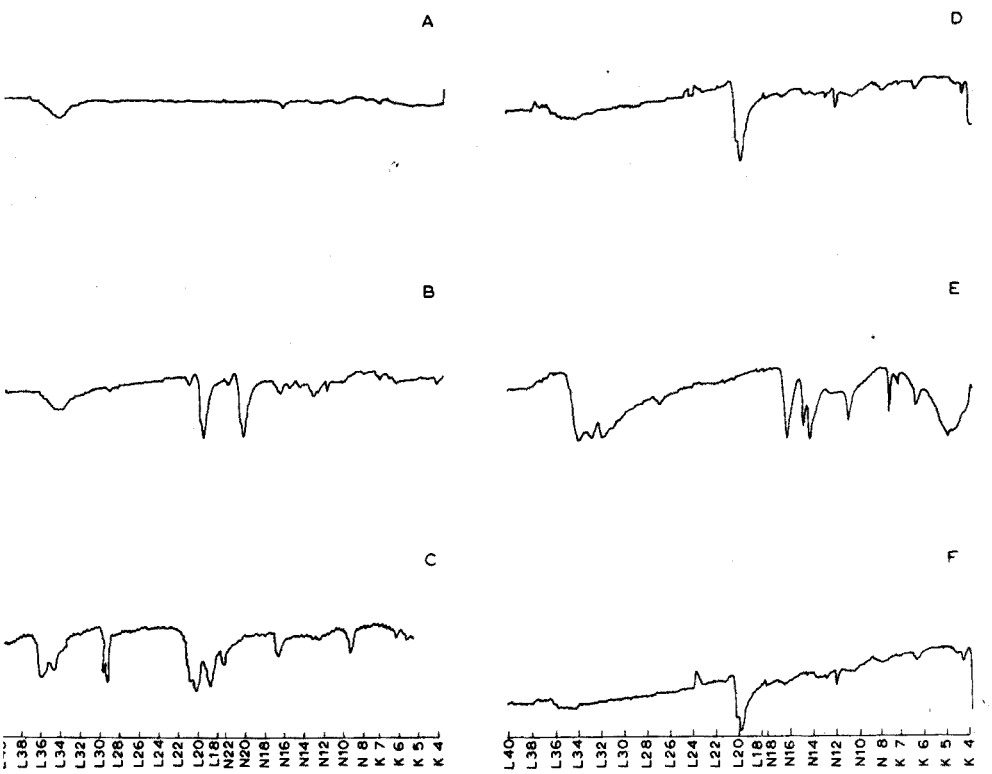


Fig. 8. Infrared spectra of species involved in the titrations. (A) The precipitate formed in the first step of the titration of thiourea; (B) the precipitate formed in the second step of the titration of thiourea. (C) cyanamide; (D) the precipitate formed in the titration of cyanamide; (E) thiourea; (F) the precipitate formed in the titration of cyanamide + thiourea.

The authors express their thanks to Dr. K. Kiss and Dr. A. Hrabéczy for taking and interpreting the infrared spectra.

SUMMARY

The determination of thiourea by direct potentiometric measurement and by potentiometric titration with silver nitrate, by means of a sulphide-selective electrode is described. The lower limit of determination in direct potentiometry is $10^{-6}$ *M* thiourea. Titrations can be successfully performed down to $10^{-3}$ *M* concentration. Two jumps appear on the titration curve, the first corresponding to the formation of silver sulphide and the second to the precipitation of silver cyanamide. Elemental and infrared analysis of the products of titration confirm the formation of silver sulphide and silver cyanamide.

RÉSUMÉ

On décrit un dosage de thiourée par potentiométrie directe et par titrage potentiométrique avec nitrate d'argent, à l'aide d'une électrode sélective au sulfure. Les concentrations limites de thiourée sont $10^{-6}$ *M* pour le dosage potentiométrique direct et $10^{-3}$ *M* pour le titrage. On observe deux sauts sur la courbe de titrage, le premier correspondant à la formation de sulfure d'argent, le second à la précipitation de la cyanamide d'argent. Ce qui est confirmé par l'analyse élémentaire et infra-rouge.

ZUSAMMENFASSUNG

Es wird die Bestimmung von Thioharnstoff durch direkte potentiometrische Messung und durch potentiometrische Titration mit Silbernitrat unter Ferwendung einer sulfidselektiven Elektrode beschrieben. Die untere Bestimmungsgrenze bei direkter Potentiometrie ist $10^{-6}$ *M* Thioharnstoff. Titrationen können bis zu $10^{-3}$ *M* herab mit Erfolg ausgeführt werden. In der Titrationskurve erscheinen zwei Sprünge; der erste ist der Silbersulfidbildung zugeordnet, der zweite der Fällung von Silbercyanamid. Elementar- und Infrarotanalyse der Titrationsprodukte bestätigen die Bildung von Silbersulfid und Silbercyanamid.

REFERENCES

1 E. PUNGOR, E. SCHMIDT AND K. TÓTH, *Proc. Intern. Measurement Confederation Symposium on Electrochemical Sensors, Veszprém, Hungary, 1968*, p. 121.
2 TONG-MING HSEN AND G. A. RECHNITZ, *Anal. Chem.*, 40 (1968) 1054.
3 T. S. LIGHT AND J. L. SWARTZ, *Anal. Lett.*, 1 (1968) 825.
4 M. J. BRAND AND G. A. RECHNITZ, *Anal. Chem.*, 42 (1970) 478.
5 R. BOCK AND H. J. PUFF, *Z. Anal. Chem.*, 240 (1968) 381.
6 J. PAPP AND J. HAVAS, *Magy. Kem. Folyoirat*, 76 (1970) 307.

*Analytica Chimica Acta*
Elsevier Publishing Company, Amsterdam
Printed in The Netherlands



# BIPOTENTIOMETRY IN ORGANIC REDOX SYSTEMS

## II. OXIDATION OF NON-AROMATICS INCLUDING SULFUR COMPOUNDS

HARVEY W. YUROW AND SAMUEL SASS
*Research Laboratories, Edgewood Arsenal, Md. 21010 (U.S.A.)*
(Received 22nd April 1971)

In Part I of this series[1], the application of bipotentiometry to oxidation of aromatic compounds with lead(IV) or cobalt(III) acetates in trifluoroacetic acid was described. It was proposed that the reactions involved formation of electrochemically reversible radical cations which depolarized a pair of polarized platinum electrodes causing a drop in the initially high potential. Since the radical ions were of limited stability, titration additions of oxidant resulted in the formation of potential "saw teeth" that went to make up unique titration curves.

In general, alkyl and cycloalkyl compounds have considerably less charge-delocalization possibility than do aromatics, but there are notable exceptions. Various alkadienes and cycloalkadienes are reported to form appreciably stable carbonium ions[2] while sulfur radicals are known to be much more stable than their oxygen analogs[3]. Finally, since theory can carry one only so far, a general screening process for classes of non-aromatic compounds to find suitable ones for bipotentiometry was necessary.

## EXPERIMENTAL

### *Reagents*

Lead(IV) acetate was prepared from red lead(IV) oxide, and cobalt(III) acetate from reaction of the lead salt with cobalt(II) acetate in trifluoroacetic acid as described in Part I[1]. The oxidant, 0.10 *N* in trifluoroacetic acid (Aldrich 99%) was standardized against bromohydroquinone as discussed previously. Stock solutions of substrate, $5.0 \cdot 10^{-3}$ *M* in dichloromethane, were prepared fresh daily from commercially available compounds.

Several of the symmetrical disulfides were synthesized by oxidation of the thiols with iodine in aqueous sodium hydroxide[4] while the methyl alkyl sulfides were prepared from the thiols and dimethyl sulfate[4]. Di-*n*-butyl diselenide was synthesized via the selenosulfate[5] and reduced with sodium to give the corresponding selenol[6].

### *Equipment*

The platinum electrodes, 1 mm in diameter and 5 cm long, generally were polarized with 7-$\mu$A direct current from a step-down transformer and selenium rectifier (2.1 V) and a series resistance (0.3 M$\Omega$). Potential measurements were made with a Beckman expanded-scale pH meter and a Sargent model MR recorder.

*Procedure*

A mixture of 1 ml of trifluoroacetic acid, 0.50 ml of stock solution and 0.5 ml of dichloromethane was placed in a 5-ml beaker provided with a microbar stirrer and a two-hole aluminum foil cap. The platinum electrodes were spaced 1 mm apart. Oxidant was added in 5-$\mu$l increments at 15-sec intervals from a Gilmont micrometer buret and the potential was recorded at a chart speed of 0.5 in $min^{-1}$.

## RESULTS AND DISCUSSION

Bipotentiometric titration curves for representative compounds are shown in Figs. 1–3. Curve classification of the compounds studied, which are given in Table I, are based upon the following. The Roman numeral refers to the number of potential

TABLE I

BIPOTENTIOMETRIC BEHAVIOR OF VARIOUS CLASSES OF NON-AROMATIC COMPOUNDS

| *Class* | *Compound* | *Curve classification with lead(IV) acetate* |
|---|---|---|
| Alkyl thiols | *n*-Butyl | IAS |
| | Isobutyl | IAS |
| | *sec.*-Butyl | IAS |
| | *tert.*-Butyl | IAS |
| | Methallyl | IAM |
| Alkyl sulfides | *n*-Butyl | IAM |
| | *sec.*-Butyl | IAM |
| | *tert.*-Butyl | 0S |
| | Methyl-*n*-butyl | IAM |
| | Methyl-*tert.*-butyl | IAM |
| | Methallyl | 0M |
| Alkyl disulfides | *n*-Butyl | IAS |
| | Isobutyl | IAS |
| | *sec.*-Butyl | IAS |
| | *tert.*-Butyl | IAS |
| | Methallyl | 0M |
| Cyclic sulfides | Ethylene | 0M |
| | Propylene | IAM |
| | Tetrahydrothiophene | IAM |
| | Pentamethylene | IAM |
| Misc. sulfur | Thiourea | |
| | Allyl isothiocyanate | IAS |
| | Mercaptoacetic acid | IBS |
| | 2,2'-Dithiodiacetic acid | 0S |
| Selenium | *n*-Butylselenol | IIAM |
| | Di-*n*-butyl diselenide | IIBM |
| | Selenourea | 0M |
| Polyene | 2,3-Dimethyl-1,3-butadiene | IAM |
| | 1,1'-Bicyclohexenyl | 0M |
| | 1,3,5,5-Tetramethyl-1,3-cyclohexadiene | 0M |
| | Cycloheptatriene | IAM |
| | Cyclooctatetraene | IAM |
| Cyclopropane | Dicyclopropylmethane | IAM |
| | Ethyl chrysanthemumate | 0M |

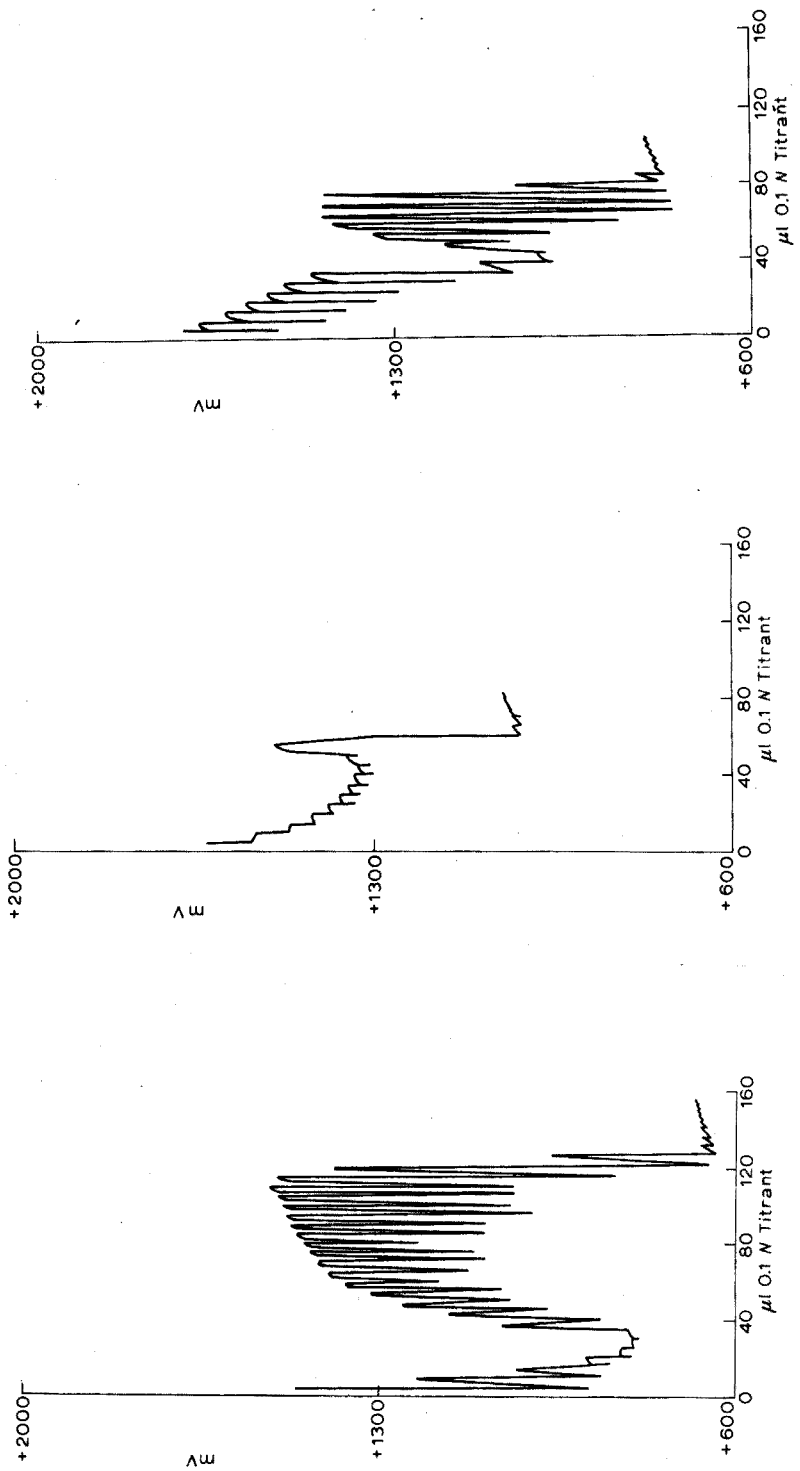


Fig. 1. Bipotentiometric titration of *n*-butanethiol with lead(IV) acetate.

Fig. 2. Bipotentiometric titration of *n*-butyl sulfide with lead(IV) acetate.

Fig. 3. Bipotentiometric titration of *n*-butyl disulfide with lead(IV) acetate.

minima ("troughs") in the curve before the end-point. Compounds with no minimum (but usually a maximum) are given the designation "0". The letters "A" and "B" refer to whether the minimum is above or below the end-point for type I curves, or whether the first minimum is above or below the second for type II curves. The relatively rare higher-order curves are not differentiated in this manner. The letters "S" and "M" refer to the type of potential increments making up the curves; "sawtooth" where the internal angle is $< 90°$, or mixed where a significant number are $\geqq 90°$.

For the majority of compounds titrated, lead(IV) acetate gave curves having better defined end-points than did cobalt(III) acetate.

Sulfides, thiols and disulfides required approximately 1.2, 1.6 and 2.5 equivalents, respectively, of lead(IV) oxidant. Curve differences within each group were noted, depending upon the nature of the alkyl substituent.

Curves useless for identification were given by a number of allyl derivatives including allyl alcohol and amine, diallyl ether and acrolein. The method was also found unsuitable for 1,3-cyclooctadiene, 2-methyl-1-buten-3-yne, 2,4-hexadiyne, 1,1,-2,2-tetramethylcyclopropane, 1,1,2-trimethylcyclopropane, methyl thiocyanate, dimethyl sulfoxide, sulfone, sulfite and sulfate.

The success of bipotentiometry in recording the oxidation of an organic substrate during a titration is based upon the formation of intermediate oxidation products which are: (*a*) electrochemically reversible and hence capable of depolarizing a pair of inert polarized electrodes, and (*b*) appreciably stable during the experimental time of measurement. However, if an intermediate is irreversible and the substrate reacts at a relatively slow rate with an oxidant which has some reversibility, "saw tooth" increments of appreciable magnitude can result. Another possibility is that certain compounds in trifluoroacetic acid (a relatively strong acid) may protonate to give salts or carbonium ions. If these are oxidized to uncharged non-depolarizing species, then one may envision formation of a type "0" curve having a potential maximum. If the carbonium ions are unstable, then polymerization products may be formed prior to titration.

The three basic types of organic oxidation intermediates are radical cations $R^{\cdot +}$, cations $R^+$, and radicals $R^{\cdot}$. The first can be half of an electrochemically reversible couple since only electron transfer is involved. The latter two can be reversible if proton transfer to nitrogen, oxygen or sulfur is involved; irreversible if a carbon–hydrogen bond is involved[7].

The degree of stabilization of the intermediate to subsequent processes such as dimerization will depend upon the extent of delocalization of the charge or the odd electron. Further, the solvent may play an important part in stabilization, and it has been suggested that the enhanced stability of radical cations in trifluoroacetic acid may be due to hydrogen–fluorine bonding with a trifluoroacetate counter-ion[8].

Although non-aromatic compounds are much more limited in their delocalization possibilities than are the aromatics, it was found that bipotentiometry could be applied to various conjugated polyenes and organosulfur compounds. Some of these polyenes are highly alkylated, the stability presumably being enhanced via a hyperconjugative effect.

The oxidation of alkenes with lead(IV) acetate in acetic acid is assumed to involve attack by $Pb(OAc)_3^+$ to give the cation $\rangle C\text{–}\overset{+}{C}\langle$ (with Pb and $(OAc)_3$ on the adjacent carbon)[9], a species that would

not be expected to be electrochemically reversible based on the rule that the redox system is reversible only if the difference in structure between substrate and product is not significant[7]. However, in trifluoroacetic acid the acetate moieties of the oxidant exchange for trifluoroacetate ones[10] to give a more polar and more powerful oxidant that may react with substrate by direct electron transfer to give a depolarizing radical cation.

Sulfur compounds gave well-defined and quite novel titration curves. Sulfur, which can expand its valence electron shell to 9 or 10 electrons, gives more stable radicals than does oxygen. Bipotentiometry is applicable to thiols, sulfides, disulfides, isothiocyanates and thioureas, but apparently not to compounds containing sulfur–oxygen bonds or to thiocyanates, based on the limited number of compounds studied.

The mechanisms of oxidation of thiols and sulfides with lead(IV) acetate in acetic acid are reported as being[9]:

$$R\text{–}SH \rightarrow R\text{–}S\text{–}Pb(OAc)_3 \rightarrow R\text{–}S^+ \xrightarrow[-H^+]{R\text{–}SH} RS\,S\,R \qquad (1)$$

$$R\text{–}S\text{–}R \xrightarrow[-Pb(OAc)_2]{(AcO)_3Pb^+} R\text{–}\overset{+}{S}\text{–}R \;(OAc) \xrightarrow[-Ac_2O]{AcO^-} R\text{–}S\text{–}R \;(=O) \qquad (2)$$

while electrochemical oxidation for the latter is[11]:

$$CH_3SCH_3 \xrightarrow{-e} CH_3\overset{+}{S}CH_3 \xrightarrow[-e]{-H^+} CH_3\overset{+}{S}{=}CH_2 \leftrightarrow$$

$$CH_3SCH_2^+ \overset{(CH_3)_2S}{\rightleftharpoons} CH_3SCH_2\overset{+}{S}(CH_3)_2 \qquad (3)$$

Reaction (1) does not appear to be valid in trifluoroacetic acid for thiols since titration curves were quite different in shape from those for disulfides, the expected product, and since the latter required a larger amount of titrant. For sulfides, the second step of eqn. (3) involves cleavage of a carbon–hydrogen bond and should be electrochemically irreversible. In support of this, it was found that titration gave approximately one equivalent of a depolarizing species.

Examination of a limited number of selenium compounds indicated that bipotentiometry should be applicable to this class. By analogy, organotellurium compounds would be expected to behave similarly, as might certain organic compounds of phosphorus, arsenic, etc.

The highly strained cyclopropane ring with its bent bonds offers the possibility of charge delocalization and is known to confer considerable stability to a carbonium ion[2]. Bipotentiometry on four cyclopropane compounds indicated that two gave well-defined curves, an insufficient number to draw any definite conclusion. Lead(IV) acetate attacks cyclopropanes, possibly via the $Pb(OAc)_3^+$ cation, to give a positively charged species that subsequently cleaves[12]. Phenylcyclopropane (which gave a well-defined titration curve) is more readily attacked than the alkyl derivatives, as are strained ring bicyclics containing the cyclopropyl moiety; *e.g.* bicyclo-(2,1,0)-pentane[9].

SUMMARY

Bipotentiometry has been found to be applicable in the oxidation with lead(IV) acetate of various polyenes and organosulfur compounds in trifluoroacetic acid. It is assumed that oxidation produces intermediates such as radical cations which are electrochemically reversible and capable of depolarizing electrodes. These radical cations are stabilized appreciably via charge delocalization through conjugated double bonds, hyperconjugation, etc. The net result is the production of titration curves composed of "saw tooth" potential increments owing to formation and decay of depolarizing species.

RÉSUMÉ

On examine les possibilités d'application de la bipotentiométrie à l'oxydation de divers polyènes et composés organosulfurés, en milieu acide fluoroacétique, par l'acétate de plomb(IV). On peut admettre que l'oxydation produit des radicaux cationiques, électrochimiquement réversibles et capables de dépolarisation des électrodes.

ZUSAMMENFASSUNG

Die Methode der Bipotentiometrie wurde bei der Oxidation verschiedener Polyene und organischer Schwefelverbindungen mit Blei(IV)-acetat in Trifluoressigsäure angewendet. Es wird angenommen, dass die Oxidation Zwischenstufen wie Radikalkationen erzeugt, die elektrochemisch reversibel sind und Elektroden depolarisieren können. Diese Radikalkationen werden über Ladungsdelokalisierung durch konjugierte Doppelbindungen, Hyperkonjugation etc. in abschätzbarem Masse stabilisiert. Das Ergebnis ist die Bildung von Titrationskurven, die aus sägezahnförmigen Potentialinkrementen zusammengesetzt sind, die durch Bildung und Zerfall von depolarisierenden Spezies hervorgerufen werden.

REFERENCES

1 H. W. YUROW AND S. SASS, *Anal. Chim. Acta*, 52 (1970) 537.
2 N. C. DENO, *Progress in Physical Organic Chemistry*, Vol. 2, Interscience, New York, 1965, p. 129.
3 C. C. PRICE AND S. OAE, *Sulfur Bonding*, Ronald Press, New York, 1962, p. 26.
4 W. J. HICKENBOTTOM, *Reactions of Organic Compounds*, Longmans Green, London, 1957, p. 163.
5 G. G. STONER AND R. W. WILLIAMS, *J. Amer. Chem. Soc.*, 70 (1948) 1113.
6 M. L. BIRD AND F. CHALLENGER, *J. Chem. Soc.*, (1942) 573.
7 Z. R. GRABOWSKI, B. CZOCHRALSKA, A. VINCENZ-CZODKOWSKA AND M. S. BALASIEWICZ, *Discussions Faraday Soc.*, 45 (1968) 145.
8 H. W. YUROW AND S. SASS, *Microchem. J.*, 15 (1970) 285.
9 R. CRIEGEE, in K. B. WIBERG, *Oxidation in Organic Chemistry*, Academic Press, New York, 1965, Chap. V.
10 R. O. C. NORMAN AND M. POUSTIE, *J. Chem. Soc.*, (1969) 196.
11 P. T. COTTRELL AND C. K. MANN, *J. Electrochem. Soc.*, 116 (1969) 1499.
12 R. J. OUELETTE AND D. L. SHAW, *J. Amer. Chem. Soc.*, 86 (1964) 1651.

*Analytica Chimica Acta*
Elsevier Publishing Company, Amsterdam
Printed in The Netherlands



# DETERMINATION OF THE MICROSTRUCTURE OF POLYBUTADIENE BY PYROLYSIS–GAS CHROMATOGRAPHY

T. SHONO AND K. SHINRA
*Department of Applied Chemistry, Osaka University, Suita, Osaka 565 (Japan)*

(Received 24th February 1971)

There have recently been rapid developments in the identification of polymers by gas chromatography of their pyrolysis products. As well as providing a convenient means of identifying polymers, pyrolysis–gas chromatography (p.g.c.) affords the possibility of investigating their microstructure[1-5]. Recently, Takeuchi *et al.*[6,7] investigated the sequence concentration of triad in vinylidene chloride–vinyl chloride copolymers and the distribution of the chlorine atoms in the chain of various chlorinated synthetic polymers by means of p.g.c. In this paper an attempt is made to determine quantitatively the microstructure of polybutadiene.

Polybutadiene can be classified into 1,4 and 1,2 structures. The former shows *cis* and *trans* forms and the latter has different tacticities. The progress of synthetic polymer chemistry has made it possible to produce polymers that are rich in only one of these microstructures.

Vacherot[8], who made a structure elucidation of polyisoprene by p.g.c., found that polyisoprene produced by 3,4-addition is characterized by a hydrocarbon peak between the peaks of isoprene and dipentene which is not given by polyisoprene produced by 1,4-addition. He reported also that the peak area ratio of this hydrocarbon and dipentene is proportional to the ratio of the 1,4-type and the 3,4-type and that this provides a method for determining the ratio of the two types in the synthetic polyisoprenes. Recently, Hackathorn and Brock[9] have examined the dimer pyrolysis fractions of several polyisoprenes. These larger fragments may retain certain microstructural features and provide information about polymer chain degradation mechanisms.

Perry[10] did similar research on polybutadiene and studied the peak area ratio of ethylene and butadiene against the ratio of the 1,2- and the 1,4-species.

TABLE I

ANALYSIS OF MICROSTRUCTURES OF STANDARD SAMPLES

| *Code* | *Microstructure*[a] (%) | | | *Intrinsic viscosity*[b] | *Catalyst used* |
|---|---|---|---|---|---|
| | *Cis*-1,4- | *Trans*-1,4- | 1,2- | | |
| 1 | 97.5 | 1.2 | 1.3 | 1.78 | Reduced nickel |
| 2 | 2.6 | 91.7 | 5.7 | 1.08 | $R_3Al$–$VCl_3$ |
| 3 | 15.2 | 0 | 84.8 | 1.34 | $R_3Al$–$Ti(OR)_4$ |
| 4 | 35.3 | 49.5 | 15.2 | 1.82 | BuLi |
| 5 | 91.8 | 5.2 | 3.0 | 1.78 | $R_3Al$–$TiI_4$ |

[a] By Morero method. [b] Measured at 30° in $CS_2$.

## EXPERIMENTAL

### *Materials*

Five kinds of polybutadiene were prepared by anionic polymerization of butadiene. Table I shows the catalyst used and the intrinsic viscosity and microstructure of the polymer. The percentage of *cis*-1,4-, *trans*-1,4- and 1,2-links was determined by the infrared spectrophotometric method of Morero[11].

### *Pyrolysis and gas chromatography*

To analyze the low boiling fragments, a heated furnace-type pyrolyser PYR-1A (Shimazu)[12] was connected to the inlet port of a gas chromatograph (Shimazu GC-2C) equipped with thermal conductivity detectors. The separation column was 4.5 m long and of 3 mm i.d., and was packed with Neosorb NP (40–60 mesh) coated with 25% hexadecane. The column temperature was 40° and the flow rate of carrier gas (helium) was maintained at 22 ml $min^{-1}$. A sample size of 5 mg was used (Fig. 1).

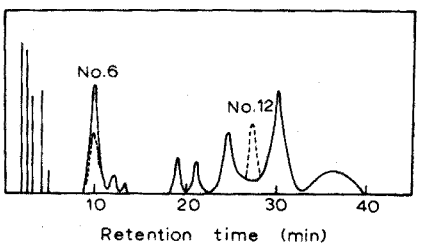


Fig. 1. Pyrolysis chromatogram of 1,4-polybutadiene (——) and 1,2-polybutadiene (-----).

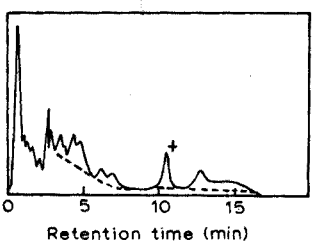


Fig. 2. Pyrolysis chromatogram of 1,4-polybutadiene (——) and 1,2-polybutadiene (----); (+) hydrocarbon peak which is given only by 1,4-*cis*-polybutadiene.

To analyze the high-boiling pyrolysate, polybutadiene rubber was pyrolyzed previously at 400° under nitrogen in a silica tube and an oil was collected. The separation column was 1.5 m long and of 3 mm i.d., and was packed with chromosorb W (40–60 mesh) coated with 1.5% silicone-gum SE30. The column temperature was programmed from 80° to 140° at the rate of 4° $min^{-1}$ and the flow rate of carrier gas (helium) was maintained at 50 ml $min^{-1}$ at 80° (Fig. 2).

To identify the characteristic hydrocarbon peak shown in Fig. 2, the Shimazu fraction collector was used. The column was 1.5 m long and of 10 mm i.d., and was packed with chromosorb W (60–80 mesh) coated with 20% silicone-gum SE30. The column temperature was maintained at 150° and the flow rate of carrier gas (helium) was maintained at 250 ml $min^{-1}$. The fractionated hydrocarbon was analyzed by n.m.r. and mass spectrometry.

## RESULTS AND DISCUSSION

Perry's relationship[10] is not linear for a high concentration of the 1,2-structure. This is believed to be due to the fact that the peak areas of ethylene and butadiene are both variables. As shown in Fig. 1, 1,4-polybutadiene and 1,2-polybutadiene can be

differentiated by the butadiene peak (peak no. 6) and the characteristic peak of 1,2-polybutadiene (peak no. 12).

For this pyrogram, operational conditions in which the *cis* form and *trans* form were the least differentiated, were selected. The characteristic peak of 1,2-polybutadiene presumably is a methylbutene, the structure of which so far has not been identified. Figure 2 shows that there exists a hydrocarbon peak which is given only by 1,4-*cis* polybutadiene.

The relationship between the area of the butadiene peak (peak no. 6, Fig. 1) and the pyrolysis temperature of various polybutadiene rubbers is shown in Fig. 3. No difference in the peak areas of the butadiene peak (peak no. 6) for *cis*-1,4-polybutadiene and *trans*-1,4-polybutadiene was noticed at 700°. With a view to obtaining the relationship between peak area and total 1,4-content, the optimal pyrolysis temperature was set at 700°. Figure 4 shows the analytical results obtained by p.g.c. against the total 1,4-structure content by i.r. analysis. The peak area ($mm^2$) of the butadiene peak (peak no. 6) and the peak height (mm) of the characteristic peak of 1,2-polybutadiene (peak no. 12) are plotted as ordinates and the content of 1,4-linkage as abscissa.

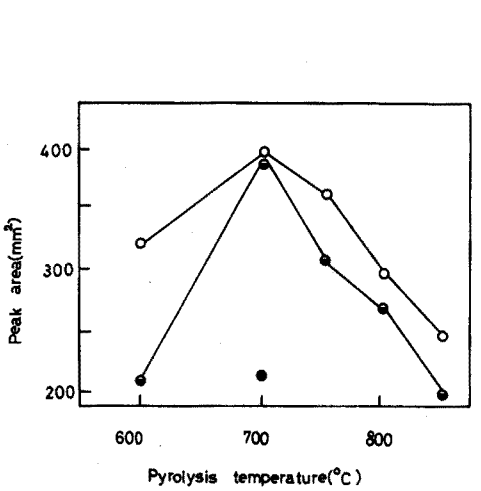


Fig. 3. The relationship between the peak area of peak 6 and pyrolysis temperature. (○) *cis*-1,4; (◒) *trans*-1,4; (●) 1,2.

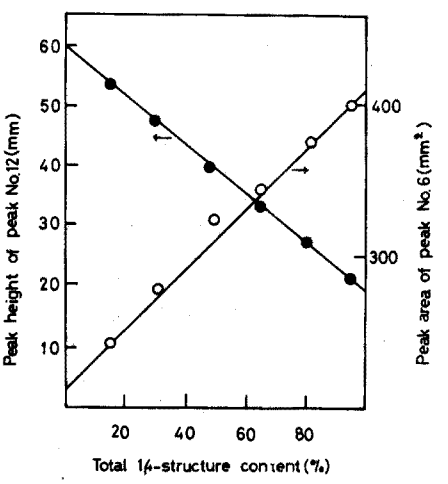


Fig. 4. Analytical results obtained by p.g.c.

The fractionated hydrocarbon peak which is given only by the 1,4-*cis* form of polybutadiene was analyzed by mass spectrometry. The mass spectrum showed the parent peak at 220 which is the tetramer of butadiene. The molecular formula $C_{16}H_{28}$ fits the data for the parent peak and P+1 peak. The pattern coefficient and retention time are in fair agreement with the authentic perhydrodimethylphenanthrene. The catalytic hydrogenation of this hydrocarbon failed in absolute ethanol with $PtO_2$ as catalyst. This means that the hydrocarbon is a saturated hydrocarbon. The n.m.r. spectrum provides conclusive confirmation for a saturated aliphatic hydrocarbon; it shows methyl hydrogens at $\tau = 9.1$ and methylene (or methine) hydrogens at $\tau =$ 7.6–9.0.

The ratio between methyl and methylene (methine) peak areas was 3:11. The polydiene ladder-type polymers are known to be prepared by polymerization of diene with complex catalysts, followed by cyclization[13-15].

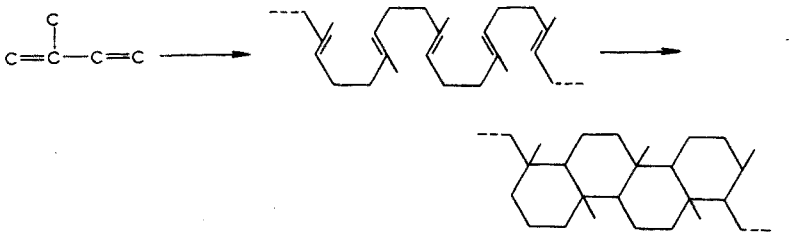

The precursor of the final conjugated ladder-type polymer presumably contains fused cyclohexane ring. From these facts, the $C_{16}H_{28}$ hydrocarbon is concluded to be 1,8-dimethylperhydrophenanthrene.

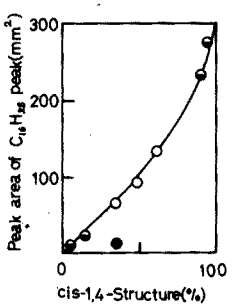


Fig. 5. The relationship between the peak area of $C_{16}H_{28}$ hydrocarbon peak and *cis*-1,4 content. (◒) standard samples (1,2,3,5); (○) mixture of 1,4- and 1,2- forms; (●) standard sample (4).

In Fig. 5 the peak area of $C_{16}H_{28}$ hydrocarbon is plotted as ordinate and the *cis* 1,4-content as abscissa. The fact that the point of sample 4 (on Fig. 5) deviates from the curve means that the microstructure of this sample differs from the other four samples. As shown in Table I, sample 4 was prepared with butyllithium as catalyst. The very low value of the $C_{16}H_{28}$ peak compared with the others means that the percentage of the unit connecting four *cis*-1,4 links (*cis*-1,4 tetrad) is undoubtedly low.

SUMMARY

Pyrolysis–gas chromatographic studies are presented for 1,4-*cis*-, 1,4-*trans*- and 1,2-polybutadiene. 1,4-Polybutadiene and 1,2-polybutadiene can be differentiated by the butadiene peak in the 1,4-polybutadiene pyrogram and a characteristic peak of 1,2-polybutadiene pyrogram. We found that there exists a hydrocarbon peak believed to be 1,8-dimethylperhydrophenanthrene, which is given only by 1,4-*cis*-polybutadiene.

RÉSUMÉ

Une étude est effectuée sur la détermination de la microstructure des polybutadiènes (1,4-*cis*-, 1,4-*trans*- et 1,2-) par chromatographie gazeuse pyrolytique. Le

polybutadiène-1,4 peut être différencié du polybutadiène-1,2 par des pics caractéristiques des pyrogrammes obtenus. On décèle un pic hydrocarbure (le diméthyl-1,8-perhydrophénanthrène) donné seulement par le *cis*-polybutadiène-1,4.

ZUSAMMENFASSUNG

1,4-*cis*-, 1,4-*trans*- und 1,2-Polybutadien wurden der Pyrolyse–Gaschromatographie unterworfen. 1,4-Polybutadien und 1,2-Polybutadien können durch den Butadien-Peak im 1,4-Polybutadien-Pyrogramm und einen charakteristischen Peak des 1,2-Polybutadien-Pyrogramms unterschieden werden. Es wurde ein Kohlenwasserstoff-Peak festgestellt, der 1,8-Dimethylperhydrophenanthren zugeschrieben und nur bei 1,4-*cis*-Polybutadien erhalten wird.

REFERENCES

1 K. J. Bombaugh, C. E. Cook and B. H. Clampitt, *Anal. Chem.*, 35 (1963) 1834.
2 J. Van Schooten and J. K. Evenhuis, *Polymer*, 6 (1965) 561.
3 L. Michajlov, P. Zugenmaier and H. J. Cantow, *Polymer*, 9 (1968) 325.
4 D. Deur-Siftar and V. Svob, *J. Chromatogr.*, 51 (1970) 59.
5 C. E. R. Jones and G. E. J. Reynolds, *Brit. Polymer J.*, 1 (1969) 197.
6 S. Tsuge, T. Okumoto and T. Takeuchi, *Makromol. Chem.*, 123 (1969) 123; *Macromolecules*, 2 (1969) 200, 277.
7 H. Ito, S. Tsuge, T. Okumoto and T. Takeuchi, *Makromol. Chem.*, 138 (1970) 111.
8 M. Vacherot, *J. Gas Chromatogr.*, 5 (1967) 155.
9 M. J. Hackathorn and M. J. Brock, *Polymer Lett.*, 8 (1970) 617.
10 S. G. Perry, *J. Gas Chromatogr.*, 5 (1967) 77.
11 D. Morero, *Makromol. Chem.*, 61 (1963) 250.
12 T. Nakagawa, K. Miyajima and T. Uno, *J. Chromatogr. Sci.*, 8 (1970) 261.
13 N. G. Gaylord, I. Kossler, M. Stolka and J. Vodefinal, *J. Polymer Sci.*, A.2 (1964) 3969.
14 M. Stolka, J. Vodehnal and I. Kossler, *J. Polymer Sci.*, A.2 (1964) 3987.
15 F. T. Wallenberger, *Angew. Chem.*, 76 (1964) 484.

*Analytica Chimica Acta*
Elsevier Publishing Company, Amsterdam
Printed in The Netherlands

## SHORT COMMUNICATIONS

### An automated method for the determination of low concentrations of polyelectrolytes

In a recent publication[1] an automated method for determining polyacrylamide in brine solution is reported. Other methods, based on organic carbon, total nitrogen, viscosity, distillation Nesslerization, and turbidimetry, have been described[2-4]. Michaels and Morelos[2] measured the light absorbed by the colloidally suspended complex formed by the reactions between Hyamine 1622 and hydrolyzed polyacrylamide, and the technique was refined by Crummett and Hummel[3]. Fuoss and Sadek[4] determined polyelectrolyte concentrations turbidimetrically by precipitation of the anionic polyelectrolyte with diisobutylphenoxyethoxyethyldimethylbenzylammonium chloride (Hyamine 1622).

The determination of large numbers of different polyelectrolytes at low concentration (0–100 p.p.m.) posed certain manipulative problems. In order to handle all the samples successfully and rapidly an automated technique was mandatory. The method outlined by Hoyt[1] was unsuitable because it was limited to polymers containing nitrogen. The various turbidimetric methods were evaluated, and although each was suitable, it was decided to adapt and automate the turbidimetric method as modified by Crummett and Hummel to the present requirements because with it only two common reagents are required, and the turbid complex forms and stabilizes rapidly. Briefly, when a large anionic polyelectrolyte, such as the sodium salt of polyacrylic acid (PAA), reacts with a large cationic molecule such as Hyamine 1622, an insoluble compound results:

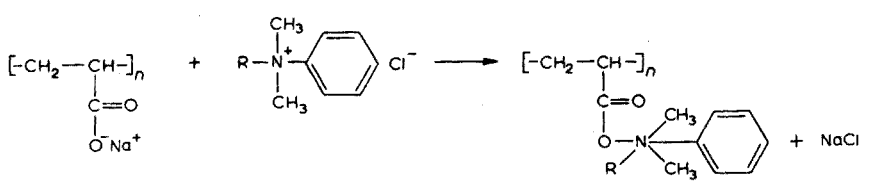


In practice the polyelectrolyte sample, citrate, and segmenting air are mixed; then Hyamine 1622 is added and mixed, and the resulting turbidity is determined at 420 nm in an 8-mm flowing cell.

*Apparatus and reagents*

*Hyamine* 1622 (Rohm and Haas) was used as 0.02–0.2% (w/v) solutions in deionized water. Except for molecular weights less than 5000, 0.2% (w/v) solution was used.

*Sodium citrate* was used as a 3% (w/v) solution in deionized water.

*Standard solutions* (0–100 p.p.m.) sere prepared for each of the polyelectrolytes studied. These included ethylenemaleic acid copolymer (EMA) and polyacrylic acid (PAA).

*Procedure*

The AutoAnalyzer was set up and prepared for operation as described in the Technicon manual. The proportioning pump manifold, fabricated as shown in Fig. 1, was placed on the proportioning pump and the proper connections were made.

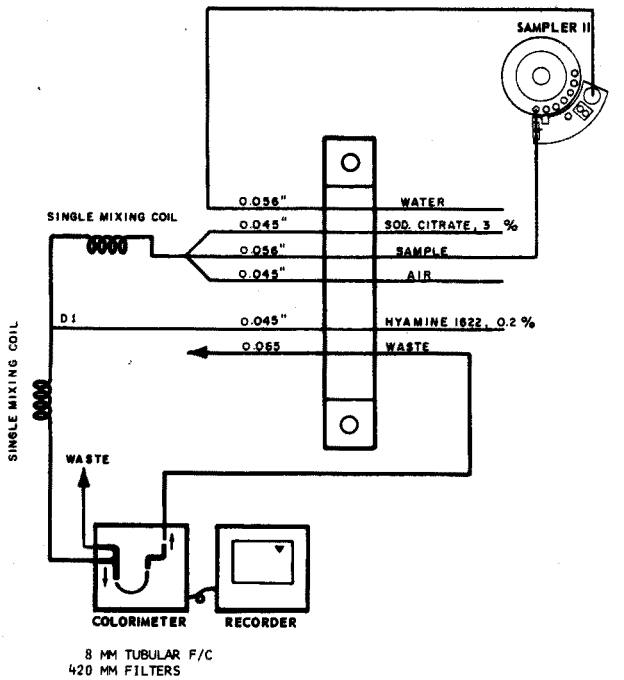


Fig. 1. Proportioning pump manifold.

The standards and sample, in 2-ml cups, were loaded into the Sampler II tray with the samples placed immediately after the standards. Then with the system at reagent equilibrium (adjusted to steady baseline) the samples were aspirated and mixed with citrate and air. Hyamine 1622 (0.2% w/v) was then added and the mixing continued through a single mixing coil where the turbid complex forms. The complex was debubbled, passed through an 8-mm flowing cell in the colorimeter and the absorbance at 420 nm recorded on a strip chart recorder. The samples of each polyelectrolyte were compared to standards of that polyelectrolyte.

*Discussion and results*

Before the final proportioning pump manifold shown in Fig. 1 was selected, several sample tube sizes were investigated to ensure that optimal sensitivity and linearity were obtained. Optimization studies were carried out with PAA but it is reasonable to assume that the other polyelectrolytes would respond similarly. The 0.065-in. I.D. sample tube gave the best sensitivity but linearity at concentrations $>20$ mg $l^{-1}$ was not observed, which indicates a lack of sufficient Hyamine or buffer or both. The 0.056-in. I.D. tube showed good linearity and greater sensitivity than the 0.045-in. I.D. tube and was used for nearly all the work here. For very low concentrations, 0.05% (w/v) Hyamine was used as described below.

The automated procedure described here is quite simple and direct in that no heating, incubation, holding, or dialysis techniques are required. The suspension is measurable within 1–2 min of its formation. When a holding coil was used to allow the suspension to age, the results were spurious because the colloidal particles grew and started to precipitate, yielding a non-uniform suspension. It was observed that the Hyamine concentration was quite significant and a study was made to determine the optimal Hyamine concentration. Three different EMA and PAA concentrations (10, 20, 40 p.p.m.) were run at seven different Hyamine concentrations (0.2, 0.3, 0.4, 0.5, 1.0, 2.0, 4.0 g $l^{-1}$).

The data showed a significant increase in absorbance with increasing Hyamine concentration with a general leveling of values near 1.0 g Hyamine per liter for PAA, but not for EMA. The anomalous behavior of EMA even at the 10-p.p.m. level is not understood but probably is a function of the polyelectrolyte structural characteristics. Also good linearity was observed for Hyamine concentrations above but not below 0.5 g $l^{-1}$. Above 4 g $l^{-1}$, Hyamine tended to precipitate and was no longer useful.

TABLE I

EFFECT OF MOLECULAR WEIGHT ON HYAMINE CONCENTRATION

| | *Response (absorbance)* | | |
|---|---|---|---|
| *Hyamine concn.* ($g\ l^{-1}$) | *EMA* 31 $MW = \sim 10^5$ | *EMA* 21 $MW = \sim 1\text{–}1.5 \cdot 10^4$ | *EMA* 11 $MW = \sim 5 \cdot 10^3$ |
| 0.2 | 1.00 | 1.04 | 1.00 |
| 0.3 | 1.00 | 1.09 | 1.06 |
| 0.4 | 1.00 | 1.00 | 1.06 |
| 0.5 | 1.00 | 1.01 | 1.14 |
| 1.0 | 1.00 | 1.09 | 1.42 |
| 2.0 | 1.00 | 1.08 | 1.48 |
| 4.0 | 1.00 | 1.03 | 1.12 |

Table I shows the effect of molecular weight on Hyamine concentration. The data are normalized, for convenience, to 1.00 for EMA 31.

Significant maxima in response are noted for Hyamine concentrations of 1.0 and 2.0 g $l^{-1}$ for lower-molecular-weight EMA 11 with only a nominal increase in response for EMA 21. Thus the optimal concentration of Hyamine is 2.0 g $l^{-1}$ and that concentration was used throughout this work for molecular weights greater than 5000. The molecular weight where the response compared to EMA 31 reverses is not known but must necessarily be below 5000.

A series of anionic moieties were analyzed to determine the lower-molecular-weight limit at which no turbidity was formed. Stearic acid, petroleum sulfonate (molecular weight 513), tridecylbenzene sulfonate and other similar samples all showed turbidity. Then a series of alkylbenzene sulfonates were studied ranging from methyl- through dodecylbenzene sulfonate. At the 100-p.p.m. level, turbidity was observed for the series from hexylbenzene sulfonate and above with 0.2% Hyamine. Concentration studies of hexyl- and dodecylbenzene sulfonates showed an anomalous behavior of

Hyamine. The data are presented in Table II. Anomalous behavior was observed for both hexyl- and dodecylbenzene sulfonate at Hyamine concentrations above 0.5 g $l^{-1}$ and in the case of hexylbenzene sulfonate also for 0.2 g $l^{-1}$. It was quite unexpected that no turbidity was detected in the lower concentrations although the range of detection did extend lower as the Hyamine concentrations decreased (except for $C_6ØSO_3^-$ at 0.2 g $l^{-1}$ of Hyamine). Such behavior may be due to ion pairs, dielectric forces or

TABLE II

CONCENTRATION STUDIES OF ALKYLBENZENE SULFONATES

| *Compound* | *Absorbance at Hyamine concentration (in g $l^{-1}$) of* | | | | |
|---|---|---|---|---|---|
| | *4* | *2* | *1* | *0.5* | *0.2* |
| $C_6ØSO_3Na$ at | | | | | |
| 100 p.p.m. | 0.387 | 0.595 | 0.581 | 0.237 | 0.049 |
| 80 p.p.m. | 0.171 | 0.475 | 0.512 | 0.217 | 0.029 |
| 60 p.p.m. | 0 | 0.222 | 0.378 | 0.170 | 0.012 |
| 40 p.p.m. | 0 | 0 | 0.134 | 0.123 | 0 |
| 20 p.p.m. | 0 | 0 | 0 | 0.058 | 0 |
| $C_{12}ØSO_3Na$ at | | | | | |
| 100 p.p.m. | 0.353 | 0.595 | 0.621 | 0.402 | 0.313 |
| 80 p.p.m. | 0.122 | 0.488 | 0.552 | 0.356 | 0.255 |
| 60 p.p.m. | 0 | 0.260 | 0.423 | 0.287 | 0.194 |
| 40 p.p.m. | 0 | 0 | 0.191 | 0.195 | 0.123 |
| 20 p.p.m. | 0 | 0 | 0 | 0.101 | 0.053 |

TABLE III

REPRODUCIBILITY OF THE METHOD

| *Compound* | *Absorbance from p.p.m. concentrations of* | | | | |
|---|---|---|---|---|---|
| | *40* | *30* | *20* | *10* | *5* |
| *EMA* | | | | | |
| Av. abs. | 0.280 ± 0.008 | 0.216 ± 0.005 | 0.147 ± 0.002 | 0.073 ± 0.002 | 0.035 ± 0.002 |
| $U_{50}$ | ± 0.004 | ± 0.002 | ± 0.0007 | ± 0.0009 | ± 0.0008 |
| $U_{99}$ | ± 0'029 | ± 0.017 | ± 0.006 | ± 0.007 | ± 0.006 |
| *PAA* | | | | | |
| Av. abs. | 0.318 ± 0.006 | 0.247 ± 0.005 | 0.162 ± 0.004 | 0.077 ± 0.003 | 0.037 ± 0.001 |
| $U_{50}$ | ± 0.003 | ± 0.002 | ± 0.002 | ± 0.001 | ± 0.0004 |
| $U_{99}$ | ± 0.025 | ± 0.019 | ± 0.019 | ± 0.009 | ± 0.003 |

colloidal phenomena. What is significant here is that for low-molecular-weight molecules present at less than 40 mg $l^{-1}$ the desired Hyamine concentration is 0.5 rather than 2.0 g $l^{-1}$ even though the greatest response at detectable concentration is still obtained at 2.0 g of Hyamine per liter.

It should be pointed out that all these data must be interpreted with care. The response is not uniform for the various types of polyelectrolytes. Thus, the polyelectrolyte under study must be known so that a correct calibration can be made.

In addition to the alkylbenzene sulfonate series, other samples similar to fragments one might expect from the polyelectrolytes studied were analyzed for turbidity formation. The sebacate anion, which is similar to fragmented PAA, and EMA, showed no detectable turbidity at the 100-p.p.m. level with the several concentrations of Hyamine studied. This seems qualitatively to indicate that fragments containing ten carbons and two carboxyl groups will show no turbidity.

Table III shows the reproducibility of the method for 5 different concentrations of the two polyelectrolytes studied in detail, together with the 50 and 99% confidence intervals.

TABLE IV

ACCURACY OF THE METHOD

| *Compound* | *p.p.m. taken* | *p.p.m. found*[a] | *% Error* |
|---|---|---|---|
| PAA | 25.0 | 24.5 | 2.0 |
| EMA | 25.8 | 27.7 | 7.4 |

[a] Average of 4 or more runs.

The accuracy of the method is difficult to determine because of response changes that occur when the molecular weight varies and because of a lack of pure known standards. Table IV shows the added and recovered data for two of the polyelectrolytes studied at a single concentration.

*Continental Oil Company,*
*Research and Development Department,*
*Ponca City, Okla. 74601 (U.S.A.)*

J. W. Wimberley
Donald E. Jordan

1 J. L. HOYT, *Adv. in Automated Analysis, Technicon International Congress, Vol. II*, 1969, p. 69–72.
2 A. S. MICHAELS AND O. MORELOS, *Ind. Eng. Chem.*, 47 (1955) 1803.
3 W. B. CRUMMETT AND R. A. HUMMEL, *J. Amer. Water Wks. Assoc.*, 55 (1963) 209.
4 R. M. FUOSS AND H. SADEK, *Science*, 11 (1949) 552.

(Received 8th March 1971)

*Anal. Chim. Acta*, 56 (1971) 308–312

## Electrochemical reduction of bis (2,5-diphenyl-1,3-oxazole-4-yl)mercury

Dessy *et al.*[1] have shown that diphenylmercury is reduced at a mercury cathode in aprotic solvent via one two-electron step to yield phenyl anion and mercury. The electrolytic cleavage of the C–Hg bond is supposedly due to a low bond strength and a high negative charge at the bonding carbon. Dessy *et al.* were unable to stabilize the C–Hg bond toward electrochemical cleavage through substitution of naphthyl and biphenyl groups but were successful upon addition of a nitro function to the aromatic fragments[2]. As a result, a series of organomercurial radical anions were pre-

pared and e.s.r. hyperfine coupling constants for mercury measured[2].

Work in this laboratory has centered on attempts to produce electrochemically radical anions of compounds in which mercury is bonded to carbons of five-membered heteroaromatic rings more reducible than the unsubstituted phenyl, biphenyl and naphthyl substituents employed by Dessy *et al.*[2]. In the present communication, work on the first of a series of oxazolylmercury compounds, bis(2,5-diphenyloxazole-4-yl)mercury, is discussed. The mechanism of the electrochemical reduction of this compound at a planar platinum disk electrode in N,N-dimethylformamide solvent is presented.

## *Experimental*

*Apparatus.* The voltammetric experiments were conducted with equipment and techniques previously described[3].

*Chemicals.* Spectroquality dimethylformamide (DMF) *ca.* 0.03% (Eastman Organic Chemicals) was vacuum distilled from anhydrous copper sulfate before use. Bis(2,5-diphenyloxazole-4-yl)mercury was prepared by the method described by Shvaika and Klimisha[4]. The preparation and purification of the supporting electrolyte has been described previously[3].

## *Results and discussion*

*Linear sweep voltammetry.* Bis(2,5-diphenyloxazole-4-yl)Hg exhibits three well defined current peaks in voltage sweep chronoamperometric experiments conducted at a planar platinum disk electrode (Table I). The first peak, appearing at a potential

TABLE I

LINEAR-SWEEP VOLTAMMETRIC DATA FOR REDUCTION OF BIS(2,5-DIPHENYLOXAZOLE-4-YL)Hg IN DMF[a]

| *Sweep rate* ($v$) ($mV\ sec^{-1}$) | $-(E_p)_c$ ($V$) | $(i_p)_c$ ($\mu A$) | $(i_p)_c/v^{\frac{1}{2}}$ ($\mu A\ sec^{\frac{1}{2}}\ mV^{-\frac{1}{2}}$) |
|---|---|---|---|
| *First wave* | | | |
| 20 | 1.96 | 37.5 | 8.4 |
| 40 | 1.97 | 56.2 | 8.9 |
| 100 | 2.01 | 91.0 | 9.2 |
| 200 | [b] | [b] | [b] |
| *Second wave* | | | |
| 20 | 2.06 | 48.6[c] | 11.0 |
| 40 | 2.06 | 71.2[c] | 11.2 |
| 100 | 2.06 | 115.0[c] | 11.5 |
| 200 | 2.07 | 161.0[c] | 11.3 |
| *Third wave* | | | |
| 20 | 2.44 | 43.0[d] | 9.65 |
| 40 | 2.44 | 59.5[d] | 9.40 |
| 100 | 2.45 | 79.5[d] | 7.95 |
| 200 | 2.47 | 102.5[d] | 7.10 |

[a] Solution was 1 m$M$ in mercury compound and 0.1 $M$ in TPAP supporting electrolyte. The platinum electrode had a cross-sectional area of 80 $mm^2$. [b] First two peaks coalesce at this sweep rate. [c] $(i_p)_c$ measured from residual current base line. [d] Base line for measurement of $(i_p)_c$ established by extrapolation of second peak current decay line.

of $-1.96$ V *vs.* saturated calomel electrode at a sweep rate of 20 mV $sec^{-1}$, shifts cathodically with increased sweep rate, coalescing with the second wave at a sweep rate of 200 mV $sec^{-1}$. The current function, $(i_p)_c/v^{\frac{1}{2}}$, of the first wave increases with an increase in potential sweep rate (Table I). This latter behavior is characteristic of an electrochemical step in which the reactant is weakly adsorbed[5]. The accompanying large cathodic shift of the peak potential suggests the existence of a rapid irreversible chemical step following a reversible electron transfer or an irreversible electrochemical step[6].

The peak potential of the second wave ($-2.07$ V *vs.* SCE) and the current function, $(i_p)_c/v^{\frac{1}{2}}$, are both independent of the potential sweep rate. This behavior indicates a reversible electrochemical step with no coupled chemical reactions[7]. Similar criteria applied to the third current peak suggest that it is the result of a reversible electrochemical step with a coupled irreversible chemical reaction[7].

*Cyclic voltammetry.* Typical cyclic voltammograms taken at a planar platinum disk electrode are shown in Fig. 1. Voltage excursion, hold and reversal past the potential of the second wave show an oxidation current corresponding to the second reduction process with a current ratio, $(i_p)_a/(i_p)_c$, of 1.0 at all sweep rates. Voltage

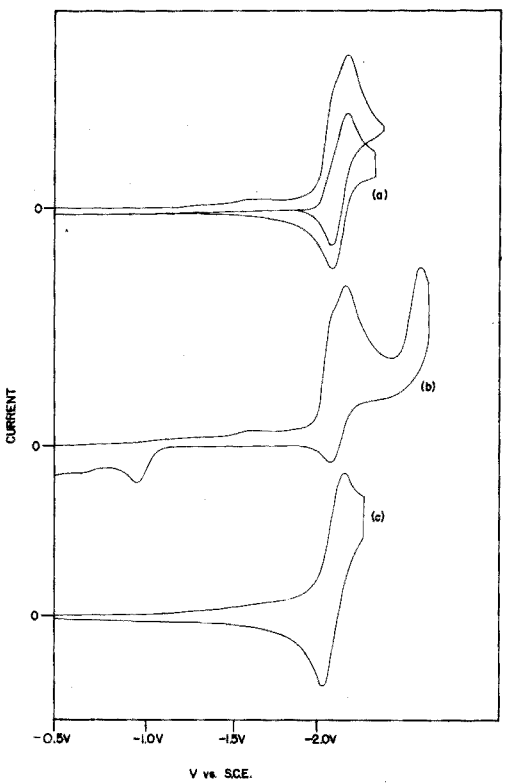


Fig. 1. (a) Cyclic voltammogram of bis(2,5-diphenyloxazole-4-yl) mercury in DMF solvent with sweep reversal past second current peak. (b) Same as (a) with sweep reversal part third current peak. (c) Cyclic voltammogram of 2,5-diphenyloxazole in DMF with sweep reversal past first current peak. Sweep rate was 100 mV $sec^{-1}$ in all experiments.

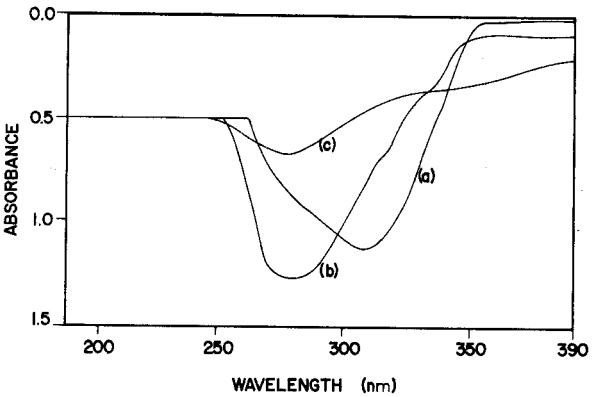


Fig. 2. U.v. spectra in DMF of (a) bis(2,5-diphenyloxazole-4-yl)mercury, (b) 2,5-diphenyloxazole, (c) exhaustively electrolyzed solution of bis(2,5-diphenyloxazole-4-yl) mercury in DMF.

excursion and reversal at potential past the third reduction peak produces a voltammogram with a diminished oxidation current corresponding to the second process and a large oxidation peak appearing near $-0.7$ V and not observed in experiments with reversal before the third wave (Fig. 1b).

The potentials and behavior of the second and third waves of the voltammograms of the organometallic compound are exactly analogous to the two voltammetric waves of the parent organic, 2,5-diphenyloxazole[3]. Comparisons of the cyclic voltammograms of the mercury compound and the parent organic are also given in Fig. 1.

*Mass electrolysis.* Bis(2,5-diphenyloxazole-4-yl) mercury was exhaustively mass electrolyzed in DMF solvent at a platinum gauze cathode. The constant electrolyzing potential was controlled at a value just exceeding the second current peak. Short-term electrolysis produced an intense yellow solution unstable to oxygen. The course of the electrolysis experiment was continuously monitored by removing portions of the solution and recording its u.v. spectrum.

The organomercury compound exhibits a broad u.v. spectrum at 309 nm in DMF solvent (Fig. 2). After mass electrolysis for *ca.* 1 h, a shoulder peak with maximal absorbance at 280 nm appears in the u.v. spectrum of the electrolyzed solution. Only a single peak with this $\lambda_{max}$ is observed in the u.v. spectrum of the exhaustively electrolyzed solution (Fig. 2). The parent organic, 2,5-diphenyloxazole, also exhibits only one u.v. absorption band with a $\lambda_{max}$ of 280 nm.

The electrochemical and spectroscopic evidence suggest that the organometallic is reduced to mercury and the parent oxazole at the first voltammetric wave. The oxazole undergoes reduction at higher potentials according to a mechanism previously discussed[3]. The total process may be represented by the following mechanism:

*First wave*

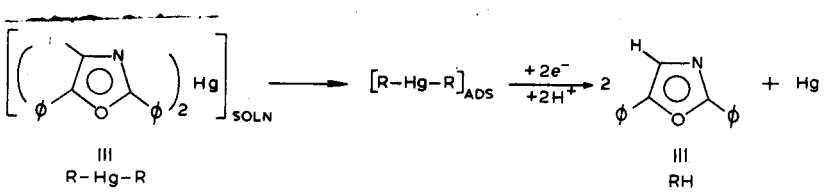


III
R–Hg–R

III
RH

*Second wave*

$$RH + e^- \rightleftarrows RH^-$$

*Third wave*

$$RH^- + e^- \rightleftarrows RH^{2-}; \quad RH^{2-} + SH \rightarrow RH_2^- + S^-$$

*Regeneration wave*

$$RH_2^- \rightarrow RH + H^+ + 2e^-$$

*Potential step chronoamperometry.* The above mechanism requires three electrons per molecule in experiments carried to potentials above the second voltammetric current peak and four electrons per molecule in experiments carried to potentials above the third. Plots of $it^{\frac{1}{2}}$ *vs.* $t$ from chronoamperometric data taken at a planar platinum disk electrode at potentials corresponding first to the second wave and next to the third, confirm the ratio of electrons per molecule as being 3/4 in the two experiments.

The authors gratefully acknowledge the financial support of the Robert A. Welch Foundation (Grant No. AO-337).

*Department of Chemistry,* G. L. Smith
*Midwestern University,* P. Zuniga
*Wichita Falls, Texas 76308 (U.S.A.)* J. W. Rogers

1 R. E. DESSY, W. KITCHING, T. PSARRAS, R. SALINGER, A. CHEN AND T. CHIVERS, *J. Amer. Chem. Soc.*, 88 (1966) 460.
2 R. E. DESSY, M. KLEINER AND S. C. COHEN, *J. Amer. Chem. Soc.*, 91 (1969) 6800.
3 W. N. GREIG AND J. W. ROGERS, *J. Electrochem. Soc.*, 117 (1970) 1141.
4 O. P. SHAVAIKA AND G. P. KLIMISHA, *Khimiya Getarotsiklicheskilh Soedineii*, 2 (1966) 19.
5 R. H. WOPSEHALL AND I. SHAIN, *Anal. Chem.*, 39 (1967) 1514.
6 R. H. WOPSEHALL AND I. SHAIN, *Anal. Chem.*, 39 (1967) 1535.
7 R. S. NICHOLSON AND I. SHAIN, *Anal. Chem.*, 36 (1964) 706.

(Received 17th February 1971)

*Anal. Chim. Acta*, 56 (1971) 312–316

## Potentiometric titrations with solid-state ion-selective electrodes. Determination of calcium and magnesium in water analysis

The calcium ion-selective electrode is probably the most important liquid membrane electrode which has been developed to date, owing to the wide variety of its applications[1]. However, when this electrode was used for direct potentiometric measurement of the concentration of calcium in river waters, the results were incorrect because of ionic strength and complexation effects[2]; in sea waters the precision attained was only *ca.* 4–5% provided that suitable standards were used[3].

In an extensive study of the calcium electrode in potentiometric titrations,

precise limits of performances were theoretically considered and experimentally checked[4,5]. In sea water analysis by potentiometric titration, it was not possible to obtain a precision better than 1%[6].

Recently the copper(II) solid-state electrode was used as the indicator electrode in titrations of several metal ions with a wide variety of chelating agents[7,8]. The analytical method is similar to the well-known method of Reilley *et al.*[9,10].

The present research was undertaken to determine if the solid-state copper(II) membrane electrode could be used for more precise end-point location in the titration of calcium by EDTA in the presence of those species that interfere with the calcium liquid-exchange electrode, *e.g.* in sea water.

*Experimental*

*Apparatus.* The titrations were performed with conventional apparatus, a Beckman 1019 Research pH meter and a standard calomel reference electrode being used.

The calcium-selective liquid-exchanger electrode was manufactured by Orion Research (Mass., U.S.A.). The copper(II)-selective solid-state electrode (AMEL, Milan, Italy) consisted of silver and copper sulfides dispersed in polyethylene[11].

*Solutions.* Reagent-grade chemicals were used.

The borate buffer was prepared by half-neutralizing a 0.2 *M* boric acid solution with 0.5 *M* sodium hydroxide and adjusting the pH to 9.2.

The phenolate buffer was prepared by half-neutralizing a 0.2 *M* phenol

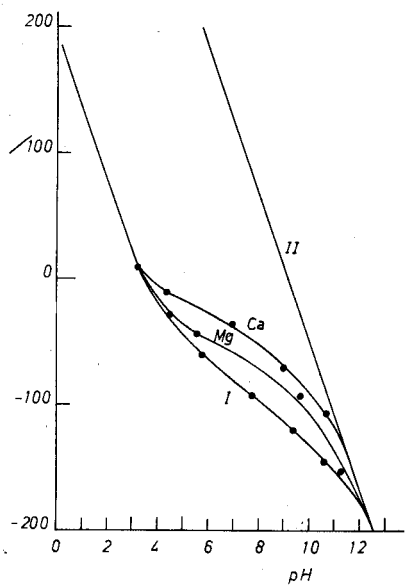


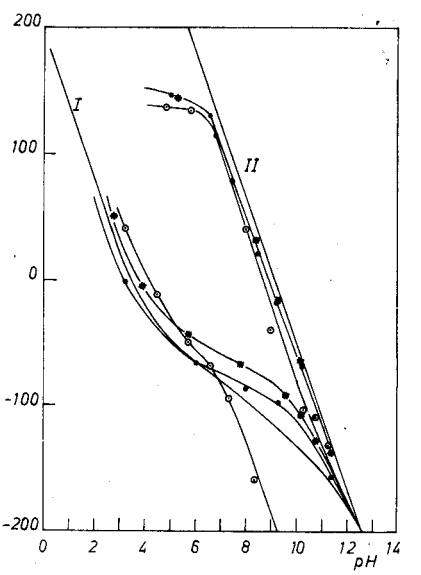


Fig. 1. Potential–pH diagram of copper(II)-selective electrode. (I) 0.001 *M* $CuEDTA^{2-}$ +0.001 *M* EDTA; (II) potential values in the presence of copper(II) hydroxide. Ca and Mg lines are for 0.001 *M* $CuEDTA^{2-}$ + 0.001 *M* $MEDTA^{2-}$ +0.001 *M* $M^{2+}$.

Fig. 2. Effect of buffers on the potential–pH diagram. (⊙) Ammonia buffer; (●) borate buffer; (*) phenolate buffer.

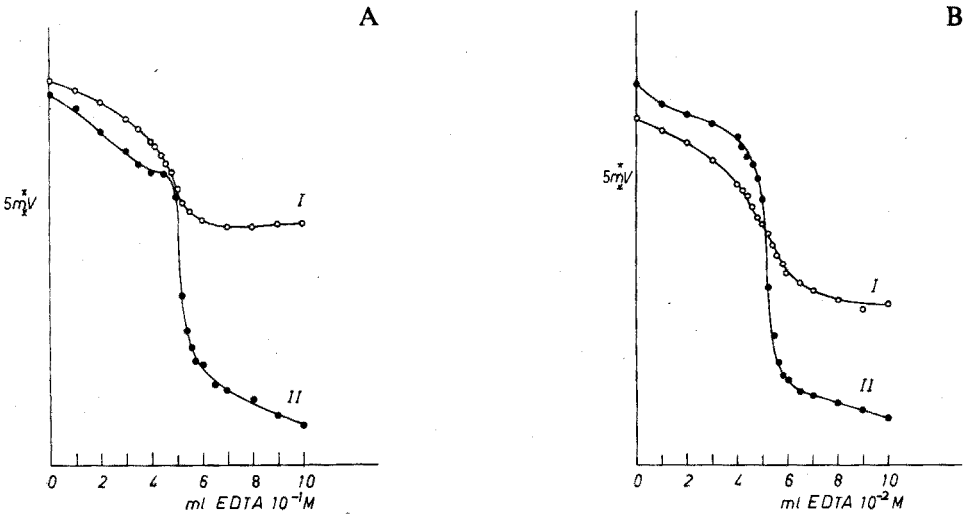


Fig. 3. Titration of calcium nitrate with the two ion-selective electrodes.(I) Calcium electrode, (II) copper(II) electrode. (A) 50 ml of $10^{-2}$ *M* $Ca(NO_3)_2$ and 50 ml of borate buffer. (B) 50 ml of $10^{-3}$ *M* $Ca(NO_3)_2$ and 50 ml of borate buffer. The curves are shifted on the ordinate axis for graphic presentation.

solution with 0.5 *M* sodium hydroxide and adjusting the pH to 10.0.

*Procedure.* A 50-ml sample of water, unless otherwise specified, was diluted with 50 ml of buffer. When the copper(II) solid-state electrode was used, 1 ml of $10^{-3}$ *M* Cu–EDTA solution was added.

The solutions were titrated with 0.1 or 0.01 *M* EDTA.

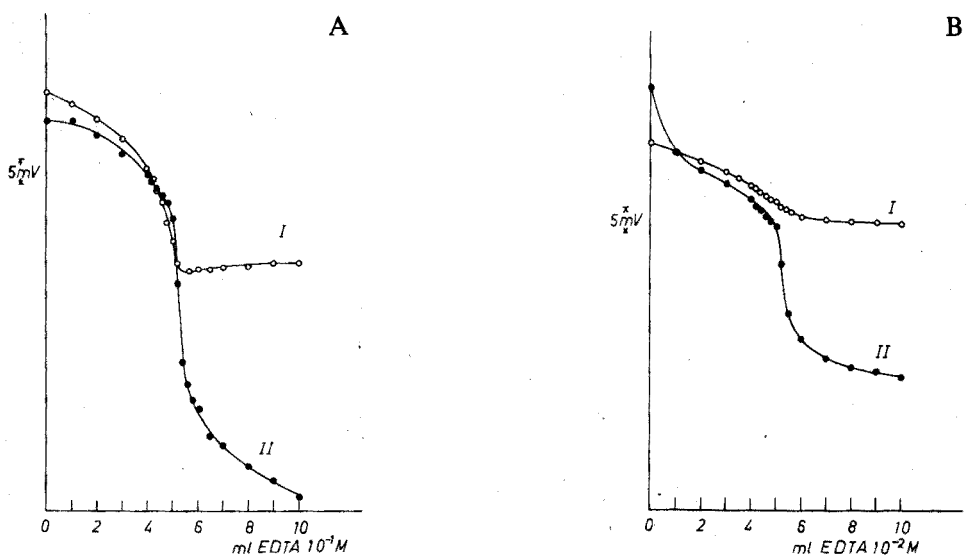


Fig. 4. Titration of calcium nitrate with the two ion-selective electrodes in the presence of 1 *M* sodium nitrate. Other data as given in the legend to Fig. 3.

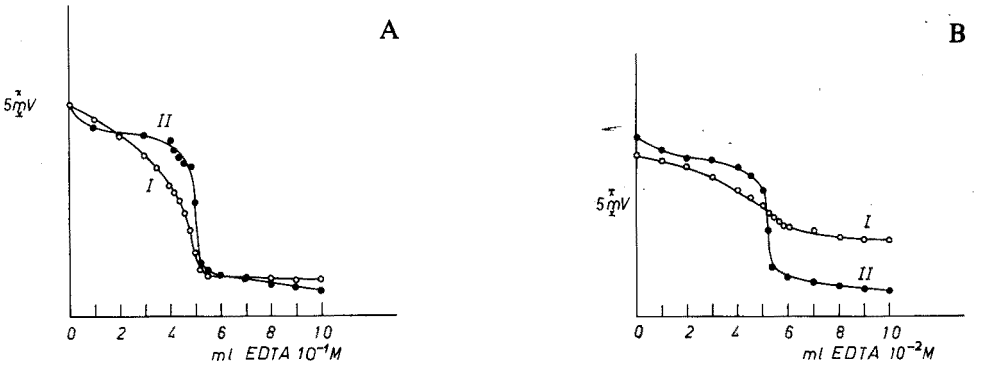


Fig. 5. Titration of calcium nitrate with the two ion-selective electrodes in phenolate buffer pH 10.0. (I) Calcium electrode, (II) Copper(II) electrode.
(A) 50 ml of $10^{-2}$ *M* $Ca(NO_3)_2$ and 50 ml of buffer. (B) 50 ml of $10^{-3}$ *M* $Ca(NO_3)_2$ and 50 ml of buffer. The curves are shifted on the ordinate axis for graphic presentation.

*Results and discussion*

Figure 1 shows the potential–pH diagram for the copper(II) system with calcium and magnesium ions as discussed by Reilley *et al.*[9]. Line II represents an upper limit of potential because of the formation of copper(II) hydroxide; the middle lines, corresponding to solutions containing equal amounts of free metal ion, and metal–EDTA complex, indicate the potential at the half-titration point; curve I indicates the potential past the end-point in the presence of a definite excess of EDTA (where $H_2Y^{2-} = CuY^{2-}$). All curves were experimentally obtained by varying the pH by addition of acid or base. The effect of buffers is shown in Fig. 2. Many common buffers form stable complexes with copper(II) ions, or with the metal ion to be titrated. The presence of those complexes varies the potential–pH diagram. The complexes formed with alkaline earth ions have been neglected, and Fig. 2 presents the curves relating to the formation of complexes between copper(II) and ammonia, borate and phenolate buffers, and relating to the formation of complexes with $CuY^{2-}$.

In Fig. 3 are shown titrations of 50 ml of $10^{-2}$ *M* and $10^{-3}$ *M* calcium nitrate with the two ion-selective electrodes in borate buffer. Figure 4 shows the same titrations in the presence of an inert electrolyte (1 *M* sodium nitrate).

The greater reliability of the copper(II) electrode over the calcium electrode is evident. It is the high level of sodium ions that limits the break at the equivalence point for the calcium electrode. Figure 5 shows the same titrations in the presence of phenolate buffer pH 10. The potential break is different as expected from the potential–pH diagrams shown in Fig. 2. A borate buffer is recommended for this titration.

The titration curves for a solution, the composition of which was similar to that of sea water, $10^{-2}$ *M* $Ca^{2+}$ and 0.5 *M* sodium chloride, are given in Fig. 6. The potentiometric titration of magnesium at pH 9.2 also gave a titration curve with an easily detectable break. Quantitative data for these titrations are presented in Table I. Total water hardness (calcium plus magnesium) can be determined by titration with EDTA with far greater confidence by means of the copper(II)-electrode than with the liquid-exchanger electrode. With the mercury–EDTA electrode, chloride is a source of interference[9,10] and samples must be passed through an ion-exchange column.

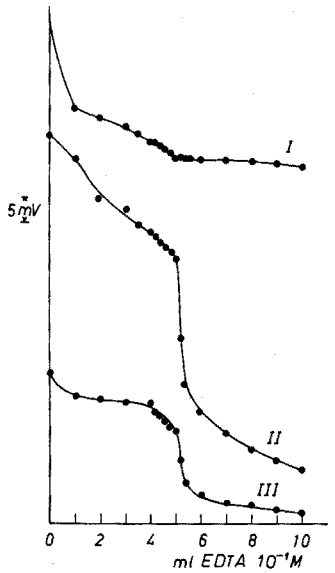


Fig. 6. Titration of 0.01 *M* calcium nitrate in the presence of 0.5 *M* sodium chloride with the two ion-selective electrodes. (I) Calcium electrode, phenolate buffer; (II) Copper(II) electrode, borate buffer; (III) Copper(II) electrode, phenolate buffer. All curves are shifted on the ordinate axis for graphic presentation.

This is not critical with the copper(II) electrode. Quantitative data on water hardness determinations are given in Table II. Some of these samples were of sea water. The method can be easily automated with currently available titrators.

## *Conclusions*

With solid-state membrane electrodes, well-defined potentiometric titration breaks can be achieved. With these electrodes, the end-point can be established

TABLE I

TITRATION OF VARYING AMOUNTS OF CALCIUM (II) AND MAGNESIUM (II)
(Conditions: 50 ml of 0.1 *M* borate buffer, 100 ml total volume, pH 9.2; 0.1 ml of $10^{-3}$ *M* $Cu(NO_3)_2$–EDTA was added)

| *Ion* | *No. of detns.* | *Taken (mg)* | *Found (mg)* | *Average error (mg)* |
|---|---|---|---|---|
| $Ca^{2+}$ | 8 | 20.0 | 20.025 | 0.175 |
| | 4 | 2.00 | 2.01 | 0.025 |
| $Mg^{2+}$ | 2 | 12.0 | 11.95 | 0.05 |
| | 2 | 1.20 | 1.20 | 0.00 |
| | | *(mmole)* | | |
| $Ca^{2+}+Mg^{2+}$ | | 0.020 +0.020 | 0.040 | |
| | | 0.020 +0.020 | 0.040 | |
| | | 0.20 +0.20 | 0.40 | |
| | | 0.20 +0.20 | 0.40 | |

TABLE II

DETERMINATION OF WATER HARDNESS
(Titrations carried out with 0.01 and 0.1 *M* EDTA at pH 9.2)

| *Water sample* | *Size of sample (ml)* | *Found (mmole)* |
|---|---|---|
| Lab water | 10 | 0.0341 |
| | | 0.0342 |
| | | 0.0341 |
| Natural water | 5 | 0.0513 |
| | | 0.0512 |
| | | 0.0505 |
| Sea water | 10 | 0.410 |
| | | 0.410 |
| | | 0.408 |

with a standard deviation of about 0.1–0.5% in the presence of inert electrolyte, *e.g.* in sea water or in river waters, far superior to the liquid-exchanger electrodes. The latter are, however, unique for determining the ion activity in a given medium with previous standardization.

*Istituto de Chimica Analytica,*
*Università di Roma,*
*Rome (Italy)*

Marco Mascini

1 *Ion Selective Electrodes*, NBS Special Publication no. 314 (1969).
2 J. B. ANDELMAN, *J. Water Pollut. Contr. Fed.*, 40(11) (1968) 1844.
3 M. E. THOMPSON AND J. W. ROSS, *Science*, 154 (1966) 1643.
4 M. WHITFIELD AND J. V. LEYENDEKKERS, *Anal. Chim. Acta*, 45 (1969) 383; 46 (1969) 63.
5 M. WHITFIELD, J. V. LEYENDEKKERS AND J. D. KERR, *Anal. Chim. Acta*, 45 (1969) 399.
6 D. DYRSSEN, D JAGNER AND H. JOHANSSON, *Report on the Chemistry of Seawater*, V Dept. Anal. Chem., University of Gothenburg, Sweden, 1968.
7 J. W. ROSS, JR. AND M. S. FRANT, *Anal. Chem.*, 41 (1969) 1900.
8 E. W. BAUMANN AND R. M. WALLACE, *Anal. Chem.*, 41 (1969) 2072.
9 C. N. REILLEY AND R. W. SCHMID, *Anal. Chem.*, 30 (1958) 947.
10 C. N. REILLEY, R. W. SCHMID AND D. W. LAMSON, *Anal. Chem.*, 30 (1958) 953.
11 M. MASCINI AND A. LIBERTI, *Anal. Chim. Acta*, 53 (1971) 202.

(Received 15th March 1971)

*Anal. Chim. Acta*, 56 (1971) 316–321

## A potentiometric determination of cesium ion

At present there is no cesium ion-selective electrode available commercially. In this work an electrode sensitive to cesium ion was prepared and used for the potentiometric determination of cesium.

The electrode was constructed from a membrane consisting of cesium 12-molybdophosphate embedded in a silicone rubber and then fixed to one end of a glass

tube. Although the dynamic response characteristics of commercial available electrodes for other cations are far better than those of this electrode, it was possible to use this electrode as end-point indicator in potentiometric titrations after application of Gran plots to the data.

*Apparatus and chemicals*

A Beckman research model pH meter was used for all e.m.f. measurements. The electrode assembly consisted fo a cesium 12-molybdophosphate–silicone rubber disc attached to a glass tube of 2.5 cm diameter; the inner solution was 0.10 *M* cesium nitrate. Saturated calomel electrodes were used both as the internal electrode and the reference electrode.

All chemicals used were of A.R. grade.

*Precipitation titrations*

Precipitation titrations with 12-molybdophosphoric acid as precipitant for

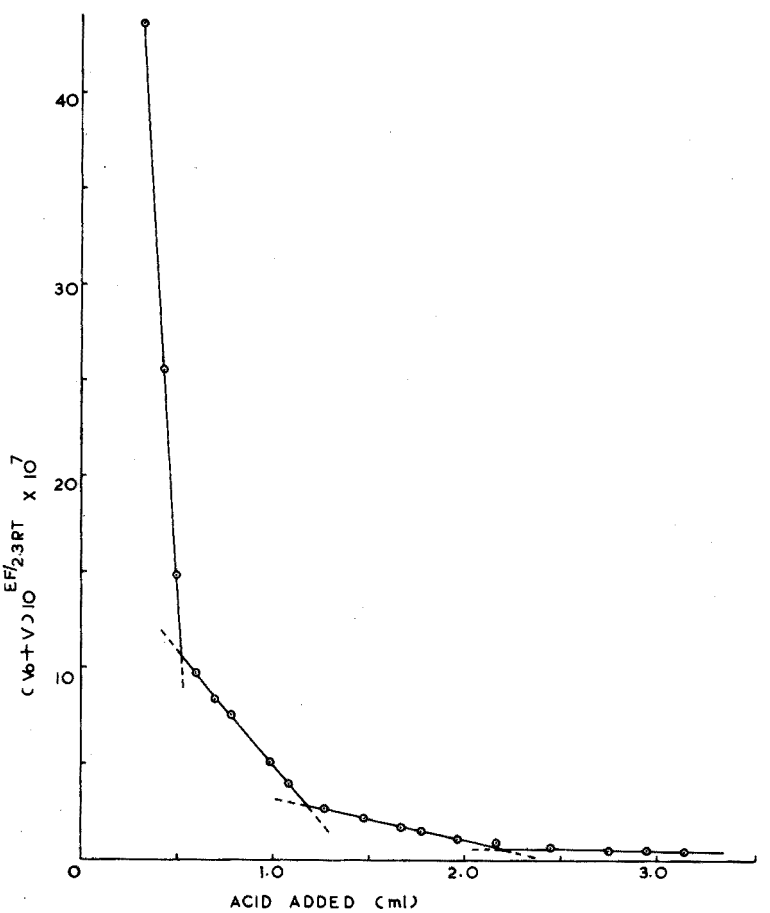


Fig. 1. Potentiometric titration of 72.4 mg of cesium in 55 ml of solution with 0.2450 *M* 12-molybdophosphoric acid solution.

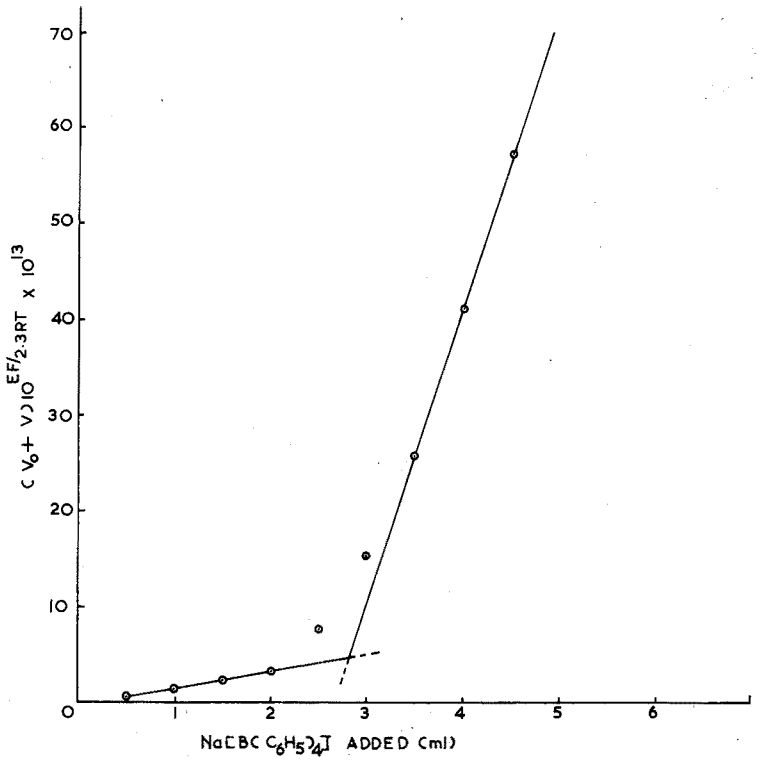


Fig. 2. Potentiometric titration of 6.55 mg of cesium in 55 ml of solution with 0.0176 *M* sodium tetraphenylborate solution.

cesium ions were done with the described electrode as indicator electrode. A very sharp end-point did not result from the usual potential–volume plot. When a Gran plot[1] of the data was done the end-point could easily be detected. The result is shown in Fig. 1 where the function $(V_0+V)\cdot 10^{EF/2.3RT}\cdot 10^7$ is plotted against $V$ ml of acid added, $V_0$ being the initial volume. The Fig. also shows the precipitation taking place in three different stages:

$$Cs^+ + H_3PMo_{12}O_{40} \rightarrow CsH_2PMo_{12}O_{40} + H^+$$
$$Cs^+ + CsH_2PMo_{12}O_{40} \rightarrow Cs_2HPMo_{12}O_{40} + H^+$$
and $$Cs^+ + Cs_2HPMo_{12}O_{40} \rightarrow Cs_3PMo_{12}O_{40} + H^+$$

In another experiment the cesium ion was precipitated with a standard sodium tetraphenylborate solution. When the same treatment was applied to the titration data, a graph as shown in Fig. 2 was obtained, giving the correct value at the intercept of the two straight portions of the curve.

*Standard addition potentiometry*

This technique may be applied to any selective electrode provided that a linear relationship exists between electrode response and logarithm of the concentration[2]. If the sample and the standard solutions are prepared in such a way that the ionic strength is kept quite high and almost constant, the activity coefficient of the

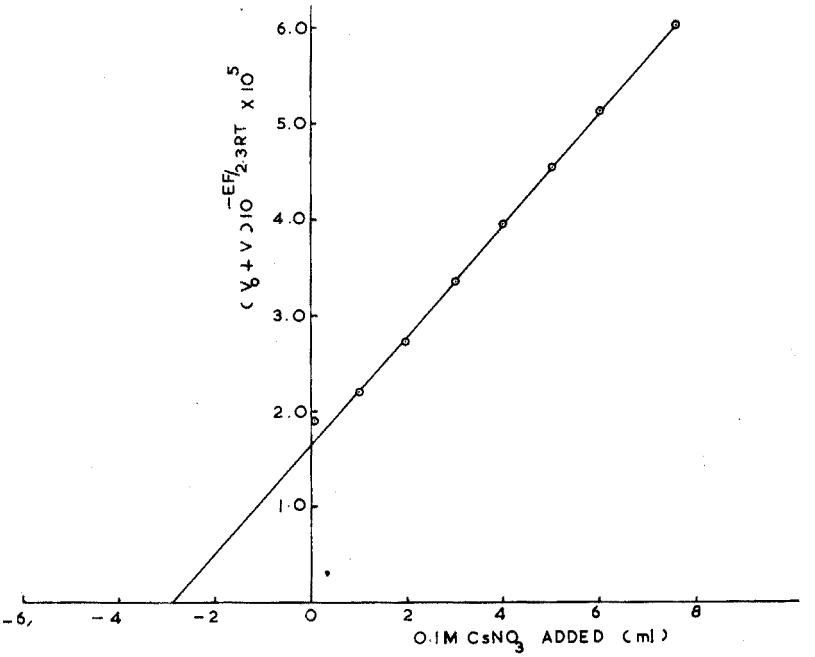


Fig. 3. Determination of 25 ml of 0.0116 *M* cesium by standard addition titration. The cesium standard solution added was 0.100 *M* in cesium and 0.1 *M* in lithium nitrate.

ion in question and the liquid junction potential does not change appreciably.

By plotting $(V_0+V)\cdot 10^{-EF/2.3RT}$ *versus* $V$ ml added, a straight line is obtained intercepting the abscissa for a value $V_e$ where $C_0V_0 = -CV_e$. The initial cesium concentration is obtained from $C_0 = CV_e/V_0$. In this experiment the ionic strength was kept constant by having both the sample solution and the standard cesium solution 0.1 *M* in lithium nitrate.

By plotting the function $(V_0+V)\cdot 10^{-EF/2.3RT}\cdot 10^5$ against volume of standard 0.10 *M* cesium nitrate added, a straight line results with an intercept $-2.90$ ml which is equal to the theoretical (Fig. 3).

It was found that of the alkali metal ions only lithium could be used to keep the ionic strength constant. When sodium was used a parallel shift of the straight line resulted, giving much larger values than the theoretical. This might be due to the sensitivity of the electrode for sodium ions.

As was found by Liberti and Mascini[2] for the fluoride electrode, the response of the cesium electrode was more rapid when going from dilute to concentrated solutions than in the other direction.

*Department of Chemistry,*
*University of the Western Cape,*
*Bellville (South Africa)*

C. J. Coetzee
A. J. Basson

1 G. Gran, *Analyst*, 77 (1952) 661.
2 A. Liberti and M. Mascini, *Anal. Chem.*, 41 (1969) 676.

(Received 29th March 1971)

*Anal. Chim. Acta*, 56 (1971) 321–324

*Analytica Chimica Acta*
Elsevier Publishing Company, Amsterdam
Printed in The Netherlands



## Titrimetric determination of ascorbic acid with cerium(IV) sulphate

Sullman[1] appears to have been the first to use cerium(IV) sulphate for the determination of ascorbic acid. Treating an aliquot with an excess of cerium(IV) sulphate solution and back-titrating after about 30 min with standard iron(II) solution, he reported that one mole of ascorbic acid consumed an amount of cerium(IV) equivalent to three oxygen atoms; the products were believed to be 1-threonic acid and carbon dioxide. Repeating the work of Sullman, Gopala Rao and Narayana Rao (unpublished work, 1957) found that the oxidation of ascorbic acid by excess of cerium(IV) does not correspond to any definite oxidation stage but is largely influenced by the time of contact of reactants, their relative ratio, the acidity of the medium and the temperature. Rao and Somidevamma (unpublished work, 1953) attempted the direct titration of ascorbic acid with cerium(IV) sulphate in dilute sulphuric acid medium using redox indicators. With diphenylbenzidine indicator, the error was observed to be $+0.6-+1.0\%$. With ferroin, N-phenylanthranilic acid and the fluorescent indicator, rhodamine 6G, the consumption of cerium(IV) was 2–3% more than that corresponding to the oxidation of ascorbic acid to dehydroascorbic acid. Evidently the excess consumption of cerium(IV) is due to the further oxidation of dehydroascorbic acid.

It has now been observed that ferriin, the oxidised product of ferroin, is reduced by both ascorbic acid and dehydroascorbic acid in 0.1–0.5 *M* sulphuric acid. The speed of reduction of ferriin by dehydroascorbic acid decreases as the acid concentration is increased, but the speed of reduction of ferriin by ascorbic acid is not affected by increased acidity even upto 1.5 *M*. The addition of 1 ml of syrupy orthophosphoric acid in a volume of 50 ml inhibits the reduction of ferriin by dehydroascorbic acid in a medium containing 0.75–1.25 *M* sulphuric acid but not that of ferriin by ascorbic acid. This concentration of phosphoric acid does not affect the speed of oxidation of ferroin by cerium(IV). These observations indicate that a direct titration of ascorbic acid with cerium(IV) sulphate can be made in 0.75–1.25 *M* sulphuric acid medium, without interference from dehydroascorbic acid, if ferroin is used as indicator and phosphoric acid is added. Phosphoric acid may also retard the direct reaction between ascorbic acid and cerium(IV) because of complexation with the latter. Suitable conditions for the accurate determination of ascorbic acid with cerium(IV) on this basis are described below. Ascorbic acid is oxidized stoichiometrically to the dehydroascorbic acid stage.

### *Experimental*

*Preparation of solutions.* A 0.1 *M* solution of cerium(IV) in 0.5 *M* sulphuric acid medium was prepared from cerium(III) oxalate by the classical method of Willard and Young and standardised against "AnalaR" sodium oxalate.

An aqueous 0.05 *M* solution of ascorbic acid (B.P. grade, Hoffmann-La Roche) was standardised daily against potassium iodate (p.a., E. Merck) as described by Ballentine[2]

The orthophosphoric acid used was guaranteed reagent (E. Merck) and all other chemicals were of analytical-reagent quality. All solutions were made with

deionized water.

*Recommended procedure.* Treat 5–20 ml of 0.05 *M* ascorbic acid with enough 2 *M* sulphuric acid to give a final acidity of 0.75–1.25 *M* on dilution to 50 ml. If the acidity falls below 0.5 *M* during the titration, cerium(IV) phosphate may precipitate. Add 1 ml of syrupy orthophosphoric acid and 1 drop of 0.01 *M* ferroin sulphate solution. Titrate with 0.1 *M* cerium(IV) sulphate solution, at normal speed with constant stirring; if any cerium(IV) phosphate precipitates, it dissolves on stirring. Near the equivalence point, add the titrant in fractions of a drop, with the aid of a thin glass rod.

The indicator correction is negligible for 0.05–0.1 *M* cerium(IV) solutions. The colour transition at the end-point is red to pale blue.

Under the above conditions, barium diphenylamine sulphonate and N-phenylanthranilic acid can also be used satisfactorily as redox indicators, the colour transitions being from colourless to violet or red-violet. Rhodamine 6G can also be used successfully; the addition of 0.1 ml of 0.035% Rhodamine 6G solution imparts in daylight a greenish fluorescence, which is sharply quenched by a slight excess of cerium(IV).

*Results and discussion*

Representative results from a large number of titrations are presented in Table I.

TABLE I

TITRIMETRIC DETERMINATION OF ASCORBIC ACID WITH CERIUM(IV) SULPHATE

| *Indicator* | *Amount of ascorbic acid (mg)* | | *Indicator* | *Amount of ascorbic acid (mg)* | |
|---|---|---|---|---|---|
| | *Taken* | *Found* | | *Taken* | *Found* |
| Ferroin | 17.33 | 17.28 | N-Phenylanthranilic | 15.11 | 15.11 |
| | 37.09 | 37.13 | acid | 29.88 | 29.83 |
| | 52.00 | 51.95 | | 59.75 | 59.85 |
| | 66.73 | 66.82 | | 72.16 | 72.06 |
| Barium diphenylamine | 12.67 | 12.67 | Rhodamine 6G | 24.66 | 24.66 |
| sulphonate | 31.00 | 31.06 | | 39.63 | 39.72 |
| | 62.36 | 62.36 | | 57.12 | 57.19 |
| | 84.14 | 83.79 | | 72.06 | 71.90 |

*Interferences.* No interferences were found from 10-fold amounts of citric acid, tartaric acid, glucose, fructose or sucrose. Oxalic acid caused an excess consumption of 0.9%–2.5% of cerium(IV), when the amount of oxalic acid added varied from 0.5 to 5 times that of the ascorbic acid taken.

*Titration of 0.01–0.005 M solutions of ascorbic acid.* In the titration of such dilute solutions with ferroin as indicator, low results were obtained. This was traced to loss of ascorbic acid by autooxidation catalysed by cerium(III). Titrations made in a carbon dioxide atmosphere gave good results.

*Titrations in phosphoric acid mesium.* It is unnecessary to maintain an inert atmosphere even for these dilute solutions of ascorbic acid, if the titration is done in 12–13 *M* phosphoric acid medium with ferroin as indicator. The Ce(IV)/Ce(III) potential in such a medium is reported to be 1.22 V[3], the value in 1–2 *N* sulphuric acid being 1.44 V. It was also found that the formal potentials of the dehydroascorbic acid/ascorbic acid system increase as the phosphoric acid concentration increases; this increased potential affords protection to the ascorbic acid against atmospheric oxidation. Moreover, phosphoric acid complexes any heavy metal ions present, thus preventing their catalytic action on the oxidation of ascorbic acid. The results obtained for small amounts of ascorbic acid by titration in 1 *M* sulphuric acid medium under an inert atmosphere, and in 12–13 *M* phosphoric acid medium without an inert atmosphere, agreed between themselves and with the theoretical value within $\pm 0.1\%$.

A further advantage with phosphoric acid as the titration medium is that oxalic acid does not interfere as it does in sulphuric acid medium. The relative error in the determination of ascorbic acid by potentiometric titration with cerium(IV) sulphate in 12–13 *M* phosphoric acid medium is within $\pm 0.1\%$. In this connection, it is interesting to note that the potentiometric titration of ascorbic acid with dichlorophenolindophenol has been reported as unsatisfactory by Kirk and Tressler[4], and that with iodine as inaccurate by Stevens[5].

TABLE II

FORMAL POTENTIALS IN PHOSPHORIC ACID MEDIA

| *Concentration of phosphoric acid (M)* | *Formal redox potential (V)* |
|---|---|
| 1.0 | 0.445 |
| 2.0 | 0.464 |
| 4.0 | 0.506 |
| 6.0 | 0.568 |
| 8.0 | 0.609 |
| 10.0 | 0.650 |
| 12.0 | 0.686 |

Phosphoric acid affords a third advantage as a titration medium. From a large number of experiments, it was observed that potentiometric titration of even high concentrations of ascorbic acid with cerium(IV) sulphate in 0.75–1.0 *M* sulphuric acid medium (even with the addition of 1.0 ml of syrupy phosphoric acid per 50 ml) gave results about 10% lower than the theoretical. Accurate titres were secured by carrying out the potentiometric titration in 12–13 *M* phosphoric acid, with a bright platinum wire as indicator electrode and a saturated calomel reference electrode; initially the potentials were measured immediately after the addition of the cerium(IV) reagent, and at 2-min intervals near the equivalence points. The potential break at the equivalence point is about 170–180 mV per 0.04 ml of the reagent. The cerium(IV) reagent is taken at double the concentration of the ascorbic acid so that the phosphoric acid concentration in the titration medium is not unduly lowered.

Formal redox potentials of the dehydroascorbic acid/ascorbic acid system at varying phosphoric acid concentrations are presented in Table II.

*Department of Chemistry,*
*Andhra University,*
*Waltair (India)*

G. Gopala Rao
G. Sitarama Sastry

1 H. SULLMAN, *Enzymologia*, 5 (1938) 326.
2 R. BALLENTINE, *Ind. Eng. Chem., Anal. Ed.*, 13 (1941) 89.
3 G. GOPALA RAO, P. KANTA RAO AND S. BHANOJEE RAO, *Talanta*, 11 (1964) 825.
4 M. M. KIRK AND D. K. TRESSLER, *Ind. Eng. Chem.*, 11 (1939) 322.
5 J. W. STEVENS, *Ind. Eng. Chem.*, 10 (1938) 269.

(Received 13th April 1971)

*Anal. Chim. Acta*, 56 (1971) 325–328

## "Quasi-isothermal" thermogravimetry

The advantage of both the static and dynamic investigation methods could be combined if it were possible to develop a thermogravimetric technique in which the temperature of the sample would be increased rapidly so long as no changes occurred, whereas isothermal conditions would be ensured during transformations connected with weight change. Although the special advantages of such a technique are obvious, its realization has been frustrated because the heating could not be programmed and automated according to the above-mentioned requirements.

Derivatography[1,2] and derivative thermogravimetry[2,3] can offer, although indirectly, a solution to this problem[4]. The new method is called "quasi-isothermal" thermogravimetry[5].

*Method of operation*

Figure 1 shows the design and operation of the device which, based on the feedback principle, regulates the heating depending on the rate of the weight change. The voltage of the heating current of the thermobalance is raised by the program regulator in the usual way at a constant speed (0.5–5° $min^{-1}$) until the weight of the sample slowly begins to decrease or increase. Because of the weight change, the balance deflects and so the light signal of the galvanometer, connected to the poles of the deriving device, also deflects. On each side of the path of the light signal are placed light-sensitive instruments, *e.g.* two photocells. In the case of weight stability the light signal stays between the two light cells, while it falls on to one or the other cell when the weight of the sample decreases or increases. The photoelectric current generated in the photocells is amplified and then actuates a relay system which reduces, usually in several steps, or cuts out the voltage of the heating current. Owing to the decrease in temperature, the rate of the thermal decomposition is reduced and accordingly the galvanometer light signal deflects, to a smaller extent. The light signal moves away from the photocell, whereupon the relay system switches on the

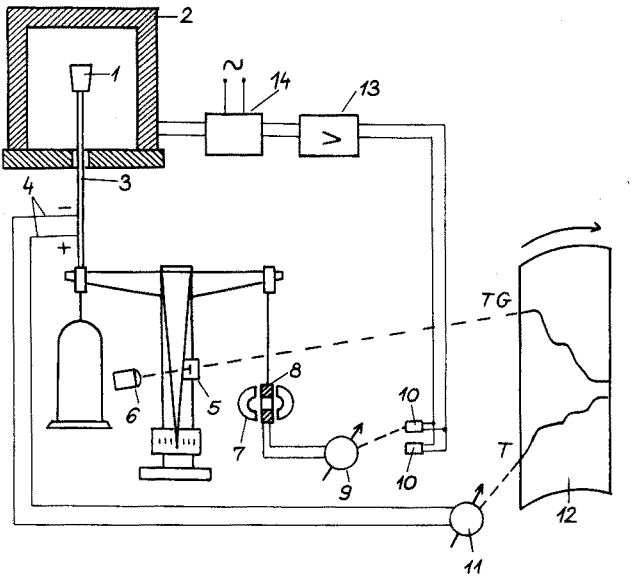


Fig. 1. "Quasi-isothermal" thermobalance. (1) Sample, (2) electric furnace, (3) corundum tube, (4) thermocouple, (5) optical slit, (6) lamp, (7) permanent magnet, (8) coil, (9) galvanometer, (10) double light cell, (11) galvanometer, (12) chart paper, (13) control mechanism, (14) heating regulator.

heating current again. The described process is repeated until the end of the thermal decomposition, at which point the temperature of the sample is again increased at the usual heating rate, up to the temperature where the next thermal decomposition process starts.

The technique described is of universal character and can be applied not only to the derivatograph, but to any other recently developed derivative thermobalance type, with minor modifications.

*Results and discussion*

The new technique was used to examine potassium hydrogencarbonate. The temperature ($T$) and weight ($TG$) changes of the 0.5-g sample were measured as functions of time in the covered platinum crucible of the derivatograph. In Fig. 2 curves a and b represent the former and latter processes, respectively. Curve c shows the weight change of the sample redrawn as a function of temperature. This latter curve can also be traced directly by means of an X–Y recorder. Curves e and d were recorded by using a heating rate of 10° $min^{-1}$. In the case of curve e the sample was measured in the conventional crucible[1,2] of the derivatograph, while curve d was obtained from examinations performed on the polyplate sample holder[2,6].

According to present knowledge, potassium hydrogencarbonate decomposes on heating according to the following simple dissociation reaction:

$$2\,KHCO_3 \rightleftharpoons K_2CO_3 + CO_2\uparrow + H_2O\uparrow$$

The partial pressure of carbon dioxide attains 760 Torr at 156°[7]. On the basis of curves e and d obtained in the conventional way, it can only be seen that the thermal decomposition takes place in one step at 140–200° or 140–240°. Curves a, b and c,

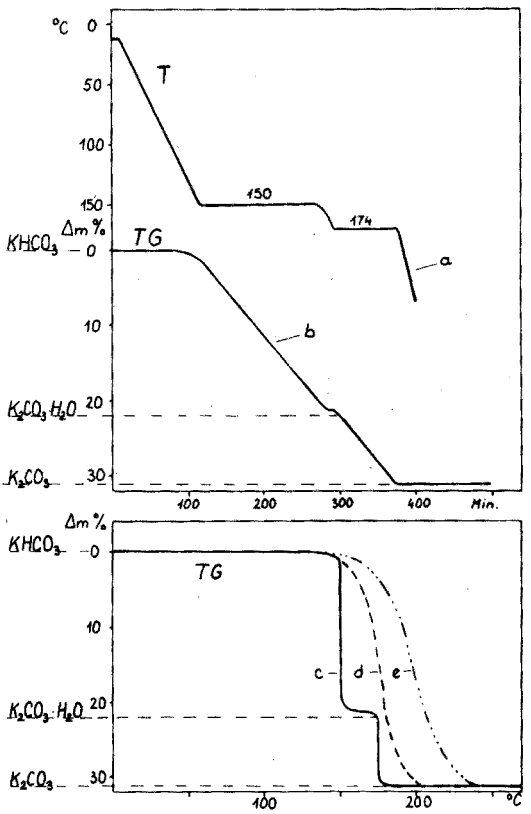


Fig. 2. Thermal decomposition of potassium hydrogencarbonate. (a) Temperature change; (b) weight change as function of time; (c) weight change as function of temperature traced by the "quasi-isothermal" technique; (d) weight change on the polyplate holder traced by the conventional thermogravimetric method; (e) weight change in the conventional crucible.

obtained with the help of the proposed device furnish new surprising information. From the course of the curve it is absolutely clear that, under the given conditions, the thermal decomposition of the sample takes place in two steps. Potassium hydrogencarbonate first decomposes at 150° to form potassium carbonate monohydrate, and this intermediate loses its water of crystallization only at 174°.

The increased selectivity attained by means of the new method can be judged from comparing the curves in Fig. 2.

A thorough analysis of curves a and b is of interest. It seems that the correctness of reaction kinetic calculations on the basis of curves obtained by dynamic thermoanalytical methods is rather questionable. According to curves a and b during the two processes that follow one another, both the rate of weight loss and the temperature are strictly constant with the exception of their small introductory and final periods. This demonstrates, however, that the conditions under which the processes occurred, were not only isothermal but also isobaric, *i.e.* the processes occurred under nearly equilibrium conditions. Moreover, this indicates that both decomposition reaction were of zero order. On the basis of the sigmoid curves a and e obtained

when the conventional heating program was used, one would conclude that the decomposition reaction was nearer first order than zero order.

The authors wish to thank Prof. E. Pungor for valuable discussions.

*Institute for General and Analytical Chemistry,*
*Technical University,*
*Budapest (Hungary)*

J. Paulik
F. Paulik

1 F. PAULIK, J. PAULIK AND L. ERDEY, *Z. Anal. Chem.*, 160 (1958) 241.
2 F. PAULIK, J. PAULIK AND L. ERDEY, *Talanta*, 13 (1966) 1405.
4 L. ERDEY, F. PAULIK AND J. PAULIK, *Acta Chim. Acad. Sci. Hung.*, 10 (1956) 61.
4 L. ERDEY, F. PAULIK AND J. PAULIK, *Hung. Patent 152.197*, 1962.
5 J. PAULIK AND F. PAULIK, *J. Thermal. Anal.*, in preparation.
6 J. PAULIK, F. PAULIK AND L. ERDEY, *Anal. Chim. Acta*, 34 (1966) 419.
7 R. M. CAVEN AND H. J. S. SAND, *J. Chem. Soc.*, 105 (1914) 2754.

(Received 5th April 1971)

*Analytica Chimica Acta*
Elsevier Publishing Company, Amsterdam
Printed in The Netherlands

## BOOK REVIEWS

R. D. Tiwari and J. P. Sharma, *The Determination of Carboxylic Functional Groups*, Pergamon Press, Oxford, 1970, vii + 132 pp., price £3.00 ($8.00).

This text, which is the third in the series of monographs on organic functional group analysis, provides a survey of the analytical methods available for carboxylic acids, acid anhydrides and chlorides, esters and amides. The analysis of binary and ternary mixtures is also discussed.

About half the book is concerned with carboxylic acids. After some general information, the titrimetric determination of the acids by visual and electrometric methods on all scales of working, is considered in detail. This is followed by spectrophotometric techniques (u.v., visible and i.r.) and chromatographic and electrophoretic procedures. The other groupings are dealt with in similar fashion. Selected analytical procedures are given in detail.

This is essentially a practical text and the information collected should be of considerable help in establishing methods for particular purposes.

A. M. G. Macdonald, (Birmingham)

*Anal. Chim. Acta*, 56 (1971) 322

*The Analytical Chemistry of Sulphur and its Compounds*, Part I, Edited by J. H. Karchmer, Wiley–Interscience, New York, 1970, xv + 534 pp., price £16.50.

This first part of a two-part treatment of the analytical chemistry of sulphur and its compounds, forming Volume 29 of the Interscience monographs on analytical chemistry and its applications, brings together for the first time a vast amount of analytically significant information on elementary sulphur and its compounds. Five chapters of the present text deal mainly with inorganic sulphur compounds, some overlap occurring into the organic field in the chapters on total sulphur and sulphur-containing gases. Considerable attention is given to oxygen- and non-oxygen-containing sulphur compounds. The sixth chapter deals with thiols and is a precursor to Part II (not yet published) which deals exclusively with organic sulphur compounds.

Each chapter forms a monograph on its particular subject matter and the individual authors have succeeded remarkably well in providing a very uniform treatment; their commission was to provide some background chemistry, with discussions on nomenclature, occurrence, physical properties, physical measurements, analytically significant physical and chemical procedures, interfering substances and recommended procedures. The result is an authoritative, comprehensive collection of material of considerable scientific and technical importance, oriented exclusively towards the requirements of the analytical chemist.

With the completion of Part II, this volume will be the most comprehensive source of information on the analysis of sulphur compounds. Although somewhat highly priced, the quality of this text is excellent, and it will undoubtedly assume the position of a standard reference work on the subject which will be of value for many years to come.

W. I. Stephen (Birmingham)

*Anal. Chim. Acta*, 56 (1971) 332

# CONTENTS



*(continued on page 4 of cover)*

*Continued from inside page of cover*